TAMPEREEN TEKNILLINEN YLIOPISTO
TAMPERE UNIVERSITY OF TECHNOLOGY

Arto Köliö

Propagation of Carbonation Induced Reinforcement Corrosion in Existing Concrete Facades Exposed to the Finnish Climate

Julkaisu 1399 • Publication 1399

Tampere 2016

Tampereen teknillinen yliopisto. Julkaisu 1399
Tampere University of Technology. Publication 1399

Arto Köliö

Propagation of Carbonation Induced Reinforcement Corrosion in Existing Concrete Facades Exposed to the Finnish Climate

Thesis for the degree of Doctor of Science in Technology to be presented with due permission for public examination and criticism in Rakennustalo Building, Auditorium RG202, at Tampere University of Technology, on the 16th of September 2016, at 12 noon.

Tampereen teknillinen yliopisto - Tampere University of Technology
Tampere 2016

Supervisors: Professor, D.Sc. Matti Pentti (custodian)

Tampere University of Technology
Department of Civil Engineering
Tampere, Finland

Adjunct Professor, D.Sc. Jukka Lahdensivu

Tampere University of Technology
Department of Civil Engineering
Tampere, Finland

Pre-examiners: Professor, Dr.-Ing. Michael Raupach

RWTH Aachen University
Faculty of Civil Engineering
Aachen, Germany

Associate professor, PhD Edgar-Emilio Bastidas Arteaga

University of Nantes
Institute for Civil and Mechanical Engineering Research

Opponent: Professor, D.Sc. Jouni Punkki

Aalto University
School of Engineering
Department of Civil Engineering

Technical advisor, CEO, Betoniviidakko Oy

ISBN 978-952-15-3774-5 (printed)
ISBN 978-952-15-3800-1 (PDF)
ISSN 1459-2045

Abstract

Reinforced concrete is present in the major part of the Finnish built environment. A vast number of concrete buildings utilizing newly developed prefabrication techniques were built from 1960 to 1979. Since then, the durability properties of the concrete building stock from this era have been found to be poor in regard to freeze-thaw action and the corrosion of the reinforcement. This building stock has now reached an age when many of the building components are due to be renovated. Because of the huge volume of this building stock, its renovation is also challenging in terms of resources.

In terms of the corrosion of the reinforcement, the service life of these concrete structures is composed of two phases. The *initiation phase* withholds the onset of favourable conditions for corrosion, while the second phase, the *propagation phase,* includes the corrosion process of the steel itself. The former is traditionally used as a measure of a building's service life, even though no damage has yet occurred at this stage. However, the service life of a building may be extended by utilising the propagation phase, which would aid in prioritising renovation projects for existing concrete structures once the initiation phase has already passed.

This thesis discusses the propagation phase (active corrosion) as part of the service life of concrete facade panels in the Nordic climate. The objective of the research is to add to our knowledge of the corrosion propagation phase in such structures under actual long-term weather exposure, and to generate data for modelling the process. The study combined a statistical analysis of a large database of condition investigation data, a more in-depth analysis of twelve building case studies and data from field measurements of reinforcement corrosion. Using regression analysis, long-term, time series weather data from the geographical locations of the buildings were compared with the actual corrosion rates. The result is a model to describe corrosion propagation in concrete facades and balcony panels in relation to the prevailing weather. The concrete facades' orientation, obstruction and shelter from vegetation were found to have a decisive impact on the rate of active corrosion. The analysis showed that propagation phase can be used to considerably extend the service life of the concrete, although for buildings in more exposed locations, this may only be a few years. This time period may, however, provide the necessary latitude for the renovation budget.

Keywords: concrete, reinforcement corrosion, corrosion rate, carbonation, service life, modelling, outdoor climate.

Preface

This research builds on, and adds to the wealth of data and knowledge gained from earlier studies of the durability and renovation of concrete facades and balconies. The particular focus of this thesis is the definition and modelling of a building's service life. The work was conducted at the Department of Structural Engineering at Tampere University of Technology from 2012 to 2015.

Quite contrary to the single author's name on the front cover of this book, the research project is actually the result of the enthusiastic and fruitful co-operation of many brilliant contributors.

I am deeply grateful for the inspired and painstaking guidance of my supervisors, Adjunct Professor Jukka Lahdensivu and Professor Matti Pentti throughout the whole doctoral project. I would also like to thank Professors Michael Raupach and Emilio Bastidas for their invaluable criticism and advice.

The entire project has also been generously guided by a highly-esteemed steering group consisting of both of my supervisors, D.Sc. Markku Leivo from the VTT Technical Research Centre of Finland and D.Sc. Jussi Mattila from the Finnish Concrete Industry Association. The author would like to thank these professionals and friends.

A special mention must go to the whole 'Service Life Engineering of Structures' research team here at TUT, especially M.Sc. Toni Pakkala, M.Sc. Petri Annila, M.Sc. Kimmo Hilliaho, B.Sc. Jussa Pikkuvirta and B.Sc. Johan Pellikka for their valuable contributions, support and advice. Special thanks are also given to M.Sc. Anssi Laukkarinen and PhD Mihkel Kiviste from the Building Physics research team at TUT for their comments and contribution to the research.

The author is grateful for the cooperation and support given by the Engineering Office Lauri Mehto Oy, especially Petri Niemelä for his support during the field studies and his participation in the analysis and dissemination of the research. The author would also like to thank D.Sc. Mari Honkanen from the department of Materials Science at TUT for her professional guidance and participation in the analysis and dissemination of the material characterization studies. Thanks are also extended to M.Sc. Harri Hohti and PhD Kirsti Jylhä of the Finnish Meteorological Institute, without whose invaluable data, this study would not have been possible.

The author is grateful to the 'Doctoral Programme in The Built Environment' (RYM-TO) financed by the Academy of Finland, and also to the Technology Development Founda-

tion (Tekniikan edistämissäätiö), KIINKO Real Estate Education (Kiinteistöalan koulutussäätiö) and the Kerttu and Jukka Vuorinen fund. Thank you for your support.

My deepest bow is reserved for my loved ones, family and friends whose presence reminds me that there is still life beyond the completion of this thesis.

Tampere 15.2.2016

Arto Köliö

Contents

Terminology

Carbonation-induced corrosion - Corrosion which is initiated by carbonation (neutralization) of the concrete cover of the reinforcement

Carbonation rate - The rate of pH drop resulting from carbon dioxide-calcium hydroxide reaction, [mm/year$^{0.5}$]

Corrosion - Degradation of metal due to its electrochemical dissolution in an electrolyte

Corrosion rate - The rate of metal loss due to corrosion commonly expressed either as corrosion current density [µA/cm^2] or as metal loss per time unit, usually [µm/year]

Degradation/Deterioration - A process that adversely affects the performance of a structure over time due to environmental actions

Degradation/Deterioration model - A conceptual and/or mathematical model that describes the performance of a structure as a function of time taking degradation into account.

Environmental actions - Those chemical and physical actions to which the concrete is exposed and which result in effects on the concrete or reinforcement or embedded metal that are not considered as loads in structural design (EN 206:2013).

Exposure classes - The classification for risks of degradation of reinforced concrete induced by different environmental actions.

Initiation phase - The first phase of the service life of reinforced concrete where favourable conditions to corrosion are formed on the depth of rebars due to carbonation (or chloride ingress)

Limit state - A predefined limit in the service life of a structure based on either visual appearance, serviceability or ultimate bearing capacity

Material characterization - Techniques which study the microscopic structure and properties of materials

Propagation phase - The second phase of the service life of reinforced concrete where the reinforcement is corroded generating rust until a predefined limit state.

Service life of a structure - The period of time after installation during which a structure meets or exceeds the performance requirements given to it.

List of Symbols and Abbreviations

α	relative volume of rust to Fe, rust volume coefficient (-)
ρ	resistivity of concrete (Ωm)
ρ_{st}	density of steel (7.85 g/cm^3)
C20/25	modern notation of the common concrete grade used in the BES-era (cylinder strength/cube strength of concrete, N/mm^2)
EDS	Energy Dispersive Spectroscopy
F	Faraday's constant (96487 As)
I_{corr}	corrosion current density (µA/cm^2)
k	carbonation coefficient (mm/√t)
M	the molar mass of a substance (for Fe 55.8452 g/mol)
p^d	corrosion penetration (µm)
Q	electric charge (C or As)
RH	relative humidity (%)
SEM	Scanning Electron Microscopy
t	time in years
t_0	the duration of the initiation phase in years
t_1	the duration of the propagation phase in years
t_{cr}	time to cracking of the concrete cover from construction
TEM	Transmission Electron Microscopy
ToW	time of wetness
V^d	corrosion penetration rate (µm/year)
w^t	time of wetness
x	carbonation depth (mm)
x^d	concrete cover thickness (mm)
x_{rust}	measured rust layer thickness (µm)
XC1…XC4	exposure classes representing the exposure to carbonation by EN 206
XRD	X-ray diffractometry
z	the valency number of the substance ions (for Fe 2)

List of original publications

This thesis is based on the following original publications in peer-reviewed scientific journals that are referenced in the text as Article I–V.

I. Köliö A., Pakkala T.A., Lahdensivu J., Kiviste M. 2014. Durability demands related to carbonation induced corrosion for Finnish concrete buildings in Changing climate. Engineering Structures, 62-63(2014). Pp. 42-52.

II. Köliö, A., Pakkala, T.A., Annila, P.J., Lahdensivu, J., Pentti, M. 2014. Possibilities to validate design models for corrosion in carbonated concrete using condition assessment data. Engineering Structures, 75(2014). Pp. 539-549.

III. Köliö, A., Niemelä, P., Lahdensivu, J. 2016. Evaluation of a carbonation model for existing concrete facades and balconies by consecutive field measurements. Cement and Concrete Composites, 65(2016). Pp. 29-40.

IV. Köliö, A., Honkanen, M., Lahdensivu, J., Vippola, M., Pentti, M. 2015. Corrosion products of carbonation induced corrosion in existing reinforced concrete facades. Cement and Concrete Research, 78(2015). Pp. 200-207.

V. Köliö, A., Hohti, H., Pakkala, T., Laukkarinen, A., Lahdensivu, J., Mattila, J., Pentti, M. 2016. The corrosion rate in reinforced concrete facades exposed to outdoor environment. Materials and Structures, <*Accepted, 8.6.2016*>.

Author’s contribution

I. The author planned the research work together with all the co-authors. The research material was gathered by Jukka Lahdensivu, while the author carried out the required calculations and simulations. The climate change parameters were prepared by Toni Pakkala. The interpretation of the results was done in cooperation with all of the other researchers while the author performed as the corresponding author to the manuscript. The literature review was prepared and written by Mihkel Kiviste.

II. The author planned the research work together with Jukka Lahdensivu and Matti Pentti. The author conducted the statistical analyses and model calculations based on the research material composed by Jukka Lahdensivu. The author wrote the manuscript as a corresponding author. The co-authors commented on the manuscript.

III. The author planned the research work together with Jukka Lahdensivu. The research material was gathered by Petri Niemelä and analysed in cooperation with the author and Jukka Lahdensivu. The author wrote the manuscript as a corresponding author. The co-authors commented on the manuscript.

IV. The author planned the research work together with Jukka Lahdensivu and Matti Pentti. The research material was gathered by the author in cooperation with the engineering office Lauri Mehto Oy by taking part in Petri Niemelä’s condition investigations. The research samples were prepared and studied by the author. Material characterization studies were conducted by Mari Honkanen (Dept. of Materials Science, TUT) assisted by the author. The author served as the corresponding author to the manuscript. Co-authors provided text passages of their own expertise and commented on the manuscript.

V. The author planned the research work together with Jukka Lahdensivu, Anssi Laukkarinen and Matti Pentti. The corrosion rate measurement data was provided by Jussi Mattila and the weather data provided by Harri Hohti. The wind-driven rain parameter was prepared by Toni Pakkala and solar radiation by Anssi Laukkarinen. The author conducted the analysis and the results interpretation. The author served as the corresponding author to the manuscript. Co-authors provided text passages of their own expertise and commented on the manuscript.

1 Introduction

As in most European countries, owning your own home is the biggest investment that most Finns make in their lives. However, an increasing percentage of Finnish home-owners are being hit with hefty bills for renovation work on their concrete apartment blocks, which have to withstand the harsh Finnish environment. There is now rising national concern about the increasing maintenance demands of our existing building stock. Many of the apartment blocks erected during the building boom of the 1960s and 70s in the new city suburbs such as Suvela in Espoo and Hervanta in Tampere are now in need of extensive renovation. In many cases, the reinforced concrete facades and balconies in these structures were built before the concept of service-life design had been properly established, and the need to extend their service-life has increased dramatically. Private and public buildings made of concrete constitute 34 % of the Finland's building stock (excl. single-family houses), and almost 40 % of these structures are now between 30 and 50 years old, a problem which Finland has in common with most European countries with significant stocks of mass housing (Huuhka et al. 2015). The concrete elements in this building stock which are most susceptible to environment-induced degradation are facades and balconies, as they are exposed to the outdoor environment. These structures are usually based on the open concrete element system (BES) developed in 1969, and are commonly built of prefabricated sandwich facade panels, balcony slabs, frames and parapet elements. The details of their joints and fittings conform to the building regulations outlined at that time (BES 1969).

In this thesis, the propagation of corrosion in concrete facades in Finnish environmental conditions was investigated through a series of field and laboratory studies conducted on twelve residential concrete buildings located in different parts of southern Finland. The studies were conducted during the normal condition assessment procedures for these buildings. In addition, the corrosion rates in concrete facades were evaluated using long-term field measurements on concrete facades under natural conditions. The experimental results were contrasted with statistical information of 947 separate building cases. This information was used to determine the parameters which are critical for modelling the service life and assessing the residual service life of these already aged buildings.

1.1 The renovation market for concrete facades and balconies

The volume of renovation projects in the whole construction sector in Finland has increased steadily in the last decade and has already surpassed the volume of new housing construction, (renovation currently accounts for approx. 58 % of building work in Finland). (Building industry, 2014). Typical renovation projects are relatively small and are normally focused on single buildings and their components. However, in the opinion of renovation contractors, it would be beneficial to combine the renovation of multiple components (facades, roof, building services, energy efficiency etc.) and to coordinate larger projects over several neighbouring buildings. In many cases, this would facilitate the practical feasibility of the renovation solutions and systems, and reduce the costs and the long-term disturbance for the residents.

The net cost of the renovation needed for the entire Finnish building stock is estimated to be €30–50 billion, which is approximately 10 % of its total value (ROTI 2013). The cost of the renovation work needed for the concrete facades and balconies alone is approximately €3.5 billion (7-12 % of the estimated cost of the total renovation needed). Due to the degradation and ageing of the structures under the strains of the harsh outdoor climatic conditions, the cost of the required renovation is increasing by €63 M a year, and this is just to maintain the building stock in its current condition. (Köliö 2011).

Managing this renovation for the national building stock is challenging, because the majority of the apartment buildings in Finland are privately owned by the residents' own housing corporations. This scattered ownership hinders the possibilities of exchanging knowledge and best practice between renovation projects, and also prevents the accumulation of experience in renovation on the owners' side, as each project is run by the individual housing corporations themselves, which have widely varying expertise in construction. All too often, the housing corporations' lack of expertise in the economics of construction leads to renovation projects being commissioned solely on the basis of what the landlords (usually homeowners' associations) can afford, rather than what really needs to be done to optimise the building's service life.

Other major parties concerned with the ownership and maintenance of a large proportion of the housing stock are national and local governmental organisations, such as the state, the cities, towns and municipalities, parishes, etc. In addition, there are large privately-owned real estate companies who own and run rented apartment blocks all over the country. These parties usually have well-developed administrative bodies to maintain their building stock. However, the problem is that the costs of the renovation often exceed the available funding for such projects. Against this background, the ability to model or forecast corrosion rates on concrete facades would greatly enhance the ability of real estate landlords and owners to deal with upcoming renovation requirements. Such a model would not only be able to predict the residual service life of a specified structure, but could also be used to create renovation strategies for larger building stocks, by revealing the order of importance or the urgency of separate renovation projects. Such a tool would enable

landlords to move towards a more predictive upkeep of their real estate, giving them the confidence to make long-term contracts with building renovation engineers and contractors.

In responding to a survey conducted for this research project, renovation architects, contractors and designers indicated that the most common renovation projects today are still concerned with suburban apartment buildings from the late 1960s to the end of the 1970s. The earliest of these buildings were subject to renovation as long ago as in the 1980s. However, due to the high volume of construction during that time, their continuing renovation will have a significant economic and social impact in Finland for the foreseeable future.

According to the survey responses, renovation designers tend to opt for heavy renovation work including cladding repair and renewal (approx. 60–70 % of the total). This is often because of the advanced state of the building's degradation, which of course necessitates the use of heavier renovation options, but such repairs are also needed to compensate for uncertainties in the initial data for the design. Usually, the delaying of the renovation will lead to higher realized renovation costs in the future. Conversely, timely preventative repairs can significantly extend the service life of a building. One key factor for the successful management of Finland's total renovation requirement is timely, proportionate renovation work which will optimize both the cost of the renovation and the extension to the service life of the building.

1.2 Risk of corrosion damage in the BES-building stock

The effects of reinforcement corrosion have resulted in high maintenance costs for concrete infrastructure in varying climates around the world, and the Finnish climate is no exception (Fasullo 1992, Wallbank 1989, Tilly 2011). The corrosion of the reinforcement in concrete structures has two basic effects. Firstly, it can cause cracking of the concrete cover, and secondly, the effective steel cross-section is reduced (Broomfield 2007). Cracking occurs in structures where the reinforcement is placed relatively close to the surface of the concrete. The cracking accelerates the penetration of agents which are harmful to concrete and causes unsightly visual defects to the concrete structures, which is especially visible on the facades. Cracking can be considered as a limit based on the appearance or serviceability of the structure where the needed intervention would be patch repairs and coatings. A further-developed form of visual damage would be spalling, where a whole segment of the concrete cover will fall from the concrete surface. However, there is still an undefined period of residual life after cracking and/or spalling, during which the structure will still continue to function adequately until a final limit is reached, when the structural failure is so severe as to require either rehabilitation or demolition. The reduction of the effective steel cross-section is a problem associated with highly-stressed structural concrete with reinforcement of very high nominal strength, such as pre-stressed concrete members (Broomfield 2007). Typical concrete facade structures do not contain pre-stressed structures.

With concrete facades, the corrosion of the reinforcement is usually initiated by the carbonation of the concrete cover. Concrete carbonation and carbonation induced reinforcement corrosion are discussed in detail in chapter 2. Secondly, corrosion can be initiated by chlorides either present or penetrated in the depth of the reinforcement. In the Finnish climate in particular, there are few environmental sources for external chlorides. (Lahdensivu 2012). This means that the likelihood of corrosion occurring in concrete facades and balconies is the combined result of carbonation and the structure's resistance to it, as well as the moisture stress level the structure is exposed to. Based on this knowledge, the ability to design structures with dense concrete with high binder content together with sufficient concrete cover of little or no variation in a way where the moisture stresses are controlled plays a decisive role in the long term durability of concrete.

1.2.1 Climate exposure

Finland lies between the 60th and 70th northern latitudes. The climate in Finland can be characterized as somewhere between humid continental and subarctic according to the Köppen-Geiger classification. Using this classification, Finland has a similar climate to the rest of Scandinavia and large parts of Russia and Canada. (Kottek et al. 2006).

Lahdensivu (2012) has shown that the most crucial climatic factors for the durability of concrete facades are the prevailing wind direction during rain and the number of freeze-thaw cycles after rain or snow. In Finland, the prevailing winds are from the south and the west, so it is the south and west-facing facades which bear the brunt of wind-driven rain. This can be clearly seen on cases of observed deterioration caused by carbonation-induced corrosion and frost damage. It also explains the lower degree of degradation generally observed on northern facades. Coastal areas tend to have higher rainfall and stronger winds than inland areas, which is reflected in the fact that the facades of buildings near the coast degrade more quickly than those inland. Autumn is usually the wettest part of the year in Finland and the air is relatively humid. The frequent wetting of the facades and their relative inability to dry out (because of the humidity) mean that the degradation of concrete structures is more severe at this time of year.

In the standardized classification of environmental actions, (SFS-EN 206, 2013), facades and balconies fall into the exposure classes XC3 and XC4. This means that the structures are composed of some parts that remain sheltered from the rain (XC3), e.g. the soffit surfaces of balcony slabs, and some parts that are subjected to cyclic wetting and drying (XC4), e.g. the vertical facades and balcony surfaces. Although the surfaces sheltered from rain are at high risk of carbonation, the fact that they don't get wet so often means they have a low risk of active corrosion. The greatest risk for the corrosion of these parts is associated with badly working details or defects in the waterproofing, which may increase the moisture stress locally. The surfaces subject to cyclic wetting and drying suffer from moderate carbonation but, once it has started, the rate of active corrosion is high. As a rule, the initiation phase (carbonation) accounts for a substantial proportion of the service life of the structure, whatever the exposure class, and is therefore essential in service-life design.

1.2.2 Typical structures and reinforcement

There are a number of structural elements common to the prefabricated construction of apartment buildings from the 1960s to the present day. These are facade sandwich panels, and balcony structures composed of individual balcony slabs, balcony side panels and balcony parapet units. Table 1.1 shows the key properties of these structures with regard to the durability of their reinforcement. In terms of durability, they can be distinguished from each by the following criteria:

a) the orientation (vertical/horizontal) of the structure units and their position in the facade, which affects their exposure to wind-driven rain
b) Monolithic balcony structures and layered facade units exhibit different drying behaviours.
c) the drying behaviour is also affected by the presence of a heat flux through the facade units in contrast to the cold balcony structures (considered as a minor effect)
d) the specified concrete grade used in balcony structures is higher than in facades, and this enhances the durability of the concrete (higher strength, lower porosity, lower water permeability etc.).
e) high local moisture stresses are often caused by inefficient water drainage on the balcony slab. Moisture stresses accumulate on the outer edge of the slab, on balconies below, and on adjacent facades.

Table 1.1 Typical dimensions and reinforcement properties of Finnish prefabricated facades and balconies

Structure/ unit	Dimensions	Reinforcement	Comments
Facade sandwich panel	Outer layer 40-70 mm, Inner layer 80 mm (non-bearing) or 150 mm (load bearing)	Outer layer: Mesh 3-4 mm with 150 mm spacing, Edge rebars 6 to 8 mm, Trusses connecting outer and inner layer spacing 600 mm, Auxiliary reinforcement/lifting straps	Thickness of thermal insulation varies with regulations, Elastic element joints (polymer sealants), Usually no ventilation gap = dries slowly
Balcony slab	Thickness 140-200 mm (sloped upper surface)	Bearing reinforcement: 10 to 12 mm spacing 100-150 mm in the lower section of the slab Upper section: tie rods, aux. reinforcement, lifting straps	Water drainage system varies: drain pipe, spout pipe through the parapet, gap between slab and parapet. Typically have no waterproofing layer.
Balcony side panel	Thickness 150-180 mm	Edge rebars 10 to 12 mm, Auxiliary reinforcement/lifting straps	Height of no more than 8 storeys allows the use of non-reinforced concrete panels.
Balcony parapet	Thickness 70-85 mm	Heavy reinforcement near both surfaces, rebars 6 to 8 mm spacing 150 mm	Often cast as one unit with the slab

The Finnish concrete code (Table 1.2) specifies the grade and thickness of concrete coverings. In addition, a common minimum requirement for the cover of auxiliary reinforcement (manufacturing reinforcement, lifting straps) has been 15 mm. Until fairly recently, the requirements for the minimum concrete cover for facade concrete were the same as those set in 1978. However, the more current codes allow the minimum requirement, to be set between 10 and 40 mm depending on the degree of exposure to climate. Nowadays, the minimum requirements for the concrete cover for carbonation-induced corrosion (exposure classes XC1 to XC4) are from 10 mm (for dry or constantly wet structures) to 25 mm (for facades and balconies) (BY 50 2012). The specified cover has proved itself sufficient for carbonation resistance in current and predicted future climatic conditions (Article I).

Table 1.2 Requirements for the minimum concrete cover of working reinforcement and concrete grade in Finnish concrete codes from 1965 to 1995. (Pentti et al. 1998).

Year	Required minimum concrete cover of reinforcement [mm]	Required concrete grade/cube strength [MPa]
1965 – 1977	20	C20/25
1978 – 1989	25	C20/25
1990 – 1992	25	C25/30
1993 – 1995	25	C32/40*

* converted from cube strength to concrete grade

However, there is significant variation in the scatter of the actual cover depths (Fig. 1.1) in existing concrete facade panels and balcony structures (Lahdensivu 2012), and this poses a risk for the durability of the buildings, as other reinforced concrete structures have shown similar problems (Lollini et al. 2012). The scatter in facade and balcony panels has mainly been caused by the poor manufacturing techniques used for these panels, e.g. lack of spacers or and workers walking on top of the panels during the casting of concrete (Hytönen and Seppänen 2009). Differences between different facade surfaces have also arisen from the casting direction, which can vary from face-up (brushed surface, good cover) to face-down (exposed aggregate and form surface, bad cover) (Pentti et al 1998).

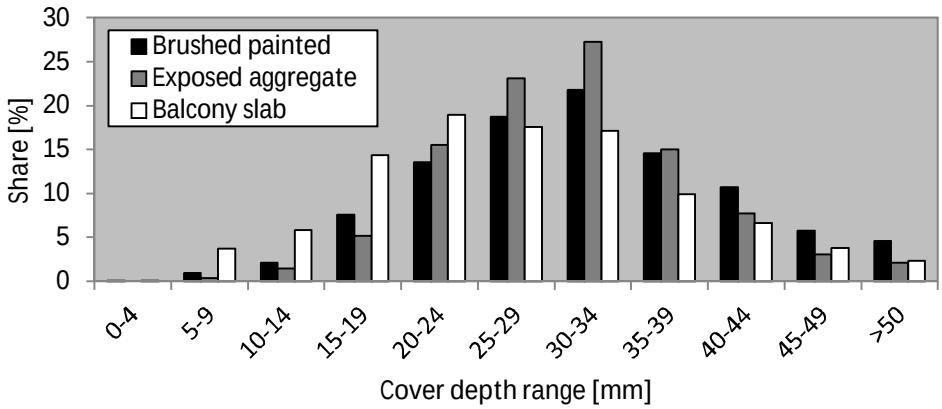

Figure 1.1 The realized scatter of reinforcement cover depths in different concrete surfaces manufactured in 1965–1989. Number of measurements is for brushed painted facade 60 640, Exposed aggregate concrete 104 958 and for the balcony slab 12 957.

The cement type most commonly used in pre-cast concrete facade panels is CEM I (42.5 N) (ordinary Portland cement) because it has good early-age strength which is an advantage when manufacturing and handling the panels. White cement, CEM I (52.5 R) has also been used in facade panels when necessary, but it only accounts for a small segment of the total building stock. In the Nordic climate, the concrete used for facades and balconies has to be air-entrained, a practice which has been common in Finland since the early 1980s. The actual composition of the concrete used during construction has not been analysed during the regular condition assessments, so this is not known precisely. Therefore, the concrete's specified values are used in evaluating the results.

The pore structure of the concrete in existing facades and balconies has been studied using simple immersion tests of capillary porosity (capillary saturation content) and the protective pore ratio (SFS 4475, 1988). The main use of these tests has been to verify the freeze-thaw resistance of the concrete, but at the same time it provides information on the diffusivity of CO_2, which is a critical factor in the corrosion of embedded steel. Judging by a large amount of experimental data, the degree of capillary saturation varies from 1.6 to 9.2 % in brushed painted concrete facade panels and from 4.4 to 10.8 % in exposed aggregate concrete. The degree of capillary saturation in balcony structures varies from 2.3 to 14.0 %. On average, these structures have a capillary saturation degree of over 6 %, which is regarded high for structures of this type (Lahdensivu 2012).

The carbonation depth (and, by extension, the carbonation coefficient) of the existing concrete facades and balconies has been determined using a standardized test procedure (SFS-EN 14630) during the regular condition inspections. The carbonation coefficient can be determined from the carbonation depth and the age of the structure at the time the measurement was taken, usually through a square-root relationship. The coefficient can be used as a measure of the carbonation rates in different structures, enabling them to be compared in terms of their corrosion risk. As a general rule, a coefficient value of ≤ 1.0 mm/year$^{0.5}$ can be considered as good quality concrete (Grantham 2011). Unfortunately, the carbonation coefficients for the BES–era buildings generally

exceed this value (average level of approx. 2.0 mm/year$^{0.5}$) which indicates that fast carbonation can be expected in these structures (Fig. 1.2).

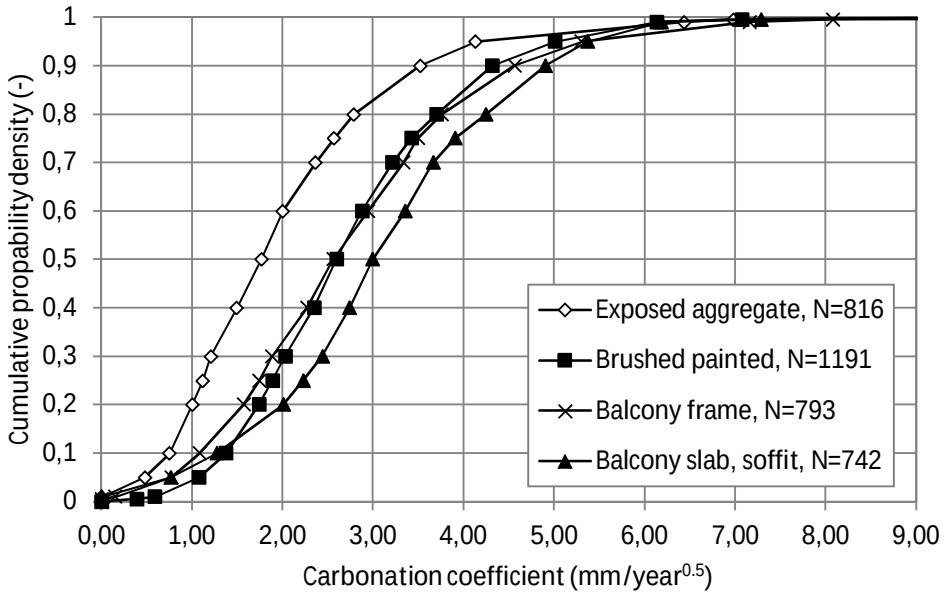

Figure 1.2 The carbonation resistance presented as the carbonation coefficient of different existing concrete facades and balcony structures manufactured in 1965–1989

The carbonation coefficient of facade and balcony structures typically has a value in the range of 0 – 8 mm/year$^{0.5}$. However, values from 1.5 to 3.5 are often observed, with average values dependent on the material, the structure and environmental conditions, and the finish on the concrete surfaces. (Fig. 1.2). The generally lower carbonation coefficients observed on exposed aggregate concrete are due to the fact that it generally has a slightly higher cement content than the brush-treated concrete. Another factor is that the brushing treatment of the brushed painted concrete while fresh leaves the concrete surface more open to carbon dioxide ingress. The high carbonation rate observed in the soffit surfaces of the balcony slabs is due to their sheltered location from rain, which keeps the RH of the concrete constantly favourable to carbonation.

1.2.3 Observed degradation

Using a comprehensive database taken from building condition inspections, Lahdensivu (2012) studied the factors that have actually affected the service life of existing concrete facades and balconies, and the occurrence and progress of different degradation phenomena in them. He found out that a proportion of the concrete facades and balconies suffer visible corrosion damage, at least to some extent. In the majority of these structures, the damage is only local. However, extensive corrosion damage was found in 5.7 % of the facades and in 15 % of the balconies. The damage was most commonly found at the splicing locations near the concrete surface and at the edge rebars of the window openings (Fig. 1.3). Corrosion damage in the actual balcony structures was most commonly found on the edge rebars of the side panels and the parapet reinforcement.

Figure 1.3 Typical corrosion damage on concrete facades

This corrosion damage was almost solely due to carbonation, which had typically reached a depth of 11-20 mm in facades built in the 1970s. Facades with clinker-clad or white concrete surfaces had resisted carbonation better. In balcony structures the carbonation rate is highly dependent on the degree of exposure to wetting. Concrete carbonation occurs faster in structures sheltered from wetting and is clearly linked to the porosity of the concrete. The capillary porosity of the concrete used for facades and balconies was found to be quite high, indicating a high water-cement ratio. Porous concrete is susceptible to reinforcement corrosion because it can easily be penetrated by both carbon dioxide and moisture.

Many of the reinforcement cover depths did not meet the minimum specified requirements. Although the proportion of small (under 10 mm) cover depths was below 3.6 % (considered minor given the size of the database), in balcony structures the proportion was found to be remarkably large, e.g. 7.7 % of the inner surfaces of the parapet panels. These shallow cover depths have allowed carbonation to lead to corrosion problems. It has to be remembered that the cover depths are not measured directly on visual damage, which could mean that the most critical cases are not represented in the statistical data.

Little attention was paid to the service life and durability of the concrete facade and balcony structures during their construction in the 1960s to the 1980s. In fact, it is only comparatively recently that building engineers and designers have started to pay attention to these factors, (a fact that can be verified by a quick glance through the concrete codes and guidelines over the years). There is a large body of data which confirms that the realized durability properties of these structures are poor and the risk of active corrosion damage in the BES building stock can be regarded as high.

1.3 Service life design of outdoor air-exposed concrete structures

1.3.1 Existing concepts and methodologies

The most common concept (Tuutti 1982) in assessing the service life of reinforced concrete is the division of the service life into two phases, an initiation phase and a propagation phase (Fig. 1.4). This dual phase model illustrates that the main pre-condition for the corrosion of steel in concrete is the de-passivation of the reinforcing steel, which occurs during the initiation phase. The de-passivation happens via carbonation of the surrounding concrete, or locally by the ingress of chlorides. Since the presence of chlorides is extremely rare in the structures studied here, chloride ingress is not discussed further in this thesis.

Carbonation has been known to advance in concrete as a front which makes determination of the location of that front relevant as it affects the achievable service life. (Broomfield 2007). It should be noted here that no actual corrosion (or damage) has yet occurred during this initiation phase. After initiation comes the propagation phase, in which the reinforcement corrodes, generating ferrous oxides, i.e. rust. As with most chemical reactions, the type and rate of corrosion is influenced by the corrosion environment, affected in this case by fluctuations in the temperature and the moisture and pH levels of the concrete (Ahmad 2003).

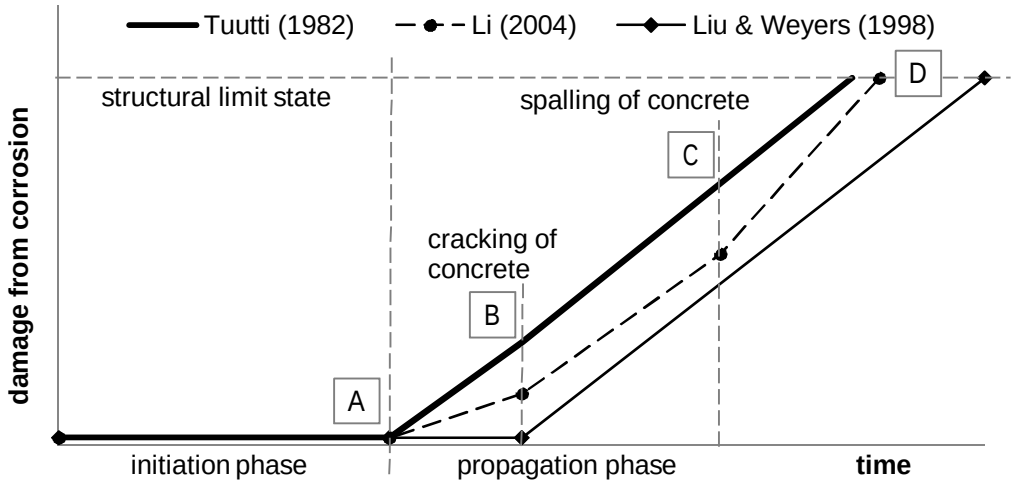

Figure 1.4 The model of reinforcement corrosion usually utilizes the principle of initiation and propagation phases.

The dual phase model can be used in service life design, either as a whole unit (comprising both phases) or only in terms of the initiation phase. In the latter case, the initiation of corrosion, (i.e. the point when carbonation has reached the reinforcement) is regarded as the end of the structure's service life (point A in Fig. 1.4). The problem with this strategy is that it sets the end of structure's service life at a point where no damage has yet occurred, i.e. there is still a wide safety margin. If both phases are taken into account, this safety margin can be effectively utilised, and a number of

other factors can be used to determine the end of the structure's service life, such as concrete cracking and/or spalling (points B and C in Fig. 1.4), critical deflection or collapse (point D in Fig. 1.4) (Li 2004).

Since the introduction of the dual phase model, the theories about what actually happens in the porous zone around the concrete reinforcement have advanced considerably. Liu and Weyers (1998), for example, have identified factors which can delay the accumulation of corrosion damage in concrete (Fig 1.4). According to their theory, the delay is caused by the fact that rust first accumulates in the vacant pores in the porous zone, which does not raise the tensile stress. Another widely discussed theory is the acceleration of the rate of damage once certain limits, such as cracking or spalling, have been reached (e.g. Li 2004). This theory has given rise to a multitude of studies on reinforcement corrosion (both initiation and propagation) in cracked concrete.

Many of the models which have so far have been proposed to illustrate carbonation make use of the square root of time relationship (Parrott 1987). However, empirical measurements have indicated using this relationship in the model results in an overestimation of the degree of carbonation, especially in cases where the concrete is exposed to rain (Tuutti 1982, Huopainen 1997). Therefore, the square root equation should be regarded as an upper limit for carbonation in such cases. The carbonation coefficient, k, is used to adjust the models so that they can describe the carbonation of different concretes in different environments. (Monteiro et al. 2012, Tuutti 1982).

Another approach has been to incorporate the effect of different environments by modifying the exponent of time (Parrott, 1987). A number of studies, such as (Thiery et al. 2007, Hyvert et al. 2010) have utilised physical models to show the reaction kinetics of carbonation. These studies were aimed at discovering the points at which the carbonation reaction is controlled by reaction kinetics, and those at which it is controlled by the diffusion resistance of concrete to carbon dioxide. Neves et al. (2012) improved the square root equation so that it distinguishes between the influences of individual internal and external factors which affect carbonation. The influences of specific factors have been isolated (fib 2006) which gives more flexible parameters than the original one-parameter model.

Corrosion propagation can be modelled by (i) empirical, (ii) numerical or (iii) analytical approaches (Otieno et al. 2011). The empirical models can be further divided into three types: expert Delphic oracle models, fuzzy logic models and models based on the electrical resistivity and/or oxygen diffusion resistance of concrete. The empirical models are based on the experimentally achieved relationship between the degree of corrosion and the controlling parameters (see DuraCrete 2000).

There are three different approaches to developing the numerical models: the finite element method (FEM), the boundary element method (BEM) and a method based on resistor networks and transmission lines. The numerical models rely on complex computation which divides the larger entities into small elements connected to each other by boundary conditions (FEM, BEM) (e.g. Gulikers and Raupach 2006).

In general, the analytical models usually apply a ‘thick-walled cylinder’ approach. Division into a cracked inner cylinder and an un-cracked outer one has also been developed. The analytical models are based on the closed-form solving of mathematical equations derived from the geometry of the problem (e.g. Goltermann 1994).

A traditional way of modelling corrosion propagation is to modify the corrosion rate with the diameter of the reinforcement and the thickness of the concrete cover. (Siemes et al. 1985) The corrosion rate itself is related to the wetness and temperature of the structure, and this can be modelled by, for example, measuring the potential electrolytical resistivity of the concrete (DuraCrete 2000).

1.3.2 The weaknesses of existing methodologies

Modelling both the initiation and propagation phases encompasses a number of uncertainties. It has to be borne in mind that a model is at best only a representation of reality, and is never able to fully capture the actual process. A number of simplifications and assumptions have to be made when producing any model, whatever the method used. In spite of these drawbacks, models are, simply, an essential tool for predicting future trends. They are a highly cost-effective way of simulating the effects of various parameters on the underlying phenomenon without having to resort to a series of expensive and complicated experimental studies. This serves as a good motivation for further research and development of the models.

Otieno et al. (2011) have highlighted some problems that commonly occur when modelling corrosion. These include: (i) the difficulty of obtaining accurate and easily quantifiable input parameters, (ii) the lack of validation of the proposed model, (iii) advance assumptions made in an attempt to simplify the numerical modelling, (iv) the use of accelerated laboratory tests, (v) the small size of the test specimens and sample size, (vi) neglecting the effect of service load-induced cracking on corrosion initiation, and (vii) the way the variability of the model’s input parameters are handled. All too often, due to the shortage of quantitative data about the scatter of material properties and degradative agents, normal distributions or arbitrarily set variables are often used in the model calculations (Otieno et al. 2011, Siemes et al. 1985). For example, Lollini et al. (2012) found that the estimation of the probability density function of the concrete cover was a substantial source of error in their analyses.

The normal service life requirement for concrete buildings today is 50 years (fib bulletin 34), which is the standard adopted in Finland’s national building guidelines. According to these guidelines, the service life of the reinforcement (by50 Concrete code 2004;2012) is only defined as corrosion initiation. This means that the target service life should be achieved by the structure’s carbonation resistance alone. Carbonation can be fairly easily accounted for in new constructions by controlling the composition of the concrete and the depth of the reinforcement’s cover. Therefore, most current corrosion research modelling is concentrated on chloride-induced corrosion (e.g. Otieno et al. 2012; Gulikers and Raupach 2006; Li 2004; Scott 2004; Liu and Weyers 1998). However, in older existing buildings, the properties of the concrete have already been set. This makes the assessment of the residual service life of these structures by the currently available means

problematic in two ways: (i) the residual service life is, by the current definition, zero, even though no damage at all has actually occurred, (ii) there are no verified calculational methods available to evaluate residual service life.

If the depth of the concrete cover is in accordance with Finnish concrete building codes (25 mm), visible corrosion damage is rare, even if the carbonation of the concrete reaches the reinforcement. In structures which are sheltered from the rain, e.g. the soffits of balcony slabs or the inner surfaces of balcony parapets, the active corrosion of the reinforcement is very slow. Visible corrosion damage will occur before the end of the designed service life in reinforced concrete structures where cover depths are low, e.g. less than 15 mm. (Article I). Therefore, modelling the cracking caused by corrosion should concentrate on the lower cover depths.

A recent study (Article I) has shown that environmental parameters such as wind-driven rain, temperature and RH are not adequately taken into account in current initiation and propagation phase models used to depict corrosion in outdoor, air-exposed concrete structures. Nevertheless, experiments have shown that these parameters can have a decisive impact on the service life of a structure (Mattila 2003). A comparison between statistical data and a modelled active corrosion phase (Article II) revealed that service-life design calculations highly overestimate the predictions for the length of the propagation phase of concrete facades and balconies. For example, the DuraCrete model (DuraCrete 2000) didn't properly take into account certain material properties or the weather exposure in the structures. The propagation phase of the soffit surfaces of the balcony slabs was also highly overestimated, due to the equivalent period of wetting which was chosen. In fact, it is perfectly valid to consider the soffit surface of a balcony slab as being sheltered from rain, which means that a long propagation phase can be expected. On the other hand, actual building condition assessments have revealed that corrosion damage in balcony slabs occurs near the edges or because of badly-worked details for rainwater runoff, which causes localised areas of wetness in the structure.

A parametric analysis was conducted (Article II) on the time of wetness and concrete resistivity which describe the environment and material quality in the DuraCrete model. Values for the parameters were varied in a range expected in the Finnish climate, and a significant influence of these parameters on the model was revealed (Figs. 1.5 and 1.6). Climate data was used to determine the time of wetness (between 0.17 and 0.43) and the concrete's resistivity was varied between 50 Ωm and 200 Ωm. The influence of time of wetness and the resistivity of the concrete can multiply the service life prediction 2 and 4 times, respectively. The climate-related temperature and time of wetness can easily be induced from statistical parameters, so their scatter can be quantified with meteorological data. In this analysis, the choice of the concrete resistivity parameter had a very substantial influence on the model's results.

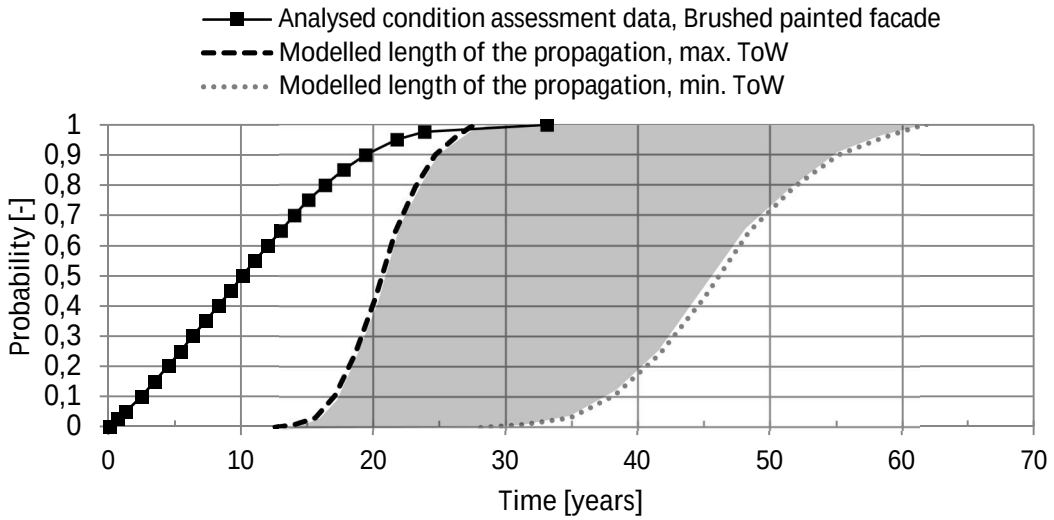

Figure 1.5 The sensitivity of the predicted corrosion propagation phase to time of wetness (ToW) of 0.17-0.43 by the DuraCrete model

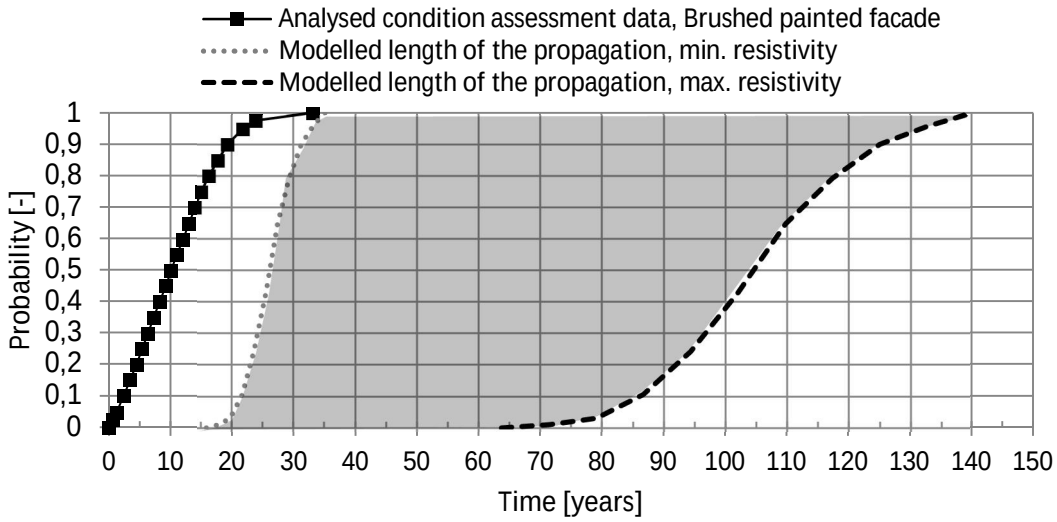

Figure 1.6 The sensitivity of the predicted corrosion propagation phase to concrete resistivity of 50-200 Ωm by the DuraCrete model

Even though the corrosion time scatters widely (depending on facade type, properties and micro-climate factors) it can still be assessed using statistical methods. These statistical analyses also provide a way to validate service life models and to narrow down the problems usually associated with such models.

2 The corrosion mechanism of steel embedded in concrete

The corrosion of steel reinforcement in concrete is commonly regarded as an electrochemical phenomenon in that the corroding reinforcement works as a mixed electrode where cathodic and anodic areas are formed on the steel surface. As stated earlier, corrosion can be initiated either by chlorides penetrating the concrete surface or by the carbonation of the concrete cover. Corrosion due to chlorides usually occurs in the form of concentrated pitting because the corrosion has a small anode opposed to a large cathode, which produces high corrosion currents, and therefore, high rates of corrosion. Corrosion due to carbonation occurs more generally over the surface of the reinforcement, as the cathode and anode areas are more evenly spaced. (Page 1988). Because the concrete acts as a protective layer for the reinforcement, corrosion is not initiated immediately. This fact is taken into account by depicting reinforcement corrosion as a process consisting of two or more consecutive phases i.e. the initiation and propagation phases (Tuutti 1982). The model presented here is aimed at illustrating the carbonation-induced corrosion process.

2.1 Carbonation of the concrete cover

Because of its alkalinity, the concrete protects the steel reinforcement from corrosion. Its high pH (approximately 13) is due to the pore solution in the microscopic pores of the concrete, which contain high concentrations of calcium, sodium and potassium hydroxides. This high alkalinity protects the steel from corrosion by creating a thin passive oxide film on the steel's surface. These passive conditions will endure as long as the environment remains alkaline. However, the alkalinity of concrete is gradually reduced by carbonation, which eventually reaches the level at which corrosion of the reinforcement steel can occur (Tuutti 1982). As well as lowering the pH of the concrete, carbonation has been observed to decrease its porosity and to increase its compressive strength and surface hardness (Parrott 1987).

Concrete carbonation is a reaction between carbon dioxide gas in the atmosphere and the alkaline hydroxides in the concrete (Broomfield 2007). Most commonly, these are calcium silicate hydrate, calcium hydroxide and various calcium aluminate or ferro-aluminate hydrates (Parrott 1987). The carbon dioxide dissolves in the pore water in the concrete and forms carbonic acid, which neutral-

izes the alkalis in the pore water. The reaction forms calcium carbonate on the pore surfaces of the concrete. The reservoir of calcium hydroxide bound in the concrete is larger than can be dissolved in the pore water, which helps maintain the concrete's high pH during the carbonation reaction (Broomfield 2007). Eventually, the reservoir is used up and the carbonation reaction penetrates further into the concrete as a carbonation front. The reaction can only occur when sufficient pore water is available. This means that concrete in low humidity does not react to any significant extent. On the other hand, the reaction also requires the diffusion of carbon dioxide gas to the carbonation front, which is slowed down when there is a lot of moisture (Parrott 1987). The propagation of the carbonation front inside concrete roughly follows the laws of diffusion, which state that the carbonation rate is proportional to the carbonation distance. The carbonation depth of concrete is therefore commonly described by a square root relationship with the exposure time (Tuutti 1982).

2.2 The corrosion process

Once the steel is depassivated it will start to corrode. The principal chemical reaction in corrosion is independent of the way the corrosion is initiated (Broomfield 2007) and can be described in simplified form by the following equations Eqs. 1 and 2. The simplification is based on the assumption of the reinforcing steel being pure iron (Fe) although it usually is composed of mainly Fe, C and Cr. Other possible anodic and cathodic reactions are presented in, e.g, (Ahmad 2003).

The anodic reaction: $Fe \rightarrow Fe^{2+} + 2e^{-}$ (1)

The cathodic reaction: $2e^{-} + H_2O + \frac{1}{2}O_2 \rightarrow 2OH^{-}$ (2)

The steel is dissolved in the pore solution in the anodic reaction and electrons are released. The electrical equilibrium is preserved because these electrons are absorbed in the cathodic reaction elsewhere on the steel surface. The cathodic reaction also consumes water and oxygen and produces hydroxyl ions that increase the alkalinity in the cathode area, thereby reinforcing the passive layer in these areas. These two reactions, especially the release of ferrous ions in the anode, precede the formation of rust, but they are not actually generating rust themselves. The released ferrous ions react with chemical substances in the pore water i.e. the electrolyte, to form the rust itself. The rust formation can be expressed in several ways. (Broomfield 2007).

As can be deduced from the above-mentioned reactions, the corrosion process is influenced by the availability of oxygen (affects the cathodic reaction) and moisture (reduces the electrical resistivity of concrete). Factors affecting corrosion of steel in concrete can be classified into external and internal factors (Ahmad 2003). The external factors include environmental and circumstantial factors, such as the availability of moisture and oxygen, while the internal factors are composed of the concrete and steel's quality parameters.

The corrosion reaction in carbonated concrete can be under reaction control (either anodic or cathodic) or under diffusion control (diffusion of oxygen through electrolyte to the cathode) (Huet et al.

2007, Marcotte 2001). Huet et al. (2007) concluded that the degree of water saturation in the concrete determines the process that controls corrosion. If the degree of water saturation is above 0.9, the corrosion reaction is under oxygen diffusion control. However, if the water saturation drops towards 0.8, the process gradually becomes under reaction control.

The amount of reinforcing steel liberated under electrolysis is commonly derived from Faraday's law. Eq. 3 has been used to shows the equivalent metal loss for a 1 µA/cm2 constant current to be 11.6 µm per year (Broomfield 2007). This calculation is, however, theoretical because the corrosion current in existing structures exposed to the outdoor environment is far from constant.

$$m = \left(\frac{Q}{F}\right)\left(\frac{M}{z}\right) \tag{3}$$

where *m* is the mass of substance liberated, *Q* is the electric charge, (for constant current this can also be expressed as *It*), *M* is the molar mass of the substance (for Fe, 55.8452 g/mol), *F* is the Faraday constant (96485 C mol-1) and *z* is the valency number of the substance ions (for Fe, 2).

Ferrous hydroxide is formed from the ferrous ions and hydroxyl ions as a combined result of the anodic and cathodic reactions. This ferrous hydroxide then reacts further with available oxygen and water to form various final reaction products, i.e. rust. (Bažant 1979). This ferrous hydroxide may react further to produce ferric hydroxide and more hydrated ferric oxide. (Broomfield 2007). The final corrosion product varies depending on the constituents available. The different corrosion products also have distinctive densities and therefore the corrosion of a certain mass of Fe may result in the formation of a greater volume of corrosion products (Fig. 2.1). This means that different corrosion circumstances generate different expansion of corrosion products.

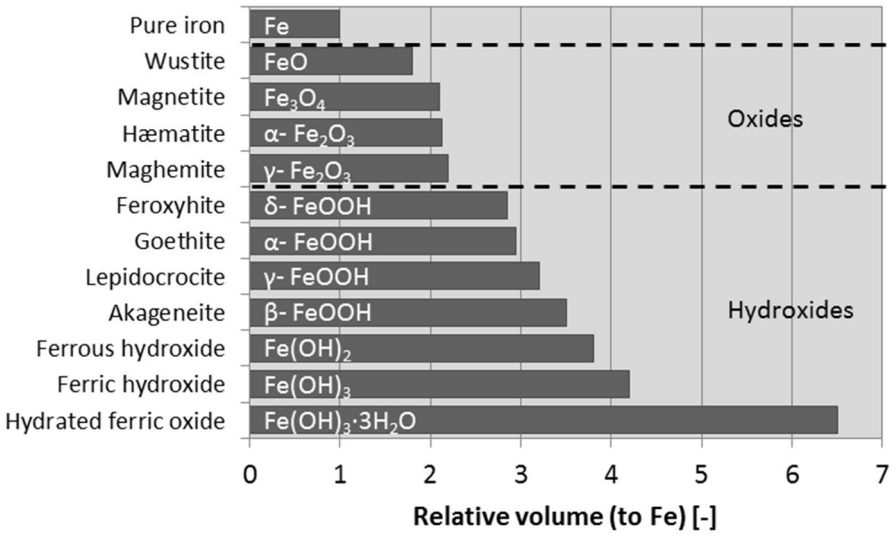

Figure 2.1 Relative volumes of corrosion products of Fe to the parent metal. Reproduced from (Broomfield 2007, Marcotte 2001, Jaffer and Hansson 2009)

The corrosion of reinforcing steel in carbonated concrete produces a multi-layer system consisting of (i) mild steel rebar, (ii) porous conductive oxide layer, (iii) non-conductive iron oxide layer, (iv) carbonated concrete cover and (v) the atmosphere (Huet et al. 2007). The main conclusion is that the corrosion products form layers of different composition around the reinforcement. According to (Huet et al. 2007), the conductive oxide layer (ii) consists mainly of magnetite (Fe_3O_4) while the non-conductive oxide layer (iii) is mainly lepidocrocite (γ-FeOOH) and/or goethite (α-FeOOH). Marcotte and Hansson (2007) have found magnetite (Fe_3O_4), goethite (α-FeOOH) and haematite (α -Fe_2O_3) in laboratory experiments on reinforcement corrosion with immersion in a NaCl solution. In their experiments, haematite in particular formed above the solution line environment, i.e. not a constantly-wet environment. These results imply that the hydroxide types of rust are formed in high moisture conditions, while the oxide type rust occurs in not-constantly-wet conditions. Suda et al. (1993) detected magnetite, goethite and lepidocrocite from a concrete specimen exposed to a marine environment for five years. Corrosion products observed on rebars by Jaffer and Hansson (2009) under chloride-induced corrosion in mechanically generated cracks included haematite, maghemite (γ-Fe_2O_3), goethite and Ferric hydroxide ($Fe(OH)_3$). From these studies it can be concluded that the expected volume increase in the final corrosion products is expected to be approximately 2-3 times the volume of the parent steel.

Hot rolled reinforcing steel is covered with a mill scale due to the manufacturing process. The mill scale is a covering layer of iron oxides a few micrometers thick, which is usually composed of magnetite with a surface layer of haematite and goethite (Marcotte 2001). Both hot rolled (typically rebars) and cold formed (typically meshes) reinforcement have been used in Finnish constructions.

Eventually, reinforcement corrosion causes damage to concrete by the expansive effect of the corrosion products (Broomfield 2007). Cracks are formed on the covering concrete, once the pressure caused by the expansion exceeds the tensile capacity of the concrete. A way of formulating this has been given e.g. by Goltermann (1994). The amount of corrosion penetration to induce concrete cracking has normally been given values of 15–100 µm in varying cases (Siemes et al. 1985, Parrott 1994, Alonso et al. 1998, Andrade 2003). Also a way of calculating the corrosion penetration needed for the initiation of a crack based on rebar diameter and concrete cover depth has been presented (DuraCrete 2000).

3 Research objectives

This research study focuses on the service life design and maintenance strategies for existing concrete facades and balconies constructed in Finland between twenty-five and fifty years ago, (1965–1990). The motivation is to find a way to manage the constantly growing need for renovation of the Finnish housing stock. The aim is to be able to combine a Carbonation model and an Active Corrosion Phase model to give a more comprehensive picture of the service life of these structures. By producing a reliable model for the corrosion propagation phase, new criteria can be applied to define the end of the service life of buildings, which can considerably extend their predicted service life. The residual service life of these facades cannot be estimated by carbonation resistance alone, since this phase has already passed.

3.1 Research questions

The following research questions were addressed:

1. How does the propagation phase of reinforcement corrosion proceed in the prevailing climate conditions after the initiation phase?
2. What is the potential extension to the residual service life by adding the propagation phase to it?
3. Can the propagation phase be reliably modeled and included in the service life estimation process?

3.2 Relevance of the results

The Finnish housing market is, and seems set to remain, highly dependent on the residential buildings built in the 1960s, 70s and 80s. There are enough of these buildings to house approximately one third of the Finnish population (OSF 2015). The majority of these residential buildings are privately owned by the inhabitants' own housing corporations, which means that the equity of a signif-

icant proportion of the Finnish population is tied up in their property. Therefore, the maintenance and renovation of Finnish housing stock is of prime importance to Finland, affecting the population's purchasing power and sense of security (often tied up in their property), which in turn has a powerful effect on the Finnish economy.

Both academics and professionals in the construction industry are increasingly concerned about the maintenance needs of the existing building stock (ROTI 2015; 2013; 2011). Many durability problems have been discovered, due mainly to the poor quality of the construction materials used when the buildings were erected. These buildings need renovation, and there are so many of them, all built in the same period, that the country needs to develop a rehabilitation strategy spanning decades. In focusing on the ongoing degradation of our building stock due to the particular conditions prevailing in Finland, this research addresses an important and pressing issue.

The results of this research project will contribute to the rehabilitation strategies of the housing stock by:

a) providing information on the active corrosion phase in concrete facade and balcony panels
b) revealing structure surfaces which are the most susceptible to corrosion for their exposure to climate
c) showing that the service life of concrete facades and balconies can be considerably extended by taking the propagation phase into account
d) developing a methodology to model the active corrosion so that it can reliably be used to define the degree of service life extension provided by the propagation phase
e) providing a way to reveal the order of importance/urgency of renovation projects through accurate modelling of the active corrosion phase, which would result in better allocation of renovation funding
f) enabling an estimation of the number of coming patch repairs of concrete structures.

Although the rehabilitation of existing buildings is the primary motivation for this research, the results can also be applied in the service life design of new structures with similar materials. The ability to forecast the future service life of new construction will enhance the competitiveness of the construction industry by providing information on the long term performance of concrete structures and promote sustainability through the ability to produce concrete buildings which are ever more-durable to the harsh Finnish climate. In the case of construction faults, e.g. inability to reach the cover depth requirement, this model could be used in describing the severity of the environmental stresses and the need for coating or sheltering of the structure.

4 Main results and discussion

4.1 Research material and methodology overview

The propagation of corrosion on concrete facades in Finnish environmental conditions was studied by a series of field and laboratory studies conducted on twelve residential concrete buildings located in different parts of southern Finland. The studies were conducted in tandem with the normal condition assessment inspections for these buildings. In addition, the extent to which the corrosion rates in concrete facades are affected by the outdoor environment was analysed using long-term (25 months) field measurements from concrete facades under natural weather conditions. These experimental results were compared with statistical information on 947 buildings. The methodology is discussed in more detail in the individual original publications. In addition, a thorough literature survey was conducted for each publication.

The additional research material for this particular study was gathered from 12 buildings, chosen because of their consistency with larger statistical data. The buildings were all located in southern Finland, and ranged from 1971 to 1984 in their years of construction. A total of 27 sample cores with a diameter of 50 mm were drilled from the outer layer of the facade panels directly on visually observable corrosion cracks or spalls (Fig. 4.1). The length of the active corrosion phase could be calculated by determining the time of initiation from carbonation depth measurements, and then subtracting that figure from the total age of the samples. The reinforcing bars trapped inside the carbonated layer of concrete were extracted from the core samples and studied under an electron microscope. The types and critical quantities of the corrosion products in the concrete and reinforcement samples, which formed visible damage, were studied by electron microscopy and X-ray diffractometry. The purpose of these studies was to resolve research questions 1 and 3 as well as to provide a value of critical corrosion penetration for the defined end of service life.

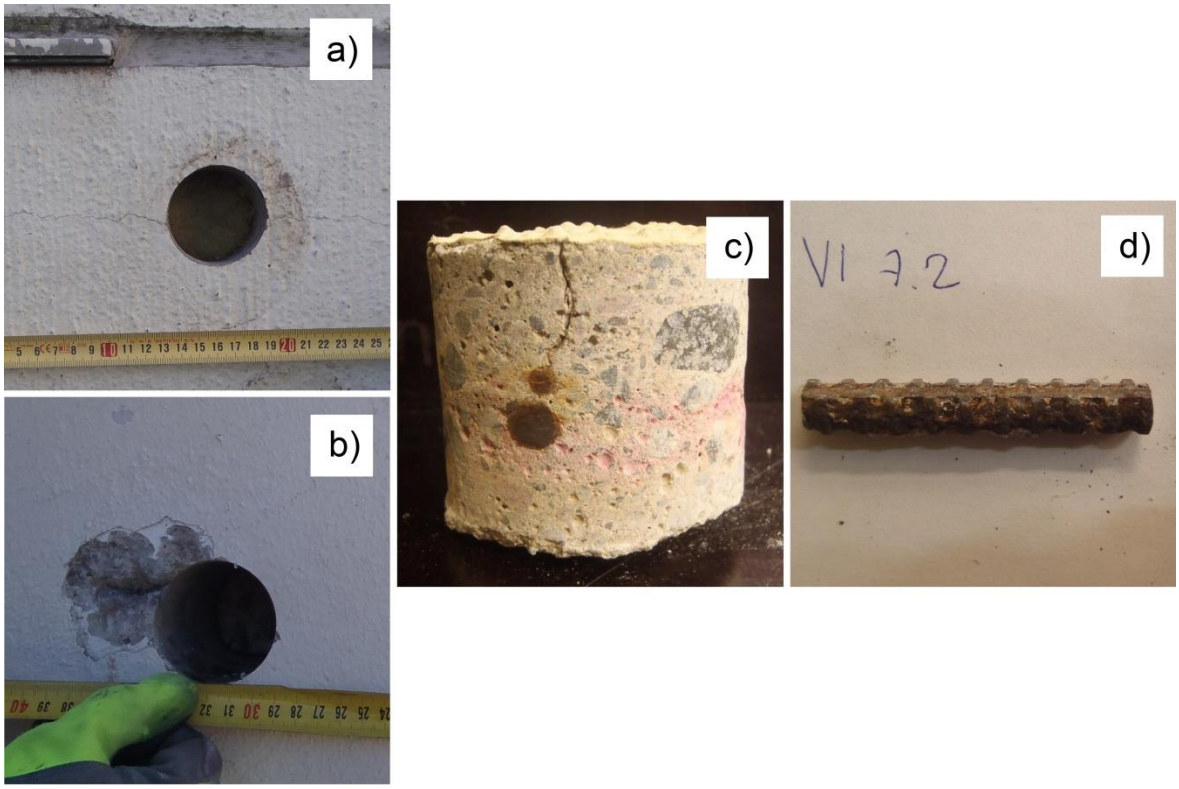

Figure 4.1 The samples were drilled directly above a corrosion induced crack (a) or a spall (b) in the facade. Steel samples (d) were extracted from the carbonated layer of the concrete cores (c) (Article IV)

Mattila (2003) took long-term corrosion current density measurements based on linear polarisation resistance between 2000 and 2002. He fitted instruments on the concrete facades and balconies of two residential buildings in Finland, one inland (Fysiikanpolku 5, Tampere), built in 1978, and the other on the coast near Helsinki, at Joupirinne 4, Espoo, also built in 1978 (Mattila 2003). The measurement facades were both in south-facing directions, the one in Tampere faces southeast (154 degrees from north, clockwise) while the one on the coast faces south-west (223 degrees from north, clockwise) (Fig. 4.2). This data was in this research combined with long term weather observation data from the same period. As well, this analysis provided answers to the research question 1 by revealing the rate of corrosion on concrete facades and its relation to prevailing weather.

The weather observation data for this study was collected by the Finnish Meteorological Institute (FMI). The data was then further refined to form four weather parameters: Temperature (*T, [ºC]*), relative humidity (*RH, [%]*), amount of wind-driven rain on the measured wall surface (I_{WA}*, [mm]*), amount of direct and diffuse solar radiation on the measured wall surface (*RAD, [kJ/m2]*). The data, taken at three-hour time intervals, was taken from the records of the weather observation stations nearest to the case buildings. Finally, multi-linear regression analysis was used to determine the partial correlation of single or a sequence of monthly averaged weather parameters on the observed monthly averaged corrosion current density. The addressed phenomena are fundamentally non-linear, however, a linear analysis can be assumed when the analysed parameters are monthly

averages. This means, that any delay caused by e.g. the transport of moisture evens out on the longer time scale, and a certain average level of monthly weather parameters induces a certain average level of corrosion rate. If transient correlation between the parameters was to be studied, the linear model could not be used.

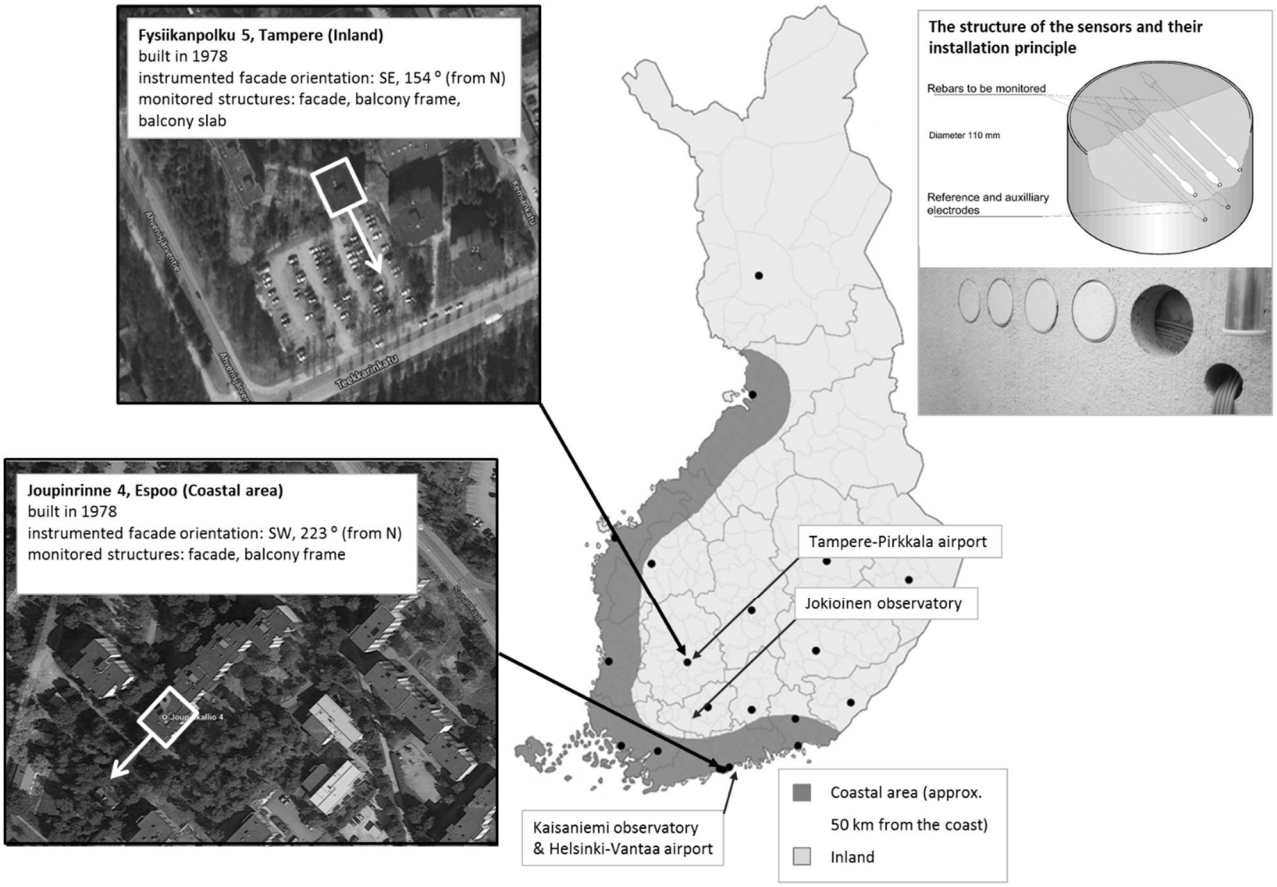

Figure 4.2 The geographical locations of the corrosion measurements and the weather data (Article V)

The research material collected from the commercial condition investigations produced a total of 18 cases where the same facade and/or balconies had been subject to two condition assessments within a certain time interval. The majority were built in the 1970s, but they ranged from 1969–1992, and were perfect for this study. This data was used to study the reliability of modelling of the carbonation of concrete facades and balconies using the square root relationship and the carbonation coefficient. During the first condition assessment, the buildings ranged from 9–36 years old (average age 27 years), and during the second assessment, they were 19–42 years old (average age 35 years). The interval between the assessments was 4–14 years (average 8 years). The properties studied were the average carbonation across the entire facade of the subject building and the carbonation depth of parallel samples. This analysis gave answers to the research question 3 and verified the research methods which were based on the tested model.

The concrete facades of buildings in Finland have been subject to condition investigations since the late 1980s and much data has been collected using standardised procedures (desk studies,

visual observations and ratings, field measurements and laboratory analyses) (Lahdensivu et al. 2013). A database has been amassed from a variety of building condition assessments conducted by various professional engineers between 1992 and 2006. This database includes the condition assessment information of 947 buildings built between 1965 and 1995. (Lahdensivu 2012). This data was subjected to statistical analysis and modelling (e.g. regression analysis, statistical distribution fitting, Monte Carlo simulation) in order to determine major trends in the degradation behaviour of concrete facades and balconies. The statistical analyses provided mainly an answer to the research question 2 and also general trends for research questions 1 and 3, which were used in verifying results from other analyses.

From 1965 until 1989, the specified concrete grade used in the facade panels was C20/25. The cement type used in these precast panels is mostly CEM I, ordinary Portland cement. The concrete composition was not analysed as part of the condition assessments, and has to be estimated from what is known.

4.2 The propagation phase in relation to the concrete facade service life

The condition assessment database was used to perform a statistical analysis of the service life of concrete facades in terms of visible damage caused by reinforcement corrosion (Article II). The visible damage ratings given in the condition assessments were studied in order to determine the age at which visible corrosion damage is generally observed in concrete facades. This damage rating was used together with the age of buildings to study the time it takes for corrosion damage to propagate. A distribution over time for the formation of visible damage was produced (Fig. 4.3).

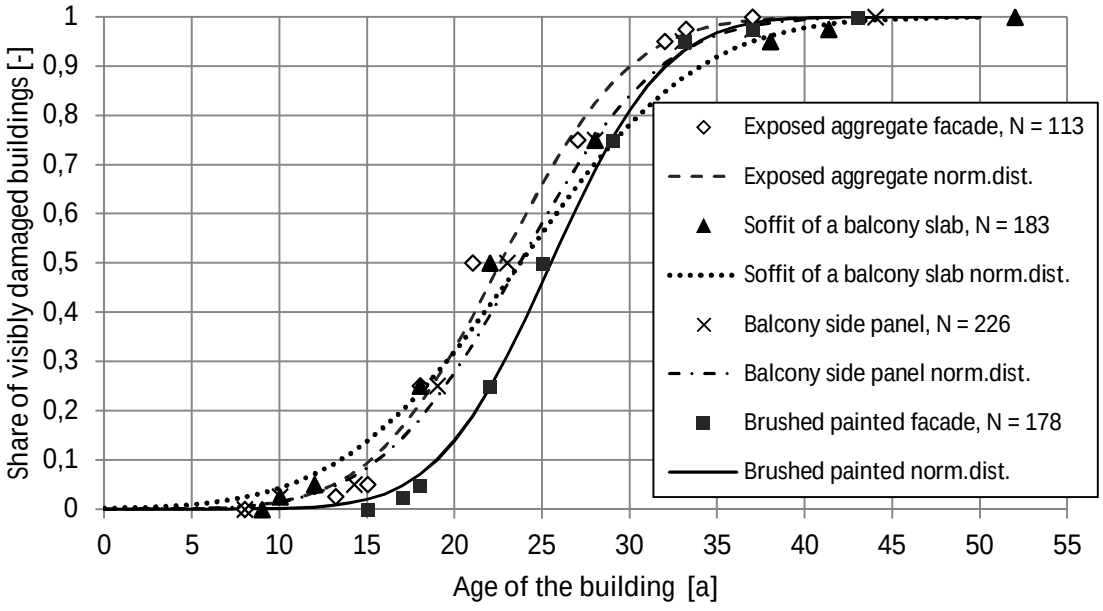

Figure 4.3 A statistical model for the evolution of corrosion damage visible on a structure‘s surface

Because the information about the age of the building is linked to the time of the condition assessment, these examinations do not take into account the fact that any cracks or other visible damage may have appeared some time before the assessment date. For the purposes of this study, how long the damage had been visible before the condition assessment was carried out is unknown, and this should be remembered when considering the results of this study.

The first visible damage had already occurred after 8 years in exposed aggregate facades, and within 15 years for brushed and painted concrete facades. In the balcony slabs, the first damage was observed after 9 years. The median figure is that visible corrosion damage had formed on the concrete facades within 21 and 25 years of construction for exposed aggregate and brushed painted concrete respectively. (Article II). The spread of corrosion-related damage has therefore been quite fast in these structures. Corrosion damage is clearly a problem, especially in cases where the concrete cover is shallow, as then both the initiation and the active corrosion occur rapidly.

This analysis has taken into account the scatter in both concrete cover depths and carbonation resistance. With a target service life of 50 years, and a 10 % safety margin, the initiation periods for corrosion (Fig. 4.4) are: 24 years for brushed and painted concrete, 21 years for exposed aggregate concrete, 11 years for the balcony side panels and 10 years for the balcony slab soffit surfaces. The target service life is therefore in these existing structures not achieved by the initiation phase alone. When the reinforcement has been placed according to requirements and with sufficient concrete cover, the target service life of 50 years can be easily achieved by the carbonation resistance alone. (Article II).

If a similar approach is applied to the statistical data on the corrosion propagation phase (with a 10 % safety margin) the propagation time can be expected to be very short, a mere 1.5 to 3 years (Fig. 4.5). This safety level relates to the most critical conditions for corrosion of the reinforcement with extremely shallow cover with very capillary concrete. However, this safety level may be too strict compared to empirical knowledge that at least some visible damage is tolerated before intervention. As the effects of corrosion in this context are mainly visual defects, a safety level of 50% could be applied, in which case the active corrosion period would be 6–12 years depending on the surface type.

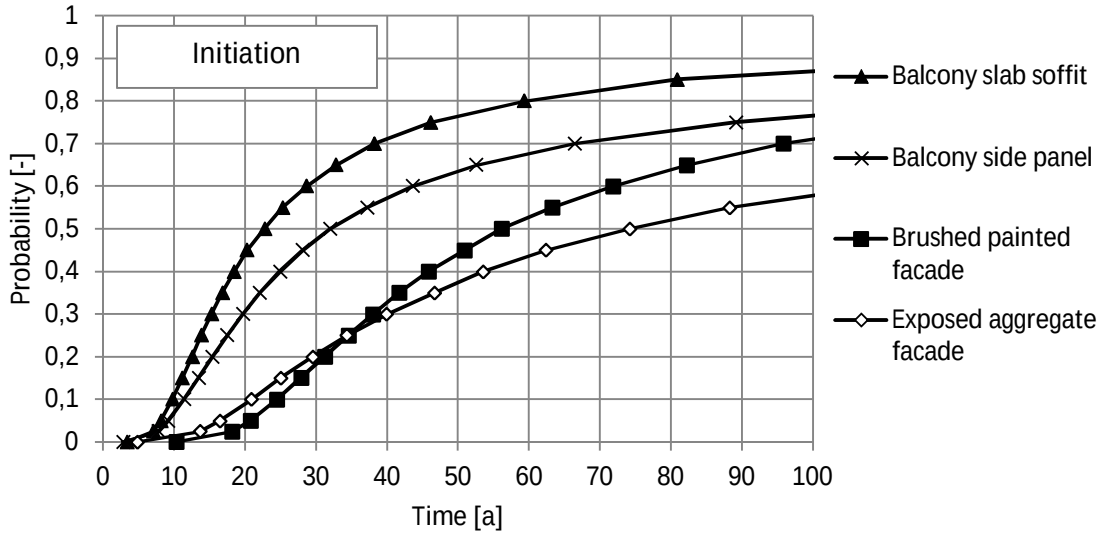

Figure 4.4 The length of the initiation phase in concrete facades and balconies based on a Monte Carlo simulation on statistical condition assessment data from buildings constructed in 1965–1990.

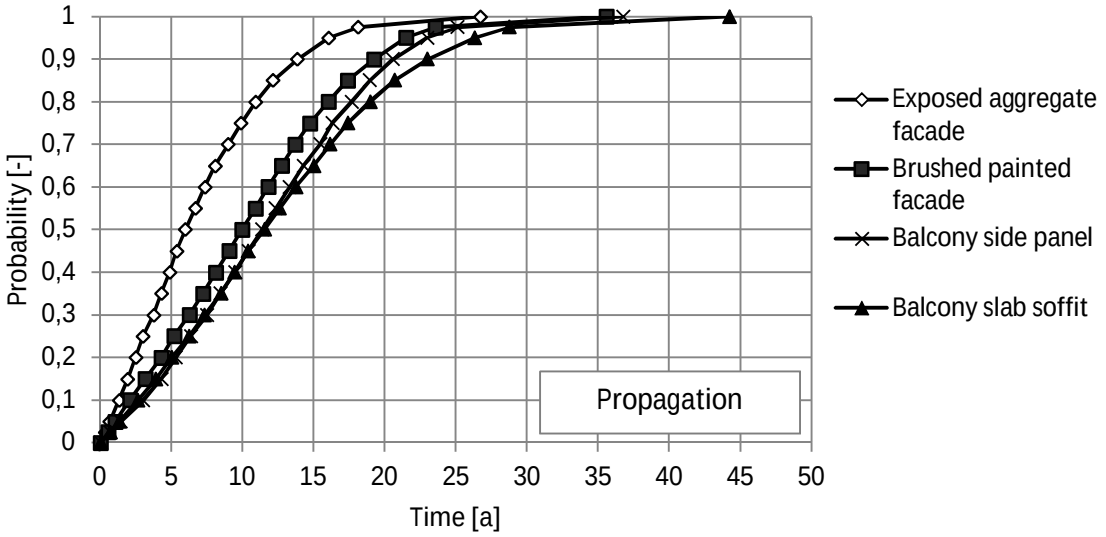

Figure 4.5 The length of the propagation phase in concrete facades and balconies based on a Monte Carlo simulation

Even though corrosion is propagated quite fast in both types of facade surfaces, their initiation phases are quite long. On the other hand, although the balcony slab soffits and balcony side panels have a significantly shorter initiation phase, their propagation phases tend to be longer. It is shown by this statistical comparison that favourable parameters and conditions for the initiation and propagation phases of corrosion tend to counteract to each other. Nevertheless, in service life design, it is still the initiation phase which is the primary measure for assessing a structure's service life.

4.3 The reliability of modelling the initiation phase by carbonation

The carbonation rate of concrete is mainly influenced by factors that affect the diffusion resistance of the material between the outdoor environment and the carbonation zone, as well as the number and type of substances taking part in the carbonation reaction. The factors that inhibit carbonation are: (1) the moisture content of the concrete, (2) the reserve of calcium hydroxide in the cement, (3) the impermeability of the concrete, (4) low CO_2 concentrations in the air, and (5) the outward diffusion of OH in water-saturated concrete (Tuutti 1982). These factors are determined by the properties of the structure and the concrete, and by external environment properties, such as the amount of CO_2 and moisture in the atmosphere.

When assessing the service life of reinforced concrete structures, the square root model (Tuutti 1982) is widely used to predict the initiation of reinforcement corrosion due to carbonation of the concrete cover. This model has also been used in this research project to calculate the duration of both the initiation and propagation phases. The model is based on diffusion laws, and although its validity can be open to question, a recent study (Article III) showed that the square root equation is highly reliable in predicting the propagation of carbonation in actual exposed outdoor structures. This is particularly true when the model is applied to aged concrete structures where the carbonation rate has already stabilized, as it was in this study. In Figs. 4.6 and 4.7 analysis on a relatively small number of parallel samples is compared to larger average data on the same structures.

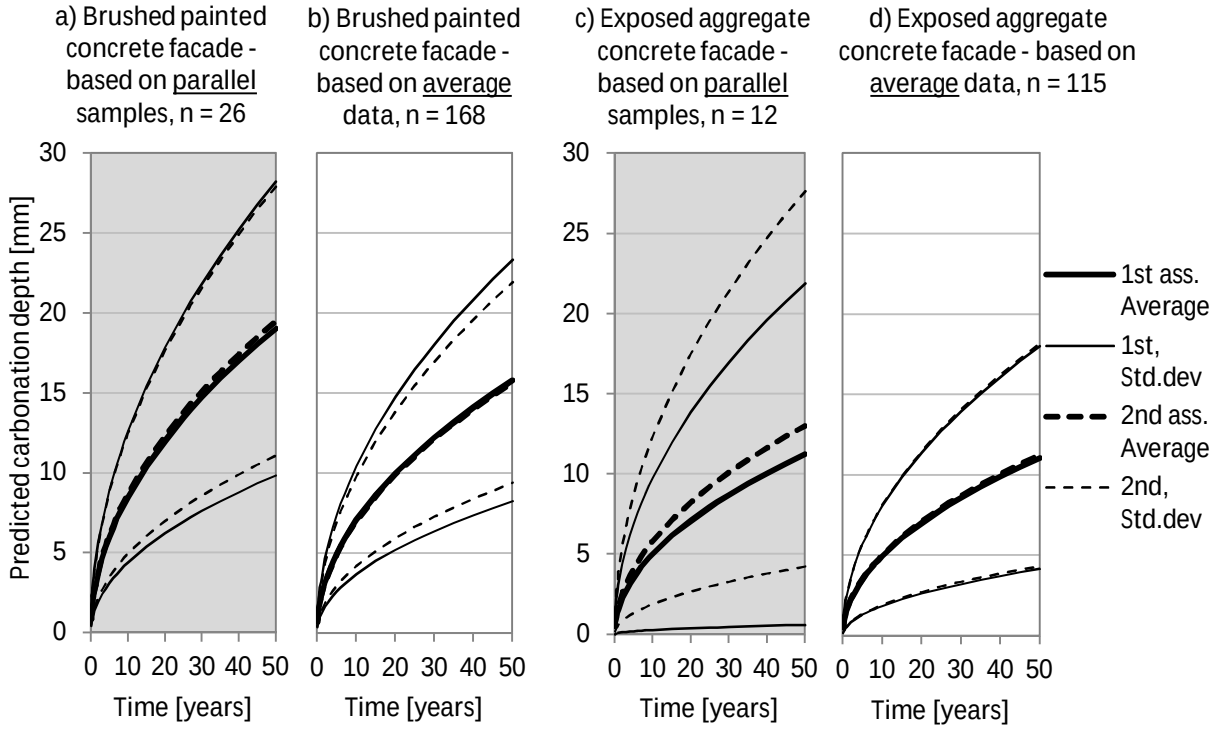

Figure 4.6 Carbonation of brushed and painted and exposed aggregate concrete facades modelled by parallel samples or by average data

The overlapping of the 1st and 2nd assessment curves in Fig. 4.6, above, shows that the square root equation provided a reasonably good fit for the propagation of carbonation in the concrete structures studied here. The predictions based on the first measurements differed from the latter measurements by 0.8–2.4 % in brushed and painted facades and by 1.5–15.8 % in the case of exposed aggregate concrete. The prediction is significantly more accurate when the sample count is high (n > 20 per case). Similar observations can be seen in the carbonation data on balcony structures (Fig. 4.7). Here, the difference in first and latter carbonation predictions was 1.0–11.5 % in the balcony slab soffit surfaces, and 0.7–38.5 % in the balcony side panels.

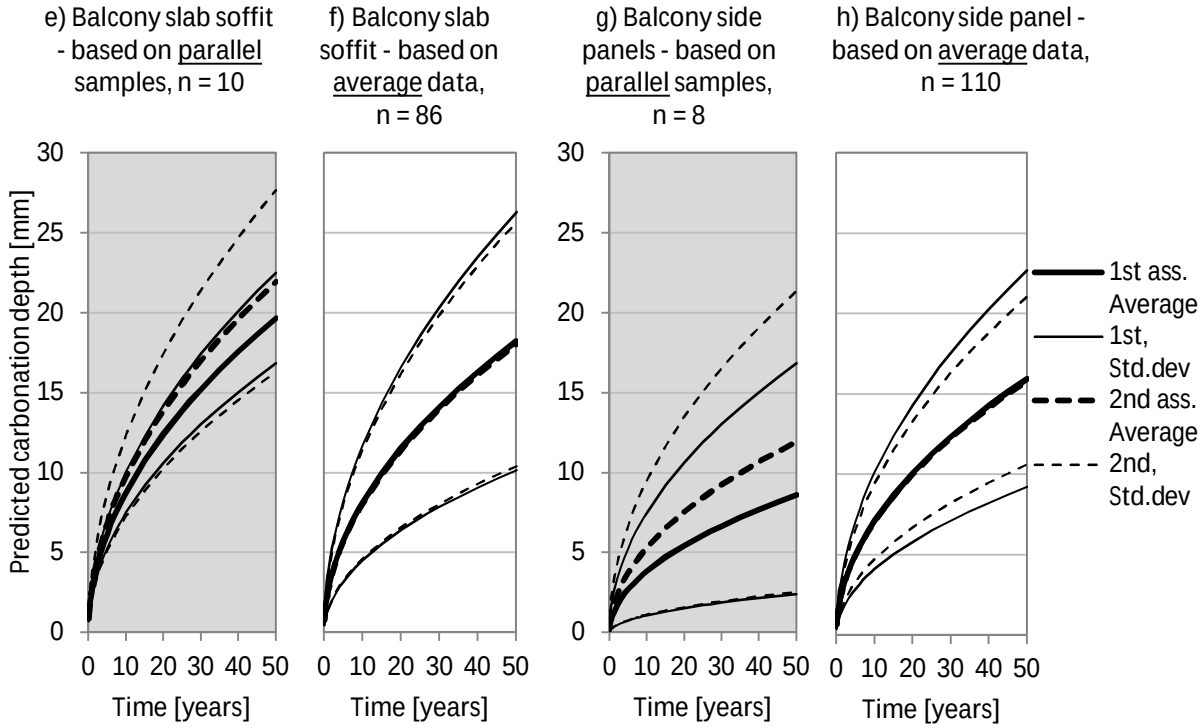

Figure 4.7 Carbonation of balcony side panels and slab soffits modelled by parallel samples or by average data

The type and quantity of cement used have been found to have an influence on the concrete's carbonation resistance and, thus, the rate of carbonation in the concrete. The cement used in most of the structures in this study was Portland cement, but the quantities used were not determined during the condition assessments. However, the type and amount of cement used are considered to have only a minor effect on the conclusions made on the basis of consecutive measurements on the same structures, since they remained unchanged over time. Variations in the amount of cement, along with variations in the composition of the concrete and its porosity, and variations in the mixing, placing and curing of the concrete all have an effect whose influence can be seen in the overall scatter of the carbonation depth. These variations contradict the initial presumption that the concrete is homogenous. The carbonation rate can also vary within a very limited area on the con-

crete surface. Taking all of these factors into consideration, it is clear that any study of the depth of carbonation must be performed on a sufficiently large sample size.

A simplified way of expressing carbonation is to describe it by its square root relationship with exposure time (Eq. 4). Where *x [mm]* is the predicted carbonation depth, *k [mm/year$^{0.5}$]* is the carbonation coefficient and *t* is the exposure time in years.

$$x = k \times \sqrt{t} \tag{4}$$

The carbonation coefficient is used to adjust the model to describe the carbonation of different concretes in different environments. The initiation phase and carbonation coefficients of different concrete facade and balcony surfaces (Table 4.1) were extensively studied by Lahdensivu (2012). The results of this earlier work are referred to here.

Table 4.1 Carbonation coefficients of different concrete facade and balcony surfaces from 1965 - 1989 (Lahdensivu 2012)

structure surface	construction year	average	standard deviation	number of measurements
brushed painted concrete facade	1965–1969	1.93	1.12	148
	1970–1979	2.76	1.16	815
	1980–1989	3.24	1.21	228
exposed aggregate concrete surface	1965–1969	1.40	0.84	143
	1970–1979	2.05	1.26	474
	1980–1989	2.28	1.42	199
balcony slab soffit	1965–1969	2.31	1.44	105
	1970–1979	3.09	1.22	366
	1980–1989	3.37	1.51	271
balcony side panel	1965–1969	2.87	2.01	52
	1970–1979	2.87	1.49	473
	1980–1989	2.51	1.32	268

The initiation of corrosion was determined as a probability curve based on these coefficients and the surface type-specific distributions of reinforcement cover depths. The initiation phase is shown in Fig. 4.4. Of the concrete surfaces studied, corrosion is initiated fastest in the balcony structures, while the aggregate facades were most resilient to carbonation. Regardless of the modelled average initiation, the carbonation of concrete depends on case-specific properties, so average results cannot be straightforwardly applied to individual structures.

4.4 The critical parameters for modelling the propagation phase

The duration of the corrosion propagation phase can be estimated using three parameters: a) the point of corrosion initiation, b) the corrosion rate, and c) the critical extent of the corrosion i.e. the end of service life. Section 3.3, above, discussed carbonation in corrosion initiation, and this chapter will look at the parameters affecting the propagation phase.

4.4.1 The critical extent of corrosion

Material characterization and microscopy studies (Article IV) were used to determine in more detail the extent of corrosion needed to cause visible damage on concrete facade surfaces. The studied concrete structures were, on average, 38.8 years old. The average time under active corrosion for the cracked locations was 26.0 years, and for the spalled locations, 33.1 years. Judging by the statistical data (Fig. 4.5) the corrosion in these structures had been active for a long time. Furthermore, all of the samples revealed that corrosion has been initiated quite fast (on average, 12.6 years) which indicates that the concrete's resistance to carbonation was poor and the environmental conditions were favourable to carbonation.

The SEM analysis confirmed that corrosion products form layers of different compositions around the steel. Based on an EDS analysis, the rust formed on the rebars was divided into two layers, the inner and outer rust layers. The corrosion products also contained veins of high-density rust and veins of what was presumably residue from the concrete pore water. Particles trapped inside the rust were also observed.

The outer layer of rust typically contained less iron and more oxygen than the inner single layers, and various other elements. The inner layer of rust had a higher iron content composed of more pure iron oxides. The particles trapped in the rust were mainly composed of calcium, silicon and oxygen and seem to originate from the calcium-silicate-hydrate (CSH) and the pore water of the concrete. The study suggests that the more porous corrosion products responsible for the largest increase in volume are located on the outer layer, nearer the concrete interface.

The majority of the x-ray diffraction patterns of the corrosion samples revealed mainly Goethite, Feroxyhite and Lepidocrocite corrosion products (Figs. 4.8 and 4.9). These rust types have a relative volume to pure iron (α) of 2.8–3.2 (Marcotte 2001). Some of the non-rust peaks could also be identified as originating from the CSH of concrete. However, more sophisticated methods, such as µRAMAN or Mössbauer spectroscopy, should be used to study the heterogeneity of the rust in more detail. TEM imagery with selected area electron diffraction (SAED) patterns agreed with the XRD results. In addition, the TEM-EDS analyses of the rust powders were similar to the cross-sectional SEM-EDS results.

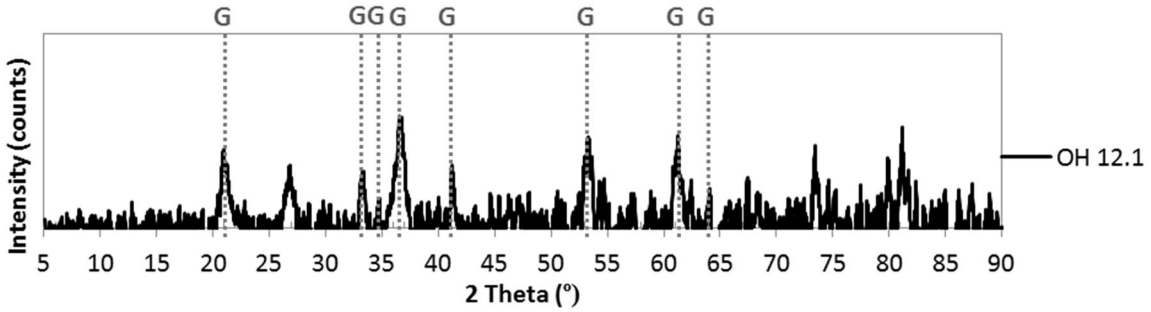

Figure 4.8 XRD pattern of the rust scraped from the sample OH 12.1, dotted lines correspond to Goethite (G)

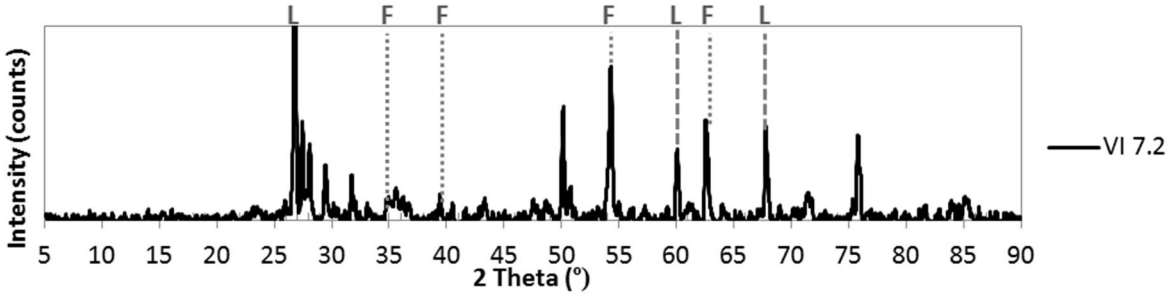

Figure 4.9 XRD pattern of the rust scraped from the sample VI 7.2, dotted lines correspond to Feroxyhite (F) and dashed lines to Lepidocrocite (L)

In the structures studied here, the main reason for the damage appearing as cracking or spalling was the depth of the concrete cover in relation to the rebar diameter, i.e. the cover/diameter ratio. If this ratio was small (below 1.5) corrosion-related damage emerged as spalling. If the ratio was well over 1.5, the damage was more likely to appear as cracking. Because the cover/diameter –ratio between the cracked and spalled samples differed significantly in the research material, determining differences in terms of the thickness of the rust layer is difficult.

The thickness of the rust layers measured in connection with cover cracking was on average 116.1 µm, with a standard deviation of 86.4 µm. In the rust layers measured where spalling had occurred, the average thickness of the rust was 71.9 µm (standard deviation of 56.9 µm). However, the spalling and cracked samples represent different cases. The total scatter in the rust thickness measurements is large (Fig. 4.10) and this has to be taken into account in determining the end of a structure's service life in practice.

In this study, the corrosion products from carbonation-initiated corrosion were mostly hydroxide types of rusts, with a rust volume coefficient $\alpha \approx 3$. This relation has to be taken into account when determining critical corrosion penetration using measured rust-layer thicknesses (division by 3). Taking the determined relative volume of the rust layer into account, the corrosion penetration required to initiate visually observable cracks in the studied facade panels was, on average, 38.7 µm, and the corresponding rust thickness was 116.1 µm. For the purposes of practical design, the scatter in the measurements is taken into account below.

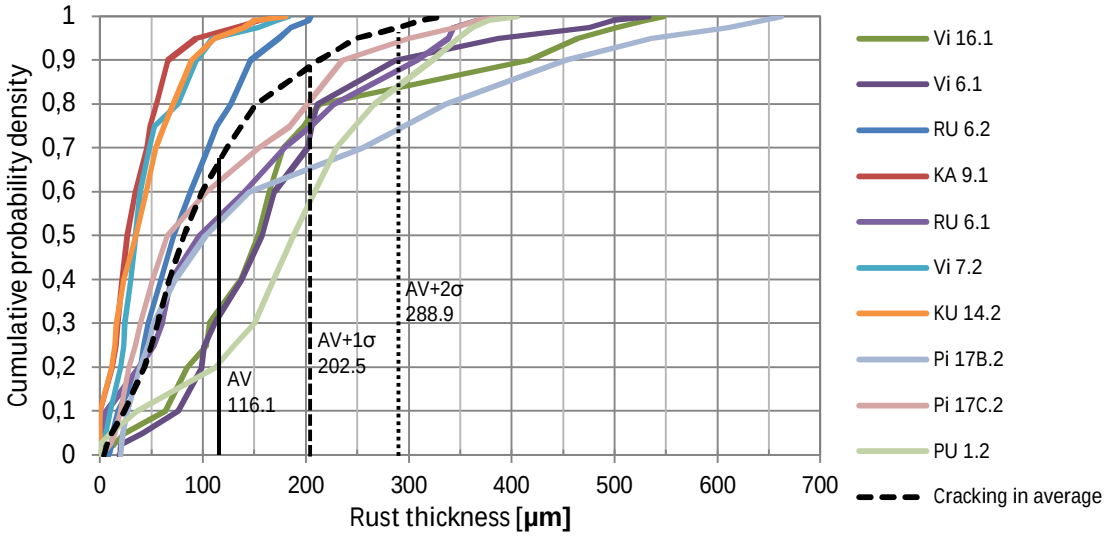

Figure 4.10 Measured rust layer thicknesses on reinforcement samples that have caused cracking of concrete cover (Average-curve, min = 4 µm, average = 116 µm, max = 332 µm)

The scatter can be taken into account by adding a deviation threshold for the scatter to the average value. In typical cases, a threshold of one standard deviation (1σ) can be used (Fig. 4.10). This will give a critical rust layer thickness of 202.5 µm for cover cracking (ranging 66.6–357.3 µm). This is equivalent to 67.5 µm in corrosion penetration (ranging 22.2–119.1 µm). This total corrosion penetration statistic is well in line with earlier literature (Table 4.2) and can be utilized in service life calculations for similar structures in which visible damage has emerged.

Table 3.2 Critical corrosion penetration regarding concrete cover cracking

Source	Critical corrosion penetration in regard of concrete cracking [µm]		
	min	design value	max
Current study	22.2	67.5	119.1
Alonso et al. 1998	15		50
Siemes et al. 1985		80	
Broomfield 2007		100	

4.4.2 Corrosion rate

The corrosion rate was determined to be the combined effect of the weather parameters on already carbonated concrete structures exposed to the outdoor environment. A set of long-term corrosion rate data from 2 locations was combined with weather data from the same locations for the same time period. Besides being somewhat scattered, the corrosion current densities are in general rather high (Fig. 4.11). However, the initial assumption that the corrosion rates would be higher

on the site located in the coastal region was not confirmed by the measurements, certainly not over the period in question, anyway. In fact, the inland structures faced 47 % more wind-driven rain than those on the coast, and their corrosion rates were 11–18 % higher. This highlights the importance of taking both the geographical position and the micro climate around the building into consideration when assessing the degradation rate. On the bottom surfaces of the balcony slabs, the corrosion rates are clearly much lower than in the other, environmentally-exposed parts. This clearly indicates that structures which are sheltered from wetting do not corrode as fast as those which are exposed to the weather.

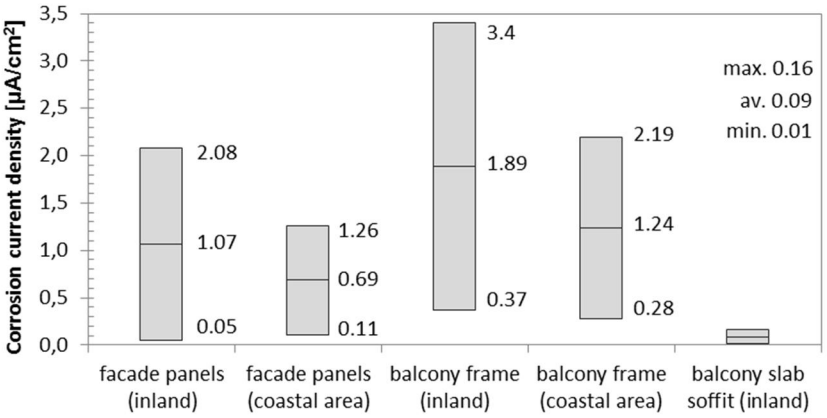

Figure 4.11 Monthly average corrosion current densities recorded in field measurements in an inland area and a coastal area in Finland

The measured corrosion current densities were compared with the four weather parameters recorded from the same time period for each area. These were temperature (T, ºC), relative humidity (RH, %), wind-driven rain (I_{WA}, mm) and solar radiation (RAD, kJ/m^2). All weather parameters but the solar radiation could be recorded close to the building site (from the distance of 12-15 km). The solar radiation is recorded only in limited number of stations in Finland thereby the longest distance to site was 79 km. The distance and differences on the building site are in calculation methods such as the wind-driven rain calculation taken into account with dedicated factors and coefficients. As a practical application the level of detail is sufficient for service life design, but for a more detailed research this have to be acknowledged as a possible error source.

The wind-driven rain was the only weather parameter that showed high seasonal variability, although most of the rain still falls in the autumn (Fig. 4.12). The curves for the wind-driven rain and the corrosion rates do match each other quite well. However, this alone will not explain all of the changes in the corrosion rates observed in the Inland site data. For example, at the inland site, in Tampere, the correlation between the WDR and the corrosion rate was lower in June of the second summer. This coincides with an exceptional rain event which occurred in the area at the time 6-7/2002. Something exceptional also seems to have occurred at the coastal site in month 4, 2001. Here, there is a rise in the corrosion rate, which is not mirrored in the WDR curve.

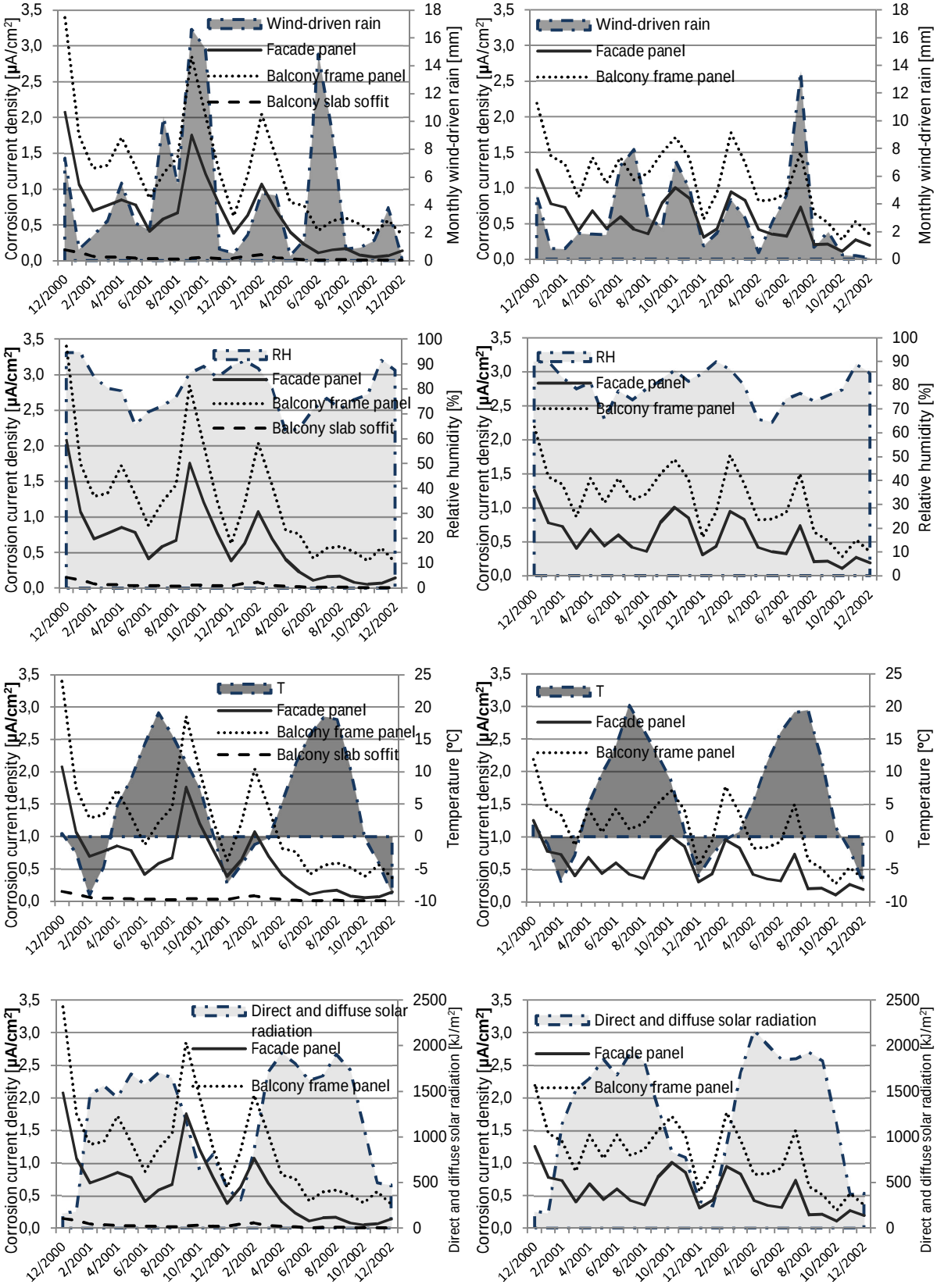

Figure 4.12 Corrosion rate contrasted to the monthly wind-driven rainfall (I_{WA}), outdoor air relative humidity (RH), outdoor air temperature (T) and solar radiation (RAD) for the inland site (left) and the coastal site (right)

The feasibility of using weather parameters to assess corrosion rates was extensively tested with regression analysis. However, a preliminary analysis of all the weather and corrosion data over the whole time period (25 months) indicates that the representativeness of single weather parameters is fairly low. The representativeness of the weather data can, however, be increased if it is analyzed seasonally.

The regression model was formed on the basis of linear regressions between the weather parameters and the corrosion rate. From a relatively large number of analyses (525 analyses with different combinations of weather parameters, seasons, etc.) the best performing combinations were judged by the coefficient of determination (R^2) of the model. Initially, separate models were produced for the facades and balconies in both the inland and the coastal areas. However, in cross-checking the models' functionality (by using the coastal area model inland and vice versa) the models were found to have a fairly good fit (R^2 of 0.49–0.53). (Fig. 4.13).

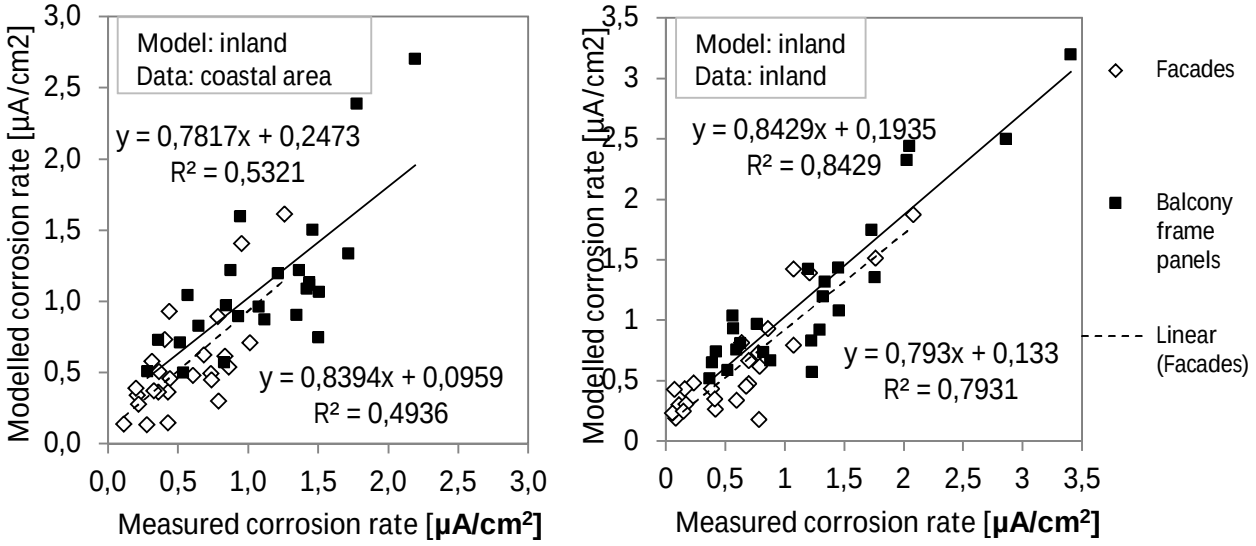

Figure 4.13 The correlation between the model generated from the inland data and the measured corrosion rate in both the inland and the coastal area

Finally, a composite model was produced utilising the spring, autumn and winter seasons from the inland data and the summer season from the coastal data (Table 4.3). This allowed a slightly better fit for both geographical locations (the R^2 for inland was 0.71 and for the coastal area, 0.55). A similar analysis was carried out also with inland balcony slab soffits, although there was no comparative data from the coastal area. The model was composed of linear relationship equations (Eq. 5) for every season, utilizing the monthly average weather parameters of T, RH, I_{WA} and RAD. The choice of parameters was made by optimizing the parameter composition in regard of the total correlation to the corrosion rate (the coefficient of determination) as well as choosing a composition of parameters where the effect of single weather parameters is of the suitable form (negative/positive).

$$y = b_0 + b_1 \times x_1 + \left(b_2 \times x_2 + b_3 \times x_3 + b_4 \times x_4\right) + n \quad (5)$$

where y = the dependent variable (corrosion current density); β_0 = interception term; β_1, x_1 = coefficient and parameter of the first weather parameter; β_2, x_2 = coefficient and parameter of the second weather parameter (optional); β_3, x_3 = coefficient and parameter of the third weather parameter (optional); β_4, x_4 = coefficient and parameter of the fourth weather parameter (optional); and v = error term. The weather parameters for the monthly weather data can be found in Table 4.3.

Table 4.3 Regression models for the reinforcement in facade panels (with heat flux) and the balcony frame panels (cold structures). The coefficients should be used together with monthly weather data

Season	Parameter	Coefficient, facades	Coefficient, balcony frames	Coefficient, balcony slab soffits
Spring	β_1, (T)	-	-	-0.0028
	β_2, (RH)	-	-	-0.0019
	β_3, (I_{WA})	0.0348	0.1260	0.0088
	β_4, (RAD)	-0.0008	-0.0007	
	β_0 (intercept)	1.9127	2.0909	0.1597
Summer	β_1, (T)	-	-	-0.0009
	β_2, (RH)	0.0107	0.0650	-0.0002
	β_3, (I_{WA})	0.0369	0.0470	-0.0006
	β_4, (RAD)	-0.0006	-0.0007	
	β_0 (intercept)	0.5620	-2.7485	0.0557
Autumn	β_1, (T)	-	-	0.0013
	β_2, (RH)	-	-	0.0012
	β_3, (I_{WA})	0.0842	0.1219	0.0008
	β_4, (RAD)	-	-	
	β_0 (intercept)	0.1121	0.4723	-0.0887
Winter	β_1, (T)	0.0682	0.1014	0.0017
	β_2, (RH)	-	-	0.0065
	β_3, (I_{WA})	0.1340	0.2349	0.0088
	β_4, (RAD)	-	-	
	β_0 (intercept)	0.8572	1.4196	-0.5239

The above-mentioned coefficients are optimized for use with monthly averaged weather data to enable corrosion service life design in practical cases.

4.5 Modelling the combined service life of initiation and propagation

As the statistical analysis presented in Chapter 4.2 shows, approximately 80 % of the service life of concrete is accounted for in the initiation phase, although there are slight differences between different structure surfaces. (Table 4.4). Therefore, when assessing the total service life of a building, it is critical to ensure the structures have the required resilience to carbonation in terms of concrete composition, concrete quality and cover depths. If the properties of the initiation phase are already fixed (as is the case in existing structures) it seems clear that accurate information about the propagation phase will have to be utilized to extend a structure's service life.

Table 4.4 The relationship of initiation and propagation phases in concrete facade panels (av. in brackets)

structure surface	share of the initiation phase in the total service life, average in parenthesis (%)	share of the propagation phase in the total service life (%)
brushed painted concrete facade	85–98 (88)	2–15 (12)
exposed aggregate concrete surface	91–99 (94)	1–9 (6)
balcony slab soffit	66–94 (72)	6–33 (28)
balcony side panel	72–99 (80)	1–28 (20)

It appears, from Table 4.4, that the balcony slab soffits have the greatest potential for extending a structure's service life with the propagation phase (28 %). Although all of the studied structure surfaces show some potential for service-life extension, the exposed aggregate surface only has a potential of (6 %) for extension. This is due to their already quite high resistance to carbonation, which in turn accounts for their fairly long initiation phase. The exposed aggregate surface is also fairly open to moisture penetration from wind-driven rain, which also keeps conditions favourable to corrosion for longer time periods.

According to the standard, EN-206, structures such as balcony slab soffits, which are sheltered from rain, fall into the exposure class XC3. The (more weather-exposed) facades fall into the exposure class XC4. In service life design, it should be recognized that the exposure of XC3 class structures can be much more severe in terms of carbonation than it is for XC4 class structures. If the scope of the service life is widened to encompass corrosion propagation, the conditions of the XC4 class structures are more likely to induce corrosion than those of the XC3 class. This means that when using carbonation resistance to assess a structure's service-life, the XC3 class requires higher attention than the preceding class. However, when the initiation and propagation phases are combined, the relationship may be the other way around. Generally, in Finland, this fact has not

been given enough weight when specifying the concrete and cover depths for each class. It is only when defining the target service life of the structure, that the final decisions about how these classes should be treated and related to each other are made (Fig. 4.14).

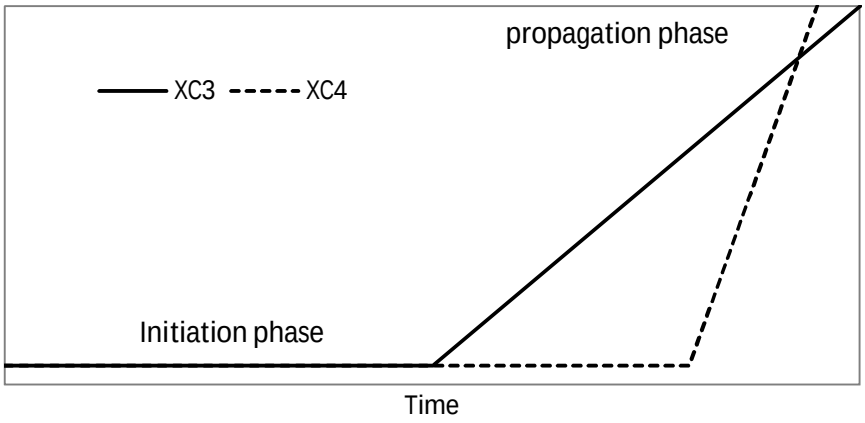

Figure 4.14 The relationship between XC3 and XC4 exposure classes in regard of initiation and propagation phases of corrosion (schematic)

The duration of the initiation phase should always be modelled using case-specific data for both the carbonation coefficient and the depth distribution of the concrete reinforcement cover. The carbonation coefficients presented in Table 4.1 can only be used for describing the general situation among a group of buildings. The generalized initiation phase is illustrated in Fig. 4.4.

Long term corrosion rates were estimated using the model proposed in chapter 3.4.3 on north and south facing facades and balconies in different geographical locations in Finland. The yearly corrosion penetration was calculated using Faraday's law of electrolysis based on the modelled corrosion rates. Both values representing the rate of corrosion are presented in Table 4.5. The average duration of the corrosion propagation phase in varying geographical locations is given by utilizing the critical corrosion penetration of 67.5 µm for concrete facades and balconies (as obtained in chapter 4.4.1).

The deduced durations of the propagation phase in different geographical locations clearly illustrate the effects of changes in climate. The weather in Northern Finland can be characterized as being drier and less windy than the weather in coastal Finland. The model can be also utilized in predicting the corrosion behaviour of these structures in changing climates with simulated weather data sets. The assumption is that corrosion will become more aggressive under higher wind velocities and rainfall, as these both result in higher moisture exposure for the facades.

Table 4.5 Modelled Corrosion rates (µA/cm^2) in facades and balconies with varying geographical locations in Finland averaged over weather data from 1979–2009 with the corresponding corrosion penetration (µm/year) in parenthesis. The corresponding length of the initiation phase (years) is presented in [square brackets] to a corrosion penetration limit of 67.5 µm

	XC4				XC3
	North facing facade	South facing facade	North facing balcony side panel	South facing balcony side panel	Balcony slab soffit
Helsinki-Vantaa (South coastal Finland)	1.00 (11.6) [5.8]	1.83 (21.2) [3.2]	1.51 (17.5) [3.8]	2.98 (34.6) [2.0]	0.07 (0.85) [79.8]
Jokioinen (Southern Finland)	0.97 (11.2) [6.0]	1.43 (16.5) [4.1]	1.46 (16.9) [4.0]	2.31 (26.8) [2.5]	0.06 (0.68) [99.8]
Jyväskylä (Mid-Finland)	0.86 (9.9) [6.8]	1.07 (12.4) [5.4]	1.33 (15.4) [4.4]	1.74 (20.2) [3.3]	0.04 (0.51) [133]
Sodankylä (Northern Finland)	0.72 (8.4) [8.0]	0.81 (9.4) [7.2]	1.08 (12.5) [5.4]	1.26 (14.7) [4.6]	0.03 (0.34) [200]

The following Figures (4.15 and 4.16) illustrate the service life of the facades and balconies when the initiation and propagation phases are combined, while Fig. 4.17 illustrates the same process applied to the soffit surface of a balcony slab. Both the monthly corrosion rates (left) and the cumulative corrosion penetration (right) are shown. The figures show that even though the corrosion rate is in the short term, highly dependent on the weather parameters, it is fairly steady when viewed over a longer time scale. As long as this is understood, the values in Table 4.5 seem appropriate for practical design. The study of future weather trends. however, requires the use of corrosion rates based on the weather data for each individual case.

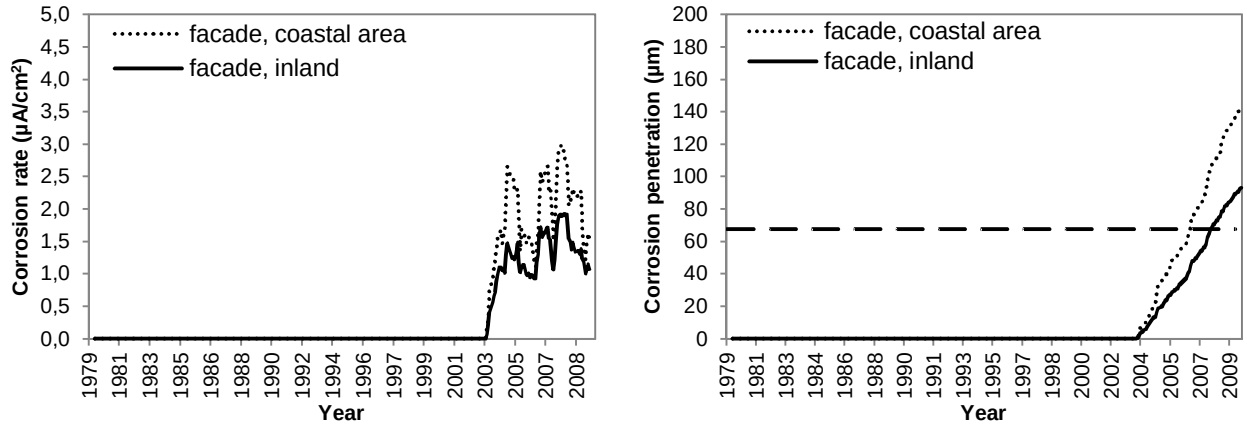

Figure 4.15 The modelled service life of concrete facades by combined initiation and propagation. The horizontal dashed line represents the occurrence of visible corrosion damage on the structure

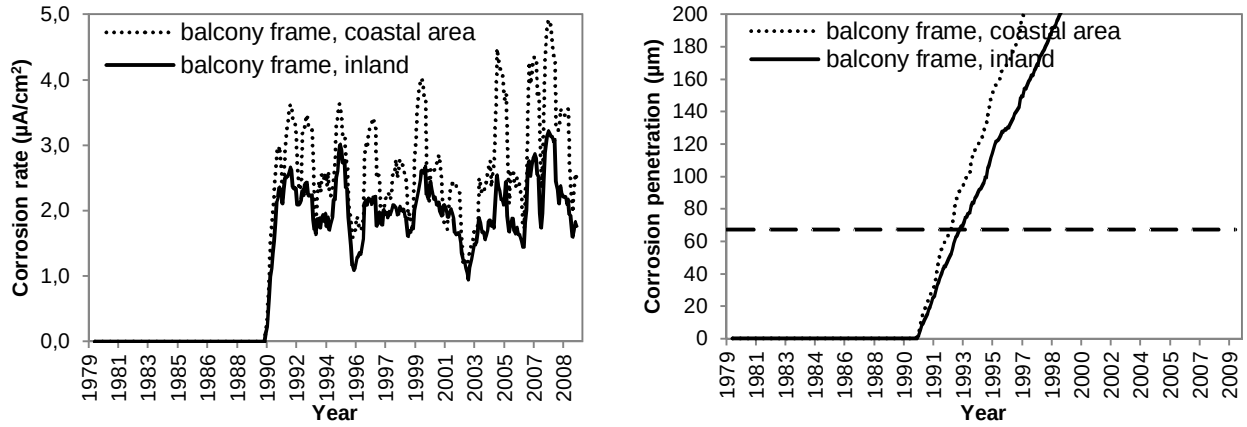

Figure 4.16 The modelled service life of concrete balcony frames (vertical structure) by combined initiation and propagation. The horizontal dashed line represents the occurrence of visible corrosion damage on the structure

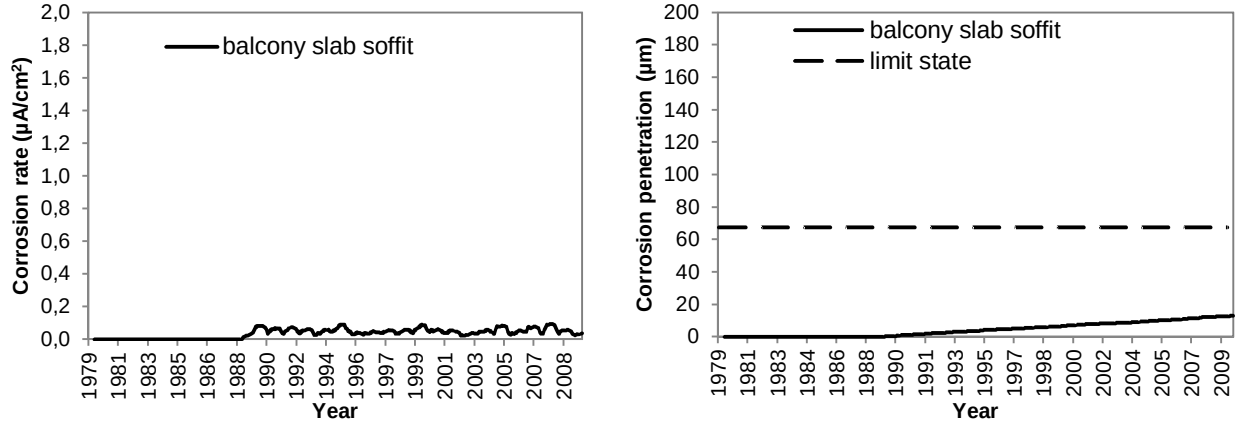

Figure 4.17 The modelled service life of concrete balcony slab soffits by combined initiation and propagation. The horizontal dashed line represents the occurrence of visual corrosion damage on the structure. Note the different Y-scale on the left figure.

In the cases studied here, visible damage appears on the structure surfaces before the common modern service-life requirement of 50 years. On facades, such damage occurs within approximately 28 years, while on balcony frames it can occur after only 13 years. In terms of practical design, the corrosion rate on these structures would have to be lowered by remedial work, such as rainwater control, recoating, or providing shelter from the elements in order to achieve the expected service life of 50 years.

In contrast, the soffit surface of the balcony slab, which belongs to the exposure class XC3, will easily achieve a service life of 50 years because the corrosion rate during the propagation phase is low. Corrosion is initiated fast by the carbonation of the concrete, but the corrosion rate is kept low due to the soffits' sheltered position in the structure. The remedial actions for the soffit surfaces should therefore include adequate rainwater control and waterproofing to maintain their dry conditions.

5 Conclusions

5.1 The outcomes of the research

The research project confirmed that the active corrosion phase can provide a considerable extension to the service life of concrete facade panels in a Nordic climate. Our statistical analyses show that the length of this period can be from a few to up to 30 years. A more in-depth analysis of the case-study buildings, however, showed that the service-life extension for XC4 exposure conditions is, in practice, likely to be limited to below ten years. It has to be noted that the limit is based on the occurrence of visible corrosion damage on the structure surfaces. Even this is therefore not the ultimate end of service life for these structures.

The occurrence of visible damage is a natural way of judging the service life of these structures, since all of the renovation and maintenance decisions are made after inspections which are usually commissioned after these visible warning signs have appeared. In the structures studied for this research, corrosion-induced damage commonly occurred on the lap splicing locations of rebars, in the edges and window openings of the panels, and in locations with a pronounced moisture load, often due to poorly functioning flashings and inadequate rainwater run-off control. If the ratio of concrete cover to reinforcement diameter was low (below 1.5),the corrosion-related damage emerged as spalling, but if the ratio was well over 1.5, the damage was more likely to emerge as cracking.

One of the objectives of the research was to determine critical parameters for the active corrosion phase, in particular, which can be used in service-life design. These factors included the critical corrosion penetration, visible damage and the corrosion rate. After the initiation phase, the general corrosion rate for these structures can be regarded as high. Thus, the average extension to service life during the active corrosion phase may only be 1–6 years, in the most severe cases. This figure may not appear to be very impressive, but this is for south-facing structures, subject to the most severe

weather. In structures which, for a variety of reasons, are more sheltered from wind-driven rain, the extension in service life can be considerably higher. This is especially true for sheltered structural surfaces, such as the soffit surfaces of the balcony slabs.

This thesis showed that the propagation phase can be modelled. We have proposed a simple, linear, active-corrosion-phase tool for modelling the onset of visible damage on concrete surfaces, This is defined by the onset by carbonation, an angle coefficient of the corrosion rate and a defined limit state. The dependence of the corrosion rate on the outdoor environment parameters was modelled as a variable which changed constantly over time. A limit state for pre-visible-damage corrosion, i.e. critical corrosion penetration was proposed for thin concrete facade panels. This is highly dependent on the reinforcement cover/diameter ratio and the corrosion environment. This model can also be utilized to study the effects of varying climate conditions on the corrosion propagation.

The ability to model or forecast corrosion rates on concrete facades will enhance the ability of property owners to react to their upcoming repair needs. This kind of model is able to predict the residual service life of a certain structure, but it could also be used in creating renovation strategies for larger ranges of building stock by revealing the order of importance or the urgency of individual renovation projects. Such a tool can thereby be used in moving towards more predictive strategies for the maintenance of real estate, giving landlords the confidence to make long-term contracts with renovation engineers and contractors.

5.2 The need for further research

Based on the work carried out for this thesis, the main avenues for future research are:

The corrosion rates on concrete structures with different surface treatments and concrete compositions

This thesis has focused on the active corrosion on brush-treated painted concrete facades and balcony structures. The reinforcement corrosion is, however, highly affected by both the concrete composition and the surface treatment of the structure. The cement type in this study was CEM I, but the effect of blended cements should be investigated as well.

Refining of the influencing factors on the weather exposure of facades

The weather exposure of building facades depends on features in the geographical location, such as shelter from the prevailing winds, or obstructions from nearby vegeta-

tion, and on the detailing of the facade. These factors are further divided into multiple parameters. The developed model could be used together with exposure models (such as the wind-driven rain calculation) in verifying the optimal obstruction and sheltering solutions for different geographical locations. The research would lead to a better understanding of the differences between exposure classes XC3 and XC4.

Studying the effect of climate change on corrosion propagation

Anticipated climate change will impose further challenges on the maintenance and renovation of concrete facades, as well as the construction of new ones. The proposed corrosion rate model could be used in climate change adaptation research simply by substituting the simulated future weather data.

Studying the combined effects of degradation phenomena on the service life of facades

In practice, concrete facades are not degraded by reinforcement corrosion alone but also by various degradation mechanisms (such as freeze-thaw action) resulting from environmental stresses. In order to design the service life of concrete holistically, the influence these phenomena have on reinforcement corrosion should be analysed. The work should be undertaken in two phases: first, developing service life models for other degradation mechanisms and, second, interconnecting them with corrosion. Time-series weather data could provide an avenue for the interconnection.

Correlating accelerated durability tests with real observed degradation

The testing of the durability properties of building materials in laboratory environment is in majority based on accelerated weathering tests conducted in accordance with specification given in standards. The comparison of the test results to actual natural degradation is, however, extremely complicated. With an abundance of proposed models available, active work on testing and verifying the proposed models with statistical data on real observed degradation is acutely needed.

References

1. Ahmad, S. 2003. Reinforcement corrosion in concrete structures, its monitoring and service life prediction – a review. Cement & Concrete Composites 25:459-471.

2. Alonso, C., Andrade, C., Rodriguez, J., Diez, J.M. 1998. Factors controlling cracking of concrete affected by reinforcement corrosion. Materials and Structures. Vol. 31. Pp. 435–441

3. Andrade C. 2003. Measurement of Polarization Resistance On-site in: Corrosion of Steel in Reinforced Concrete Structures. Final report of COST action 521, Office for Official Publications of the European Communities, Luxembourg. Pp. 82–98.

4. Bažant, Z.P. 1979. Physical model for steel corrosion in concrete sea structures—theory. J. of the Engrg. Mech. Div., Proc. ASCE, 105, Pp. 1137–1153.

5. BES – Development of open concrete element system, Research report. 1969. Suomen Betoniteollisuuden Keskusjärjestö ry (in Finnish).

6. Broomfield, J. 2007. Corrosion of steel in concrete. 2nd ed. Oxon: Taylor & Francis.

7. Building industry association. 2014. Tilastot ja suhdanteet, kuviopankki. available, 4.1.2016 https://www.rakennusteollisuus.fi/Tietoa-alasta/Talous-tilastot-ja-suhdanteet/ (in Finnish)

8. BY50. 2004. Concrete code 2004. Helsinki, The Concrete Association of Finland. (in Finnish).

9. BY50. 2012. Concrete code 2012. Helsinki, The Concrete Association of Finland. (in Finnish).

10. DuraCrete project. 2000. Probabilistic performance based durability design of concrete structures. The European union – Brite EuRam III, DuraCrete. Final technical report of DuraCrete project, document BE95-1347/R17. CUR, Gouda, Nederland.

11. Fasullo, E. 1992. Infrastructure: the Battlefield of Corrosion, ASTM STP 1137.

12. fib Bulletin No.34. 2006. Model Code for Service Life Design. International Federation for Structural Concrete, Lausanne.

13. Grantham, M. (editor) 2011. Concrete repair – A practical guide. New York, Taylor & Francis. 302 p.

14. Goltermann, P. 1994. Mechanical predictions on concrete deterioration. Part 1: Eigenstresses in concrete. ACI Materials Journal 91(6):543–50.

15. Gulikers, J., Raupach, M. 2006. Numerical models for the propagation period of reinforcement corrosion: comparison of a case study calculated by different researchers. Materials and Corrosion 57(8):618–27.

16. Huet, B., L'hostis, V., Santarini, G., Feron, D., Idrissi, H. 2007. Steel corrosion in concrete: Determinist modeling of cathodic reaction as a function of water saturation degree. Corrosion Science, 49(4):1918–1932.

17. Huopainen, J. 1997. Carbonation of Concrete Facades - a Field Study (MSc thesis), Tampere University of Technology. (in Finnish).

18. Huuhka, S., Kaasalainen, T., Hakanen, J.H., Lahdensivu J. 2015. Reusing concrete panels from buildings for building: Potential in Finnish 1970s mass housing. Resources, Conservation and Recycling, Volume 101, August 2015, Pp. 105–121.

19. Hytönen, A., Seppänen, M. 2009. Tehdään elementeistä – suomalaisen betonielementtirakentamisen historia (Let’s prefabricate it). Suomen rakennusmedia. 332 p. (in Finnish)

20. Hyvert, N., Sellier, A., Duprat, F., Rougeau, P., Francisco, P. 2010. Dependency of C-S-H carbonation rate on CO2 pressure to explain transition from accelerated test to natural carbonation. Cement and Concrete Research 40:1582-1589.

21. Jaffer, S.J., Hansson, C.M. 2009. Chloride-induced corrosion products of steel in cracked.concrete subjected to different loading conditions. Cement and Concrete Research 39:116–125.

22. Kottek, M., Grieser, J., Beck, C., Rudolf, B., Rubel, F. 2006. World Map of the Köppen-Geiger climate classification updated. Meteorologische Zeitschrift, 15(3):259–263.

23. Köliö, A. 2011. Degradation induced repair need of concrete facades. MSc thesis. Tampere University of Technology. 74p. (in Finnish).

24. Lahdensivu, J. 2012. Durability properties and actual deterioration of Finnish concrete facades and balconies. Tampere University of Technology, TUT Publ. 1028. 117p.

25. Li, C.Q. 2004. Reliability service life prediction of corrosion affected concrete structures. ASCE J Struct. Eng. 130(10):1570–7.

26. Liu, Y., Weyers, R.E. 1998. Modelling the time-to-corrosion cracking in chloride contaminated reinforced concrete structures. ACI Materials Journal 95(6):675–81.

27. Lollini, F., Redaelli, E., Bertolini, L. 2012. Analysis of the parameters affecting probabilistic predictions of initiation time for carbonation-induced corrosion of reinforced concrete structures. Materials and Corrosion 2012;63(12):1059–68.

28. Marcotte, T.D. 2001. Characterization of chloride-induced corrosion products that form in steel-reinforced cementitious materials, PhD thesis in Mechanical Engineering. University of Waterloo, Waterloo, Canada. 330 p.

29. Marcotte, T. D., Hansson, C. M. 2007. Corrosion products that form on steel within cement paste. Materials and Structures 40:325–340.

30. Mattila, J. 2003. On the durability of cement-based patch repairs on Finnish concrete facades and balconies. Tampere University of technology, TUT Publ. 450, 111 p.

31. Monteiro, I., Branco, F.A., de Brito, J., Neves R. 2012. Statistical analysis of the carbonation coefficient in open air concrete structures, Construction and Building Materials 29 263-269.

32. Neves, R., Branco, F. A., de Brito, J. 2012. A method for the use of accelerated carbonation tests in durability design. Construction and Building Materials 36:585-591

33. Otieno, M., Beushausen, H., Alexander, M. 2011. Modelling corrosion propagation in reinforced concrete structures – a critical review. Cement & Concrete Composites 33:240–5.

34. Otieno, M., Beushausen, H., Alexander, M. 2012. Prediction of corrosion rate in reinforced concrete structures – a critical review and preliminary results. Materials and Corrosion 63(9):777-790.

35. OSF. 2015. Official statistics, Buildings and free-time residences. Statistics Finland. available 4.1.2016: http://www.tilastokeskus.fi/til/rakke/tau_en.html

36. Page, C.L. 1988. Basic principles of corrosion. In: Schiessl P, editor. Corrosion of steel in concrete. London: Chapman and Hall. Pp. 3–21.

37. Parrott, L.J. 1987. A Review of Carbonation in Reinforced Concrete, Cement and Concrete Association, Slough, UK.

38. Parrott, LJ. 1994. Design for avoiding damage due to carbonation-induced corrosion, in Proceedings of Third International Conference on Durability of Concrete, Nice, Special Publication SP-145, American Concrete Institute, Pp. 283-298.

39. Pentti, M., Mattila, J., Wahlman, J. 1998. Repair of concrete facades and balconies, part I: structures, degradation and condition investigation. Tampere, Tampere University of Technology, Structural Engineering. Publication 87. 157 p. (In Finnish)

40. ROTI. 2015. Rakennetun omaisuuden tila –raportti (State of the built environment –report). available, 4.1.2016 http://www.roti.fi (in Finnish)

41. ROTI. 2013. Rakennetun omaisuuden tila –raportti (State of the built environment –report). available, 4.1.2016 http://www.roti.fi (in Finnish)

42. ROTI. 2011. Rakennetun omaisuuden tila –raportti (State of the built environment –report). available, 4.1.2016 http://www.roti.fi (in Finnish)

43. Scott, A. N. 2004. The influence of binder type and cracking on reinforcing steel corrosion in concrete. PhD Thesis, Department of Civil Engineering, University of Cape Town.

44. SFS 4475. 1988. Concrete. Durability. Freeze-thaw resistance.

45. SFS-EN 14630. 2007. Products and systems for the protection and repair of concrete structures. Test methods. Determination of carbonation depth in hardened concrete by the phenolphthalein method.

46. SFS-EN 206. 2013. Concrete. Specification, performance, production and conformity.

47. Siemes, A.J.M., Vrouwenvelder, A.C.W.M., van den Beukel, A. 1985. Durability of buildings: a reliability analysis. Heron 30(3):3–48.

48. Suda, K., Misra, S., Motohashi, K. 1993. Corrosion products of reinforcing bars embedded in concrete. Corrosion Science 35(5-8):1543–1549.

49. Thiery, M., Villain, G., Dangla, P., Platret, G. 2007. Investigation of the carbonation front shape on cementitious materials: Effects of the chemical kinetics. Cement and Concrete Research 37:1047-1058.

50. Tilly, G. 2011. Durability of Concrete Repairs, in Grantham, M. Concrete Repair - a Practical Guide, Taylor & Francis, New York. Pp. 231–247.

51. Tuutti, K. 1982. Corrosion of steel in concrete. Stockholm. Swedish Cement and Concrete Research Institute. CBI Res 1982;4(82):304.

52. Wallbank, E. 1989. The Performance of Concrete Bridges: a Survey of 200 Highway Bridges, HMSO Publication, London.

ORIGINAL PAPERS

I

DURABILITY DEMANDS RELATED TO CARBONATION INDUCED CORROSION FOR FINNISH CONCRETE BUILDINGS IN CHANGING CLIMATE

by

Köliö A., Pakkala T.A, Lahdensivu J. & Kiviste M., Mar 2014

Engineering Structures vol 62-63, 42-52

http://dx.doi.org/10.1016/j.engstruct.2014.01.032

Engineering Structures 62–63 (2014) 42–52

Contents lists available at ScienceDirect

Engineering Structures

journal homepage: www.elsevier.com/locate/engstruct

Durability demands related to carbonation induced corrosion for Finnish concrete buildings in changing climate

Arto Köliö *, Toni A. Pakkala, Jukka Lahdensivu, Mihkel Kiviste

Tampere University of Technology, P.O. Box 600, FI-33101 Tampere, Finland

ARTICLE INFO

Article history:
Received 24 June 2013
Revised 17 December 2013
Accepted 20 January 2014

Keywords:
Concrete structure
Corrosion
Carbonation
Durability
Climate change
Modelling
Service life

ABSTRACT

The study is based on durability properties of concrete collected in condition assessments and climate change prediction. According to the prediction facades will face more driving rain in the future because of increasing precipitation and windiness. Outdoor circumstances in southern Finland will ease remarkably already 2030. Initiation by carbonation dominates service life of facades because active corrosion phase is only 5–8 years for surfaces exposed to rain. However, sheltered location will remarkably lengthen active corrosion. Properties that influence initiation time are highly important in ensuring eligible service life of the structure. Present requirements are enough also in the future climate but the required cover must always be achieved.

1. Introduction

During their service life new buildings are going to face more rapidly changing climate than before. The structures in the future have to be durable enough to cut unnecessarily frequent repairs that are not part of their maintenance plan. This does not only promote sustainable development but is also cost effective property management. Even today there are known cases where durability properties have not been met which indicates that the importance of durability design in construction and repair projects has not yet been fully recognized.

Climate change itself has been studied worldwide for a long time. In this context, climate change is referred to as a global-scale warming caused by an increase in greenhouse gases, especially carbon dioxide (CO_2). Climate change will affect the geographical and seasonal distribution of precipitation, wind conditions, cloudiness, air humidity and solar radiation. Modelling of future climate is based on alternative scenarios of greenhouse gas and aerosol particle emissions. In the scenarios, different assumptions are made about the future development of population growth, economic development, energy production modes, etc. The impact of climate change on the performance of structures is becoming an important research issue from an engineering point of view.

The future of European construction industry (under Horizon 2020) will involve the adaptation of current and future infrastructure towards climate-resilience (document SWD 137 [1]). Projected impacts of climate change and associated threats concerning the construction sector are as follows: (1) extreme precipitation, e.g. leading to water intrusion, damage to foundations and basements; (2) extreme summer heat events [2], e.g. leading to material fatigue and accelerated aging, high energy use for cooling; (3) exposure of structures to heavy snowfall; (4) rising sea and river levels that increase the risk of flooding, soil subsidence risks are likely to increase.

The Finnish Meteorological Institute (FMI) has examined in the ACCLIM project the different climate models, built models for Finnish climate conditions and adaptation to climate change. In all gas emission scenarios, based on three IPCC (2007) [3] scenarios for the evolution of greenhouse gas and aerosol particle emissions, the average temperature and the change of precipitation rises equally fast until 2040. Differences among the scenarios start to emerge only after the middle of the century [4]. The FMI has also made new calculations based on IPCC recently published new scenarios. In new scenarios differences in the average temperature and change of precipitation starts earlier but the values of the most severe scenario are not going to differ significantly from the values published in ACCLIM project which are used in this study.

Nowadays the estimated life cycle in building design is typically 50–100 years, and efforts are made to lengthen the service life of the older building stock by renovation. Thus, there is a great need

* Corresponding author. Tel.: +358 40 849 0837.
E-mail addresses: arto.kolio@tut.fi (A. Köliö), toni.pakkala@tut.fi (T.A. Pakkala), jukka.lahdensivu@tut.fi (J. Lahdensivu), mihkel.kiviste@tut.fi (M. Kiviste).

http://dx.doi.org/10.1016/j.engstruct.2014.01.032
0141-0296/

to study the performance of repaired structures and repair methods exposed to future climates. These studies are a major part of the FRAME project recently carried out at Tampere University of Technology (TUT). The project was based on data of the ACCLIM project [4]. However, the ACCLIM project is based only on a single future scenario of greenhouse gas emissions.

The ACCLIM and FRAME projects have shown that in the future climate conditions are likely to get worse in terms of durability of facades and other structures. It has been shown in the case of precast concrete buildings that presently deterioration of facades and balconies is faster in the coastal areas and southern Finland than inland and eastern and northern Finland [5]. According to the data of the ACCLIM project, precipitation during the winter season is also going to increase while the form of precipitation is going to be increasingly rain and sleet. At the same time, the conditions for drying are going to get worse. Thus, the degradation rate of structures will accelerate in most of Finland if maintenance and protection actions are neglected [6].

Research objective was to study whether the durability properties regulated by Finnish building codes are enough for the changing climate conditions. In this work a database of concrete material properties and observed degradation was combined with climate data projections from FMI.

2. Background

2.1. Corrosion of reinforcement due to carbonation

Because of its nature, corrosion of concrete reinforcement is in general depicted by a model with two distinct phases as in Fig. 1 [7].

2.1.1. Initiation phase and its modelling

Concrete reinforcement is protected from corrosion by high alkalinity of concrete pore water. This alkalinity is over time neutralized by carbon dioxide in the surrounding air or chlorides penetrating the concrete cover leaving the reinforcement susceptible to corrosion. Concerning concrete facades in a non-marine environment, the corrosion of reinforcement is mainly initiated by carbonation [5].

Although chloride-induced corrosion is considered to be worse than carbonation-induced corrosion, Parrott [8] and Jones et al. [9] states that 2/3 of all structural concrete is exposed to environmental conditions that favour carbonation-induced corrosion. Carbonation of concrete is a chemical reaction between alkaline hydroxides of concrete and carbon dioxide gas both dissolved in concrete pore water. The reaction product is calcium carbonate, which lowers the pH of the pore water (and concrete) gradually to a level where steel can corrode. As the alkaline hydroxide reservoir in concrete is limited, it is eventually used up leading to the neutralization of concrete.

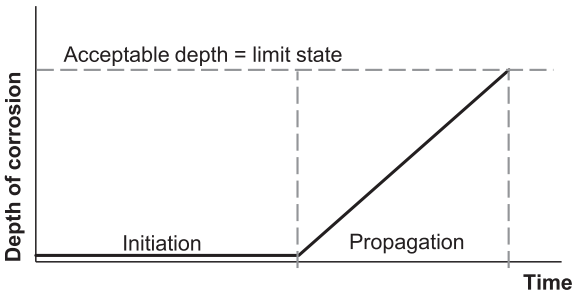

Fig. 1. The two-phase model of corrosion of reinforcement in concrete by Tuutti [7].

The evaluation of the service life of reinforced concrete structures has led to the development of several models to model carbonation evolution [7,10–17]. Carbonation has been found to involve a number of processes, from the aggressive environment of gas diffusion to the beginning of the corrosion itself, and there are several other parameters whose variability cannot be ignored. Neves et al. [18] provided a simple analytical model for the initiation period, calibrated with long-term carbonation results, which used the accelerated carbonation resistance and the environmental class as input parameters (semi-probabilistic approach). Recent work also focused on the assessment of climate change on the durability of concrete structures in specific locations. Wang et al. [19] studied the impact of climatic change on corrosion-induced damage in Australia. Talukdar et al. [20] estimated the effects of climate change on carbonation in Canadian cities. Based on those results Talukdar and Banthia [21] developed a model of carbonation in concrete infrastructure in the context of global climate change. The serviceable life, from construction through to cracking due to carbonation induced corrosion of concrete infrastructure is considered in all continents. It was concluded that global climate change will affect the progression and will result in much higher ultimate carbonation depths in the long term. Guiglia and Taliano [22] compared the carbonation measured on in-field exposed existing reinforced concrete structures with predictions made using fib-Model Code 2010. This comparison has highlighted the key role played not only by the environment, but also by the quality of the concrete through the inverse effective carbonation resistance of concrete on the evolution of the carbonation depth in time.

2.1.2. Propagation phase and its modelling

Corrosion of steel embedded in concrete is an electrochemical reaction where anode and cathode areas are formed on the steel surface as a result of differences in pH and moisture. Anode areas release positively charged hydrated ions in oxidation reaction into the pore water acting as an electrolyte. The excess electrons flow through metal from the anode to cathode where they are consumed in reduction reaction by hydrogen ions or by dissolved oxygen. The ions released in electrolyte react forming corrosion products. Corrosion, especially with shallow cover depths, leads to cracking or spalling of surrounding concrete as the reinforcing bar starts to rust forming residue greater in volume than the original bar [23]. To happen, electrochemical corrosion requires [24]:

- a reactive metal where anodic oxidation can take place,
- a reducible substance which acts as a cathodic reactant,
- electrolyte allowing the migration and movement of ions,
- an electron conduction between anodic and cathodic areas.

Therefore, amount of pore water is one of the critical preconditions for corrosion meaning that the moisture of reinforced concrete has a paramount effect on the rate of corrosion. The rise in temperature is considered to increase the solubility of chemical compounds thereby increasing also the rate of corrosion [7].

The corrosion propagation phase is now appreciated as a significant component in the service life of RC structures and a good understanding of the propagation process is paramount. Various models have been developed to simulate and/or predict the propagation phase. Empirical models are sub-divided into three types i.e.: (i) Expert Delphic oracle models, (ii) fuzzy logic models, (iii) models based on electrical resistivity and/or oxygen diffusion resistance of concrete. Three different approaches can be used to develop numerical models viz: (i) finite element method (FEM), (ii) Boundary element method (BEM) and (iii) resistor networks and transmission line method. Analytical models apply usually thick-walled cylinder approach. Division into cracked inner

cylinder and an uncracked outer have also been developed. Otieno et al. [25] presented a critical review of some of the available models for corrosion propagation, and proposed ways forward to overcome some of these problems.

The influence of the amount of precipitation to the behaviour of reinforcement corrosion was observed in research depicted in Refs. [26,27]. In his research Mattila measured the corrosion current in measurement devices embedded in existing concrete facades. High corrosion current was observed during a year when annual precipitation was exceptionally high. Vice versa, when annual precipitation was low also very low corrosion currents were observed. Refs. [28–30] establish a basis for estimating the relationships between aggressiveness of corrosion, corrosion rates and loss of cross section of reinforcing bar due to corrosion.

2.1.3. Limit state of reinforcement corrosion

Corrosion of reinforcement affects concrete structures basically either by cracking of concrete cover caused by corrosion products or by reduction of effective steel cross-section. Which one of these effects is more crucial depends on the functionality of the corroding structure. Cracking occurs in structures where the reinforcement is placed quite near the concrete surface and the pressure generated by corrosion products is sufficient. Cracking accelerates the penetration of harmful agents to concrete and causes visual defects in concrete facades ultimately leading to spalling of areas of concrete. In this context, the occurrence of cracks is not the ultimate limit for the life of the structure, but rather a limit based on the appearance and serviceability of the facade. There still exists an undefined residual life after this. As induced by carbonation, the corrosion of relatively small reinforcement with normal cover depths can go on for remarkably long time without showing any visual signs thus making it difficult to diagnose. Principles [7] and threshold values [28,31,32] for estimating the amount of corrosion needed to cause visual damage are discussed in literature for various corrosion cases.

2.2. Precast facade elements and balconies

Since 1970s almost all prefabricated concrete structures in Finland are based on the Concrete Element System [33]. That open system defines, for instance, the recommended floor-to-floor height and the types of prefabricated panels used. In principle, the system allows using the prefabricated panels made by all manufacturers in any single multi-storey building.

2.2.1. Facades

The concrete panels used in exterior walls of multi-storey residential buildings were, and still are, chiefly prefabricated sandwich-type panels with thermal insulation placed between two concrete layers. Facade panels are made up of two relatively thin reinforced concrete layers connected to each other by steel trusses. The thermal insulation between the layers is most often mineral wool of 240 mm nominal thickness according to the building regulations in force.

The usual nominal thickness of the outer layer is nowadays 80–85 mm. The layers are most typically reinforced with steel mesh of a wire diameter of 3 mm and spacing of 150 mm. Rebars 6–8 mm in diameter are typically used as so-called edge bars and often also diagonally at the corners of windows and other major openings in the layers. The bars are spliced by lap splices, which increase the overall thickness of the reinforcement, see Fig. 2.

The outer layer is generally supported by the inner layer. Sandwich facade panels are connected to the building frame by the inner layer, usually by means of cast concrete joints and reinforcement ties.

2.2.2. Balconies

The most common balcony type in Finland from the late 1960s until today consists of a floor slab, side panels and a parapet panel of precast concrete. These stacked balconies have their own foundations, and the whole stack is connected to the building frame only to brace it against horizontal loads. All structural members of a precast balcony are load-bearing. The cross-section of a typical balcony constructed of precast panels is presented in Fig. 3 [35].

The typical nominal thickness of a load-bearing wall panel is between 150 and 180 mm depending on the number of floors. In general, multi-storey residential buildings have no more than eight floors. This allows using plain concrete side panels as a bearing structure and rebars only 10–12 mm in diameter as so-called edge bars to take the forces caused by the shrinkage of concrete and the erection of the balcony.

The nominal thickness of a bearing concrete slab is between 140 and 200 mm. It varies a lot depending on the slope of the upper surface of the slab panel. The bearing reinforcement, typically 10–12 mm in diameter and with a spacing of 100–150 mm, is in the bottom section of the slab. Without exception there is not any waterproofing on the top of balcony slab.

The nominal thickness of parapets is from 70 to 85 mm. Parapets usually have quite heavy reinforcement near both surfaces, vertical rebars 6–8 mm in diameter spaced 150 mm apart. Parapets are most often joined to the slab by casting them together.

2.3. Climate projections in Finland

Although the climate is relatively steady for the latitudes and compared to size, it still varies considerably. However, the Finnish building stock is mainly focused on the few biggest cities and certain growth areas near them. Due to both the climate differences and the concentration areas of the population Finland can be divided to four main areas: coastal area, southern Finland, inland and Lapland. Coastal area includes 30 km wide sector of the coast from the city of Vaasa to Russian border. Southern Finland includes the rest of southern parts to the level of the Tampere city (150 km north from Helsinki). Inland area includes the rest of the country except Lapland.

The Finnish Meteorological Institute (FMI) has weather data since 1961 in digital form from several meteorological stations covering all of Finland. The data consist of temperature, relative humidity, rain intensity, wind speed and direction, solar radiation variables, etc. These observations have been collected at least daily and three times a day at best. In the REFI-B project [36], the FMI also forecast the climates of four localities (coastal area, southern Finland, inland, Lapland) in three periods (2030, 2050 and 2100). The forecasts are based on an average of 19 different models which are all based on greenhouse gas emission scenario A2. The A2 scenario involves a situation where greenhouse gases are assumed to increase significantly – it is a sort of worst-case scenario. The FMI also has other significant greenhouse gas emission scenarios: A1B (quite large emissions) and B1 (small emissions). The increase of the CO_2-level is depending highly on the scenario used. According to the IPCC [3], while using A2 scenario the CO_2-level can rise up to 840 ppm until the end of the century and about 540 when using B1 scenario. However, the increase is significant compared to present level (390 ppm) [36] (see Fig. 4).

The annual precipitation does not get evenly distributed over facades. The distribution depends on the height of the building and prevailing wind directions during rain. According to Jerling and Schechninger, the upper parts and corners of facades get more precipitation than lower and central parts [37]. Prevailing wind directions and wind speeds also have a strong influence on the distribution of precipitation across a building. In Finland most of the rain and sleet in wintertime comes with southerly to westerly

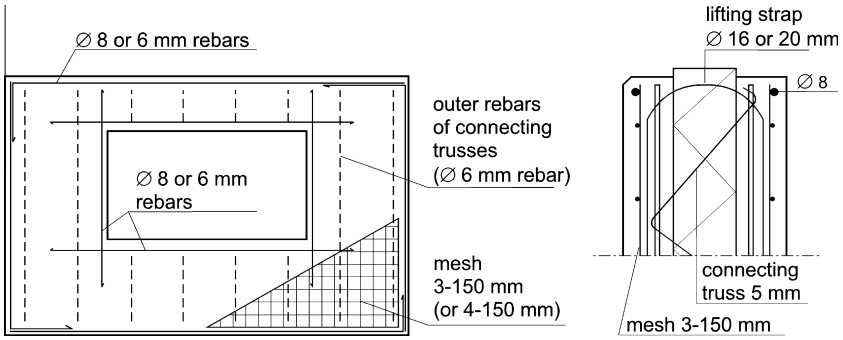

Fig. 2. Typical reinforcement of outer layer of a concrete facade panel [34].

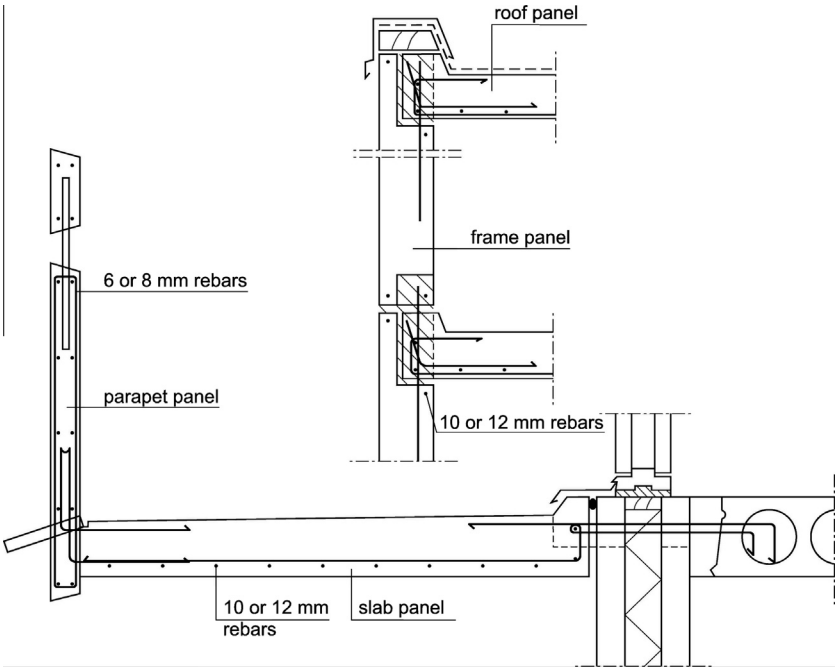

Fig. 3. Cross-section of a typical Finnish balcony made of precast structural members [35].

winds. Rain events with wind from other directions have been rare. Due to stronger winds, about 60% of the rain and sleet load in the coastal area hits the facades and balconies; the corresponding share inland is about 40%. Combined with the higher amount of precipitation in coastal areas, facades and balconies there are subject to considerably higher moisture stress than inland resulting in clearly more corrosion and frost damage. Winds are stronger at higher reaches of buildings than close to ground level which naturally leads to upper sections of high buildings receiving more rain and sleet stress than lower buildings, and lower sections of buildings in general [38].

3. Research methods and material

3.1. Research material

Research material for this study is composed of data on concrete durability assembled in condition assessments conducted on prefabricated concrete facades and balconies built in 1961–1996. As this study discusses the current concrete codes the data is delimited to 72 buildings built 1990 or after. The database withholds measurements of concrete pore structure, tensile strength, chloride content, carbonation depths as well as concrete cover depths of reinforcement. In addition it includes results from thin section analyses and visual observations made from the building facades and balconies.

Practical design of concrete structures is in Finland governed by national concrete codes [39]. Besides guidelines for structural design, it also gives recommendation on durability properties and service life design. These requirements are compared to the actual observed degradation processes and their progress in the future.

Future climate projections and their effects on weather conditions critical to concrete degradation have been prepared by the Finnish Meteorological Institute. This data is utilized in this study.

3.1.1. Quality of concrete

In Finland the concrete grade used in concrete facade panels as well as most structural members of balconies has been C30/37 since late 1980s by the guidelines for durability and service life of concrete [40]. The cement type used in those concrete panels is mostly CEM I (42.5 N) (ordinary Portland cement) because of good early age strength of concrete which allows rapid formwork rotation at precast concrete panel factory. White cement, CEM I (52.5 R) is also used in facade panels if necessary, but its share of total amount of used cement is small. In Nordic outdoor climate the concrete used for facades and balconies is always air-entrained.

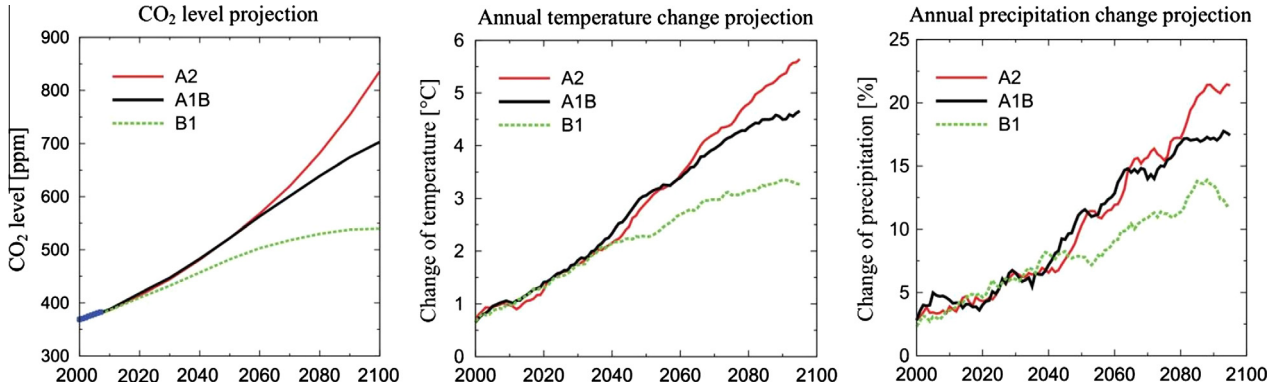

Fig. 4. Projections for CO_2 level increase, the annual mean temperature and the precipitation change for the period 2000–2100, relative to the mean of the reference period 1971–2000. The curves depict 11 year running means, averaged over Finland and the responses of 19 global climate models. Projections are given separately for the three greenhouse gas scenarios (A2, A1B and B1) [4].

3.2. Calculating the service life by reinforcement corrosion

3.2.1. Initiation phase

Corrosion of reinforcement in concrete facades and balconies is evaluated by a combined model for future climate in Finland by Finnish Meteorological Institute and carbonation initiated corrosion. Initiation is depicted with the square root model of carbonation (Eq. (1)), based on Fick's 2nd law on diffusion, using measured coefficients. The progression of carbonation inside the concrete is commonly acknowledged to follow a square root equation relationship with the time of exposure modified with a carbonation coefficient [7]. However, the square root model does not specify the influence of the rise in CO_2 in the environment due to climate change. For estimating the influence of CO_2 the model given in fib model code for service life design [41] was used (Eq. (2)). Propagation phase is estimated by combining future climate data and preset boundary conditions obtained through research and from literature. The service life of the reinforcement withholds the time of initiation and active corrosion to the limit state when first cracking occurs.

The demands in Finnish concrete codes for reinforcement cover depths are given in Table 1.

Carbonation time is calculated using the presumed square root dependence of carbonation depth x with time of exposure t to CO_2 in surrounding air [7]:

$$x = k \cdot \sqrt{t} \tag{1}$$

The carbonation coefficient k is highly dependent on (and includes the effect of all) type of structure, time of wetness, material properties, etc. These coefficients for different types of facade finishes and balcony units have been determined in facade condition assessments and thus, the values used in this study represent actual measured carbonation depths from existing buildings. The large amount of data enables statistical evaluation. The statistical numbers calculated were average, standard deviation (to the worse direction) and 95% percentile.

To study the effect of change in CO_2 in the environment and the amount of precipitation by climate change, the fib model for carbonation [41] was used with parameters given in Table 2:

Table 2
Parameters used in Eq. (2).

k_e	k_c	R_{NAC}^{-1}	t_0	w	C_s
0.466	1.00	28,500	0.0767	Varied	Varied

$$x_c = \sqrt{2 \cdot k_e \cdot k_c \cdot R_{NAC}^{-1} \cdot C_s} \cdot \sqrt{t} \cdot \left(\frac{t_0}{t}\right)^w \tag{2}$$

3.2.2. Propagation phase

As idealized in the model by Tuutti, corrosion of reinforcing steel in concrete is a phenomenon with two consecutive phases. It is also assumed here that active corrosion begins after the initiation phase has been completed. For a single point inside the structure this assumption is valid, but not for a whole structure resulting from the variations in structure's properties. The corrosion rate of a reinforcing bar varies depending greatly on the moisture of the surrounding concrete. Coarse boundary values for annual precipitation for very fast and very slow reinforcement corrosion have been established in an earlier study by Mattila [26]. According to Mattila corrosion is fast in Finnish climate conditions when the annual precipitation is over 480 mm/year. These results were combined with known corrosion rates obtained from literature. Rates at which corrosion penetrates reinforcing steel are presented by Andrade [29]. Negligible corrosion advances less than 1 μm/a and high corrosion over 10 μm/a. The respective corrosion rates are less than 0.1 $\mu A/cm^2$ and over 1 $\mu A/cm^2$.

Active corrosion phase was modelled as the penetration depth x_{corr} by the following rules:

$$x_{corr} = \sum_{i=1}^{t_{prop}} r_i \tag{3}$$

where x_{corr} = corrosion penetration depth, r_i = average annual corrosion rate during year i (1 μm/a if annual precipitation <480 mm and 10 μm/a if annual precipitation $\geqslant$480 mm), and t_{prop} = the age in years when critical corrosion depth is achieved.

Table 1
Demands for concrete cover in different stress class when designed service life is 50 or 100 years [39].

Designed service life (a)	Stress class	Minimum concrete cover (mm)	Crack width (mm)
50	XC3/XC4	25	$\leqslant$0.2
100	XC3/XC4	30	$\leqslant$0.13

Table 3
Average annual change (%) in precipitation and temperature (°C) compared to present climate (2000) in four different observation station.

	Vantaa (south coastal area)			Jokioinen (south inland)			Jyväskylä (inland)			Sodankylä (Lapland)		
	2030	2050	2100	2030	2050	2100	2030	2050	2010	2030	2050	2100
Precipitation	3.8	7.1	17.7	3.1	6.1	15.2	3.6	7.1	18.2	3.9	7.9	21.3
Temperature	1.2	2.1	5.1	1.2	2.1	5.0	1.3	2.3	5.5	1.5	2.7	6.4

The average annual corrosion rate was chosen based on the amount of annual precipitation for each year *i*. For this data of measured annual precipitation from the period 1979–2009 was used to describe current climate. This data was then increased according to FMI predictions, see Table 3, to describe the change in 2030, 2050 and 2100. The change in the amount of precipitation will be higher during autumn and winter when drying of structures is slower in general. Again, according to FMI, the prevailing wind directions during rain events will stay same as present. It intends that facades faced from South-East to West will get more precipitation also in the future.

The fib model [41] for propagation phase until first cracking (Expert Delphic oracle based log–normal distribution with parameters $m = 4.5$ years and $s = 1.5$ years) was applied to study the effect of change in temperature in the environment by climate change.

3.2.3. Limit state of reinforcement corrosion

Alonso et al. [28] have presented estimates for the amount of corrosion in concrete reinforcement that can cause cracks and chipping of concrete cover. The critical amount is 15–50 μm presented as depth of corrosion or loss of bar diameter. The formation of cracks due to corrosion is, however, dependent on multiple factors including bar diameter and thickness of concrete cover, which can deviate considerably from the design value. In this study 50 μm was chosen as the critical depth of corrosion x_{limit} depicting the time of the first cracking of concrete.

4. Results and discussion

4.1. Initiation of corrosion of reinforcement in facades

The carbonation coefficients that have been used in the calculations of this study are presented in Fig. 5 as cumulative distribution functions. All of the carbonation coefficients have been determined from existing prefabricated concrete buildings constructed in 1990–1995 that have been subjected to a condition assessment.

Concrete facades with white concrete or brick tile finishing are generally less susceptible to carbonation that ordinary painted concrete facades. The difference of painted concrete is due to the brushing surface treatment that leaves the concrete surface more open to carbonation. Higher cement content of the white concrete and the compacting effect of the capillary suction of brick tiles while casting are influencing more slow carbonation in these facades [5]. Statistical numbers for carbonation coefficients used later in the assessment of carbonation depths by Eq. (1) are average and 95% percentile as shown in Table 4. The large standard deviation for both facades and balconies, in Tables 4 and 5, describes the large scatter in carbonation of these surfaces in practice.

Probable lengths of carbonation phase for different facades calculated using the above carbonation coefficients are shown in Fig. 6. Standard design service life of concrete facades (50 years) is marked with a horizontal line in the figure. The figures have been limited to illustrate more clearly the first 100 years. Very long estimates are also quite theoretical.

Fig. 6 indicates that by average the 50 year service life is always achieved by carbonation in facades with white concrete or brick tile finish. Painted concrete facade requires successful concrete cover to achieve 50 years. By the 95% percentile, painted concrete facades reach a service life of 20 years when reinforcement is placed according to the concrete codes (25 mm cover). With white concrete and brick tile finish a service life of 100 and 40, respectively, years are achieved.

As the service life by reinforcement corrosion is in Finnish guidelines managed only by the initiation phase, namely carbonation of the concrete cover, the ones to fill the requirement of 50 year service life with 5% safety margin are white concrete facades. As an average, it can be said that majority of facades fulfill the required service life. This is of course when the placing of the reinforcing bars/mesh has been successful according to the codes with sufficient concrete cover. The importance of sufficient concrete cover is clearly pointed out by Fig. 6. Even a decrease of 5 mm will shorten the service life through carbonation easily by 10 years.

4.2. Initiation of corrosion of reinforcement in balconies

The carbonation of prefabricated balcony units was analyzed with the same principle as with different facade types. Carbonation coefficients describing the aggressiveness of carbonation in different structure units are presented in Fig. 7 and the ones used in further studies are presented in Table 5.

The one balcony surface carbonating much faster than others is the lower surface of a balcony slab. This is affected mainly by the casting direction which is upside down. Therefore the lower surface has higher w/c ratio due to the effect of floating of fresh concrete surface. Secondly, the lower surface of the balcony slab is sheltered from the rain, which keeps the surface dry allowing easier carbonation [5]. That behaviour is illustrated in Fig. 8.

Probable lengths of carbonation phase for different balcony units are shown in Figs. 8–10. Standard design service life of concrete facades (50 years) is marked with a horizontal line in the figures.

According to Figs. 8–10, based on average carbonation rate the 50 year service life requirement is always fulfilled. Based on 95% percentile the 50 year service life is not certain with balcony parapet outer surface and balcony side panel inner surface. It is also questionable with parapet inner surface and side panel outer surface.

In balcony structures described in Fig. 2 the main reinforcement is located in the lower part of the prefabricated balcony slab. Thus the carbonation of the lower surface of a balcony slab is the most relevant in the question of service life. As an average, 50 years is achieved by initiation also in the case of the lower surface. However, based on 95% percentile the length of initiation is only 17 years.

4.3. The effect of climate change on initiation

In Nordic climate the climate change affects the carbonation of concrete by increasing the CO_2 concentration in air and by increasing raininess. The both have an opposite effect on carbonation. The effect of these factors have been presented in Fig. 11.

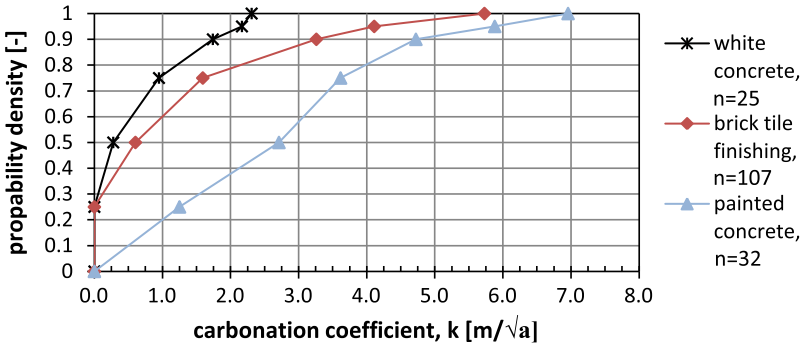

Fig. 5. Carbonation coefficients as cumulative graphs determined in facade condition assessments of buildings built in 1990–1995.

Table 4
Carbonation coefficients of concrete facades surfaces of different finishing (mm/√a).

	Brick tile finishing	Painted concrete	White concrete
Average	1.06	2.62	0.59
Std. deviation	1.31	1.64	0.70
95% percentile	4.11	5.88	2.17

Table 5
Carbonation coefficients in balcony units (mm/√a).

	Slab		Side panel		Parapet	
	Upper s	Lower s	Outer s	Inner s	Outer s	Inner s
Average	1.15	3.21	1.50	1.63	1.09	1.48
Std. deviation	0.90	1.42	1.02	1.24	1.13	1.02
95% percentile	2.82	6.02	3.47	4.14	3.95	3.49

The scenarios in Fig. 11 are based on the climate change scenario A2 (significant increase). According to the fib model [41] the increase in rain reduces the carbonation by 5.7% until 2050 and by 15.4% until 2100. The increase in carbonation by CO_2 level is 17.0% until 2050 and 48.2% until 2100. The results indicate that the influence of CO_2 level is dominating of these two factors in regard of concrete carbonation and, thus, the carbonation is likely to increase as the result of climate change. However, the weather function w in Eq. (2) is somewhat questionable for it takes into account only the number of rainy days and the probability of wind driven rain. The distribution and duration of rain events (seasonal rains or small amounts constantly) is also likely to have an effect on carbonation.

Fig. 12 shows the comparison between the average carbonation by the fib model [41] and the scatter in the carbonation coefficients measured from existing structures by the Tuutti's model.

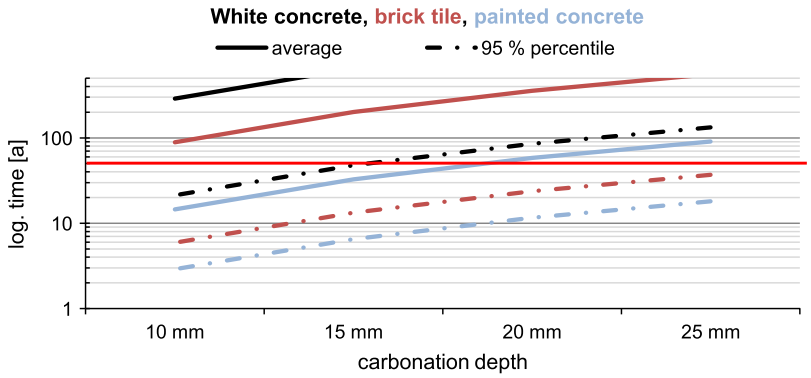

Fig. 6. Service life of reinforcement regarding the initiation phase (carbonation) for different cover depths and surface treatments of facades.

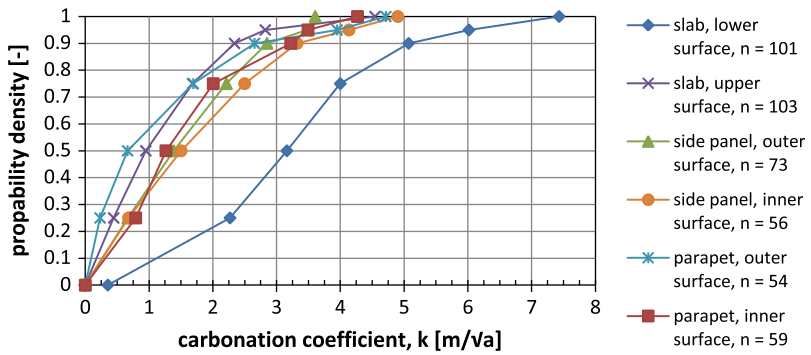

Fig. 7. Carbonation coefficients determined from prefabricated concrete balconies in facade condition assessments of buildings built in 1990–1995.

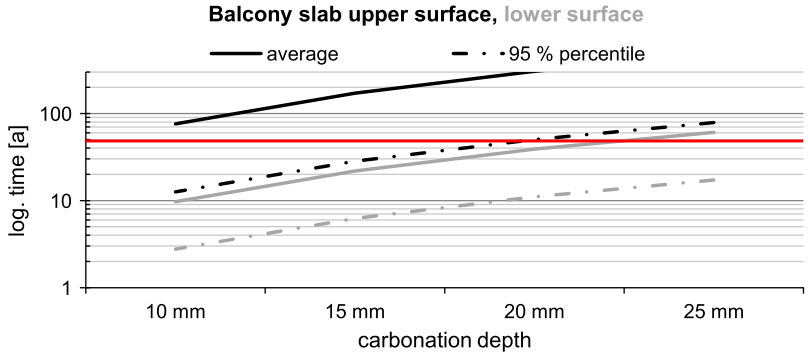

Fig. 8. Service life of reinforcement regarding the initiation phase (carbonation) for different cover depths in upper and lower surface of a balcony slab.

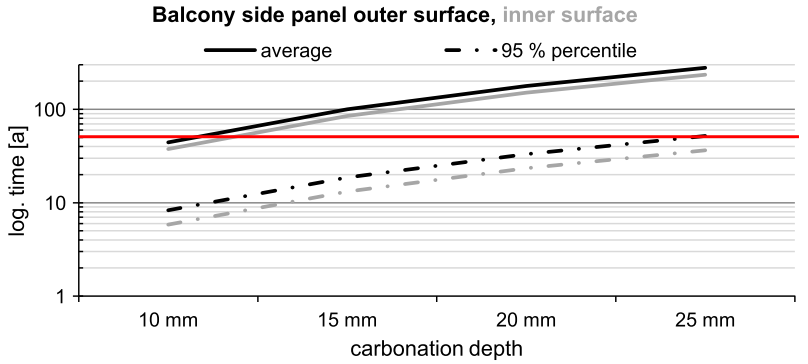

Fig. 9. Service life of reinforcement regarding the initiation phase (carbonation) for different cover depths in outer and inner surface of a balcony side panel.

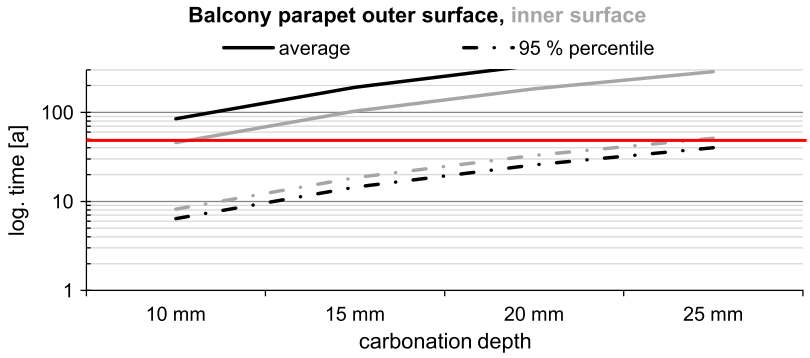

Fig. 10. Service life of reinforcement regarding the initiation phase (carbonation) for different cover depths in outer and inner surface of a balcony parapet.

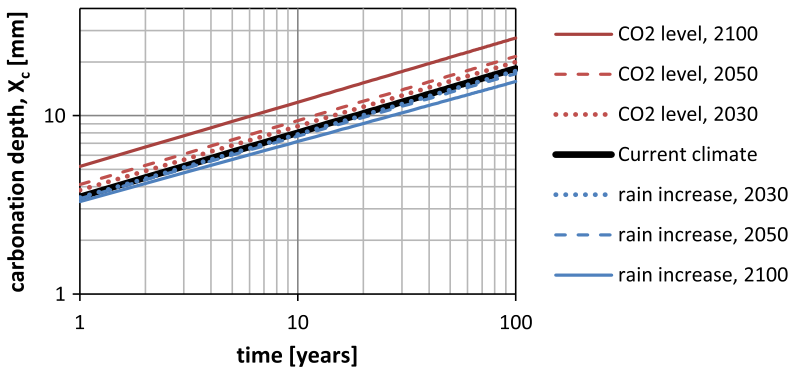

Fig. 11. The influence of CO_2 level and increase in raininess on corrosion initiation by carbonation.

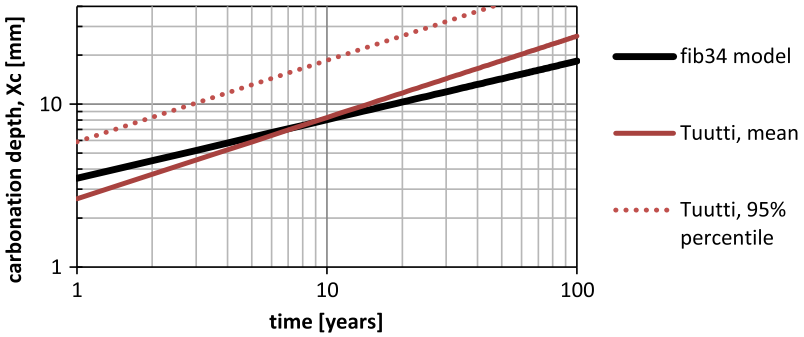

Fig. 12. Comparison between the carbonation coefficients of Tuutti model and the model by fib [41].

Table 6
The length (in years) of active corrosion phase in respect of crack initiation in different parts of Finland.

	Helsinki-Vantaa airport (coastal area)	Jokioinen observatory (southern Finland)	Jyväskylä-Tikkakoski airport (inland)	Sodankylä observatory (Lapland)
Current climate (1980–2009)	5.7	6.1	8.2	37.5
2030	5.5	5.7	7.8	37.5
2050	5.3	5.5	7.4	37.5
2100	5.3	5.1	6.1	19.7

Carbonation rate according to the fib model is slower than Tuutti's model based on measured carbonation depth of concrete. The fib model gives higher carbonation depth for young concrete but after 100 years fib model gives 8 mm lower carbonation depth than Tuutti's model in average. The difference is remarkable in case of service life of concrete structure. By extrapolating the fib model the difference of 8 mm equals 168 years in service life prediction.

The fib model is based on DuraCrete-project [17]. Concrete studied in that project has generally been of better quality than in existing Finnish concrete facades and balconies. For that reason Tuutti's model has been used in this study with measured coefficients leading to higher predictions in carbonation depth in 100 years.

4.4. The effect of increase in rain on propagation phase

The length of active corrosion phase to the initiation of cracks in concrete was estimated by using the background established in Refs. [26,28,29]. This knowledge was combined with future weather data by FMI in Table 2. Table 6 presents the calculated durations of active corrosion phase in respect to the weather conditions (annual raininess) of different locations in Finland.

Taking the active corrosion phase into consideration will lengthen the service life of reinforcement by 5–8 years in southern parts of Finland and up to 35 years in Lapland in current climate. Climate change will as a rule shorten the active corrosion phase by subjecting concrete structures to weather conditions more favourable to corrosion. The change is slow at first but will increase by the end of this century especially in northern parts of Finland.

Table 6 shows that the most severe conditions regarding active corrosion are in the coastal area and southern Finland. In these regions of Finland active corrosion phase is remarkably short. The climate change will not affect it significantly compared to Lapland. The active corrosion phase in Lapland will remain at the same level until 2050 and then drop dramatically. This change is due to much bigger precipitation prediction by FMI.

If the building is in Lapland combining initiation and active corrosion will easily give enough service life. However, the majority of Finnish building stock is located and construction activities are in the southern part of Finland. In the southern part of Finland initiation period dominates service life because active corrosion phase adds only 5–8 years. Therefore cover depth of reinforcement and the quality of concrete, that influence the initiation time, are highly important in ensuring the 50 year service life.

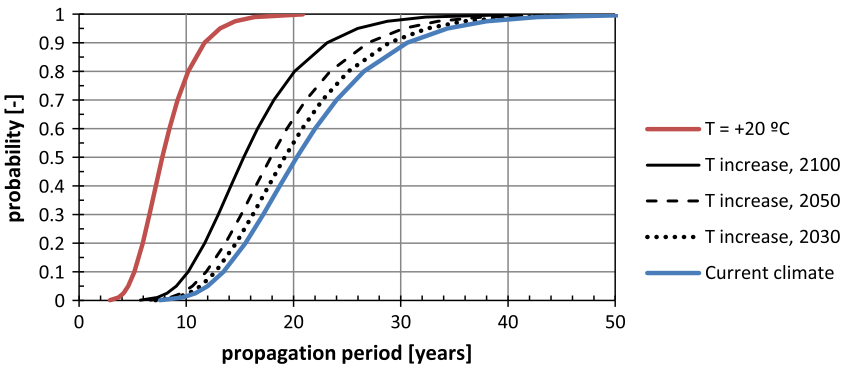

Fig. 13. The effect of increase in temperature on active corrosion of reinforcement in carbonated concrete according to fib 34 [41].

4.5. The effect of temperature change on propagation phase

Propagation model given in [41] represents a temperature relationship of active corrosion using a reference propagation time modified by a temperature related factor. This has been applied in Fig. 13 to predict the influence of increase in air temperature induced by climate change. According to FMI the annual average temperature in Finland varies from +5.9 °C (south coastal area) to −0.4 °C (Lapland). In calculations presented in Fig. 13 has been used +2.0 °C which is suitable for large areas in southern Finland.

Active corrosion phase takes 12 years in present climate when studying 95% percentile. The active corrosion phase decrease to 9.6 years by the end of century as a result of temperature increase caused by climate change. According to fib model, temperature has significant effect on corrosion rate; in 20 °C active corrosion phase takes 4.6 years. This is theoretically right and reasonable. However, according to field measurements made by TUT outdoor temperature does not have so significant influence on corrosion rate in practice. Corrosion rate remain approximately at the same level in temperature range of −5 to +25 °C, only very low rise was detected [27].

In current climate corrosion rate presented in Table 6 is rather close to 20 °C probability curve presented in Fig. 13. The raininess as well as properties of concrete (capillarity) are the crucial factors affecting on corrosion rate of reinforcement in carbonated concrete.

5. Conclusions

According to Finnish concrete codes the service life of reinforced concrete structure will end when carbonation achieves the reinforcement. In practice corrosion can start in that time if circumstances are favourable to corrosion (enough moisture, availability of oxygen, temperature, etc.). Active corrosion phase is not included to service life of concrete structure.

The carbonation rate of concrete varies a lot according to properties of concrete. Concrete is not a homogenous material, the durability properties varies due to e.g. compaction and curing of fresh concrete. Great difference might occur between patches due to e.g. moisture content of aggregate leading to different water–cement ratio. Concrete technology has a great influence on the capillarity of concrete. In general, the carbonation rate of concrete is slow in dense, low water–cement ratio concrete, where curing has been careful.

Regarding service life by reinforcement corrosion, for the majority of Finnish building stock the initiation period by carbonation dominates service life because active corrosion phase can add only 5–8 years. Therefore cover depth of reinforcement and the quality of concrete, that influence the initiation time, are highly important in ensuring the 50 year service life.

For buildings located in northern Finland the active corrosion phase can increase service life remarkably. Precipitation in northern Finland occurs mostly as snow. The above estimation of active corrosion time is valid for surfaces exposed to rain. Since the amount of rain has a paramount influence on active corrosion, also a sheltered location will remarkably lengthen the period of active corrosion. This is valid for the soffit surface of a balcony slab.

Visible corrosion damage in facades and balcony structures are rather unusual if the cover depth is in the level required in Finnish concrete codes (25 mm) even if the carbonation of concrete would achieve the reinforcement. Especially structures sheltered from the rain, like soffits of balcony slabs or inner surface of balcony parapets, the active corrosion of reinforcement is very slow.

Facades will get higher driving rain stress in the future because climate change will increase the amount of rain and sleet and also windiness. The increase of precipitation in the future will have only small effect to the corrosion rate during active corrosion period, because the active corrosion period is rather short even now, only 6–8 years which will accelerate to 5–6 year in the beginning of century in southern and middle Finland.

Visible corrosion damage will be noticed before designed service life has been achieved in the reinforced concrete structures where cover depths are low, e.g. less than 15 mm. During manufacturing of concrete structures sufficient cover depths should be ensured with spacers and careful installation of the reinforcement.

The fib 34 model gave a longer service life in both initiation and propagation phase than Tuutti's model and propagation phase studies conducted at TUT. The differences in initiation time were caused by different concrete quality and grade of research material. The increase of CO_2 dominates over the increase in precipitation during initiation. Thus, the initiation will be faster in future. Based on FMI predictions in Finnish climate the current study shows that the increase in precipitation affects the propagation phase more than the increase in temperature.

Acknowledgements

The authors would like to acknowledge the researchers in Finnish Meteorological Institute for preparing the future climate projections. This study was part of FRAME research project conducted at Tampere University of Technology in 2009–2012.

References

[1] SWD 137. Adapting infrastructure to climate change. Brussels; 2013.
[2] E.E.A. Report 12. Climate change, impacts and vulnerability in Europe 2012. European Environment Agency, Copenhagen; 2012.
[3] IPCC. Climate change 2007: the physical science basis. Contribution of working group I to the fourth assessment report of the intergovernmental panel on climate change. Cambridge University Press, Cambridge, UK; 2007. 996 p.
[4] Jylhä K, Ruosteenoja K, Räisänen J, Venäläinen A, Tuomenvirta H, Ruokolainen L, et al. The changing climate in Finland: estimates for adaption studies. ACCLIM project report 2009. Finnish Meteorological Institute. Reports 2009:4. Helsinki; 2009. 78 p. 36 app [in Finnish].
[5] Lahdensivu J. Durability properties and actual deterioration of Finnish facades and balconies. Tampere University of Technology, Faculty of Built Environment, Tampere. Publication 1028; 2012. 117 p. 37 app.
[6] Lahdensivu J. The durability of facades and balconies in a changing climate. Ministry of the Environment, Department of the Built Environment, The Finnish Environment 17/2010. Helsinki; 2010. 64 p. [in Finnish].
[7] Tuutti K. Corrosion of steel in concrete. Stockholm. Swedish Cement and Concrete Research Institute. CBI Research 4:82; 1982. 304 p.
[8] Parrott L. Some effects of cement and curing upon carbonation and reinforcement corrosion in concrete. Mater Struct 1996;29(3):164–73.
[9] Jones M, Dhir R, Newlands M, Abbas A. A study of the CEN test method for measurement of the carbonation depth of hardened concrete. Mater Struct 2000;33(2):135–42.
[10] Ho DWS, Lewis RK. Carbonation of concrete and its prediction. Cem Concr Res 1987;17(3):489–504.
[11] Bakker RFM. Initiation period. In: Schiessl P, editor. Corrosion of steel in concrete. RILEM; 1988.
[12] Papadakis VP, Vayenas CG, Fardis MN. Fundamental modelling and experimental investigation of concrete carbonation. ACI Mater J 1991;88(4):63–373.
[13] Parrott LJ. Design for avoiding damage due to carbonation-induced corrosion. TC104/WG1/Panel 1, CEN; 1992.
[14] Saetta A, Schreflerb BA, Vitaliani RV. 2-D model for carbonation and moisture/heat flows in porous materials. Cem Concr Res 1995;25(8):1703–12.
[15] RILEM Report 14 – durability design of concrete structures. London: E&FN Spon Press; 1996.
[16] CEB Bulletin d'information N° 238. New approach to durability design – an example for carbonation induced corrosion; 1997.
[17] DuraCrete. Probabilistic performance based durability design of concrete structures. The European Union – Brite EuRam III, DuraCrete. Final technical report of duracrete project, document BE95-1347/R17. CUR, Gouda, Nederland; 2000.
[18] Neves R, Branco FA, de Brito J. A method for the use of accelerated carbonation tests in durability design. Constr Build Mater 2012;36:585–91. http://dx.doi.org/10.1016/j.conbuildmat.2012.06.028. ISSN 0950-0618.
[19] Wang X, Stewart MG, Nguyen M. Impact of climate change on corrosion and damage to concrete infrastructure in Australia. Clim Change 2012;110:941–57.

[20] Talukdar S, Banthia N, Grace JR, Cohen S. Carbonation in concrete infrastructure in the context of global climate change: part 2. Canadian urban simulations. Cem Concr Compos 2012;34:931–5.
[21] Talukdar S, Banthia N. Carbonation in concrete infrastructure in the context of global climate change: development of a service lifespan model. Constr Build Mater 2013;40:775–82.
[22] Guiglia Matteo, Taliano Maurizio. Comparison of carbonation depths measured on in-field exposed existing r.c. structures with predictions made using fib-Model Code 2010. Cem Concr Compos 2013;38:92–108.
[23] Broomfield J. Corrosion of reinforcement in concrete. London: E&F Spon; 1997.
[24] Page CL. Basic principles of corrosion. In: Schiessl P, editor. Corrosion of steel in concrete. London: Chapman and Hall; 1988. p. 3–21.
[25] Otieno MB, Beushausen HD, Alexander MG. Modelling corrosion propagation in reinforced concrete structures – a critical review. Cem Concr Compos 2011;33(2):240–5.
[26] Mattila J. On the durability of cement-based patch repairs on Finnish concrete facades and balconies. Tampere, Tampere University of Technology. Publication 450; 2003. 111 p.
[27] Mattila J, Pentti M. Suojaustoimien tehokkuus suomalaisissa betonijulkisivuissa ja parvekkeissa. Tampere University of Technology, Research report 123; 2004 [in Finnish].
[28] Alonso C, Andrade C, Rodriguez J, Diez JM. Factors controlling cracking of concrete affected by reinforcement corrosion. Mater Struct 1998;31:435–41.
[29] Andrade C. Measurement of polarization resistance on-site. In: Corrosion of steel in reinforced concrete structures. Final report of COST action 521. Office for Official Publications of the European Communities, Luxembourg; 2003. p. 82–98.
[30] Andrade C, Castillo A. Evolution of reinforcement corrosion due to climatic variations. Mater Corros 2003;54(2003):379–86.
[31] Parrott L. Design for avoiding damage due to carbonation-induced corrosion. In: Proceedings of third international conference on durability of concrete, nice. Special Publication SP-145, American Concrete Institute. p. 283–98.
[32] Siemes AJM, Vrouwenvelder ACWM, van den Beukel A. Durability of buildings: a reliability analysis. Heron 1985;30:3–48.
[33] BES – Development of open concrete element system. Research report. Suomen Betoniteollisuuden Keskusjärjestöry; 1969 [in Finnish].
[34] Pentti M, Mattila J, Wahlman J. Repair of concrete facades and balconies. Part 1: structures, degradation and condition investigation. Tampere, Tampere University of Technology, Structural Engineering. Publication 87; 1998. 156 p. [in Finnish].
[35] Pentti M. Repair of building envelope. In: Kaivonen J-A, editor. Repair techniques and economy of buildings. Rakennustieto Oy: Saarijärvi; 1994. p. 287–358 [in Finnish].
[36] Jylhä K, Ruosteenoja K, Tietäväinen H, et al. Rakennusfysiikan ilmastollisten testivuosien sääaineistot nykyisessä ilmastossa ja arviot tulevaisuuden muutoksista. Väliraportti. Finnish Meteorological Institute, Helsinki; 2011. 6 p. 20 app. [in Finnish].
[37] Jerling A, Schechninger B. Fogars beständighet. Byggforskningrådet. Rapport R89:1083. Stockholm; 1983. 172 p. [in Swedish].
[38] Lahdensivu J, Mäkelä H, Pirinen P. Durability properties and deterioration of concrete balconies of inadequate frost resistance. J Sustain Build Urban Develop 2013;4(2):160–9.
[39] Concrete Association of Finland. Finnish concrete code BY 50. Helsinki, Concrete Association of Finland; 2012. 251 p.
[40] Guidelines for durability and service life of concrete structures. BY 32. Helsinki. Concrete Association of Finland; 1989. 60 p.
[41] fib Bulletin No. 34. Model code for service life design. International Federation for Structural Concrete, Lausanne; 2006. 116 p.

II

POSSIBILITIES TO VALIDATE DESIGN MODELS FOR CORROSION IN CARBONATED CONCRETE USING CONDITION ASSESSMENT DATA

by

Köliö A., Pakkala T.A, Annila, P.J., Lahdensivu J. & Pentti M., Sep 2014

Engineering Structures vol 75, 539-549

http://dx.doi.org/10.1016/j.engstruct.2014.06.038

Engineering Structures 75 (2014) 539–549

Contents lists available at ScienceDirect

Engineering Structures

journal homepage: www.elsevier.com/locate/engstruct

Possibilities to validate design models for corrosion in carbonated concrete using condition assessment data

Arto Köliö *, Toni A. Pakkala, Petri J. Annila, Jukka Lahdensivu, Matti Pentti

Tampere University of Technology, P.O. Box 600, FI-33101 Tampere, Finland

ARTICLE INFO

Article history:
Received 28 March 2014
Revised 19 June 2014
Accepted 23 June 2014
Available online 9 July 2014

Keywords:
Concrete facades
Corrosion
Carbonation
Service life
Durability properties
Modelling

ABSTRACT

This study analyses the actual observed corrosion damage and active corrosion in concrete facades in Nordic outdoor climate and compares this data with the DuraCrete design model for carbonation initiated corrosion propagation phase. Active corrosion was examined in this study by calculating backwards the age of the building and the initiation time by carbonation from a large condition assessment data from concrete facades and balconies using statistical simulation methods. The earliest visible corrosion damage on concrete facades was observed in condition assessments already after 8–15 years from construction. In a large group of buildings the damage occurrence was found to reasonably well follow a normal distribution. The design model was found in the case of concrete facades and balconies in Finnish climate conditions to overestimate considerably the propagation phase predictions in all of the studied structure types compared to the statistical analysis. The overestimation in the model is due to the high influence of concrete resistivity and the definition of corrosion penetration needed for the initiation of a crack.

1. Introduction

Starting from the 1960s, concrete structures have become prevalent in Finnish construction. This is a result mainly from urbanization and domestic housing policy in Finland which triggered the production of prefabricated concrete buildings. Corrosion is responsible for approximately 11–40% of the repair costs of prefabricated concrete facades in Finland depending on the surface finishing [1], and along with insufficient frost resistance, carbonation induced corrosion is the most significant degradation mechanism of concrete buildings in Finnish environment. The damage caused by the both mechanisms accounts for € 3.5 billion in repair need and is increasing [1]. It alone makes 1.8% of yearly GDP of Finland [2]. This is an issue that cannot be solved instantly, but requires a rehabilitation plan over several years.

There must be a subjective methodology to compare different repair options technically as well as economically including instant and life cycle costs. Large amount of information on the durability properties of single buildings and their repair possibilities can be gathered in condition assessments but to estimate the residual service life of a concrete structure it is necessary to utilize predictive models.

Degradation models can be divided into empirical, numerical and analytical ones depending on how they have been developed [3]. Empirical models such as [4] are based on assumed direct relationship between corrosion rate and influencing parameters such as experimentally determined coefficients or material properties. Also the use of Delphic oracle method [5] falls under the category of empirical models. Numerical models such as [6,7] are mathematical models that provide approximate solutions using boundary conditions and differential equations inside a medium divided in element matrix (e.g. FEM). Analytical models such as [8,9] are based on closed-form solutions of mathematical equations.

This study analyses the actual observed corrosion damage and active corrosion in concrete facades in Nordic outdoor climate and compares this data with the DuraCrete design model [4] for carbonation initiated corrosion propagation phase. The statistical analysis is based on condition assessment data gathered from the assessment reports of 443 concrete facades and 331 concrete balconies built in 1965–1995. Lollini et al. [10] have conducted a similar study on the initiation phase by carbonation using the fib initiation model [5] and a case study on eight reinforced concrete buildings. This study aims at finding out what is the correspon-

* Corresponding author. Tel.: +358 40 849 0837.
E-mail addresses: arto.kolio@tut.fi (A. Köliö), tonia.pakkala@tut.fi (T.A. Pakkala), petrij.annila@tut.fi (P.J. Annila), jukka.lahdensivu@tut.fi (J. Lahdensivu), matti.pentti@tut.fi (M. Pentti).

http://dx.doi.org/10.1016/j.engstruct.2014.06.038
0141-0296/

dence of the design model to actual observed corrosion damage on concrete facades in Finnish outdoor climate conditions.

2. Background

2.1. Effects of reinforcement corrosion in concrete

The effects of reinforcement corrosion have resulted in high maintenance costs in concrete infrastructure around the world in varying climates but also in climates similar to Finland [11–13]. Regarding concrete facades, corrosion of reinforcement is usually initiated by carbonation. In Finnish outdoor climate in particular there are scarce environmental sources for external chlorides [14].

Corrosion of reinforcement affects concrete structures basically either by cracking of concrete cover caused by corrosion products or by reduction of effective steel cross-section. Cracking occurs in structures where the reinforcement is placed quite near the concrete surface. Cracking accelerates the penetration of harmful agents to concrete and causes visual defects in concrete facades. The performance requirements for structures are many and the suitability of each depends on the type of structure. Therefore the occurrence of cracks is not the ultimate limit for the life of the structure, but rather a limit based on the appearance or serviceability of the structure. There exists an undefined period of residual life after cracking, where the structure will still continue to function adequately until the final limit state were it structural failure, rehabilitation or deconstruction.

2.2. Concrete facades and balconies in Finland

The concrete structures of this building stock that are subject to degradation are facades and balconies, commonly built of prefabricated sandwich facade panels and balcony slab, frame and parapet elements. Building even today is based on an open concrete element system (BES) developed in 1969 that standardizes building units and their details of joints. Table 1 shows a collection of key properties of these structures in regard of durability.

The Finnish building stock, concrete blocks of flats in particular, is highly homogenous by structural solutions. These structures and their construction techniques have remained comparatively uniform for many decades. Finishing, thermal insulation and dimensions of units have changed over time with building regulations but the basic structural idea remains. The concrete panels used in exterior walls of multi-storey residential buildings have been chiefly prefabricated sandwich-type panels with thermal insulation placed between two concrete layers. The surface finishing in 1965–1995 has typically been either exposed aggregate surface or brushed concrete surface that has been painted with a more or less permeable paint. The most common balcony type in Finland from the late 1960s until today consists of a floor slab, side panels and a parapet panel of precast concrete. These stacked balconies have their own foundations and are braced to the building frame horizontally. Balcony slabs are typically cast upside down to form the necessary slope and chutes for the runoff water. The soffit surface of a balcony slab is thereby most commonly floated and painted with a permeable paint.

The requirements given for reinforcement in national concrete code are shown in Table 2. In addition, a common requirement for the cover of auxiliary reinforcement (manufacturing reinforcement, lifting straps) has been 15 mm. Basically, the requirement for concrete cover has remained the same from 1978 to this date (concerning facade concrete). However, in current code the minimum requirement is set, according to climate exposure class, to 10–40 mm. For carbonation induced corrosion, minimum requirements of 10 mm (dry or constantly wet structures) to 25 mm (e.g. facades and balconies) are nowadays used [15]. Nevertheless large scatter is associated with the cover depths of existing concrete facade panels [14] as is later illustrated in Fig. 9. The same was also observed in [10] in the case of reinforced concrete nuclear power plant buildings.

2.3. Climate exposure conditions

Lahdensivu [14] has shown that the most crucial climatic factor for durability of concrete facades are prevailing wind directions during rain and amount of freeze–thaw cycles after liquid precipitation. The most common wind directions during liquid precipitation in Finland are concentrated on south and west direction. Thus, the distribution of rainfall is concentrated on southern and western facades and that can be seen also on cases of observed deterioration caused by carbonation induced corrosion and frost damage. On coastal area annual precipitation is on average mildly higher than in inland. Typically facades and balconies fall into the exposure classes XC3 and XC4 in European standards [17].

Finnish climate is much milder than its location on mid-latitude predicts, mostly due to the warm and steady Atlantic Ocean. Also Scandinavian Peninsula prevents Finland for the most extreme conditions of e.g. coastal areas of Norway. In the Köppen Climate

Table 2
Requirements for the minimum concrete cover of working reinforcement and concrete grade in Finnish concrete codes from 1965 to 1995 [16].

Year	Required minimum concrete cover of reinforcement (mm)	Required concrete grade/ cube strength (MPa)
1965–1977	20	C20/25
1978–1988	25	C20/25
1989–1992	25	C25/30
1993–1995	25	C32/40[a]

[a] Converted from cube strength to concrete grade.

Table 1
Typical dimensions and reinforcement properties of Finnish prefabricated facades and balconies.

Structure/unit	Dimensions	Reinforcement	Comments
Facade sandwich panel	Outer layer 40–70 mm, inner layer 80 mm (non-bearing) or 150 mm (load bearing)	Outer layer: mesh 3–4 mm with 150 mm spacing, edge rebars 6–8 mm, trusses connecting outer and inner layer spacing 600 mm, aux. reinforcement/lifting straps	Thickness of thermal insulation varies with regulations, elastic element joints (polymer sealants), usually no ventilation gap = dries slowly
Balcony slab	Thickness 140–200 mm (sloped upper surface)	Bearing reinforcement: 10–12 mm spacing 100–150 mm in the lower section of the slab upper section: tie rods, aux. reinforcement, lifting straps	Water drainage system varies: drain pipe, spout pipe through the parapet, gap between slab and parapet. No waterproofing
Balcony side panel	Thickness 150–180 mm	Edge rebars 10–12 mm, aux. reinforcement/lifting straps	Height of no more than 8 floors allows the use of non-reinforced concrete panels
Balcony parapet	Thickness 70–85 mm	Heavy reinforcement near both surfaces, rebars 6–8 mm spacing 150	Often cast as one unit with the slab

Classification system (developed by Wladimir Peter Köppen around 1900) Finland locates in the subarctic climate zone in which warm summers and freezing winters are typical.

Although the climate is relatively steady for the latitudes and compared to size, it still varies annually considerably. For example, from 1961 to 2005 annual precipitation in southern Finland varied between 300 and 700 mm which is considerable low and the monthly distribution of precipitation is also relatively minor. However, for durability the most crucial precipitation period is at wintertime because the relative humidity of outdoor air is constantly high as a result of low outdoor temperature, thus the drying conditions being inadequate. In Finland conditions mentioned above are considered to occur between September and April [18] while liquid precipitation has varied between 100 and 480 mm [14]. Due to both the climate differences and the concentration areas of the population, Finland can be divided into four main areas: coastal area, southern Finland, inland and Lapland.

2.4. Models for reinforcement corrosion in concrete structures

Corrosion of steel reinforcement in concrete is commonly regarded as an electrochemical phenomenon meaning that corroding reinforcement works as a mixed electrode where cathodic and anodic areas are formed on the steel surface [19]. The size of anodes and cathodes determine the nature of corrosion. Corrosion due to chlorides usually forms very concentrated pitting corrosion that has a small anode opposed to large cathode and forms high corrosion currents and high rates of corrosion where corrosion due to carbonation is more general over the reinforcement surface with more evenly spaced cathode and anode areas [20]. Therefore, the nature of corrosion plays a role in choosing the fundamental mechanism by which corrosion is modelled. Because concrete protects steel from corrosion as a protective layer for the reinforcement, corrosion does not initiate immediately. This has been taken into account by depicting reinforcement corrosion as a process consisting of two or more consecutive phases [9,21,22] as shown in Fig. 1. The initiation phase of carbonation induced corrosion is well known [21,23,14], but information on the propagation phase is more limited.

The protection to corrosion by concrete alkalinity can be lost by lowering of the pH by carbonation phenomenon between CO_2 and $Ca(OH)_2$ in concrete or the ingress of chlorides. Carbonation is often depicted as a diffusion phenomenon following a square root relationship with exposure time [21]. This model has since been developed further to specify the effect of multiple factors [4] and to include the influence of prevailing weather [5]. Later the original model has been improved by statistical methods [24].

Models for active corrosion of reinforcing steel have been actively developed for chloride induced corrosion, e.g. [4,5,9,25–29] but models given for carbonation induced corrosion cases are more rare, e.g. [4,5,30,31,10]. Reason for this has been assumed to be easy avoidance of carbonation problems in new construction by increasing concrete cover or concrete quality [32]. These measures however cannot be utilized in existing building stock making the modelling of carbonation induced corrosion a relevant issue in renovation and timing of repairs of existing structures.

Corrosion propagation phase until cracking has been traditionally modelled by the corrosion rate and the diameter and cover depth of reinforcement [30]. Propagation phase is lengthened by increasing concrete cover for the reinforcement whereas increasing reinforcing bar diameter will lead to shorter propagation phase. Additionally, relative time of wetness [4] and temperature [4,5] are used to describe environment conditions. For the modelling of the corrosion rate itself, the potential electrolytical resistivity of concrete is used together with factors relating it to different environmental conditions [4,33–35].

Corrosion rate of steel in carbonated concrete has been experimentally observed on existing concrete facades to be greatly dependent on the moisture of the surrounding concrete [36]. High corrosion current was recorded during times when monthly rainfall was exceptionally high. Vice versa, during times when monthly rainfall was low also very low corrosion currents were observed. Active corrosion time in carbonated concrete in Finnish climate was studied recently by combining annual precipitation and its effect to corrosion rate with critical amount of corrosion in regard of concrete cracking [37]. This calculation was valid for rain exposed structures, i.e. concrete facades.

Critical corrosion rates and attack penetration to form cracking are proposed for the estimation of limit states in [30,38–40]. Also a way of calculating corrosion penetration needed for initiation of a crack is presented in [4]. The formation of cracks due to corrosion is dependent on multiple factors including bar diameter, thickness of concrete cover and the type of corrosion products. In the service life by reinforcement corrosion the small cover depths (left tail of the cover depth distribution) are critical. Cover depths of less than 15 mm and fast carbonating concrete have been empirically found to be responsible for the formation of visual defects in concrete facades [14]. Therefore it is important, from the point of view of service life design, to model this left tail precisely.

Otieno et al. [3] have highlighted that problems regarding modelling of corrosion most commonly arise from (i) difficulty in obtaining accurate and easily quantifiable input parameters, (ii) the lack of validation of the proposed model, (iii) advance assumptions made in an attempt to simplify the numerical modelling, (iv) the use of accelerated laboratory tests, (v) small size of test specimens and sample size, (vi) neglecting the effect of service load-induced cracking on corrosion initiation and (vii) from the handling of the variability of model input parameters. Due to the shortage of quantitative data on the scatter of material properties and degradative agents, normal distributions or arbitrarily set variables are often used in calculations in the lack of better alternatives [3,30]. The estimation of the probability density function of concrete cover was concluded by Lollini et al. [10] to be a substantial source of error.

2.5. Condition assessment and database

Concrete facades of buildings in Finland have been subjected to condition assessments since late 1980s and data measured by standardized procedures [41] has been produced in majority of these assessments. The condition assessments consist of preliminary desk top studies, visual observation and rating in situ, measurements and sampling in situ and laboratory tests [42]. Thus, the database includes information on both the durability properties of structures and the actual observed degradation in real outdoor environment conditions. A database has been collected from condition assessments conducted by various professional engineers during 1992–2006. The database includes the condition assessment information of 947 buildings built 1965–1995 [14]. The assessments have been conducted in connection to renovation or systematic maintenance of the building. Typically the same building has not yet been subjected to assessment more than once. This means that each building in the database represents an individual case. The practice has been similar due to uniform guidelines used by all condition assessment practitioners. The database can thereby be argued to be very well suitable for statistical analyses.

The inspected structures have during the assessment been given a visual damage rating. This rating is (1) no visual damage, (2) local damage and (3) wide spread damage. The rating is based on visual observations by the engineer conducting the assessment. In these condition assessments the facade has been inspected for

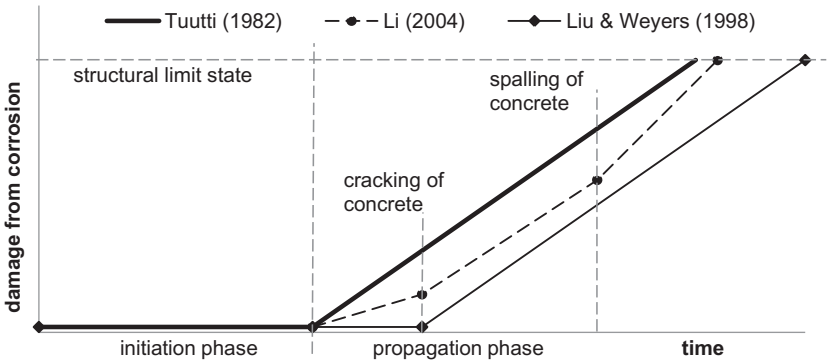

Fig. 1. Models for reinforcement corrosion utilizing the principle of initiation and propagation.

damage as one unit. Therefore, e.g. differences in signs of damage on facades facing different directions have not been recorded. Differences between the degradation of northern and southern facades are common due to the characteristics of driving rain in Finnish climate [14]. This is not however represented by the database.

Carbonation depth has been measured from core samples taken during the field investigation by spraying freshly cut surface with phenolphthalein pH indicator. By average 12 samples have been taken from one building [42]. Reinforcement cover depths have been mapped from the facade and balcony surfaces using a cover meter and the readings have been verified by measuring the cover depth from core samples.

3. Research methods and material

3.1. Research material

Three types of surfaces were analysed in the statistical study: facade with brushed and painted surface, facade with exposed aggregate surface and the soffit surface of a balcony slab (which commonly is floated and painted with permeable paint). These are the most commonly used surface finishes of concrete buildings from 1965 to 1980 in Finland. This definition limits the database for this study to cover 250 brushed painted concrete buildings, 193 exposed aggregate concrete buildings and 331 concrete balcony slabs. The data used in the statistical calculations are depicted in Table 3.

The age at which visual corrosion damage is generally observed in concrete facades was studied using visual damage ratings given in condition assessments. This damage rating was used together with the age of buildings to study the time it takes for corrosion damage to propagate. A distribution over time was produced for the formation of visual damage based on damage ratings 2 and 3. The facades rated 1 (no visual damage) were excluded from the analysis for the moment of visual damage occurrence is not known for this part of the data. This limitation will cause the analysis to underestimate the time to visual damage. Because the damage rating of the buildings is linked to the time of condition assessment these examinations do not take into account the fact that visual cracks or damage have, in fact, emerged some time before the assessment date. This time before the condition assessment is in this study unknown. Thus, the time to visual damage is, in consequence to this, overestimated. These two features produce error to the statistical analyses that, however, partly overlap, i.e. partly cancel each other out. The results of this study should be treated accordingly.

3.2. Statistical analysis

Initiation phase by carbonation was studied by using carbonation depth measurements and reinforcement cover depth measurements produced in condition assessments. Carbonation coefficient was calculated from the measured carbonation depths by the square root relationship in Eq. (1) [21]. This coefficient was then fitted as a statistical distribution to produce probabilities for carbonation times to different depths on different facade surfaces.

$$x = k \cdot \sqrt{t_0} \tag{1}$$

where x is the carbonation depth, k the carbonation coefficient (mm $a^{-1/2}$), and t_0 is the initiation time (years).

Reinforcement cover depths were fitted as distributions to calculate the actual initiation period to the depth of reinforcement in different facade surfaces. To match the research data of visual damage the left tail of cover depth distributions, i.e. covers of $\leqslant$15 mm was used in both statistical analyses and model calculations. This selection is further discussed in Section 4.1.

Finally, the active corrosion period was calculated backwards from the ages at which corrosion damage was observed and the initiation period on these facade surfaces by Eq. (2).

$$t_{CRACK} = t_0 + t_1 \tag{2}$$

where t_{CRACK} is the age at which visual corrosion damage is observed (years), t_0 the initiation phase by carbonation (years), and t_1 is the active corrosion phase (years).

An approximation for the active corrosion period was produced with a Monte Carlo simulation using these statistical variables by sampling 10,000 calculations having an estimated statistical error of $\leqslant$1%. If the normal distributions produced a negative value for carbonation coefficient it was neglected from the calculations as false result. The calculation of carbonation progress is based on a simplified model which has also been questioned many times among the researchers in this field of science. It is, however, justified to use the model here for the coefficients are based on actual measurements of carbonation depth on these facade surfaces and the same model has been used to calculate the coefficients. Thus, the coefficients are calibrated for this model. The use of normal distribution for carbonation coefficients fits well for the data within 95% of the values. It, however, leads to very small and even negative values (which is false already by definition) in the far end of the left tail of the distribution thereby leading to exaggerated carbonation time. The use of log-normal distribution would eliminate the possibility of negative values but would also shift the balance of the distribution and overestimate the amount of very high coefficient values ($k \geqslant 5.00$).

Table 3
Research material for the statistical analysis based on condition assessment database.

	Brushed painted concrete facades	Exposed aggregate concrete facades	Concrete balcony slab
Age of the structure (years)	9–43	7–37	7–52
Visual ratings (number of observations)	250	193	331
Carbonation coefficient (number of samples)	1285	849	884
Reinforcement cover depth (number of measurements)	60,640	104,958	12,957

3.3. Propagation phase modelling

Statistically calculated active corrosion phase was compared to active corrosion phase proposed by DuraCrete model for carbonation induced corrosion [4]. This model was chosen for it represents current widely agreed design methodology for service life regarding carbonation initiated corrosion. This model is empirical using concrete resistivity as a decisive factor.

Corrosion penetration was calculated by Eq. (3) utilizing corrosion rate V^d determined by Eq. (4). The corrosion rate is influenced by characteristic resistivity of concrete ρ^c calculated by Eq. (5) which in part is influenced by temperature in Eq. (6). The parameters used in calculation are given in Table 4. Average time of wetness and temperature calculated from meteorological data were used where applicable in the model. The resistivity was given values based on references [4,33–35]. Since the concrete discussed here has a considerably high w/c-ratio, it is reasonable to presume a low resistivity. For a detailed description of the propagation phase model and the model specific parameters the reader is advised to reference [4].

$$p^d = \begin{cases} 0 \\ V^d w^t (t - t_i^d) \end{cases} \tag{3}$$

where p^d is corrosion penetration, V^d is corrosion rate, w^t is the time of wetness, t is time and t_i^d is the service life design value.

$$V^d = \frac{m_0}{\rho^c} \cdot \alpha^c \cdot F_{cl}^c \cdot \gamma_V \tag{4}$$

where m_0 is the constant for corrosion rate versus resistivity, ρ^c is the characteristic concrete resistivity, α^c is the pitting factor, F_{cl}^c is the chloride corrosion rate factor and γ_v is the partial safety factor.

$$\rho^c = \rho_0^c \cdot \left(\frac{t_{hydr}}{t_0}\right)^{n_{res}^c} \cdot k_{c,res}^c \cdot k_{T,res}^c \cdot k_{RH,res}^c \cdot k_{cl,res}^c \tag{5}$$

where ${\rho_0}^c$ is the potential electrolytic resistivity, t_{hydr} is hydration age of concrete, t_0 age of the concrete at the compliance test, n_{res}^c is the age factor for the electrolytic resistivity and $k_{c,res}^c, \ldots, k_{cl,res}^c$ are factors that take into account curing, temperature, humidity and the presence of chlorides, respectively.

$$k_{T,res}^c = \frac{1}{1 + K^c(T_{mean} - 20)} \tag{6}$$

where K^c is the temperature factor and T_{mean} is mean annual temperature.

The corrosion penetration needed for initiation of a crack is calculated by Eq. (7) where a_1, a_2 and a_3 are regression parameters, x^d is the cover thickness, d is the reinforcement diameter and $f_{c,sp}^d$ is concrete splitting tensile strength. Reinforcement diameter and concrete strength were chosen according to the structure. The left tail of cover depth distributions of $\leqslant$15 mm concrete covers derived from condition assessment data was used to match the visual damage data. The parameters are given in Table 4.

$$p_0^d = a_1 + a_2 \frac{x^d}{d} + a_3 f_{c,sp}^d \tag{7}$$

4. Results and discussion

4.1. Time to cracking

The age of the buildings at the time of damage observation have varied from 8 to 52 years as shown in Fig. 2. The first visual damage had occurred after 15 years from construction in brushed and painted concrete facades and after 8 years in exposed aggregate facades. In balcony slabs first damage was observed after 9 years. By median, visual corrosion damage has formed on concrete facades after 21–25 years from construction (exposed aggregate and brushed painted respectively). Although the exposed aggregate surface is carbonated slower than brushed concrete, it is after initiation damaged faster owing to higher porosity and the lack of paint coating which would keep the structure more dry. In balcony slab corrosion damage has formed, by median, after 22 years from construction.

Fig. 3 shows the age distribution of observations of visual damage on concrete facades with painted concrete surface and exposed aggregate surface and on soffit surfaces of balcony slabs. By assuming the appearance time of corrosion damage to follow a normal distribution, the mean value, standard deviation and thereby the coefficient of variation can be estimated as in Table 5.

In approximately half of the facades subjected to condition assessment (52–65% depending on the facade type) visual corrosion damage had not occurred. The ages of these undamaged structures were 9–40 years for brushed painted concrete facades, 7–33 years for exposed aggregate facades and 7–46 years for balcony slabs. The moment of visual damage occurrence is not known for this part of the data and they were excluded from the statistical analysis. Although buildings in both groups are of similar ages, variation in the durability properties of the structure or in the climate stress will result in variation in visual damage occurrence. The durability properties of these structures, e.g. cover depths and capillary porosity of concrete scatter widely [14] and thereby only the more susceptible structures have been damaged.

4.2. The initiation phase

Carbonation coefficients describing the rate of carbonation were fitted normal distributions, see Fig. 4. Fig. 4 shows that the normal distribution provides a fairly good fit for the measured data. The free form upper boundary curve reveals that the data is not (or at the most extremely slightly) skewed from the mean value (3.08). However, it can be argued that the normal distribution produces in this case negative values for the carbonation coefficient and on this ground cannot be entirely correct. Also, in the case of single buildings, skewed distribution of carbonation depths have been observed [43]. However, in a large group of buildings, slight differences in concrete production, casting and curing as well as different age of buildings tend to shift the distribution more normal. In practical case the normal distribution works well for at least 95% of the value range if possible zero or negative values are eliminated. Carbonation coefficients determined for different facade surfaces are shown in Fig. 5. In general, a large scatter is

Table 4
Parameters for Eqs. (3)–(7).

Parameter	Min.	Mean	Max.	Constant	Comments
$w^t_{facades}$ (−)	0.17	0.30	0.38		Meteorological data, facades
$w^t_{balconies}$ (−)	0.09	0.1	0.11		Set value for the soffit surface
m_0 (μm Ωm/a)				882	Characteristic value
α^c (−)				2	Carbonation case
F^c_{cl} (−)				1	Carbonation case
γ_v (−)				1	Safety factors set as 1
ρ^c_0 (Ωm)	50		200		Wet, OPC concrete
t_0 (years)				0.0767	Characteristic value
t_{hydr} (years)				1	Characteristic value
n^c_{res} (−)				0.23	Characteristic value, OPC
$k^c_{c,res}$ (−)				1	
$k^c_{cl,res}$ (−)				1	Carbonation case
$k^c_{RH,res}$ (−)				1.44	Unsheltered
T_{mean} (°C)	0.6	3.4	5.3		Meteorological data
K^c (°C^{-1})				0.025	Characteristic value
a_1 (μm)				74.4	Characteristic value
a_2 (μm)				7.3	Characteristic value
a_3 (μm)				−17.4	Characteristic value
$f^{tl}_{c,sp}$ (μm/MPa)				2.2	Based on C20/25 concrete
d (mm)				8	Edge reinforcement
x^d (mm)	Varies	Varies	15		Normal distribution, varies depending on the structure (Figs. 9 and 10)

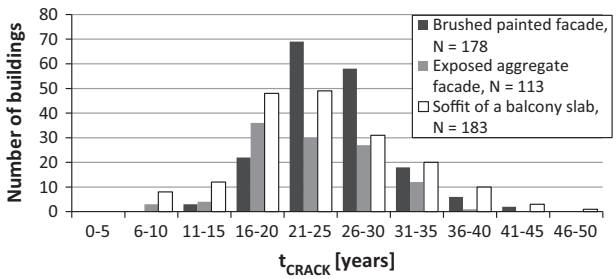

Fig. 2. Age at which visual corrosion damage has been observed on facades and balcony slabs.

Table 5
Time to observed corrosion cracking in different types of facades.

Type of structure	Observed corrosion cracking in 95% of cases (years)	Mean, μ	Coefficient of variation	Number of observations, N
Brushed, painted concrete facades	17–37	27	0.19	178
Exposed aggregate concrete facades	13–33	23	0.22	113
Concrete balcony slab soffit surface	10–41	25.5	0.30	183

associated with the carbonation coefficients of all structures. Owing to a higher cement content, exposed aggregate concrete is carbonated slower that the brushed and painted concrete. In balcony slab soffit surface the carbonation is fast because the surface is kept rather dry.

As shown in Figs. 6–8, when the reinforcement is placed according to requirements with sufficient concrete cover, the corrosion initiation time is by median 85 years for brushed and painted concrete, 163 years for exposed aggregate concrete and 66 years for the soffit of a balcony slab. However, by service life consideration with a target service life of 50 years and a 5% safety level, the initiation period is 28 years for brushed and painted concrete, 38 years for exposed aggregate concrete and 22 years for the balcony slab soffit surface. The target service life is not achieved by the initiation phase alone. Furthermore, the initiation is even faster when considering the smaller than required cover depths. Taking the estimate the other way around reveals that, with specified concrete cover, the safety level for the target service life of 50 years is 25%, 11% and 37% respectively for brushed and painted concrete,

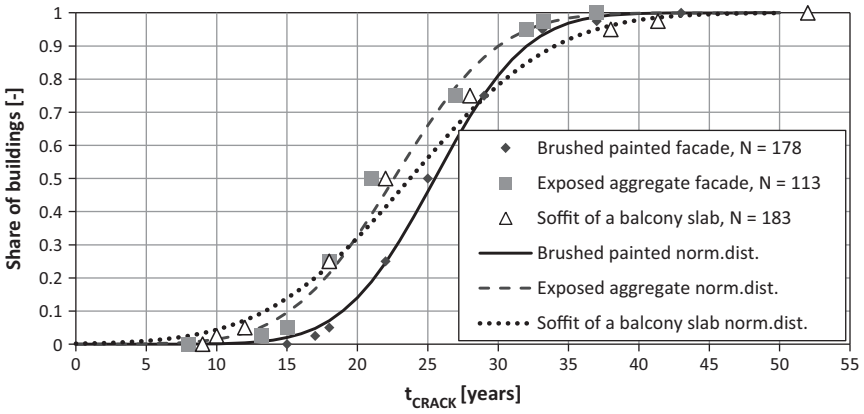

Fig. 3. Statistical distributions for ages at which visual corrosion damage was observed on concrete facades.

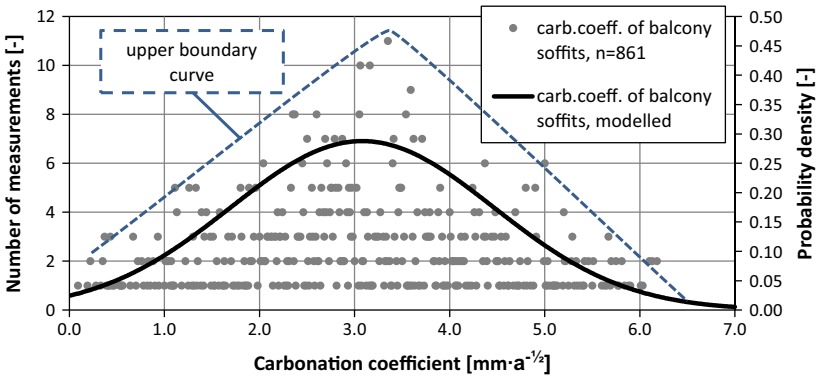

Fig. 4. Fitting of distribution for the carbonation coefficient of balcony slab soffit surfaces.

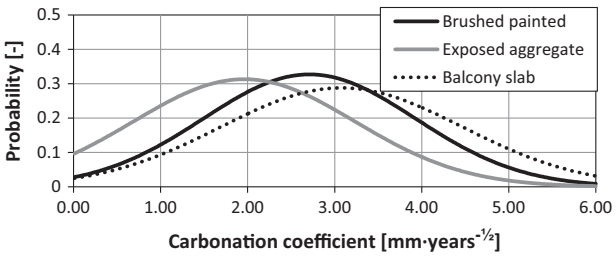

Fig. 5. Differences in carbonation coefficients on diferent facade surfaces.

exposed aggregate concrete and the balcony slab soffit surface meaning that this share of structures fails to meet the requirement.

The left tails of cover depth distributions of reinforcement in the three different types of structures were used to decide how large portion of the reinforcement is partial in the formation of visual corrosion damage. Measured cover depths of reinforcement for edge bars (facades) and bearing reinforcement (balcony slab) are presented in Fig. 9. The distributions used in statistical analyses as well as in DuraCrete model calculations are presented in Fig. 10.

4.3. Propagation phase in carbonated concrete

The active corrosion time was calculated as the remainder of time from construction to the occurrence of visual damage and the time of corrosion initiation. The results in Fig. 11 show the propagation phase in the structures most susceptible to corrosion. The active corrosion periods scatter widely due to different case specific geographical and micro climatic conditions and there are differences between different facade surfaces and balconies.

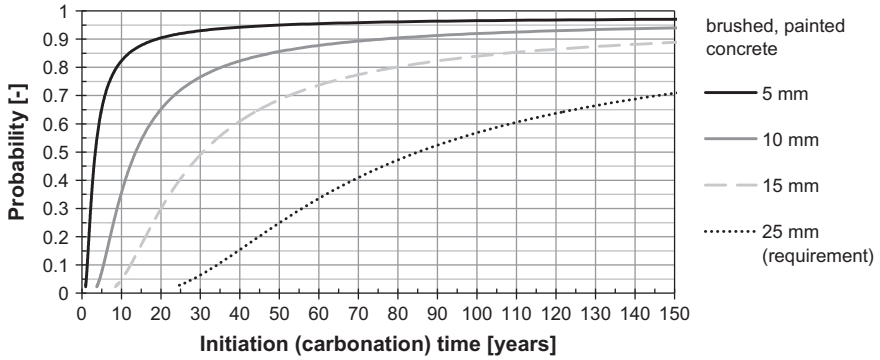

Fig. 6. The distribution of initiation time by carbonation to different depths of cover of reinforcement in brushed and painted concrete facades.

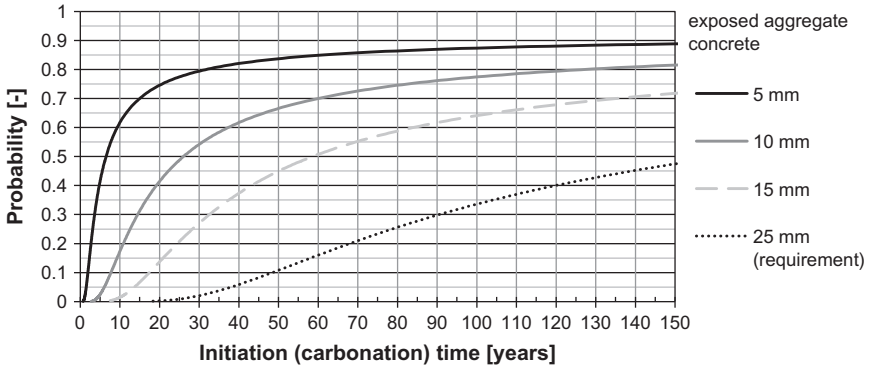

Fig. 7. The distribution of initiation time by carbonation in exposed aggregate concrete facades.

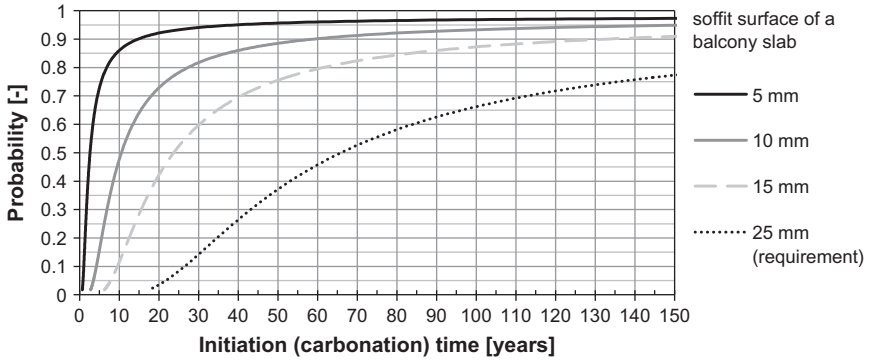

Fig. 8. The distribution of initiation time in the soffit surface of balcony slabs.

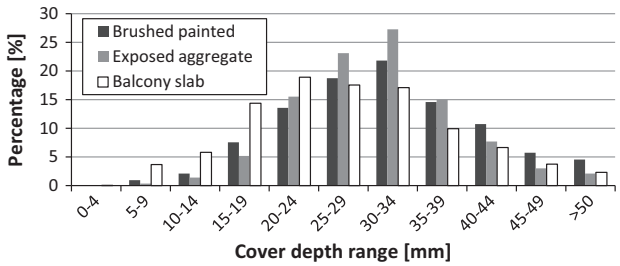

Fig. 9. Distribution of reinforcement cover depths in different concrete surfaces.

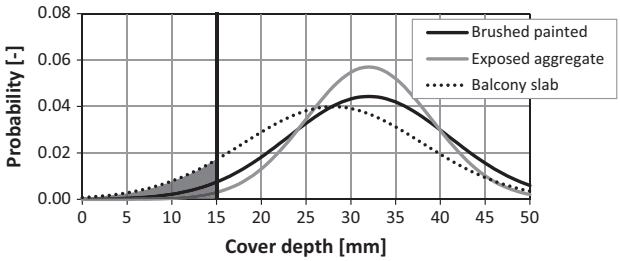

Fig. 10. Normal distributions for concrete cover were used in the modelling of the propagation phase. Covers of ⩽15 mm were used in modelling consistent to the statistical analyses.

According to the calculation, the active corrosion period is 0.6–1.4 years when adopting a commonly used 5% safety level. It relates to corrosion of reinforcement with extremely small cover depth or in very capillary concrete. However, this safety level may be too strict compared to empirical knowledge. As the effects of corrosion in this context are mainly visual defects, a safety level of 50% could be applied. In these cases the active corrosion period would be 6–12 years depending on the surface type. Because the share of below 15 mm cover depths is usually small, see Fig. 9, the safety level could in practice be tied to the amount of small cover depths, for example 100% minus the share of ⩽15 mm cover depths. This means that active corrosion in reinforcement deep inside concrete could be taken into account in service life considerations as a fairly long period of time.

4.4. Comparison of the statistical calculation with modelled results

By utilizing the idea presented in [37] but varying the critical corrosion depths by values from the literature, the active corrosion times (to cracking) shown in Table 6 were produced for different parts of Finland.

The lowest limit in Table 6 (15 μm) could depict the case of reinforcement with a small cover depth. These active corrosion times are also similar to the 5% safety level in Fig. 11. The active corrosion times obtained with 80 μm limit describe better the reinforcement deeper inside concrete and give results in the same magnitude as 50% safety level. The differences between localities in Table 6 result from varying exposure of facade surfaces to wind-driven rain in different parts of Finland. Naturally, due to higher annual rainfall corrosion is fastest in coastal areas. Exposure to climate of facade surfaces varies monthly and yearly because of the variation in monthly/yearly rainfall, windiness, etc. meaning that reinforcement corrosion in outdoor environment is far from steady state phenomenon. Therefore, the modelling of corrosion should be taken towards straight relationship between environment factors rather than only time-dependency.

Fig. 12 shows the comparison of the statistical study and the DuraCrete design model calculation using characteristic parameter values for C20/25 facade concrete in Finnish climate (values to the more severe side from Table 4). As represented, a service life design calculation with no included partial safety factors would produce

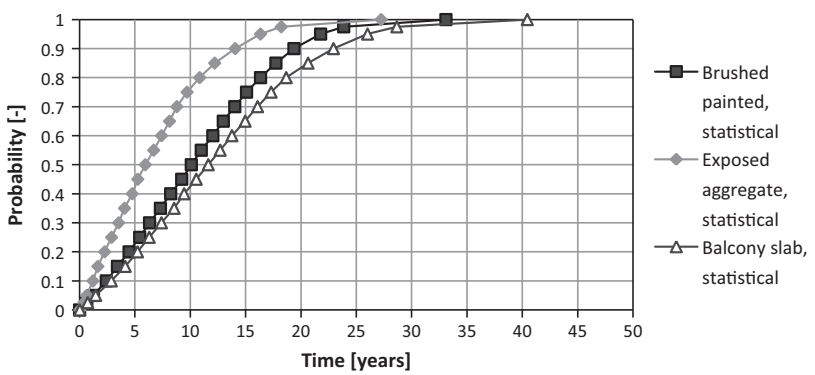

Fig. 11. Propagation time to form visual damage observed in different facade structures by statistical simulation.

Table 6
Active corrosion time in years from corrosion initiation to the formation of cracks in current climate (years 1979–2009). Formation of cracks is modelled with different critical depths of corrosion proposed in literature.

Critical depth (μm)	Helsinki-Vantaa airport (coastal area)	Jokioinen observatory (southern Finland)	Jyväskylä-Tikkakoski airport (inland)	Sodankylä observatory (Lapland)
15 lower limit [39]	1.7	1.8	2.4	11.3
50 upper limit [39]	5.7	6.1	8.2	37.5
80 [30]	9.1	9.7	13.0	60.0
100 [38]	11.3	12.1	16.3	75.0

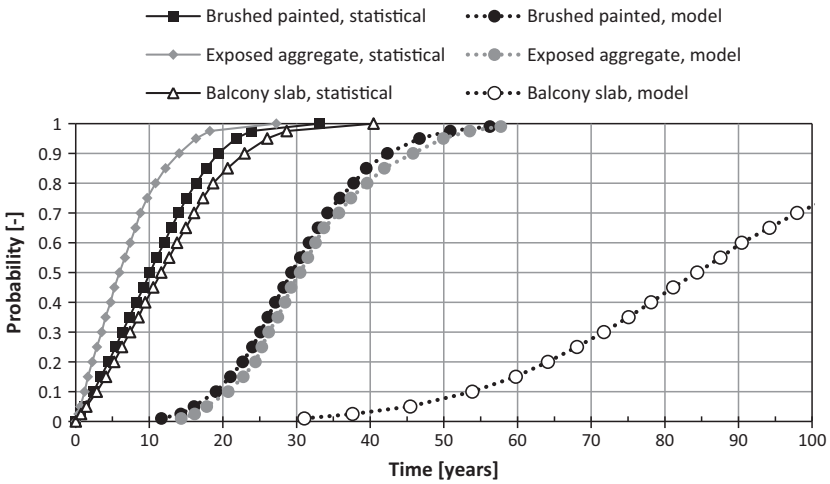

Fig. 12. Lengths of the active corrosion phase in reinforced concrete calculated statistically from condition assessment data and modelled using the DuraCrete propagation phase model.

overestimated predictions for the propagation phase of concrete facades and balconies. Differences between model predictions of different structures are inherent from different weather exposure and cover depth distribution.

The propagation phase of the soffit surface of a balcony slab is highly overestimated due to the choice of the equivalent period of wetting. Generally, estimating the soffit surface of a balcony slab to be sheltered from rain is valid and thereby a long propagation phase is expected. However, as is observed in condition assessments in practice, corrosion damage in balcony slabs is formed near the edges and badly working details of rainwater runoff which is keeping the structure wet locally. Thereby, the actual propagation time until cracking is quite short, as shown by the statistical results. Knowing this, the model does not in this case predict service life sufficiently as illustrated in Fig. 12.

Parametric analysis conducted on the yearly mean temperature, time of wetness and concrete resistivity with minimum and maximum values presented in Table 4 revealed a high influence from the two latter parameters as shown in Figs. 13–15. The temperature was assumed by climate data to vary between the minimum and maximum of 0.6 °C and 5.3 °C respectively. Time of wetness was assumed, also by climate data, to vary between 0.17 and 0.43. Concrete resistivity was varied between 50 Ωm and 200 Ωm.

The influence of time of wetness parameter and concrete resistivity parameter on the propagation phase can be even of the order of 2 and 4 respectively. The climate related temperature and time of wetness are easily understood as statistical parameters and thereby their scatter can be quantified by meteorological data. Especially the choice of concrete resistivity parameter has a substantial influence on the model results.

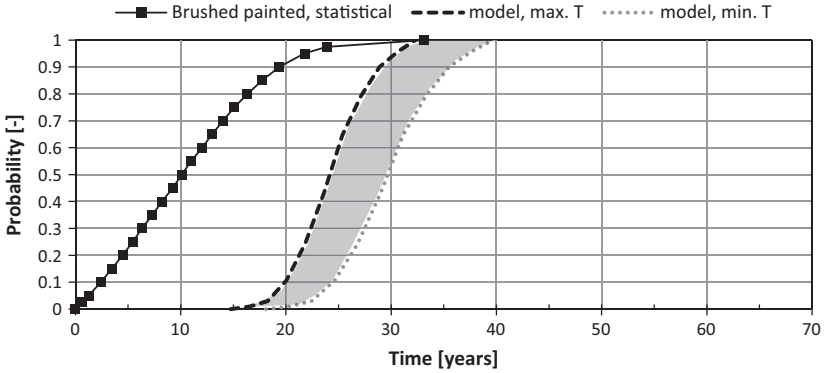

Fig. 13. The influence of annual mean temperature on the propagation phase prediction by the DuraCrete model.

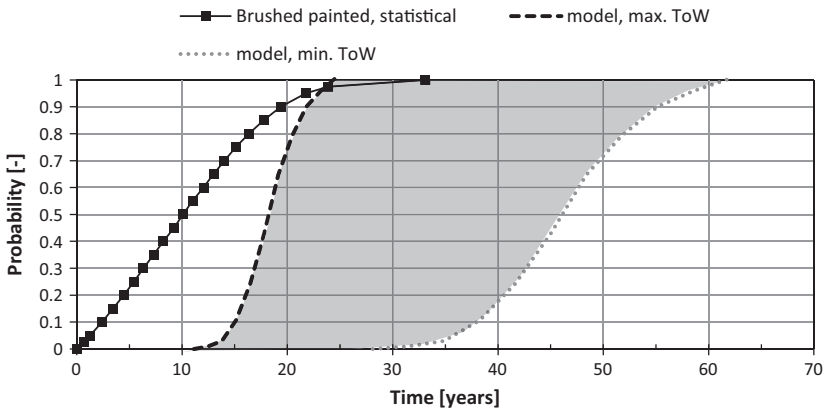

Fig. 14. The influence of time of wetness vertical facade surfaces on the propagation phase prediction.

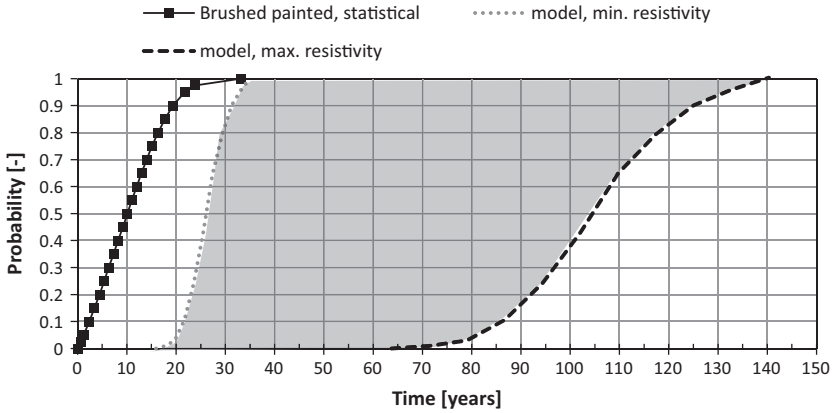

Fig. 15. The influence of concrete resistivity on the propagation phase prediction.

5. Conclusions and recommendations

Even though the corrosion time scatters widely depending on facade type, properties and microclimate factors it can be assessed using statistical methods. These statistical analyses also provide a way to validate service life models and to narrow down the problems usually associated with models. The propagation phase of reinforcement corrosion is found from condition assessment cases to scatter from practically zero to 30–40 years depending on the structure and climate. A recent study at Tampere University of Technology on the effect of precipitation to active corrosion has shown similar results. The DuraCrete design model was found not to provide adequate predictions for the propagation phase in the assessed situation. The prediction of the model is general and does not reasonably take into account the actual micro climate and the properties of the facade. These properties are the realized cover depths and resistivity of the specific concrete used as well as moisture load, runoff water handling and possible local increase in moisture load, e.g. as seen with the edge area of a balcony slab. In reality, these details are the first to damage from moisture related degradation phenomena.

Especially the concrete resistivity parameter and the definition of corrosion penetration needed for the initiation of a crack have a substantial influence on the model results. Therefore, more emphasis should be put on the determining of the parameter in each concrete and moisture state related case. Studies are needed to determine correct statistical variables for the case specific parameters in order to enable geography dependent design of service life. The modelling of corrosion should, in principle, be taken towards straight relationship between environment factors rather than straight time-dependency, because reinforcement corrosion in outdoor environment is not a steady-state process. This would also produce versatile models capable of taking into account different climates.

The question about the safety level in regard of reinforcement corrosion in concrete facades is closely tied to the desired visual appearance. A safety level of 5% represents the case of a very small cover depth and porous concrete. In the case of concrete facade a safety level of 50% or a safety level tied to the share of small cover depths could be used in assessing the active corrosion period in connection to service life design. The amount of accepted visual signs of damage should go with the discussion on the proper safety level. Allowing more visual damage could enable the use of more broad safety level. In a high standard case the safety level could be chosen more strictly.

Because the statistical method of studying corrosion propagation gives valuable information regarding actual exposure conditions it would be beneficial to further improve it by eliminating the possible sources for error mentioned in this paper. This is possible by a specific sampling study in connection with a certain series of condition assessments by:

- targeting samples on visually damaged areas on the facades (This has not been done in condition investigations, because the sample does not reveal anything new from the point of view of repair planning.) From these samples the concrete cover of

corroded reinforcement and the depth of carbonation (as well as other concrete properties) can be measured from the right (and same) spot,
- focusing the visual inspection of corrosion damage on each facade individually and more precisely, e.g. where exactly these are,
- quantifying the amount of damage more accurately, e.g. meters of corroded steel per m^2 of facade.

These suggestions do not improve the condition assessment practice on the point of view of selecting proper repair measures for the individual case, but will, through the results of the study, greatly improve the investigator's ability to estimate the residual life of the reinforcement.

Acknowledgement

The study was made possible by the Doctoral Programme of Built Environment (RYM-to) under the funding of the Academy of Finland.

References

[1] Köliö A. Degradation induced repair need of concrete facades. MSc thesis. Tampere University of Technology; 2011. 74p [in Finnish].
[2] Statistics Finland. Statistics on dwellings and housing conditions. Internet source; 2011. <http://www.tilastokeskus.fi/til/asas/index_en.html>.
[3] Otieno M, Beushausen H, Alexander M. Modelling corrosion propagation in reinforced concrete structures – a critical review. Cem Concr Compos 2011;33(2011):240–5.
[4] DuraCrete. Probabilistic performance based durability design of concrete structures. The European union – Brite EuRam III, DuraCrete. Final technical report of DuraCrete project, document BE95-1347/R17. CUR, Gouda, Nederland; 2000.
[5] Fib Bulletin No. 34. Model code for service life design. International federation for structural concrete, Lausanne; 2006. 116p.
[6] Gulikers J, Raupach M. Numerical models for the propagation period of reinforcement corrosion: comparison of a case study calculated by different researchers. Mater Corros 2006;57(8):618–27.
[7] Sanad AM, Moussa MA, Hassan HA. Finite element modelling of steel corrosion in reinforced concrete cylinders. Adv Mater Res 2013;785–786:273–8.
[8] Goltermann P. Mechanical predictions on concrete deterioration. Part 1: Eigenstresses in concrete. ACI Mater J 1994;91(6):543–50.
[9] Liu Y, Weyers RE. Modelling the time-to-corrosion cracking in chloride contaminated reinforced concrete structures. ACI Mater J 1998;95(6):675–81.
[10] Lollini F, Redaelli E, Bertolini L. Analysis of the parameters affecting probabilistic predictions of initiation time for carbonation-induced corrosion of reinforced concrete structures. Mater Corros 2012;63(12):1059–68.
[11] Fasullo EJ. Infrastructure: the battlefield of corrosion. Corrosion forms and control for infrastructures, ASTM STP 1137. p. 1–16.
[12] Wallbank EJ. The performance of concrete bridges: a survey of 200 highway bridges. London: HMSO Publication; 1989. 96p.
[13] Tilly GP. Durability of concrete repairs. In: Grantham M, editor. Concrete repair – a practical guide. New York: Taylor & Francis; 2011. p. 231–47.
[14] Lahdensivu J. Durability properties and actual deterioration of Finnish concrete facades and balconies. Tampere University of Technology, TUT Publ. 1028; 2012. 117p.
[15] Concrete Association of Finland. BY 50 concrete code 2012. Helsinki, The Concrete Association of Finland; 2012 [in Finnish].
[16] Pentti M, Mattila J, Wahlman J. Repair of concrete facades and balconies, Part I: Structures, degradation and condition investigation. Tampere: Tampere University of Technology, Structural Engineering. Publication 87; 1998. 157p [in Finnish].
[17] SFS-EN 206-1 + A1 + A2. Concrete. Part 1: Specification, performance, production and conformity. Finnish Standards Association SFS; 2005. 71p.
[18] Ruosteenoja K, Jylhä K, Mäkelä H, Hyvönen R, Pirinen P, Lehtonen I. Weather data for building physics test reference years in the observed and projected future climate – results from the REFI-B project. Finnish meteorological institute reports, Helsinki, vol. 1; 2013. 48p [in Finnish].
[19] Page CL. Basic principles of corrosion. In: Schiessl P, editor. Corrosion of steel in concrete. London: Chapman and Hall; 1988. p. 3–21.
[20] Schiessl P, editor. Corrosion of steel in concrete. London: Chapman and Hall; 1988. 101p.
[21] Tuutti K. Corrosion of steel in concrete. Stockholm. Swedish Cement and Concrete Research Institute. CBI Res 1982;4(82):304.
[22] Li CQ. Reliability service life prediction of corrosion affected concrete structures. ASCE J Struct Eng 2004;130(10):1570–7.
[23] Monteiro I, Branco FA, de Brito J, Neves R. Statistical analysis of the carbonation coefficient in open air concrete structures. Constr Build Mater 2012;29:263–9.
[24] Ann KY, Pack S-W, Hwang J-P, Song H-W, Kim S-H. Service life prediction of a concrete bridge structure subjected to carbonation. Constr Build Mater 2010;24(8):1494–501.
[25] Bažant ZP. Physical model for steel corrosion in concrete sea structures—theory. J Eng Mech Div Proc ASCE 1979;105:1137–53.
[26] Jin W-L, Wang X-Z, Song Z-G. A.probabilistic model for corrosion prediction of steel reinforcement. Int J Model Ident Control 2008;4(3):268–77.
[27] Al-Harthy AS, Stewart MG, Mullard J. Concrete cover cracking caused by steel reinforcement corrosion. Mag Concr Res 2011;63(9):655–67.
[28] Schiessl P, Beck M, Burkert A, Harnisch J, Isecke B, Osterminski K, Raupach M, Tian W, Warkus J. Deterioration model and input parameters for reinforcement corrosion. Struct Concr 2012;13(3):145–55.
[29] Osterminski K, Schiessl P. Design model for reinforcement corrosion. Struct Concr 2012;13(3):156–65.
[30] Siemes AJM, Vrouwenvelder ACWM, van den Beukel A. Durability of buildings: a reliability analysis. Heron 1985;30(3):3–48.
[31] Marques PF, Costa A. Service life of RC structures: carbonation induced corrosion. Prescriptive vs. performance-based methodologies. Constr Build Mater 2010;24(3):258–65.
[32] Raupach M. Models for the propagation phase of reinforcement corrosion – an overview. Mater Corros 2006;57(8):605–13.
[33] Glass GK, Page CL, Short NR. Factors affecting the corrosion rate of steel in carbonated mortars. Corros Sci 1991;32(12):1283–94.
[34] Polder R. Test methods for onsite measurement of resistivity of concrete – a RILEM TC-154 technical recommendation. Constr Build Mater 2001;15(2-3):125–31.
[35] Redaelli E, Bertolini L, Peelen W, Polder R. FEM-models for the propagation period of chloride induced reinforcement corrosion. Mater Corros 2006;57(8):628–35.
[36] Mattila J, Pentti M. Suojaustoimien tehokkuus suomalaisissa betonijulkisivuissa ja parvekkeissa (The efficiency of protective measures in Finnish concrete facades and balconies). Tampere University of Technology, Research report 123; 2004. 69p [in Finnish].
[37] Köliö A, Pakkala TA, Lahdensivu J, Kiviste M. Durability demands related to carbonation induced corrosion for Finnish concrete buildings in changing climate. Eng Struct 2014;62–63(2014):42–52.
[38] Broomfield J. Corrosion of steel in concrete. 2nd ed. Oxon: Taylor & Francis; 2007.
[39] Alonso C, Andrade C, Rodriguez J, Diez JM. Factors controlling cracking of concrete affected by reinforcement corrosion. Mater Struct 1998;31:435–41.
[40] Andrade C. Measurement of polarization resistance on-site. In: Corrosion of steel in reinforced concrete structures. Final report of COST action 521, Office for official publications of the European communities, Luxembourg; 2003. p. 82–98.
[41] Concrete Association of Finland. BY 42, Condition assessment manual of concrete facades and balconies. Helsinki: The Concrete Association of Finland; 2002 [in Finnish].
[42] Lahdensivu J, Varjonen S, Pakkala T, Köliö A. Systematic condition assessment of concrete facades and balconies exposed to outdoor climate. Int J Sustain Build Technol Urban Dev 2013;4(3):199–209.
[43] Pentti M. The accuracy of the extent-of-corrosion estimate based on the sampling of carbonation and cover depths of reinforced concrete facade panels. TUT Publ.; 1999. p. 105. 274.

III

EVALUATION OF A CARBONATION MODEL FOR EXISTING CONCRETE FACADES AND BALCONIES BY CONSECUTIVE FIELD MEASUREMENTS

by

Köliö A., Niemelä P. & Lahdensivu J., Jan 2016

Cement and Concrete Composites vol 65, 29-40

http://dx.doi.org/10.1016/j.cemconcomp.2015.10.013

Cement and Concrete Composites 65 (2016) 29–40

Contents lists available at ScienceDirect

Cement and Concrete Composites

journal homepage: www.elsevier.com/locate/cemconcomp

Evaluation of a carbonation model for existing concrete facades and balconies by consecutive field measurements

Arto Köliö [a, *], Petri J. Niemelä [b], Jukka Lahdensivu [a]

[a] Tampere University of Technology, P.O. Box 600, FI-33101, Tampere, Finland
[b] Engineering Office Lauri Mehto Oy, Finland

ARTICLE INFO

Article history:
Received 28 January 2015
Received in revised form
19 August 2015
Accepted 7 October 2015
Available online 22 October 2015

Keywords:
Concrete
Carbonation
Corrosion
Field measurement
Service life
Modelling

ABSTRACT

The square root model is widely used to predict the initiation phase of reinforcement corrosion induced by carbonation of the concrete cover. The model is based on diffusion laws which makes its validity arguable. The model has been accused of not being able to model accurately carbonation in structures exposed to drying/wetting cycles. The model was evaluated by field measurements on 18 existing concrete buildings conducted twice at an average interval of 8 years. Data from individual parallel samples as well as averaged measurement data were produced. The propagation of carbonation over a certain period of time and variation in the carbonation coefficient were studied using the data. Individual measurements indicated high variation and even inconsistency in carbonation depth. Thus, the carbonation coefficient calculated for the square root model also varied widely. Despite the high scatter, the averaged carbonation of many buildings was found to be closely in line with the prediction of the square root model.

1. Introduction

Reinforcement corrosion has resulted in high maintenance costs of concrete infrastructure around the world in different climates including climates similar to that of Finland [1–3]. Carbonation of the concrete cover is one factor behind the initiation of corrosion damage in reinforced concrete structures. In the case of concrete facades, it is also usually the major cause of corrosion initiation. In Finnish conditions chloride-induced corrosion of facades and balconies is extremely rare [4].

The concrete structures of the building stock subject to degradation are facades and balconies, commonly built of prefabricated sandwich facade panels and balcony floor slabs and side and parapet panels. The open concrete element system (BES) developed in the late 1960's uses standardised precast concrete panels and joint details. The concrete panels used in exterior walls of multi-storey residential buildings have been chiefly prefabricated sandwich-type panels with thermal insulation between two concrete layers. The most common balcony type in Finland from the late 1960's until today consists of a floor slab, side panels and a parapet panel of precast concrete. These stacked balconies have their own foundations and are fastened horizontally to the building frame. More information about these structures can be found in other sources [4,5].

Corrosion of reinforcement ultimately affects concrete structures either by cracking of the concrete cover as a result of stresses exerted by the deposition of corrosion products or by reducing effective steel cross-section. These are considered limit states in service life predictions concerning the initiation and propagation phases of reinforcement corrosion [6]. Commonly used service life predictions only consider the initiation phase, and thus make corrosion initiation a limit state. That introduces additional safety to service life predictions since actual corrosion damage has not occurred by then. The method is, however, justified since it sets an unambiguous service life limit state and limits the complexity of the examination to just carbonation (controlled by the diffusion of CO_2). This study considers only the initiation phase of reinforcement corrosion due to carbonation of concrete.

Carbonation models have been widely used to predict the service life of concrete structures. Since the late 1950's, many researchers have conducted both laboratory research on accelerated carbonation [7–11] and field studies [12,4,13] on natural carbonation in an attempt to determine design parameters and their relation to carbonation rate, to produce service life design methods

* Corresponding author.
E-mail addresses: arto.kolio@tut.fi (A. Köliö), petri.niemela@laurimehto.fi (P.J. Niemelä), jukka.lahdensivu@tut.fi (J. Lahdensivu).

http://dx.doi.org/10.1016/j.cemconcomp.2015.10.013
0958-9465/

and to correlate accelerated and natural carbonation. However, no study using data from repeated measurements of natural carbonation of the same concrete structure within a certain time interval in an actual outdoor environment has been found in the literature. Such data would be valuable for validating laboratory research.

This study analyses the actual observed progress of carbonation on concrete facades in Nordic climate by repeated condition assessments at certain time intervals. The results are compared to those of the widely used square root model to evaluate its use in predicting the progression of natural carbonation in concrete structures exposed to Nordic climate.

2. On concrete carbonation and its modelling

Carbonation of concrete is a chemical reaction between the alkaline hydrates of concrete and carbon dioxide gas, both of which are dissolved in concrete pore water. The reaction product is mainly calcium carbonate, which lowers the pH of the pore water (and concrete) gradually to a level where steel can corrode. Carbonation has been acknowledged to advance in concrete as a front which makes determination of the location of that front relevant as it affects the achievable service life [14].

2.1. Principal factors affecting concrete carbonation

The carbonation rate of concrete is influenced mainly by factors that affect the diffusion resistance of the material between outdoor air and the carbonation zone and the amount of substances taking part in the carbonation reaction of the carbonating material. Factors that limit carbonation are (1) moisture content of concrete, (2) reserve of calcium hydroxide in cement, (3) impermeability of concrete, (4) low CO_2 concentrations in air, and (5) outward diffusion of OH^- in water saturated concrete [15]. These factors are related to structural and concrete properties and to external environment properties such as the amount of atmospheric CO_2 and precipitation.

The moisture content of the pore system has a major influence on the diffusion resistance of concrete as the diffusion rate of carbon dioxide in air is about 10,000 times greater than in water-filled pores [16]. In practice, carbon dioxide cannot penetrate into the pore system of concrete while the surfaces of capillary pores are covered by condensation moisture.

The amount of carbonating substance determines how much carbon dioxide is consumed in carbonation reactions at different levels to allow the carbonation front to penetrate deeper into the concrete. The amount depends on the type and amount of binder and hydration rate.

Diffusion resistance of concrete is mainly affected by the amount and type of pores and the moisture content of the pore system [11]. The porosity of concrete, i.e. the amount and size of pores, depends on the water-cement ratio and hydration rate of cement as well as the amount of binder used. The capillary porosity of concrete varies a lot between different types. The lower the capillary porosity of concrete, the lower the carbonation rate of concrete [4].

Carbon dioxide content of ambient air, temperature and narrow cracking (0.1–0.4 mm) have been found to have a minor influence on carbonation rate [15–17]. Carbon dioxide content in the air increases an average annual rate of 2 ppm [18]. The average age of the subject buildings at the time of the 1st assessment was 27 years and at the time of the 2nd assessment 35 years. During the intervening period of about 8 years, the carbon dioxide content of the atmosphere still accounted for 0.04% of all atmospheric gases.

Lahdensivu [4] analysed the carbonation of concrete facades and balconies in an actual outdoor environment in a study of 947 concrete buildings built between 1960 and 1996. The study showed statistically the differences in the carbonation of facades with different surface treatment. Facades with a brushed concrete carbonated fast whereas facades clad with clinker or brick tiles carbonated remarkably slowly. Differences were also observed in balcony structures where the surface treatment and sheltered location caused fast carbonation of soffits of balcony slabs compared to other balcony components.

Recent work has focused on the assessment of the effects of climate change on the durability of concrete structures and the progression of carbonation in different locations and environments [5,19–21].

2.2. The modelling of carbonation

The basic assumption of carbonation models is the homogeneity of concrete, i.e. that the properties that determine the carbonation rate are similar at all concrete depths. However, actual concrete structures are not ideally homogenous, but vary e.g. as to required compaction and curing period and, especially, prevailing moisture conditions. Thus, it is natural that the carbonation of the concrete used in facades and balconies only rarely follows closely the presented model. Since concrete is often denser and hydration has progressed further inside a concrete structure than on its surfaces, carbonation of concrete with respect to time is often slower than in the commonly used parabolic model. Likewise, the higher moisture content within concrete compared to the surface layers may also result in slower carbonation [16].

Because carbonation is controlled by the diffusion of carbon dioxide within concrete, it is commonly modelled using the square root of time relationship, see Eq. (1) [15], derived from the differential equation of diffusion [14]. The rate of carbonation, including the effect of both internal and external factors, is in this model denoted by k (the carbonation coefficient).

$$x = k \cdot \sqrt{t} \tag{1}$$

where,

x = carbonation depth
k = carbonation coefficient [mm/year$^{1/2}$]
t = exposure time [years]

Many models have been proposed for depicting carbonation, all of which make use of the square root of time relationship [11]. However, empirical measurements have indicated it to overestimate carbonation especially in cases where the concrete is exposed to rain [15,22]. Therefore, the square root equation should be regarded as an upper limit for carbonation in such cases. The carbonation coefficient k is used to adjust the model to describe the carbonation of different concretes in different environments [12,15]. Another approach has been to incorporate the effect of different environments by modifying the exponent of time [11]. A number of studies e.g. Refs. [23,24] have been concentrated on the reaction kinetics of carbonation by utilizing physical models. The square root equation has also been improved to distinguish between the influences of different individual internal and external factors affecting carbonation [7], and to isolate the influences of specific factors [25] opposed to the one parameter in Eq. (1). A statistical analysis of a carbonation coefficient based on field measurements has been recently presented in Portugal [12] and in Finland [4]. Lollini et al. [13] have brought to light issues concerning the reliability of statistical service life estimates using the fib model for carbonation.

The main difference between the carbonation model proposed in fib model code [25] and the one and two parameter models by

Tuutti [15] and Neves et al. [7] is the requirement for a specific accelerated carbonation test performed in a laboratory environment to determine the carbonation resistance parameter. The latter models, on the other hand, are applicable in practice based on natural carbonation measurements conducted on site. A proposal to bridge this gap by a linear relationship between natural and accelerated carbonation has been presented in Ref. [8] based on extensive carbonation field studies on 21 viaducts 4–32 years old in inland Portugal.

3. Research methods and material

3.1. Research material

3.1.1. Condition assessment

The research material of this study has been collected in connection with commercial condition assessments conducted as part of building management. Concrete facades of buildings in Finland have been subjected to condition assessments since the late 1980's, and data measured by standardised procedures [26] has been produced as part of most of these assessments. The condition assessments consist of preliminary desk top studies, visual observation and rating in situ, measurements and sampling in situ and laboratory tests [27].

Carbonation depth has been measured from core samples taken during field investigations by spraying the freshly cut surface with a phenolphthalein pH indicator. The phenolphthalein pH indicator is commonly used in determining the depth of the carbonation front. However, this method is acknowledged to slightly underestimate the carbonation front and its effect on steel depassivation due to the difference in the pH of the colour change and the carbonation itself [15,11]. To minimise this effect in the comparison of consecutive measurements, both measurement rounds were conducted applying the same method based on the phenolphthalein indicator.

Carbonation depth was measured from the samples as an average and maximum depth of the carbonation front. The average depth was determined from multiple (>10) measurements using a feeler blade. The maximum depth was the highest carbonation depth measured from the sample. The average carbonation depth was used in the analyses of this study. Twelve samples were taken from one building on average [27]. Fig. 1 shows the typical distribution of core samples in a building.

Concrete composition was not analysed in connection with the condition assessments and is therefore not known precisely. The concrete grade used in facade panels and most structural members of balconies was C20/25 from 1965 until 1989. Thereafter, the grade was raised to C25/30. The cement type used in these precast panels is mostly CEM I ordinary Portland cement because its good early age strength has been an advantage in manufacturing and handling the panels.

3.1.2. Repeated condition assessments at certain time intervals

A total of 18 cases were identified where the same facade and/or balconies had been subject to two condition assessments within a certain time interval, see Table 1. The first condition assessments were conducted in 1998–2008 and the second round in 2007–2013, both by the same engineering office. Since the first edition of the condition assessments manual [26] for concrete facades and balconies in Finland was published in 1997, it can be argued that both assessment rounds have been conducted according to the same guidelines and, therefore, provide comparable information.

The buildings subjected to consecutive condition assessments were built in 1969–1992, the majority in the 1970's. During the first condition assessment, the buildings were 9–36 years old (average age 27 years), and during the second assessment 19–42 years old (average age 35 years). The interval between the assessments was 4–14 years (average 8 years).

In 15 of the assessed facades, the whole facade or parts of it were of brushed and painted concrete while six were of exposed aggregate concrete. In the case of the 15 assessed balconies, on case considered only slabs and one only side panels making the total number of examined structures 14 for both. All of the balconies were of painted concrete. These facades and balconies were not subject to any renovation or maintenance measures during the assessment interval.

The studied properties were average carbonation across the entire facade of the subject building and carbonation depth of parallel samples. A varying number of parallel samples were taken in the latter condition assessment from the same locations as in the first assessment in an attempt to eliminate local variation in concrete properties and environmental loading. An example of taken parallel samples is presented in Fig. 2.

3.2. Calculating the progression of carbonation

In this study, consecutive carbonation depth measurements are compared to the square root model for predicting progress of carbonation (Eq. (1)) [15]. The data from consecutive condition assessments is used to evaluate the model's representativeness of actual observed natural carbonation. The comparison can be carried out by using the carbonation coefficients calculated by this model for the studied cases.

If measured carbonation is closely in line with the predictions of the square root model, the carbonation coefficient remains unchanged over time. The goodness of the fit with the square root model can be determined by comparing the differences that occur in consecutive calculations of carbonation coefficients.

There were some cases among the research data where the measured carbonation depth was smaller in the latter assessment than in the former measurements which produced a negative difference between them. This inconsistency in the data is due to large scatter in the properties, especially porosity, of the concrete used in these facades and balcony slabs and panels. Thus, they have to be taken into account also in the statistical analysis in order to consider the whole scatter and to produce an undistorted average. However, when individual cases or measurements are dealt with in Chapter 4 in this article, the negative difference is interpreted so that carbonation has not advanced in their case (zero difference).

The square root curve resembles a parabolic curve whose differential (representing carbonation rate) decreases over time. Carbonation is, thus, fast in the beginning phase (1.1–0.4 mm/year over the first 10 years with a carbonation coefficient of 2.2 mm/year$^{1/2}$) and decreases over time (0.21–0.19 mm/year in 27–35 year old structures). Therefore, the carbonation depth measurements are more sensitive with regard to service life considerations in the old existing building stock than in measurements conducted on new constructions, see Fig. 3.

4. Results and discussion

4.1. Measured progression of carbonation – parallel samples

4.1.1. Brushed and painted concrete surface

The carbonation progression between the individual parallel samples of brushed and painted concrete was −9 to +14 mm, the average progression being 2.2 mm, as shown in Table 2. The time interval between measurements was on average 8.4 years. Carbonation coefficients were determined separately from the data of both assessments. The difference between the carbonation

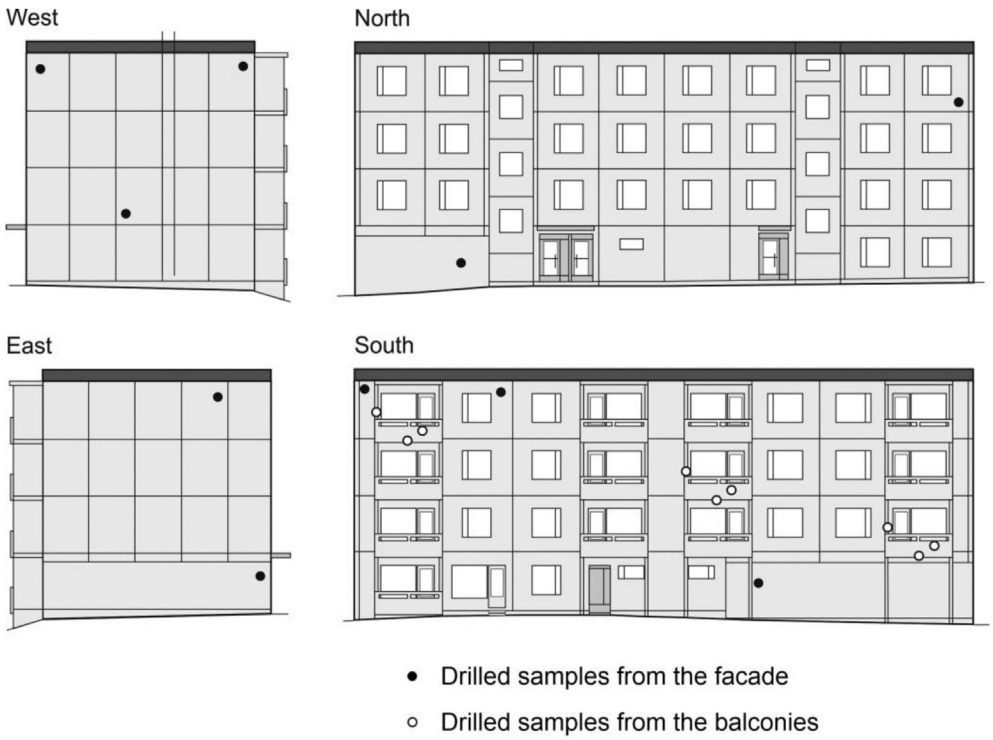

Fig. 1. An example of sampling locations in a typical situation where samples were drilled for laboratory tests.

Table 1
Characterisation of the condition assessment cases as research material.

	Facades	Balconies	Year of construction	1st assessment		2nd assessment	
				Year	N[a]	Year	N[a]
1	Brushed & painted/exposed aggregate	Painted concrete	1979	2005	4/5 + 6/4	2012	4/2 + 5/2
2	Brushed & painted	Painted concrete	1975	2004	12 + 5/4	2011	6 + 2/2
3	Exposed aggregate	Painted concrete	1976	2003	44 + 3/5	2011	10 + 2/3
4	Exposed aggregate	–	1982	1998	9 + 0	2012	7 + 0
5	–	Painted concrete	1973	2007	0 + 8/6	2013	0 + 7/6
6	–	Painted concrete	1972	2008	0 + 2/4	2012	0 + 5/3
7	–	Painted concrete	1981	2004	10 + 3/3	2012	8 + 2/3
8	Brushed & painted	Painted concrete	1971	2001	6 + 2/2	2012	9 + 4/3
9	Brushed & painted	–	1981	2004	11 + 0	2012	6 + 0
10	Brushed & painted	Painted concrete	1973	2006	8 + 4/2	2013	9 + 3/3
11	Brushed & painted	Painted concrete	1977	2005	8 + 2/2	2012	7 + 5/3
12	Brushed & painted	–	1972	2003	15 + 0	2008	26 + 0
13	Brushed & painted	Painted concrete	1977	2004	7 + 3/3	2012	6 + 4/2
14	Brushed & painted	Painted concrete	1969	2000	6 + 2/2	2011	9 + 3/3
15	Exposed aggregate	Painted concrete	1969	1999	5 + 4/2	2011	7 + 3/2
16	Brushed & painted	Painted concrete	1992	2001	3 + 0/2	2011	6 + 0/3
17	Exposed aggregate	Painted concrete	1973	2002	9 + 5/4	2007	5 + 2/3
18	Exposed aggregate	Painted concrete	1977	2002	8 + 9/0	2012	4 + 5/0

[a] The number of samples is denoted by N [surface type 1/surface type 2/surface type 3 + balcony side panels/balcony slabs].

coefficient determined in the latter assessment and the first assessment was on average + 0.07 mm/year$^{1/2}$ with a standard deviation of 1.02 mm/year$^{1/2}$. A negative difference would indicate that the progression of carbonation has been slower than predicted by the square root model and a positive difference would indicate faster than predicted progression. As shown in Table 2, there was large scatter between the results.

4.1.2. Exposed aggregate concrete surface

The carbonation progression in the individual parallel samples of exposed aggregate concrete, Table 3, was 0 to +6 mm, the average progression being 2.7 mm. The time interval between measurements was on average 10.2 years. The difference between the carbonation coefficient determined in the latter assessment and the first assessment was on average + 0.25 mm/year$^{1/2}$ with a standard deviation of 0.53 mm/year$^{1/2}$.

4.1.3. The soffit surfaces of balcony slabs

The carbonation progression in the individual parallel samples from soffit surfaces of balcony slabs, Table 4, was 0 to +10 mm, the average progression being 3.8 mm. The time interval between measurements was on average 7.0 years. The difference between the carbonation coefficient determined in the latter assessment and the first assessment was on average + 0.32 mm/year$^{1/2}$ with a standard deviation of 0.46 mm/year$^{1/2}$.

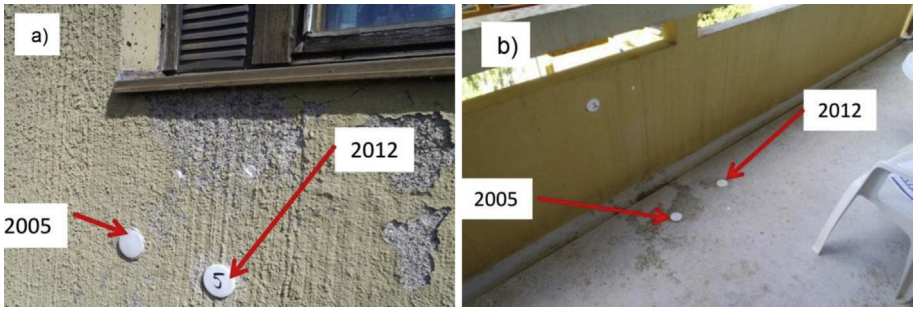

Fig. 2. Parallel samples taken from the a) facade and b) balcony of the subject building A1 in condition assessments conducted in 2005 and 2012.

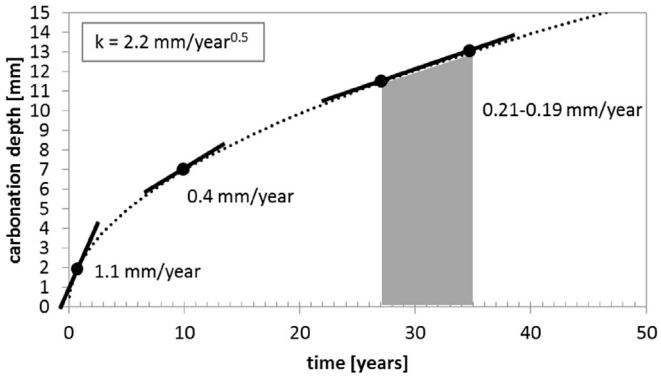

Fig. 3. Higher sensitivity of initiation phase predictions of carbonation depth measurements due to decrease of the differential over time. The gray area describes the average age of the buildings in this study (27–35 years). The carbonation coefficient used in the illustration is the average of brushed and painted facades in this study.

4.1.4. Balcony side panels

Finally, the carbonation progression between the individual parallel samples from balcony side panels, as presented in Table 5, was −1 to +9 mm, the average progression being 4.0 mm. The time interval between measurements was on average 9.5 years. The difference between the carbonation coefficient determined in the latter assessment and the first assessment was on average + 0.47 mm/year$^{1/2}$ with a standard deviation of 0.54 mm/year$^{1/2}$.

Negative progression of carbonation depth, meaning that carbonation depth was actually smaller in the latter assessment than in the former, was observed at four sampling points of brushed and painted facades and at one point on balcony side panels. This inconsistency is due to a large scatter in the properties of the concrete used in these facades and balcony side panels. That means that individual samples taken from different parts of the facade are not directly comparable with each other. Instead, there is a high probability of producing false or even inconsistent information (negative values with no physical equivalent). Local variation in material and coating properties should be minimised by working

Table 2
Parallel samples of carbonation measurements of brushed and painted concrete facades.

Sample #	1st assessment carbonation depth mm	2nd assessment carbonation depth mm	1st assessment carbonation coefficient mm/year$^{1/2}$	2nd assessment carbonation coefficient mm/year$^{1/2}$	Difference in carbonation depth mm	Difference in carbonation coefficient mm/year$^{1/2}$	Time interval years
1.1	13	12	2.55	2.09	−1	−0.46	7
1.2	18	21	3.53	3.66	3	0.13	7
8.1	8	11	1.46	1.72	3	0.26	11
10.1	23	26	4.00	4.11	3	0.11	7
11.1	14	8	2.65	1.35	−6	−1.29	7
12.1	20	26	3.59	4.33	6	0.74	5
12.2	18	15	3.23	2.50	−3	−0.73	5
12.3	26	30	4.67	5.00	4	0.33	5
14.1	5	19	0.90	2.93	14	2.03	11
14.2	22	13	3.95	2.01	−9	−1.95	11
14.3	6	14	1.08	2.16	8	1.08	11
14.4	15	18	2.69	2.78	3	0.08	11
14.5	4	8	0.72	1.23	4	0.52	11

Table 3
Parallel samples of carbonation measurements of exposed aggregate concrete facades.

Sample #	1st assessment carbonation depth mm	2nd assessment carbonation depth mm	1st assessment carbonation coefficient mm/year$^{1/2}$	2nd assessment carbonation coefficient mm/year$^{1/2}$	Difference in carbonation depth mm	Difference in carbonation coefficient mm/year$^{1/2}$	Time interval years
4.1	4	6	1.00	1.10	2	0.10	14
15.1	6	6	1.10	0.93	0	−0.17	12
17.1	25	25	4.64	4.29	0	−0.35	5
18.1	6	8	1.20	1.35	2	0.15	10
18.2	3	9	0.60	1.52	6	0.92	10
18.3	5	11	1.00	1.86	6	0.86	10

Table 4
Parallel samples of carbonation measurements from soffit surfaces of balcony slabs.

Sample #	1st assessment carbonation depth mm	2nd assessment carbonation depth mm	1st assessment carbonation coefficient mm/year$^{1/2}$	2nd assessment carbonation coefficient mm/year$^{1/2}$	Difference in carbonation depth mm	Difference in carbonation coefficient mm/year$^{1/2}$	Time interval years
1.3	15	18	2.94	3.13	3	0.19	7
1.4	13	16	2.55	2.79	3	0.24	7
14.6	19	29	3.41	4.47	10	1.06	11
17.2	14	14	2.60	2.40	0	−0.20	5
17.3	13	16	2.41	2.74	3	0.33	5

Table 5
Parallel samples of carbonation measurements on outer surfaces of balcony side panels.

Sample #	1st assessment carbonation depth mm	2nd assessment carbonation depth mm	1st assessment carbonation coefficient mm/year$^{1/2}$	2nd assessment carbonation coefficient mm/year$^{1/2}$	Difference in carbonation depth mm	Difference in carbonation coefficient mm/year$^{1/2}$	Time interval years
11.2	4	3	0.76	0.51	−1	−0.25	7
14.7	14	23	2.51	3.55	9	1.03	11
18.4	5	10	1.00	1.69	5	0.69	10
18.5	3	6	0.60	1.01	3	0.41	10

with average values across the facade. Thus, an analysis based on average values for each facade or balcony structure type was carried out.

4.2. Measured progression of carbonation – average data

4.2.1. Brushed and painted concrete surface

The carbonation measurements on brushed and painted concrete facades targeted on average 7.9 samples/facade in the first assessment and 8.8 samples/facade in the latter assessment. The difference in carbonation depth between the assessments was −4.0 to +5.6 mm (on average + 1.5 mm), see Table 6. The time interval between assessments was on average 8.3 years.

Carbonation coefficients were determined separately from the data of both assessments. The difference between the carbonation coefficient determined in the latter assessment and the first assessment was −1.12 to +0.64 mm/year$^{1/2}$, the average difference being −0.02 mm/year$^{1/2}$.

4.2.2. Exposed aggregate concrete surface

The measurements on exposed aggregate facades targeted on average 13.3 samples/facade in the first assessment and 5.8 samples/facade in the latter assessment. The difference in carbonation depth between the assessments was +0.1 to +3.2 mm (on average + 1.4 mm). The time interval between assessments was on average 9.4 years. The difference between the carbonation coefficients determined separately in the latter assessment and the first assessment was −0.39 to +0.35 mm/year$^{1/2}$, the average difference being +0.02 mm/year$^{1/2}$, see Table 7.

4.2.3. The soffit surfaces of balcony slabs

In the carbonation measurements on the soffit surfaces of balcony slabs, the average sample size was 2.9/building in both assessments. The difference in carbonation depth between the assessments was −5.5 to +6.8 mm (on average + 1.6 mm). The time interval between assessments was on average 7.9 years. The difference between the carbonation coefficients determined separately in the latter assessment and the first assessment was −1.20 to +0.84 mm/year$^{1/2}$, the average difference being −0.03 mm/year$^{1/2}$, see Table 8.

4.2.4. Balcony side panels

In the carbonation measurements on balcony side panels the average sample size was 4.1/building in the first assessment and

Table 6
Average carbonation depth measured in consecutive condition assessments of brushed and painted concrete facades.

Subject building #	1st assessment carbonation depth mm	2nd assessment carbonation depth mm	1st assessment carbonation coefficient mm/year$^{1/2}$	2nd assessment carbonation coefficient mm/year$^{1/2}$	Difference in carbonation depth mm	Difference in carbonation coefficient mm/year$^{1/2}$	Time interval years
1	19.0	15.0	3.73	2.61	−4.0	−1.12	7
2-A[a]	14.0	14.8	2.60	2.47	0.8	−0.13	7
2-B	15.4	14.5	2.86	2.42	−0.9	−0.44	7
8-A	15.3	15.0	2.79	2.34	−0.3	−0.45	11
8-B	10.3	14.7	1.88	2.30	4.4	0.42	11
9	12.7	10.3	2.65	1.85	−2.4	−0.80	8
10	14.5	20.0	2.52	3.16	5.5	0.64	7
11-A	4.8	7.0	0.91	1.18	2.2	0.28	7
11-B	7.8	9.0	1.47	1.52	1.2	0.05	7
12	17.5	20.8	3.14	3.47	3.3	0.32	5
13-A	18.8	19.0	3.62	3.21	0.2	−0.41	8
13-B	13.3	16.0	2.56	2.70	2.7	0.14	8
14-A	11.4	17.0	2.05	2.62	5.6	0.58	11
14-B	4.0	8.0	0.72	1.23	4.0	0.52	11
16	0.0	0.7	0.00	0.16	0.7	0.16	10

[a] A stands for the average for long facades and B for the average for end facades of long buildings.

Table 7
Average carbonation depth measured in consecutive condition assessments of exposed aggregate concrete facades.

Subject building #	1st assessment carbonation depth mm	2nd assessment carbonation depth mm	1st assessment carbonation coefficient mm/year$^{1/2}$	2nd assessment carbonation coefficient mm/year$^{1/2}$	Difference in carbonation depth mm	Difference in carbonation coefficient mm/year$^{1/2}$	Time interval years
1	5.2	5.5	1.02	0.96	0.3	−0.06	7
3	5.0	7.7	0.96	1.30	2.7	0.34	8
4	6.0	6.1	1.50	1.11	0.1	−0.39	14
15	6.2	6.3	1.13	0.97	0.1	−0.16	12
17	20.2	21.8	3.75	3.74	1.6	−0.01	5
18-A[a]	6.3	9.5	1.26	1.61	3.2	0.35	10
18-B	6.8	8.5	1.35	1.44	1.75	0.09	10

[a] A stands for the average for long facades and B for the average for end facades of long buildings.

Table 8
Average carbonation depth measured in consecutive condition assessments of soffit surfaces of balcony slabs.

Subject building #	1st assessment carbonation depth mm	2nd assessment carbonation depth mm	1st assessment carbonation coefficient mm/year$^{1/2}$	2nd assessment carbonation coefficient mm/year$^{1/2}$	Difference in carbonation depth mm	Difference in carbonation coefficient mm/year$^{1/2}$	Time interval years
1	14.0	17.0	2.75	2.96	3.0	0.21	7
2	17.8	18.0	3.31	3.00	0.2	−0.31	7
3	14.6	17.7	2.81	2.99	3.1	0.18	8
5	11.5	17.8	1.97	2.81	6.3	0.84	6
6	20.8	20.7	3.47	3.27	−0.1	−0.19	4
7	10.3	11.0	2.15	1.98	0.7	−0.17	8
8	15.5	19.3	2.83	3.01	3.8	0.18	11
10	24.0	23.7	4.18	3.75	−0.3	−0.43	7
11	2.5	3.7	0.47	0.63	1.2	0.15	7
13	24.3	24.0	4.68	4.06	−0.3	−0.62	8
14	12.5	19.3	2.25	2.98	6.8	0.73	11
15	12.5	7.0	2.28	1.08	−5.5	−1.20	12
16	2.5	2.7	0.83	0.62	0.2	−0.21	10
17	11.3	15.0	2.10	2.57	3.7	0.47	5

3.7/building in the latter assessment. The difference in carbonation depth between the assessments was −4.0 to +11.3 mm (on average + 1.5 mm). The time interval between assessments was on average 7.9 years. The difference between the carbonation coefficients determined separately in the latter assessment and the first assessment was −1.01 to +1.87 mm/year$^{1/2}$, the average difference being −0.02 mm/year$^{1/2}$, see Table 9.

The results show that carbonation depth scatters widely also within samples from the same facade. Highest scatter in carbonation depths was observed in balcony side and parapet panels and the second highest in balcony slab soffit surfaces. The scatter in carbonation depths was smallest on exposed aggregate facades. As shown by the results, measurements from a single facade can deviate greatly. However, the deviation decreases significantly if the average of the results for a group of similar buildings is used.

Negative progression of carbonation depth was also shown by the average data on four brushed and painted facades, four soffit surfaces of balcony slabs and six balcony side panels.

4.3. Comparison of the carbonation predictions

Predictions of the progression of carbonation were calculated by Eq. (1) based on carbonation coefficients determined in both assessments either from parallel samples or from average carbonation measurement data. In general, the square root equation provided a good fit for the propagation of carbonation in the studied concrete structures, indicated by the overlapping of the 1st and 2nd assessment curves in Figs. 4 and 5. Using the average of a

Table 9
Average carbonation depth measured in consecutive condition assessments of outer surfaces of balcony side panels.

Subject building #	1st assessment carbonation depth mm	2nd assessment carbonation depth mm	1st assessment carbonation coefficient mm/year$^{1/2}$	2nd assessment carbonation coefficient mm/year$^{1/2}$	Difference in carbonation depth mm	Difference in carbonation coefficient mm/year$^{1/2}$	Time interval years
1	11.3	10.0	2.22	1.74	−1.3	−0.48	7
2	17.0	13.0	3.16	2.17	−4.0	−0.99	7
3	1.7	13.0	0.33	2.20	11.3	1.87	8
5	18.9	21.1	3.24	3.34	2.2	0.09	6
6	13.5	18.4	2.25	2.91	4.9	0.66	4
7	7.7	7.5	1.61	1.35	−0.2	−0.26	8
8	16.5	12.8	3.01	2.00	−3.7	−1.01	11
10	14.0	17.3	2.44	2.74	3.3	0.30	7
11	3.7	3.0	0.70	0.51	−0.7	−0.19	7
13	19.7	17.5	3.79	2.96	−2.2	−0.83	8
14	13.5	16.3	2.42	2.52	2.8	0.09	11
15	13.3	18.0	2.43	2.78	4.7	0.35	12
17	12.8	13.5	2.38	2.32	0.7	−0.06	5
18	8.0	10.8	1.60	1.83	2.8	0.23	10

larger sample size, Fig. 4 b and d, the predicted 50 year carbonation depth differed from the latter measurements by only 0.1 mm (0.8%) in the case of brushed and painted facades and 0.2 mm (1.5%) in the case of exposed aggregate facades. In predictions based on the parallel samples, Fig. 4 a and c, the difference was 0.5 mm (2.4%) and 1.8 mm (15.8%) for brushed and painted facades and exposed aggregate facades, respectively. A larger scatter was also observed in the prediction based on parallel samples because the use of single paired samples pronounces the effect of variation in concrete material properties on the facade surface.

The same difference in accuracy was also observed in the carbonation predictions on balcony structures, see Fig. 5. The 1st prediction based on average data differed from the latter measurements by 0.2 mm (1.0%) in the case of balcony slab soffits and 0.1 mm (0.7%) in the case of balcony side and parapet panels, Fig. 5 f and h. In predictions based on parallel samples, Fig. 5 e and g, the difference was 2.3 mm (11.6%) in the case of balcony slab soffits and 3.3 mm (38.8%) in the case of balcony side panels.

The impact of these two methods on the prediction of the initiation time was pronounced in the case of balcony side panels, where the number of parallel samples was the lowest. At the age of 35 years, the average age of the case buildings during the 2nd measurements, the surfaces of the side panels were carbonated to a depth of 13.3 mm based on average data with a good general agreement between the results of the 1st and 2nd measurements. Carbonation depth predicted by parallel samples of the same age based on the 2nd round of measurements was 10.0 mm. The difference to the average data prediction is thus 3.3 mm which equals 17 years as initiation time by the differential in Fig. 3. The difference between both parallel sample predictions was 2.8 mm which equals 15 years as initiation time. A difference this large cannot be accepted in service life design where the target service life of conventional buildings is 50 years.

4.4. Carbonation coefficient comparison

The differences between the carbonation coefficients found in both assessment rounds were studied with respect to the structure's surface type. In the parallel sample data on different facade surfaces, see Fig. 6, the change in the carbonation coefficient between measurements was +0.06 mm/year$^{1/2}$ in the case of brushed and painted concrete and +0.25 mm/year$^{1/2}$ in the case of exposed aggregate concrete facades. The differences between balcony structures were +0.47 mm/year$^{1/2}$ in the case of balcony side panels and +0.32 mm/year$^{1/2}$ in the case of balcony slab soffit surfaces. The positive differences imply that the progression had been faster than first predicted. In the case of facades, the total range of deviation was −1.95 to +2.03 mm/year$^{1/2}$ and with the soffit surface of the balcony −0.25 to +1.06 mm/year$^{1/2}$.

A perfect match with the square root model would give a zero difference between the 1st and 2nd measurement rounds. Deviation from zero indicates an error between the predicted carbonation from the first measurements and the carbonation measured after a time interval. The severity of the error was assessed as a percentage of the average carbonation coefficient of the structure determined in the first measurements. An error of 10% was studied in Figs. 6 and 7.

The carbonation coefficients of the consecutive measurements differed by an average of −0.02 mm/year$^{1/2}$, the total range being −1.12 to +0.64 mm/year$^{1/2}$ in the case of brushed and painted concrete facades. The same difference in the case of exposed aggregate concrete facades was on average 0.02 mm/year$^{1/2}$, the total range being −0.39 to +0.35 mm/year$^{1/2}$. The difference between the carbonation coefficients of the soffits of balcony slabs was on average −0.03 mm/year$^{1/2}$, the total range being −1.20 to +0.84 mm/year$^{1/2}$. In the case of balcony side panels the average difference was −0.02 mm/year$^{1/2}$, the total range being −1.01

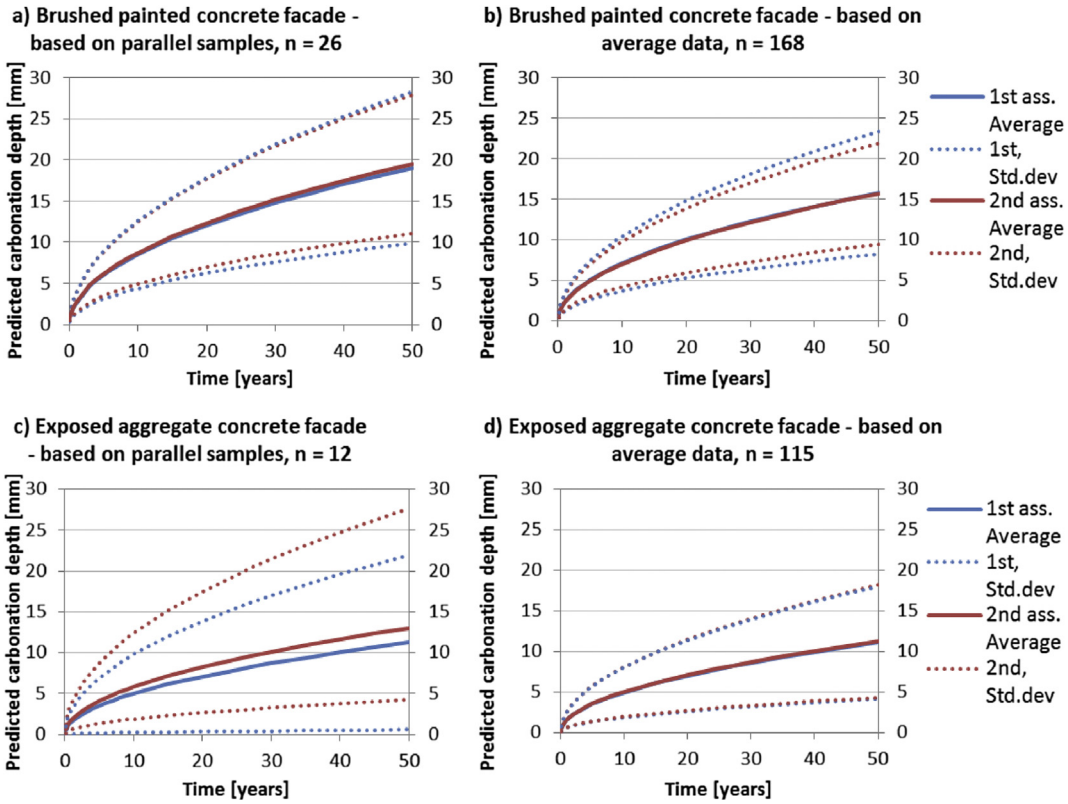

Fig. 4. Carbonation of brushed and painted and exposed aggregate concrete facades modelled by parallel samples or by average data.

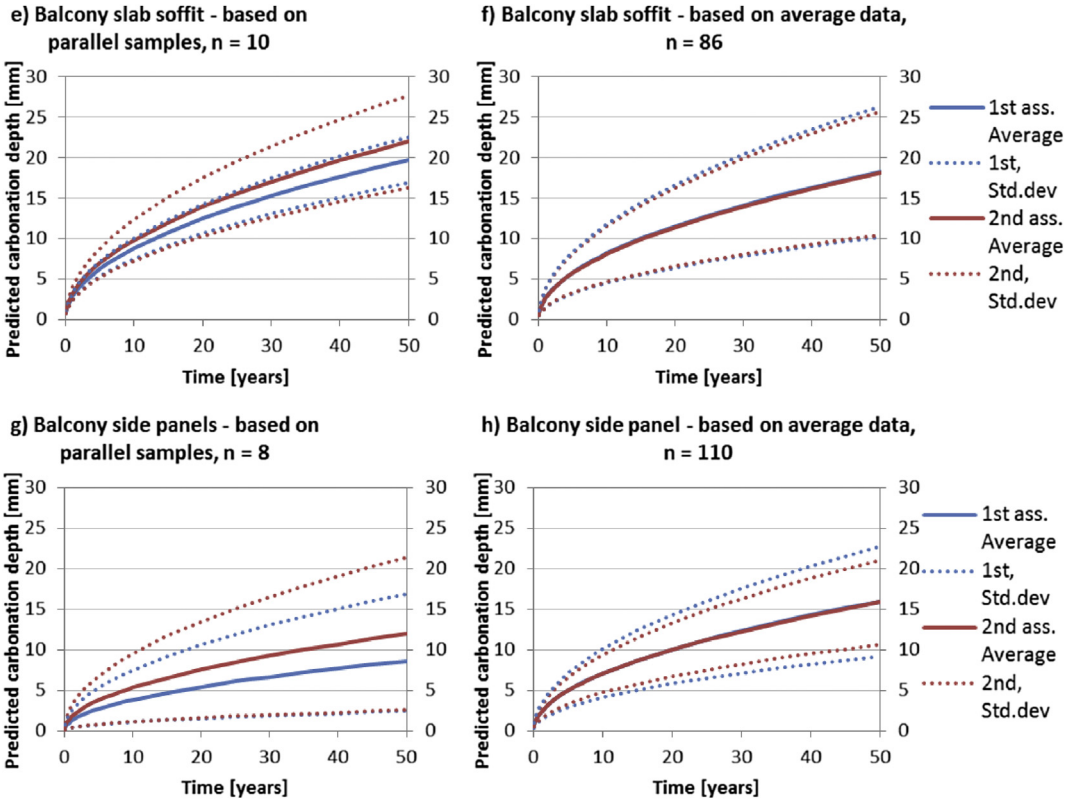

Fig. 5. Carbonation of concrete balcony soffits and balcony side panels modelled by parallel samples or average data.

to +1.87 mm/year$^{1/2}$.

Deviation of the average data was very close to zero (−0.03 to +0.02 mm/year$^{1/2}$ depending on the surface type) which implies a very close correlation with the square root Eq. (1). The correlation was verified with Student's t-test for paired samples at 95% significance level. That means that the square root equation is capable of predicting the propagation of carbonation in practical cases in exposed outdoor structures with high reliability. The significance of the prediction based on average values was higher (p-values > 0.83) than that based on parallel samples (p-values < 0.29). Thus, a small sample size cannot in this case be compensated for by using parallel samples. In the case of brushed and painted facades, the test indicated high significance in the case of both parallel samples (p-value 0.82) and large sample size (p-value 0.90). This implies that the sample size of the parallel samples of brushed and painted facades (n = 26) is already large enough for prediction.

4.5. Evaluation of the carbonation influencing factors

The type and amount of cement have been found to influence carbonation resistance and, thus, the carbonation rate of concrete. In general, the carbonation of ordinary Portland cement concrete has proven slower than that of blended cement concrete [11]. The cement type used in the structures of this study has been mostly Portland cement, but the amounts used have not been determined during the condition assessments and, therefore, their impact was not included in this analysis. The type and amount of cement used over time can be considered to have remained the same (apart from the chemical reactions involved in carbonation). Therefore, they are considered to have only a minor effect on the conclusions made on the basis of consecutive measurements on the same structures.

Variation in the amount of cement along with variation in other concrete properties – such as porosity and concrete composition, mixing, placing and curing – do, however, influence the overall scatter of carbonation depth. Changes in these factors related to construction usually negate the initial presumption of homogeneity of concrete in field studies on existing concrete structures. Therefore, the properties of concrete that affect the carbonation rate can differ also within a very limited area on the concrete surface. Thus, it is not recommended to use individual parallel samples in carbonation studies. Instead, a proper sample size should be ensured.

The concrete grade used in the structures of this study has been mainly C20/25. Studies that relate carbonation rate and concrete compressive strength, e.g. Refs. [12], have suggested a very high carbonation rate with a carbonation coefficient even above 5.0 mm/year$^{1/2}$ for concrete compressive strengths < 25 MPa. All of the carbonation coefficients observed by the authors of this study were below 5.0 mm/year$^{1/2}$, the averages being about 1.5 mm/year$^{1/2}$ (exposed aggregate facades) and 2.6 mm/year$^{1/2}$ (balcony slab soffits). This means that, apart from using a higher concrete grade, carbonation can be reduced significantly by the environmental conditions the existing structures are subjected to e.g. humidity and driving rain. The micro climate at the facade and the pore structure of concrete play a significant role in quantifying their impact.

4.5.1. Impermeability of concrete

In the studied samples capillary porosity, which affects both the permeability and wetting of concrete, varied between 4.9 and 8.4 wt% in all samples, while average value was 6,7 weight-%. The concrete of the samples was not homogenous. Capillary porosity of concrete varies a lot in existing concrete facades and balconies made in 1960s–1980s. According to Lahdensivu [4] the average capillary porosity of balconies is usually 6,4 weight-% (n = 1928) as well as in facades (n = 2311). The share of small carbonation

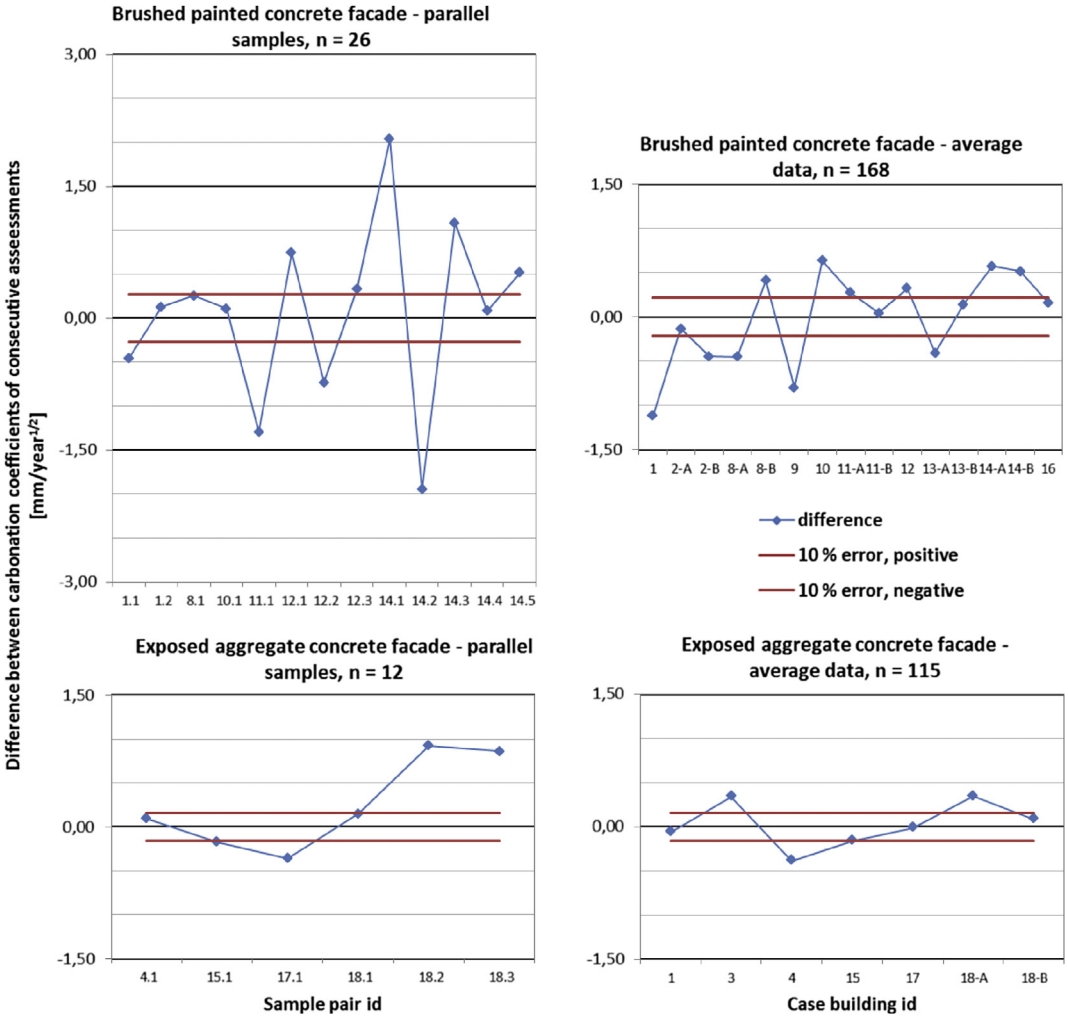

Fig. 6. Deviation of the difference between the carbonation coefficients from zero determined from facades in consecutive assessments.

coefficient ($k < 1.0$) was found on samples with low capillary porosity (<5 weight-%) and the share of carbonation coefficients higher than 3.0 was remarkably higher in the samples where capillary porosity of concrete was ≥7.0 weight-%.

4.5.2. Moisture content of concrete

In addition to the material-related factors, the micro climate around a structure influences carbonation causing different carbonation rates for structures sheltered from rain (balcony slab soffits) and structures exposed to rain (facades) as was observed in the case of different structures in this study. According to the standard EN-206, sheltered from rain structures e.g. balcony slab soffits fall into exposure class XC3 and rain exposed facades to XC4. In design it should be recognized that the exposure of XC3 class can be much more severe regarding carbonation than the following class XC4, as is observed e.g. in Fig. 5. If the scope of the service life is widened to withhold corrosion propagation, the conditions of the exposure class XC4 favour more corrosion propagation than the conditions of XC3. This means that in the design of structure service life based on carbonation resistance, the XC3 class requires higher attention than the preceding class. On national level e.g. in Finland [28] this has not been included properly in the concrete and cover depth specification given for each class. It is the defining the target service life that finally decides how these classes should be treated and related to each other.

5. Conclusions

The square root model is widely used to predict the initiation of reinforcement corrosion due to carbonation of the concrete cover in service life considerations of reinforced concrete structures. The model is based on diffusion laws and its validity is therefore arguable. The model has been accused of not taking into account the changes in the moisture content of concrete during its lifetime, i.e. it has been acknowledged to depict carbonation in structures sheltered from rain. However, this study showed that the square root equation is capable of predicting the propagation of carbonation in actual exposed outdoor structures with high reliability. That was proven by a study on existing 27–35 year old structures that were subjected twice to carbonation depth measurements within a period of approx. 8 years. The prediction made in this study can be assumed to represent the average situation on facades. The measurements analysed in this study imply that although there was high scatter between individual samples and sampling points, on average, carbonation progresses in a similar manner in facades made of similar materials with similar surface treatment.

Carbonation may vary considerably in a certain spot on a structure due to concrete composition, mixing, placing and curing. Therefore, individual or parallel spots are not likely to describe adequately the progression of carbonation across the whole structure. Surface treatment and micro climate can either

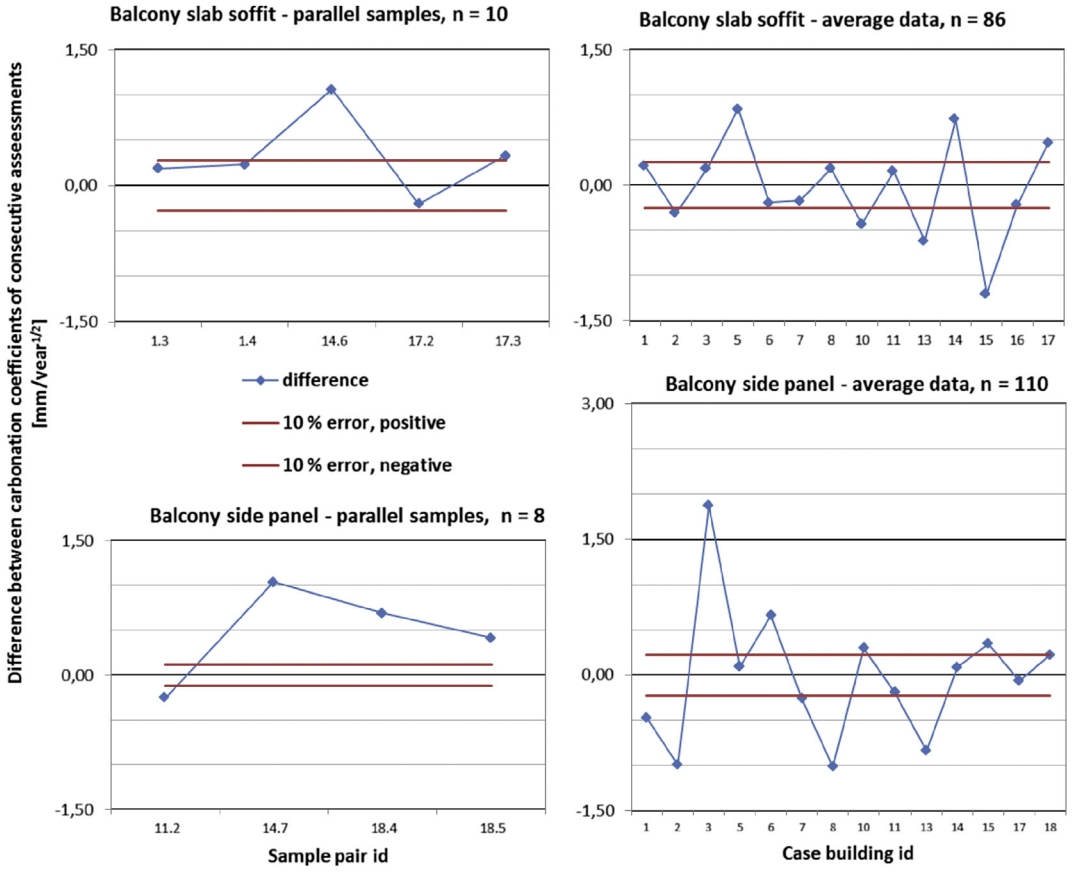

Fig. 7. Deviation of the difference between the carbonation coefficients from zero determined from balconies in consecutive assessments.

accelerate carbonation or shelter concrete from it by altering the moisture content of concrete. That can lead to a systematically lower carbonation rate (exposed aggregate concrete facade) or a higher carbonation rate (balcony slab soffits). When the concrete surface is treated while fresh (e.g. brushed or floated) it leaves the pore system on the surface more open for the penetration of CO_2 as well as driving rain. This will increase the carbonation rate in dry periods, but also allow faster wetting of the structure during driving rain.

These results show that the square root model is capable of predicting quite accurately the average carbonation rate of concrete facades and balconies under Finnish climate conditions.

Acknowledgements

This study was funded by the Doctoral Programme of Built Environment (RYM-to) under the Academy of Finland (grant number T20500/913615/RYM-TO). The field measurement data of the consecutive condition assessments was provided for this study by Engineering Office Lauri Mehto Oy.

References

[1] E. Fasullo, Infrastructure: the Battlefield of Corrosion, ASTM STP 1137, 1992.
[2] E. Wallbank, The Performance of Concrete Bridges: a Survey of 200 Highway Bridges, HMSO Publication, London, 1989.
[3] G. Tilly, Durability of Concrete Repairs, in Concrete Repair - a Practical Guide, Taylor & Francis, New York, 2011, pp. 231–247.
[4] J. Lahdensivu, Durability Properties and Actual Degradation of Finnish Concrete Facades and Balconies, Tampere University of Technology, 2012. TUT Publ. 1028.
[5] A. Köliö, T.A. Pakkala, J. Lahdensivu, M. Kiviste, Durability demands related to carbonation induced corrosion for Finnish concrete buildings in changing climate, Eng. Struct. 62–63 (2014) 42–52.
[6] C.Q. Li, Reliability based service life prediction of corrosion affected concrete structures, ASCE J. Struct. Eng. 130 (2004) 1570–1577.
[7] R. Neves, F.A. Branco, J. de Brito, A method for the use of accelerated carbonation tests in durability design, Constr. Build. Mater. 36 (2012) 585–591.
[8] R. Neves, F.A. Branco, J. de Brito, Field assessment of the relationship between natural and accelerated concrete carbonation resistance, Cem. Concr. Compos. 41 (2013) 9–15.
[9] J.B. Aguiar, C. Júnior, Carbonation of surface protected concrete, Constr. Build. Mater. 49 (2013) 478–483.
[10] F. Duprat, N.T. Vu, A. Sellier, Accelerated carbonation tests for the probabilistic prediction of the durability of concrete structures, Constr. Build. Mater. 66 (2014) 597–605.
[11] L.J. Parrott, A Review of Carbonation in Reinforced Concrete, Cement and Concrete Association, Slough, UK, 1987.
[12] I. Monteiro, F.A. Branco, J. de Brito, R. Neves, Statistical analysis of the carbonation coefficient in open air concrete structures, Constr. Build. Mater. 29 (2012) 263–269.
[13] F. Lollini, E. Redaelli, L. Bertolini, Analysis of the parameters affecting probabilistic predictions of initiation time for carbonation-induced corrosion of reinforced concrete structures, Mater. Corros. 63 (2012) 1059–1068.
[14] J. Broomfield, Corrosion of Steel in Concrete, Taylor & Francis, Oxon, 2007.
[15] K. Tuutti, Corrosion of Steel in Concrete, in: CBI Research 4, Swedish Cement and Concrete Research Institute, Stockholm, 1982, p. 82.
[16] R. Bakker, Initiation Period, in Corrosion of Steel in Concrete, Chapman and Hall, London, 1988.
[17] A.V. Saetta, B.A. Schefler, R.V. Vitaliani, The carbonation of concrete and the mechanism of moisture, heat and carbon dioxide flow through porous materials, Cem. Concr. Res. 23 (1993) 761–772.
[18] Finnish Meteorological Institute, Carbon Dioxide and Circulation of Carbon, 2010 [Online]. Available: http://ilmasto-opas.fi/fi/ilmastonmuutos/ilmio/-/artikkeli/1e92115d-8938-48f2-8687-dc4e3068bdbd/hiilidioksidi-ja-hiilenkiertokulku.html [accessed 07.11.14].
[19] X. Wang, M.G. Stewart, M. Nguyen, Impact of climate change on corrosion and damage to concrete infrastructure in Australia, Clim. Change 110 (2012) 941–957.
[20] S. Talukdar, N. Banthia, J.R. Grace, S. Cohen, Carbonation in concrete infrastructure in the context of global climate change: part 2, Canadian urban simulations, Cem. Concr. Compos. 34 (2012) 931–935.

[21] S. Talukdar, N. Banthia, Carbonation in concrete infrastructure in the context of global climate change: development of a service lifespan model, Constr. Build. Mater. 40 (2013) 775–782.
[22] J. Huopainen, Carbonation of Concrete Facades - a Field Study (MSc thesis), Tampere University of Technology, 1997 (in Finnish).
[23] M. Thiery, G. Villain, P. Dangla, G. Platret, Investigation of the carbonation front shape on cementitious materials: effects of the chemical kinetics, Cem. Concr. Res. 37 (2007) 1047–1058.
[24] N. Hyvert, A. Sellier, F. Duprat, P. Rougeau, P. Francisco, Dependency of C-S-H carbonation rate on CO2 pressure to explain transition from accelerated test to natural carbonation, Cem. Concr. Res. 40 (2010) 1582–1589.
[25] fib Bulletin No.34, Model Code for Service Life Design, International Federation for Structural Concrete, Lausanne, 2006.
[26] Concrete Association of Finland, BY42 Condition Assessment Manual of Concrete Facades and Balconies, Concrete Association of Finland, Helsinki, 2013 (in Finnish).
[27] J. Lahdensivu, S. Varjonen, T. Pakkala, A. Köliö, Systematic condition assessment of concrete facades and balconies exposed to outdoor climate, Int. J. Sustain. Build. Technol. Urban Dev. 4 (2013) 199–209.
[28] Concrete Association of Finland, BY 50 Concrete Code 2012, The Concrete Association of Finland, Helsinki, 2012 (in Finnish).

IV

CORROSION PRODUCTS OF CARBONATION INDUCED CORROSION IN EXISTING REINFORCED CONCRETE FACADES

by

Köliö A., Honkanen M., Lahdensivu J., Vippola M. & Pentti M., Dec 2015

Cement and Concrete Research vol 78, 200-207

http://dx.doi.org/10.1016/j.cemconres.2015.07.009

Cement and Concrete Research 78 (2015) 200–207

Contents lists available at ScienceDirect

Cement and Concrete Research

journal homepage: http://ees.elsevier.com/CEMCON/default.asp

Corrosion products of carbonation induced corrosion in existing reinforced concrete facades

Arto Köliö [a,*], Mari Honkanen [b], Jukka Lahdensivu [a], Minnamari Vippola [b], Matti Pentti [a]

[a] Tampere University of Technology, Department of Civil Engineering, P.O. Box 600, FI-33101 Tampere, Finland
[b] Tampere University of Technology, Department of Materials Science, P.O. Box 589, FI-33101 Tampere, Finland

ARTICLE INFO

Article history:
Received 8 April 2015
Accepted 28 July 2015
Available online 14 August 2015

Keywords:
E. Concrete
D. Reinforcement
C. Corrosion
B. SEM
B. X-ray diffraction

ABSTRACT

Active corrosion in reinforced concrete structures is controlled by environmental conditions and material properties. These factors determine the corrosion rate and type of corrosion products which govern the total achieved service life. The type and critical amount of corrosion products were studied by electron microscopy and X-ray diffractometry on concrete and reinforcement samples from existing concrete facades on visually damaged locations. The corrosion products in outdoor environment exposed concrete facades are mostly hydroxides (Feroxyhite, Goethite and Lepidocrocite) with a volume ratio to Fe of approximately 3. The results can be used to calibrate calculation of the critical corrosion penetration of concrete facade panels.

1. Introduction

1.1. Overview

The effects of reinforcement corrosion have resulted in high maintenance costs in concrete infrastructure around the world in varying climates but also in climates similar to Finland [1–3]. Corrosion is responsible for approximately 11–40% of the repair costs of prefabricated concrete facades in Finland depending on the concrete surface finishing [4]. Regarding concrete facades, corrosion of reinforcement is usually initiated by carbonation [5]. Corrosion damage in concrete structures becomes visible as cracks or spalls. The formation of cracks is usually the first sign of damage thereby making it a suitable limit state in service life considerations that try to take into account both initiation and active corrosion phases of reinforcement service life. When corrosion is far advanced or the spacing of reinforcing bars is small spalling may occur where a piece of the thickness of the concrete cover will be cut off from the surface [6,7]. A method to calculate the critical corrosion penetration exists [8] but it has not been validated especially in the case of carbonation initiated corrosion in slender concrete panel structures.

The concrete cover of reinforcement protects the steel during initiation phase but also determines the amount of corrosion needed to facilitate damage. If the cover is high enough a sufficient stress to generate damage on concrete surface may never occur [5]. The requirement for sufficient concrete cover is usually specified in national codes of practice such as [9]. In spite of the requirements, a large scatter is associated with the cover depths of existing concrete structures [5,10]. Because the facade panels in Finland are usually very slender (nominal thickness of 40–70 mm) the manufacturing of the panel and the installation of the reinforcement are sensitive in regard of achieving proper cover depth.

1.2. Corrosion products

The type of rust formed in corrosion is found to have a significant impact on the cracking behaviour of concrete due to the different volume expansion of corrosion products, see Fig. 1 [6,11,12]. This volume expansion is essential in studies that aim at relating corrosion induced damage and corrosion penetration used in determining the residual service life of corrosion affected structures [8].

The final corrosion products in reinforced concrete have mainly been studied in the case of chloride induced corrosion either in laboratory conditions [14–16], or under marine environment [17]. Zhao et al. [14] concluded that the mechanism of concrete cover cracking due to reinforcement corrosion can be described by two main stages: of stresses caused by the growth of rust thickness and the migration of rust to the pores at the steel/concrete interface. The experiments of Marcotte and Hansson [14] imply that hydroxide types of rusts (in Fig. 1) are formed in high moisture conditions and oxide type rusts in not constantly wet conditions. Characterization studies of corrosion products formed on archaeological ferrous artefacts have been published e.g. in [18,19]. The observed phases in both studies were mainly of goethite, lepidocrocite and magnetite and/or maghemite. Dehoux et al. [19]

* Corresponding author. Tel.: +358 40 849 0837.
E-mail addresses: arto.kolio@tut.fi (A. Köliö), mari.honkanen@tut.fi (M. Honkanen), jukka.lahdensivu@tut.fi (J. Lahdensivu), minnamari.vippola@tut.fi (M. Vippola), matti.pentti@tut.fi (M. Pentti).

http://dx.doi.org/10.1016/j.cemconres.2015.07.009
0008-8846/

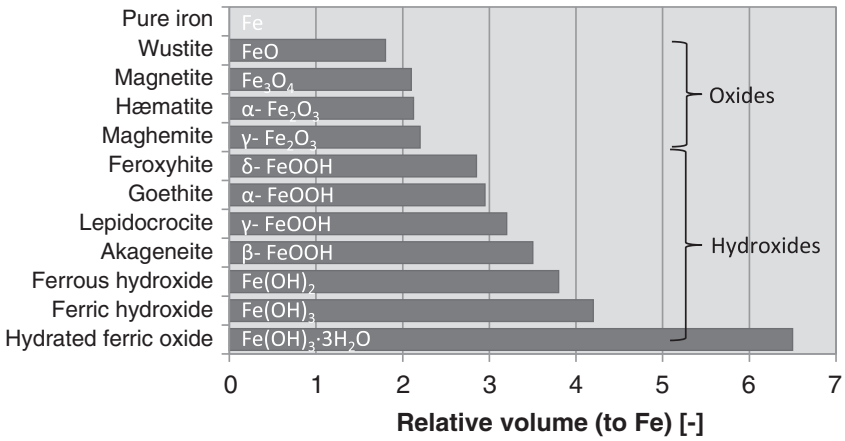

Fig. 1. Relative volumes of corrosion products of Fe to the parent metal. Compiled from [6,12,13].

observed differences in the mechanical properties i.e. elastic moduli of the different phases of these corrosion products. Chitty et al. [18] observed that the corrosion products form layers of different composition, density and permeability around the reinforcement. The layered structure was composed of the metallic substrate (M), dense product layer (DPL), transformed medium (TM) of final corrosion products and compounds from the binder and the surrounding binder (B). Since, similar layered structure has been observed also by Jaffer and Hansson [13] in their studies on reinforced concrete specimens produced in the laboratory. Huet et al. [20] used the same structure in mathematical modelling of the corrosion process. Duffó et al. [21] conducted characterization studies on reinforcement embedded in concrete in a 65 year old structure. A layered structure of rust was found, where the inner layer was dense and well adhered to the steel surface and mainly composed of magnetite. The outer layer of rust was mainly composed of goethite and lepidocrocite and was porous. Corrosion was concluded to have been initiated by fast carbonation, but the time taken for the initiation was not known. Analysis on the generated products was presented and a reaction path proposed for the rusts formed.

Hot rolled reinforcing steel is covered with a few micrometre thick mill scale due to the manufacturing process composed of magnetite with a surface layer of haematite and goethite [12]. Zhao et al. [15] measured a thickness of the mill scale of average 34.5 μm. This mill scale does not take part in the corrosion stresses and was therefore not included in corrosion thickness evaluation in their studies. Both hot rolled (typically rebars) and cold formed (typically meshes) reinforcement have been used in the construction of the facade panels currently under study.

1.3. Corrosion modelling and the critical corrosion penetration

Studies depicting the propagation phase of reinforcement corrosion in concrete have been presented e.g. in references [11,13,14,22,23]. These studies are based on accelerated laboratory experiments on laboratory specimens. One study on the effect of climatic variations on reinforcement corrosion has been reported in [24] based on observations and measurements on laboratory specimens. The capabilities of models created using laboratory experiments to universally predict time-to-cracking with various reference cases have been under debate [25]. Thus, a new approach is proposed in this paper to contribute to the knowledge on the corrosion propagation phase using investigation methods from condition assessments of concrete facades.

The extent of corrosion is presented as corrosion penetration on the steel circumference. The critical corrosion penetration to form cracking has been studied e.g. in [15,26–29]. The critical penetration values varied in this literature from 15 to 100 μm depending on the experiment, exposure or material.

1.4. The objective of this research

This study addresses the determination of the type and thickness of corrosion products formed especially in carbonation induced corrosion in outdoor exposed concrete facade panels. The objective is to produce reliable information on the extent of corrosion that causes visual damage on these structures. The studies are performed on concrete samples taken from visually damaged locations on existing concrete facades that have been in use for 30–43 years.

2. Research methods and material

2.1. Acquisition and preparing of the research material

The research material for this study was gathered in the period of April–August 2013 in the facade condition assessment of 12 buildings chosen deliberately for this study. The buildings were located in the southern parts of Finland and their construction years ranged from 1971 to 1984. The facades were constructed using prefabricated sandwich panels. Of the studied facades seven were of painted concrete, four of exposed aggregate and one of untreated form surfaced concrete.

In all 27 sample cores of the diameter of 50 mm were drilled from the outer layer of the facade panels directly on visually observable corrosion cracks or spalls, see Fig. 2. The samples contained the corroded rebar and its surrounding concrete. The core samples were sprayed by phenolphthalein solution to measure average and maximum carbonation depth from the freshly cut surface and were then wrapped airtight for transport and storage for further investigations.

Carbonation depth measurements were used to investigate the time of corrosion initiation in these samples and thereby calculate the length of the active corrosion phase by subtracting from the total age of the samples the time of initiation, see Table 1. The initiation time was calculated by the square root model for carbonation [30]. The studied concrete structures were on average 38.8 years old. The average time under active corrosion was for the cracked locations 26.0 years and for spalled locations 33.1 years. This information is further discussed in chapter 5. It should also be noted that for all of the samples corrosion has been initiated quite fast (by average 12.6 years) which indicates that both concrete resistance against carbonation has been poor and the environmental conditions favourable to carbonation.

The concrete core samples were broken in laboratory and the reinforcing bars trapped inside the carbonated layer of concrete were extracted from the core samples. The diameter of reinforcing steel samples varied from 3 to 10 mm. The total number of steel samples was 35 of which 16, ranging from different diameter and corroded surface, were chosen for electron microscopic studies. The properties of the steel samples are shown in Table 1.

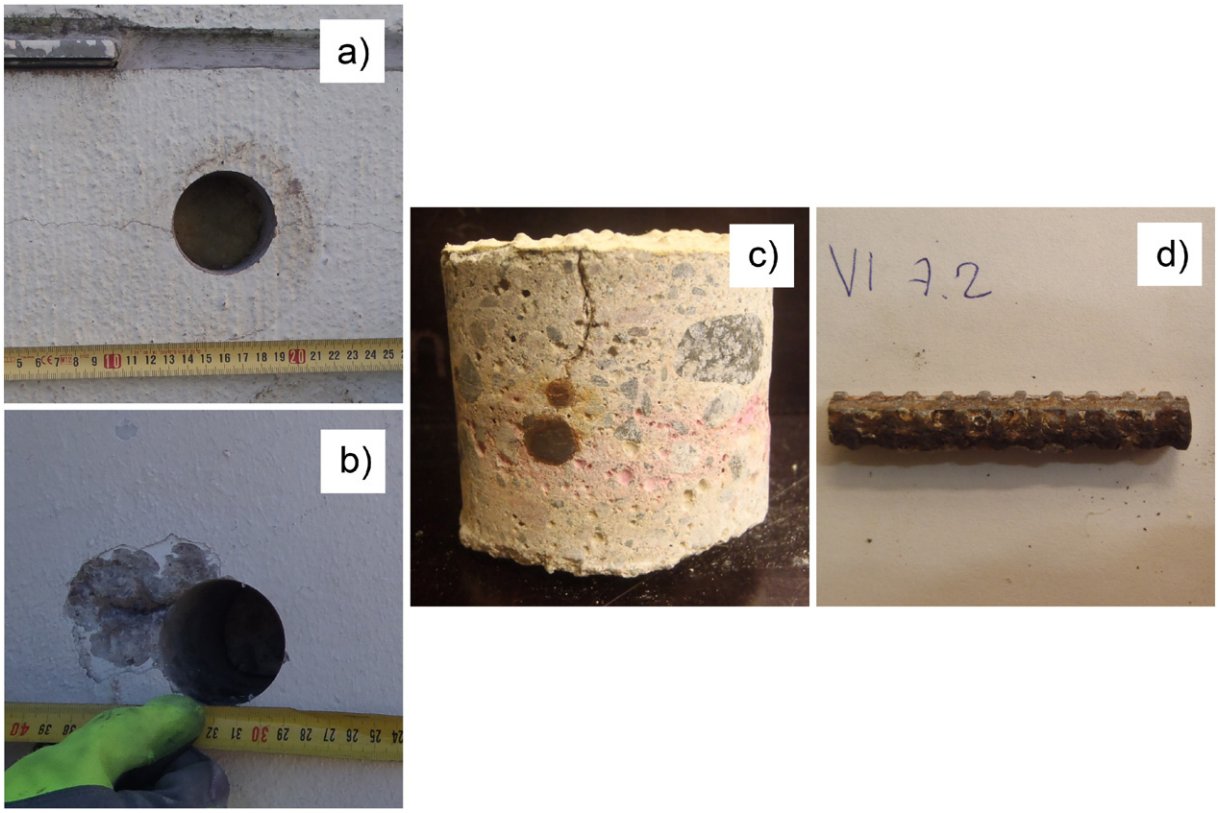

Fig. 2. The samples were drilled directly above a corrosion induced crack (a) or a spall (b) in the facade. Steel samples (d) were extracted from the carbonated layer of the concrete cores (c).

The corroded surface area was estimated by wrapping the reinforcing bars into a transparent plastic film and drawing on it the corroded areas. The plastic films were then removed and scanned to a computer to calculate the relative corroded areas.

In 53% of the total 35 steel samples nearly the whole steel surface (above 90% of the surface) was corroded. Less than half of the surface area was corroded in 28% of the samples. Thus, the corrosion in these samples is general.

2.2. Rust characterization methods

Cross sections of the reinforcing steel samples were prepared with conventional metallographic sample preparation method: moulding into resin followed by mechanical grinding and polishing. Grinding, polishing, and cleaning of the cross-sectional samples were performed without water to avoid dissolution of rust. The cross-sectional samples were characterized with a scanning electron microscope (SEM, ULTRAplus, Zeiss) equipped with an energy dispersive spectrometer (EDS, INCA Energy 350 analyzator with INCAx-act detector, Oxford Instruments). The overall thickness of corrosion products was measured from the SEM images of the samples by utilizing an image analysis software imageJ. Thicknesses were measured in evenly spaced lines perpendicular to the circumference of the reinforcing steel, see Fig. 3, and averaged over the outward and inward semicircle of the reinforcement circumference. The orientation of the reinforcing steel was identified using photographs taken for this purpose during sample preparation.

Table 1
Properties of the steel corrosion samples.

Sample id	Steel diameter [mm]	Concrete cover [mm]	Estimate of the corroded surface [% of steel surface]	Damage on the concrete structure [crack, spall, no crack]	Sample age [years]	Time under active corrosion [years]
OR 13.1	3	2	69%	Spall	36	32.0
PU 3.1	3	3	100%	Spall	40	39.7
Vi 16.1	3	10	100%	Crack	41	30.8
Vi 6.1	3	14	87%	Crack	41	20.9
Pi 17D.1	4	11	28%	No crack	37	0
RL 4.1	4	3	100%	Spall	29	28.6
RU 6.2	4	13	100%	Crack	39	24.4
KA 9.1	5	9	100%	Crack	37	12.2
OH 12.1	6	8	100%	Spall	41	39.1
RU 6.1	6	11	70%	Crack	39	24.4
Vi 7.2	6	21	70%	Crack	41	24.2
KU 14.2	8	13	36%	Crack	42	33.5
Pi 17B.2	8	24	100%	Crack	37	25.8
Pi 17C.2	8	23	90%	Crack	37	29.8
PU 1.2	8	30	90%	Crack	40	34.4
Vi 5.1	10	4	49%	Spall	41	25.0

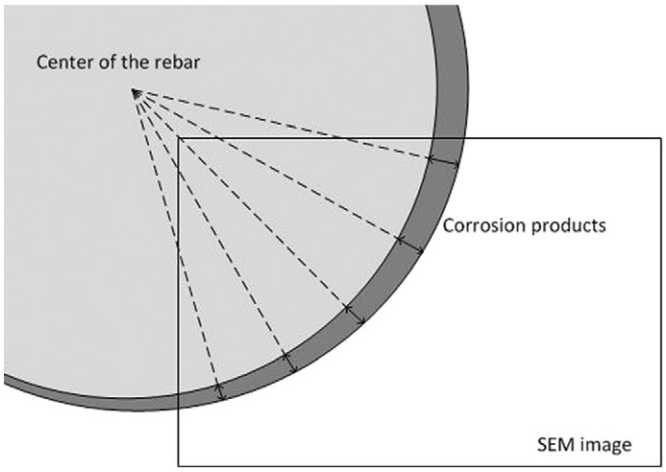

Fig. 3. Thicknesses were measured in evenly spaced lines perpendicular to the circumference of the reinforcing steel.

EDS analyses were performed on the samples to study the elemental composition of the rust layer. Further on scraped rust powder from 12 samples was studied with X-ray diffractometer (XRD, Empyrean, PANanalytical) to analyse compounds of the corrosion products. Scraped rust powder was also studied by transmission electron microscope (JEM 2010, Jeol) equipped with EDS (Noran Vantage with Si(Li) detector, Thermo Scientific). Samples for TEM studies were prepared by crushing the scraped rust powder between two laboratory glass slides and dispersing the powder with ethanol onto a copper grid with a holey carbon film.

It must be noted that the characterization methods used are not capable of separating magnetite and maghemite phases. These methods can, however, distinguish between the phases on a more coarse level that have the greatest differences in volume and therefore the highest relevance in the service life estimation purpose.

2.3. Calculation of the corrosion penetration needed to generate cracks

The critical corrosion penetration to form cracks on concrete surface was calculated for the sample cases following the DuraCrete model [8] by Eq. (1) where a_1, a_2 and a_3 are regression parameters, x^d is the cover thickness, d is the reinforcement diameter and $f_{c,sp}^{d}$ is concrete splitting tensile strength. The cover thickness and reinforcement diameter were taken from Table 1. The regression parameters used were a1 = 74.4 μm, a2 = 7.3 μm and a3 = −17.4 μm/MPa as recommended in [8]. Concrete composition was not analysed in connection with the condition assessments and is therefore not known precisely. The specified concrete grade used in facade panels was C20/25 from 1965 until 1989. Thereafter, the grade was raised to C25/30. The cement type used in these precast panels is mostly CEM I ordinary Portland cement. The concrete splitting tensile strength was chosen according to C20/25 concrete grade as 2.2 MPa.

$$p_0^d = a_1 + a_2 \frac{x^d}{d} + a_3 f_{c,sp}^d \quad (1)$$

A noteworthy observation on the calculation is that for a given concrete grade there exists a minimum value for the critical corrosion penetration. For C20/25 concrete this minimum value is 36.1 μm and for a d C40/50 concrete grade 13.5 μm. Compared to the experimental values given in the literature this minimum value is considerably high and does not take into account the most critical cases with cover depth below 10 mm often encountered in facade panels. The minimum value is inherent from the pre-set regression parameters.

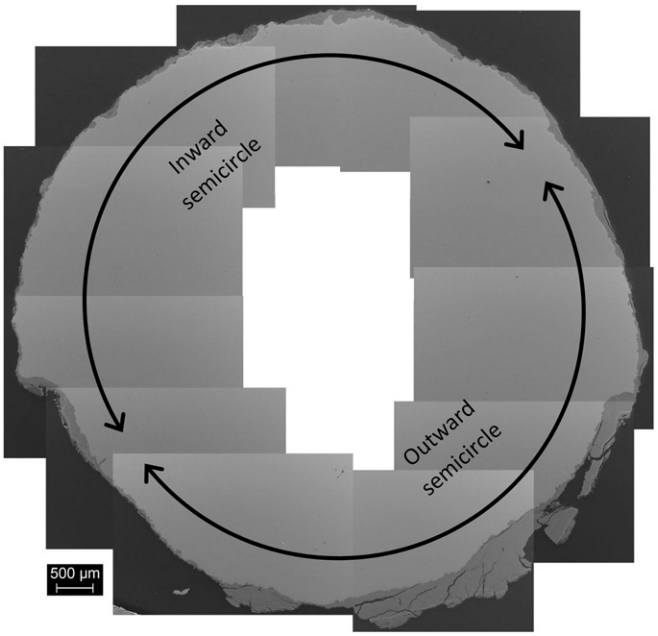

Fig. 4. A compilation of 11 SEM images of the cross-section of sample PI17B.2 The thickness of corrosion products was measured using image analysis software. The outside surface is facing the lower right corner in the figure.

3. Results and discussion

3.1. Thickness of corrosion products

Multiple SEM images of one steel sample have been compiled in Fig. 4 illustrating the differences between the semicircle of the circumference of the rebar facing to the carbonating surface of the structure denoted as “outward semicircle” and the opposite semicircle denoted as “inward semicircle”. Fig. 4 shows the high variability in the thickness of corrosion products around the same cross-section of a reinforcing bar owing to differences in external factors, e.g. orientation, pH and moisture and the time corrosion has been active on that side of the circumference. The corrosion products are visible in the SEM image as a dark grey layer on the surface of the reinforcing bar. The parent metal is of light grey colour and the dark grey area surrounding the sample is the epoxy resin used in preparing the samples.

Thickness of corrosion products measured from scanning electron microscope images of corroded steel samples are presented in the following Table 2 (cracked samples) and Table 3 (spalled samples). The

Table 2
Rust formation observed in SEM images of cracked samples.

Sample id, (diameter, mm)	Rust layer thickness, outward semicircle		Rust layer thickness, inward semicircle		Cover depth/steel diameter
	Average [μm]	Std.dev [μm]	Average [μm]	Std.dev [μm]	[–]
Vi 16.1 (3)	178.1	130.1	105.8	71.2	3.3
Vi 6.1 (3)	170.7	103.1	67.8	43.5	4.7
Pi 17D.1 (4)	– [a]	– [a]	– [a]	– [a]	2.8
RU 6.2 (4)	80.5	49.8	45.4	27.0	3.3
KA 9.1(5)	34.8	31.9	14.9	14.1	1.8
RU 6.1 (6)	131.9	107.4	44.7	42.1	1.8
Vi 7.2 (6)	44.8	37.2	35.8	26.5	3.5
KU 14.2 (8)	42.0	37.0	6.6	5.8	1.6
Pi 17B.2 (8)	182.3	174.9	62.3	38.4	3.0
Pi 17C.2 (8)	109.5	94.6	40.6	35.1	2.9
PU 1.2 (8)	186.1	98.0	158.4	158.2	3.8

[a] Steel orientation not detectable.

Table 3
Rust formation observed in SEM images of spalled samples.

Sample id, (diameter, mm)	Rust layer thickness, outward semicircle		Rust layer thickness, inward semicircle		Cover depth/steel diameter
	Average [μm]	Std.dev [μm]	Average [μm]	Std.dev [μm]	[–]
OR 13.1 (3)	13.1	14.1	6.0	7.4	0.7
PU 3.1 (3)	23.0	29.9	31.1	28.7	1.0
RL 4.1 (4)	154.5	73.4	136.8	95.1	0.8
OH 12.1 (6)	77.1	42.9	62.3	92.0	1.3
Vi 5.1 (10)	92.0	124.1	18.5	6.3	0.4

samples represent reinforcement with varying diameter and cover depth, see Table 1.

The data suggests, that majority of the rust layer is formed on the outward semicircle of the steel. This is expected in concrete structures where corrosion is initiated by carbonation advancing inside concrete as a barrier. This means that corrosion begins earlier on the outside facing surface and is, thus, advanced further. The outward surface is also most affected by driving rain. The rust layer formed on the outer semicircle of the reinforcing steel circumference is the most responsible for corrosion cracking and spalling. By average 60% of rust was formed on the outer semicircle.

The average measured rust thickness on the outer half circumference was 116 μm in cracked samples and 72 μm in spalled samples. The result is opposite to the presumption that spalling requires more far advanced corrosion than cracking. However, all of the spalled samples have also had a very shallow cover depth as opposed to the cracked samples. This may have caused the spalling to occur far earlier since the reinforcing steel was located so near to the outside surface. Thereby the limit state (rust thickness) given for cracking or spalling of concrete due to corrosion should, in fact, be contrasted to the specific cover depth of the reinforcement or to the ratio of cover depth and steel diameter.

In the case of sample Pi 17D.1 the orientation of the steel was unclear thereby making the determining of the outward and inward semicircle impossible. The average overall corrosion thickness on the whole circumference was 14.4 μm. However, owing to the uncertainty, this result was not utilized in the further analysis.

3.2. Type of corrosion products

The examined samples confirmed that corrosion products form layers of different composition around the steel, see Fig. 5. The rust layer contained typically thin veins of varying element composition and density. This observation is similar to [18,21] on the multi-layered

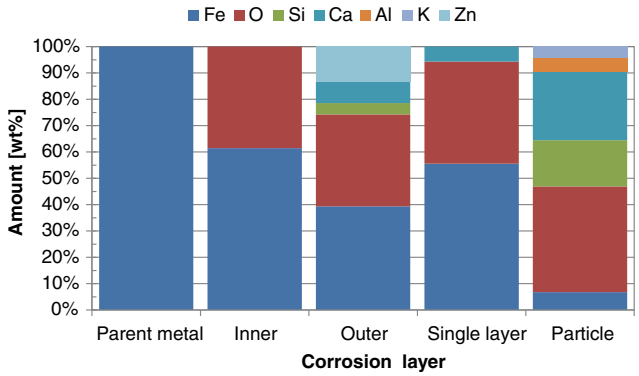

Fig. 6. The element composition (wt%) of different rust layers on corroded reinforcing steel samples. (Only elements >5 wt%).

composition of rust. Based on the EDS analysis the rust formed on rebars was divided into inner and outer rust layers. In the case of the rust layers being very thin, it was treated as single layer. The corrosion products also contained veins of highly dense rust and veins of presumably residue of concrete pore water. Also particles that were trapped inside the rust were observed, see Fig. 5. The samples KU14.2, PI17B.2, PI17C.2, RU6.1 and VI5.1 showed also residue of a mill scale inherent from the production of the reinforcing steel. The thicknesses of the mill scale were respectively 11.8, 2.9, 17.5, 11.6 and 14.5 μm in these samples.

The element composition of the rust layer based on EDS analysis is illustrated in Fig. 6. The figure is composed of different identified rust layers which are divided into shares by mass of elements present in the corresponding layer. Only elements >5 wt% were taken account.

Fig. 6 shows the differences in element composition of the different rust layers. The outer rust layer contains typically less iron and on the other hand more oxygen and various other elements than inner and single layers. In the inner rust layer the amount of iron is higher and the layer is composed more strictly of pure iron oxides i.e. the amount of other substances is low. The composition of the thin rust layer is a compilation of the inner and outer layers. Particles that were entrapped in the rust were mainly composed of calcium, silicon, and oxygen. These constituents originate from calcium-silicate-hydrate (CSH) and the pore water of concrete.

The rust layer near the parent steel is more strictly of iron and less oxygen than other layers and the amount of oxygen is increased when moving outwards to the concrete interface. This suggests that the more porous corrosion products responsible for the most volume increase are located on the outer circumference near the concrete interface. A similar observation has also been made in [21,31].

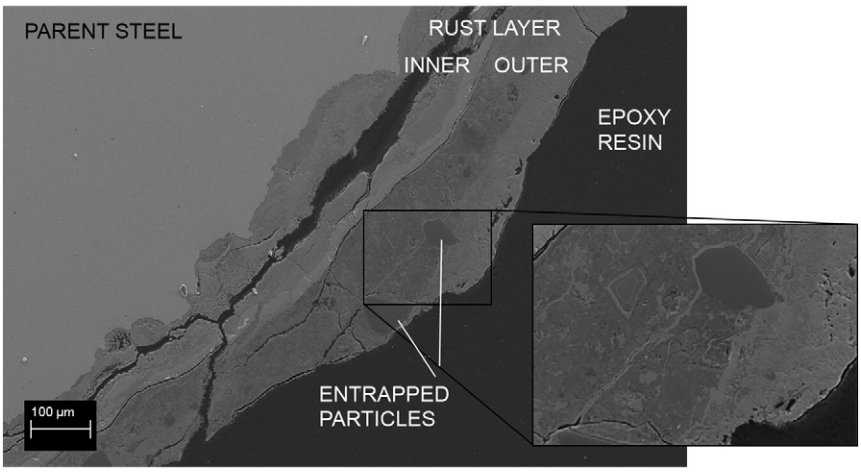

Fig. 5. Multi-layer composition of the corrosion products shown in a SEM image of the sample PI17C.2.

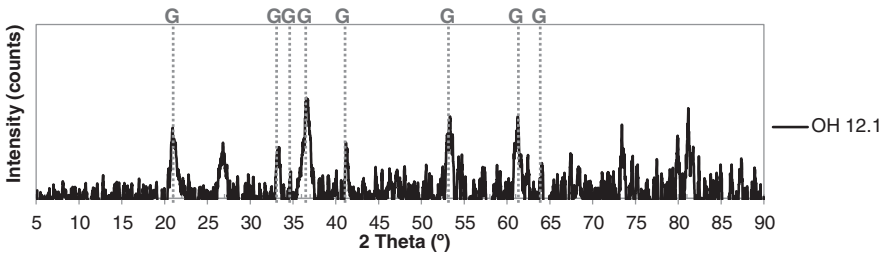

Fig. 7. XRD pattern of the rust scraped from the sample OH 12.1, dotted lines correspond to Goethite (G).

XRD patterns of the rust scraped from the samples OH 12.1 and VI 7.2 are presented in Figs. 7 and 8, respectively. The samples of this study originate from existing concrete facade structures from real outdoor conditions. Mainly Goethite, Feroxyhite and Lepidocrocite corrosion products were identified in majority of the samples by comparing the diffraction patterns to literature and powder diffraction files [32, 33] and (PDF 00-060-0344, PDF 01-079-1971). Magnetite/Maghemite (oxide) was also identified in three samples (PU 1.1, VI 7.2 and VI 16.1), but in general they were rare. Some of the non-rust peaks could also be identified to originate from the CSH of concrete. According to XRD results, the rust products in this case were mainly hydroxides (Feroxyhite, Goethite, Lepidocrocite). These rusts have unit volume of approximately 3 times the volume of iron.

TEM image with selected area electron diffraction (SAED) patterns of the rust powder from the sample OH 12.1 is presented in Fig. 9. SAED patterns indicated a nanocrystalline structure of rust and d-values (a distance between atomic layers calculated by measuring the radius of the rings in the SAED patterns) corresponded to goethite, lepidocrocite, and feroxyhite (PDF 00-013-0087, PDF 98-007-1808, PDF 00-060-0344). Thus, these results agree with XRD results. In addition, the TEM-EDS analyses of the rust powders were similar to the cross-sectional SEM-EDS results.

3.3. Application to corrosion modelling

The performed characterization studies imply that rust is mainly formed on the outward semicircle of the reinforcing bar and the corrosion products are mainly composed of hydroxides with a volume ratio to Fe of approximately 3. It is thereby proposed that this value can be utilized in service life analyses in similar carbonation induced corrosion cases. The volume ratio is a simplification made for service life modelling purposes and it assumes a homogenous layer of the main rust phases found. In reality the rust layer contains veins of multiple rust phases and the real relative volume to Fe is a compilation of the phases present. More sophisticated methods could be used to study the heterogeneity of the rust in more detail e.g. transmission Mössbauer spectroscopy [21] or micro-Raman spectroscopy [18]. The measured rust thickness in this study represents the total rust layer thickness including both corrosion stages presented in [15]. Characteristics of the porous zone around rebars should be known if one wanted to distinguish between the corrosion stages. Critical corrosion penetration to form cracks calculated for the sample cases by Eq. (1) [8] compared to the ones determined experimentally by the rust layer measurements and characterization is presented in Table 4.

Uncertainties that have to be acknowledged in utilizing the experimental data presented in this paper concern the age of the visual damage on the building facade which is linked to the time of condition assessment. In order for the crack or spall to be detected in the assessment these signs of damage have to have occurred before the assessment date. This time period before the condition assessment is in this study unknown. Thus, the visual damage is likely to be formed even earlier than the critical corrosion penetration values indicate. The error associated overestimates the measured rust thickness, and the results of this study should be treated accordingly. If the response time for the assessment was one year, it would cause overestimation of 3–4 μm with a moderate corrosion rate. The inherent error is greater considering small penetration values and lower considering the larger values. Even though care has been taken in protecting the rust layer of the samples during their preparation some amount of rust may have been lost during the experiments. This on its behalf underestimates the results since a smaller amount of rust is detected. To some extent these two uncertainties cancel each other out thereby lowering the error caused by uncertainty in the age of cracking.

An attempt to eliminate the uncertainty related with the response time of the assessment can be made by subtracting from the measured rust thickness the amount of rust that can be produced during the response time of one year for the assessment with the obtained corrosion rate for each sample (0.9–4.1 μm/year). An iteration of subtracting the corrosion penetration of one year and then recalculating the corrosion rate was performed. The calculation reached a fast convergence after three iterations. The error corrected values are included in Table 4.

The calculation (by DuraCrete) of the critical corrosion penetration gives values ranging 41.6–70.2 μm. It must be noted that with the concrete grade (C20/25) the ultimate minimum given by Eq. (1) is 36.1 μm regardless of the cover/diameter ratio of the reinforcement. This behaviour results from the fixed parameters a_1 and a_3 when cover/diameter ratio is set to zero. The critical corrosion penetration determined experimentally ranged 14.5–90.4 μm with an average value of 53.6 μm. The experimentally determined penetration values adjust well to literature [26–29]. The critical corrosion penetration was however observed to be highly dependent on the corrosion environment, thickness of concrete cover, the cover/diameter ratio of the reinforcement

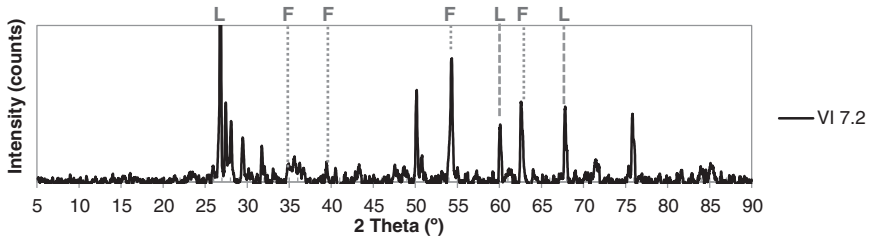

Fig. 8. XRD pattern of the rust scraped from the sample VI 7.2, dotted lines correspond to Feroxyhite (F) and dashed lines to Lepidocrocite (L).

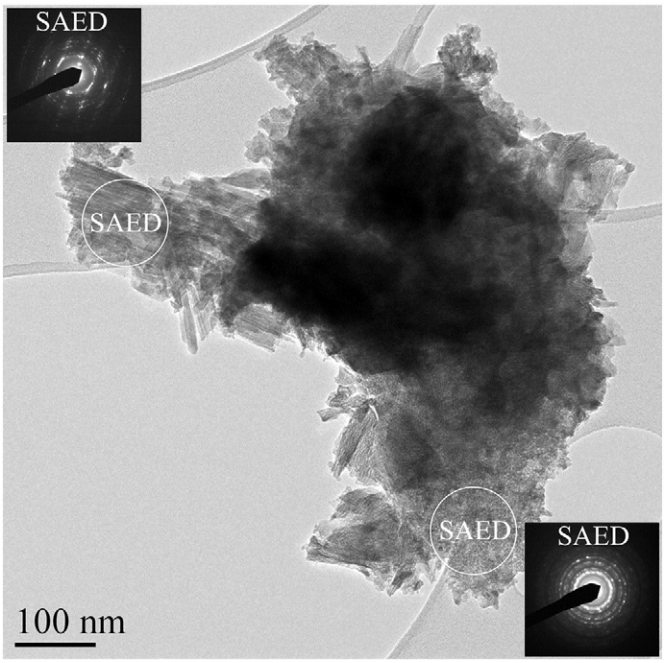

Fig. 9. TEM image with selected area electron diffraction (SAED) patterns of the rust powder from the sample OH 12.1.

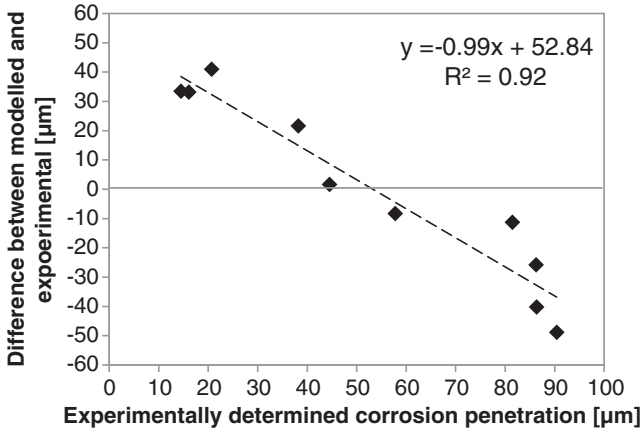

Fig. 10. The difference (error) caused by the Eq. (1) calculation compared to experimentally determined corrosion penetration.

and the tensile capacity of the cover concrete. The latter may vary considerably from the specified concrete grade due to e.g. the surface finish and curing of the concrete surface. The modelling is therefore specific to the structures and climate in question.

By average, the calculation method and the experimental values seem to be in good agreement. The calculation was however observed to overestimate the cases where the experimentally determined corrosion penetration has been small, see Fig. 10. Thereby, the most critical cases tend to be overestimated causing inherently too long service life predictions if the calculation method is used. On the other hand the cases where considerably large corrosion penetration is found experimentally the calculation vice versa underestimates and is thereby on the safe side. These cases usually have large concrete cover depth for the reinforcement compared to the reinforcement diameter and good quality concrete with high tensile capacity. This behaviour should be compensated for when Eq. (1) is used to describe the critical corrosion penetration of slender concrete panels.

The average rust thickness in the measurements of cracked samples was 111.7 µm and the corresponding average corrosion penetration was 53.6 µm with the determined volume ratio of 3. Spalling of concrete cover had occurred in average measured rust thickness of 72 µm with a corresponding average corrosion penetration of 36 µm. The results of the two cases seem to contradict the presumption that spalling is subsequent to cracking. However, the comparability of the two sample sets is low because the cover/diameter-ratio of the samples where spalling has occurred was considerably smaller (cover/diameter < 1.3) than that of the cracked samples (cover/diameter 1.6–4.7), see Tables 2 and 3. A more crucial risk for concrete spalling is thus associated with low cover/diameter ratio cases. Presumably, a crack has occurred first also in these low cover/diameter spalling cases. Further conclusions on the damage sequence cannot therefore be made.

The average time under active corrosion was for the cracked locations 26.0 years and for spalled locations 33.1 years. This information allows estimating the average corrosion rate during the active corrosion phase in these structures. For cracked locations the average corrosion rate after error correction was 2.2 µm/year (ranging 0.6–3.9 µm/year) and for spalled locations 1.1 µm/year. Again, the comparability of these two damage cases is poor because the main reason for the different damage mode has been the cover/diameter-ratio. Also regarding the spalled cases a quantity of corrosion products may have been detached with the spalled concrete or washed away.

4. Conclusions

Visual damage on the studied concrete facade panels had begun to emerge after 35 years of service life (The average age of the studied damaged cases was 38.8 years). Corrosion cracks emerged after 26 years of active corrosion. Corrosion induced damage was found on the lap splicing locations of rebars, in the edges and window openings of the panels and in locations with pronounced moisture load due to poorly functioning flashings and rain water runoff control. In the studied structures the main reason for the damage to emerge in the studied time span

Table 4
Comparison of the experimentally determined and calculated critical corrosion penetration until cracking of concrete cover.

Sample id	Rust thickness on the steel samples, [µm]	Critical corrosion penetration, rust volume ratio = 3, [µm]	Error corrected corrosion penetration, [µm]	Duracrete critical corrosion penetration, [µm]	Difference, model − experimental, [µm]
Vi 16.1	178.1	89.1	86.2	60.5	−28.6
Vi 6.1	170.7	85.4	81.5	70.2	−15.2
Pi 17D.1	–	–	–	56.2	–
RU 6.2	80.5	40.3	38.2	59.8	19.6
KA 9.1	34.8	17.4	16.1	49.3	31.9
RU 6.1	120.3	60.2	57.8	49.5	−10.6
Vi 7.2	44.8	22.4	20.7	61.7	39.3
KU 14.2	30.2	15.1	14.5	48.0	32.9
Pi 17B.2	179.4	89.7	86.3	46.2	−43.5
Pi 17C.2	92	46.0	44.5	46.2	0.2
PU 1.2	186.1	93.1	90.4	41.6	−51.5
Average	111.7	55.8	53.6	53.5	

as cracking or spalling was the concrete cover depth in relation to the rebar diameter, i.e. the cover/diameter ratio. If the ratio is small (below 1.5) corrosion related damage probably emerges as spalling. If the ratio is well over 1.5 the damage more probably emerges as cracking.

Corrosion products associated with carbonation initiated corrosion on the studied concrete facade panels were mostly hydroxide type of rusts (e.g. Goethite and Lepidocrocite) which have a unit volume of roughly 3 times the volume of iron. More sophisticated methods could be used to study the heterogeneity of the rust in more detail.

Taking the determined relative volume of the rust layer into account the required corrosion penetration to initiate visually observable cracks in the studied facade panels was by average 53.6 μm with a corresponding rust thickness of 111.7 μm. This total corrosion penetration can be utilized in service life calculations of similar structures because it is the sum of the corrosion stages responsible for crack emergence. Uncertainties stated in chapter 4 should be taken into account when the information is applied for further uses.

The results obtained in this study can be used to calibrate Eq. (1) to describe better the critical corrosion penetration of slender concrete panels. Two main points should be taken into account: i) The ultimate minimum value should be adjusted to fully take into account the small cover depths and ii) Sensitivity to both small and large corrosion penetration values should be increased by adjusting the regression parameters case specifically for different structures.

Acknowledgements

This study was made possible by the Doctoral Programme of Built Environment (RYM-to) under the funding of the Academy of Finland (grant number T20500/913615/RYM-TO). The authors would like to thank the Engineering office Lauri Mehto Oy for providing the opportunity for additional core sampling and participating in the condition assessments.

References

[1] E.J. Fasullo, Infrastructure: The Battlefield of Corrosion, Corrosion Forms and Control for Infrastructures, ASTM STP11371992 1–16.
[2] E.J. Wallbank, The Performance of Concrete Bridges: A Survey of 200 Highway Bridges, HMSO Publication, London, 1989 96 p.
[3] G.P. Tilly, Durability of concrete repairs, in: M. Grantham (Ed.), Concrete Repair—A Practical Guide, Taylor & Francis, New York 2011, pp. 231–247.
[4] A. Köliö, Degradation induced repair need of concrete facades(MSc thesis) Tampere University of Technology2011 (74 p (in Finnish)).
[5] J. Lahdensivu, Durability Properties and Actual Deterioration of Finnish Concrete Facades and Balconies, 1028Tampere University of Technology. TUT Publ, 2012 (117 p.).
[6] J. Broomfield, Corrosion of Steel in Concrete, 2nd edition Taylor & Francis Oxon, 2007 (277 p).
[7] M.G. Richardson, Fundamentals of Durable Reinforced Concrete, Spon Press, New York, USA, 2002 (240 p).
[8] DuraCrete., Probabilistic performance based durability design of concrete structures, The European Union—Brite EuRam III, DuraCrete. Final technical report of duracrete project, document BE95-1347/R17. CUR, Gouda, Nederland, 2000.
[9] Concrete Association of Finland, BY 50 Concrete Code 2012. Helsinki, The Concrete Association of Finland, 2012 (in Finnish).
[10] F. Lollini, E. Redaelli, L. Bertolini, Analysis of the parameters affecting probabilistic predictions of initiation time for carbonation-induced corrosion of reinforced concrete structures, Mater. Corros. 63 (12) (2012) 1059–1068.
[11] Y. Liu, R.E. Weyers, Modelling the time-to-corrosion cracking in chloride contaminated reinforced concrete structures, ACI Mater. J. 95 (6) (1998) 675–681.
[12] T.D. Marcotte, Characterization of chloride-induced corrosion products that form in steel-reinforced cementitious materials, PhD thesis in Mechanical Engineering. University of Waterloo, Waterloo, Canada, 2001 (330 p).
[13] S.J. Jaffer, C.M. Hansson, Chloride-induced corrosion products of steel in cracked-concrete subjected to different loading conditions, Cem. Concr. Res. 39 (2009) (2009) 116–125.
[14] Y. Zhao, Y. Jiang, H. Bingyan, J. Weiliang, Crack shape and rust distribution in corrosion-induced cracking concrete, Corros. Sci. 55 (2012) (2012) 385–393.
[15] Y. Zhao, Y. Jiang, W. Yingyao, J. Weiliang, Critical thickness of rust layer at inner and out surface cracking of concrete cover in reinforced concrete structures, Corros. Sci. 59 (2012) (2012) 316–323.
[16] T.D. Marcotte, C.M. Hansson, Corrosion products that form on steel within cement paste, Mater. Struct. 40 (2007) (2007) 325–340.
[17] K. Suda, S. Misra, K. Motohashi, Corrosion products of reinforcing bars embedded in concrete, Corros. Sci. 35 (5-8) (1993) 1543–1549.
[18] W.-J. Chitty, P. Dillmann, V. L'Hostis, C. Lombard, Long-term corrosion resistance of metallic reinforcements in concrete—a study of corrosion mechanisms based on archaeological artefacts, Corros. Sci. 47 (2005) (2005) 1555–1581.
[19] A. Dehoux, F. Bouchelaghem, Y. Berthaud, D. Neff, V. L'Hostis, Micromechanical study of corrosion products layers. Part I: Experimental characterization, Corros. Sci. 54 (2012) (2012) 52–59.
[20] B. Huet, V. L'hostis, G. Santarini, D. Feron, H. Idrissi, Steel corrosion in concrete: determinist modeling of cathodic reaction as a function of water saturation degree, Corros. Sci. 49 (4) (2007) 1918–1932.
[21] G.S. Duffo, W. Morris, I. Raspini, C. Saragovi, A study of steel rebars embedded in concrete during 65 years, Corros. Sci. 46 (2004) (2004) 2143–2157.
[22] L. Abosrra, A.F. Ashour, M. Youseffi, Corrosion of steel reinforcement in concrete of different compressive strengths, Constr. Build. Mater. 25 (2011) (2011) 3915–3925.
[23] C.Q. Li, Reliability based service life prediction of corrosion affected concrete structures, J. Struct. Eng. ASCE 130 (2004) (2004) 1570–1577.
[24] C. Andrade, A. Castillo, Evolution of reinforcement corrosion due to climatic variations, Mater. Corros. 54 (2003) (2003) 379–386.
[25] A. Jamali, U. Angst, B. Adey, B. Elsener, Modeling of corrosion-induced concrete cover cracking: a critical analysis, Constr. Build. Mater. 42 (2013) (2013) 225–237.
[26] A.J.M. Siemes, A.C.W.M. Vrouwenvelder, A. van den Beukel, Durability of buildings: a reliability analysis, Heron 30 (3) (1985) 3–48.
[27] L.J. Parrott, Design for avoiding damage due to carbonation-induced corrosion, in Proceedings of Third International Conference on Durability of Concrete, Nice, Special Publication SP-145, Am. Concr. Inst. (1994) 283–298.
[28] C. Alonso, C. Andrade, J. Rodriguez, J.M. Diez, Factors controlling cracking of concrete affected by reinforcement corrosion, Mater. Struct. 31 (1998) 435–441.
[29] C. Andrade, Measurement of Polarization Resistance On-site in: Corrosion of Steel in Reinforced Concrete Structures. Final report of COST action 521, Office for Official Publications of the European Communities, Luxembourg, 2003 82–98.
[30] K. Tuutti, Corrosion of steel in concrete. Stockholm. Swedish Cement and Concrete Research Institute, CBI Res. 4 (82) (1982) (304 p).
[31] H. Cano, D. Neff, M. Morcillo, P. Dillmann, I. Diaz, D. de la Fuente, Characterization of corrosion products formed on Ni 2.4 wt%–Cu 0.5 wt%–Cr 0.5 wt% weathering steel exposed in marine atmospheres, Corros. Sci. 87 (2014) (2014) 438–451.
[32] M.A. Legodi, D. de Waal, The preparation of magnetite, goethite, hematite and maghemite of pigment quality from mill scale iron waste, Dyes Pigments 74 (2007) (2006) 161–168.
[33] V.A. Drits, B.A. Sakharov, A. Manceau, Structure of feroxyhite as determined by simulation of X-ray diffraction curves, Clay Miner. 28 (1993) (1993) 209–222.

V

THE CORROSION RATE IN REINFORCED CONCRETE FACADES EXPOSED TO OUTDOOR ENVIRONMENT

by

Köliö A., Hohti H., Pakkala T.A, Laukkarinen A., Lahdensivu J., Mattila J. & Pentti M., Jun 2016

Materials and Structures, Accepted manuscript 10.6.2016

The corrosion rate in reinforced concrete facades exposed to outdoor environment

(Accepted manuscript version, 10.6.2016, Materials and Structures, Springer)

Arto Köliö[a,c], Toni A. Pakkala[a], Harri Hohti[b], Anssi Laukkarinen[a], Jukka Lahdensivu[a], Jussi Mattila[a], Matti Pentti[a]

[a] *Tampere University of Technology, Deparment of Civil Engineering, P.O.Box 600, FI-33101, Tampere, Finland, email: arto.kolio@tut.fi, toni.pakkala@tut.fi, anssi.laukkarinen@tut.fi, jukka.lahdensivu@tut.fi, jussi.mattila@tut.fi, matti.pentti@tut.fi*

[b] *Finnish Meteorological Institute, email: harri.hohti@fmi.fi*

[c] *corresponding author: arto.kolio@tut.fi, tel. +358 40 849 0837*

Abstract

Outdoor concrete structures such as concrete facade panels and balcony frame panels are subjected to various environmental actions causing reinforcement corrosion problems. Long-term field measurement data on reinforcement corrosion in carbonated concrete on these structures was utilized in the creation of a corrosion rate regression model combining weather parameters such as temperature, relative humidity, wind-driven rain and solar radiation to corrosion rate. A versatile model capable of predicting the effect of varying environmental actions on the corrosion rates of carbonation induced corrosion was produced. Wind-driven rain was found to have the greatest impact on corrosion rate in tandem with the micro climate surrounding the building. Due to changes in air temperature, air relative humidity as well as in the amount of wind-driven rain and solar radiation, the corrosion rate on concrete facades and balconies is constantly changing. Despite the high seasonal and yearly variation, the average level of the modelled corrosion rate was quite steady on a longer 30-year perspective. This information is substantial for the long term service life design of concrete structures.

keywords: concrete; reinforcement; carbonation; corrosion; field measurement; modelling; service life design

1. Introduction

1.1 Overview

Corrosion of steel reinforcement in ageing concrete structures has caused globally extensive need of repair and large maintenance costs in concrete infrastructure and buildings (Fasullo 1992, Tilly 2011). While chlorides are the main reason for corrosion in marine and coastal region as well as where de-icing salts are used, the carbonation of concrete cover is behind the corrosion phenomenon in many concrete structures exposed to outside air, such as facades and balconies. This article focuses on corrosion initiated by carbonation on concrete facades and balconies.

Corrosion of steel reinforcement in concrete is commonly regarded as an electrochemical phenomenon meaning that corroding reinforcement works as a mixed electrode where cathodic and anodic areas are formed on the steel surface. Corrosion due to carbonation is considered to be general over the reinforcement surface with fairly evenly spaced cathode and anode areas. (Page 1988). Concrete protects steel from corrosion chemically by creating a passive film on the steel surface and physically as a protective layer for the reinforcement, thus, corrosion does not initiate immediately. This has been taken into account by depicting reinforcement corrosion as a process consisting of two or more consecutive phases (Tuutti 1982).

During the initiation phase carbon dioxide penetrates the concrete cover and reacts with hydroxides in concrete pore water. The carbonation reaction begins from the concrete surface and advances inside the concrete as a front. As the carbonation front reaches the depth of the reinforcing steel it initiates the corrosion process. Until this point, no actual damage has occurred. In the propagation phase, the corrosion of the reinforcement in concrete structures has two basic effects. Firstly, it can cause cracking of the concrete cover, and secondly, the effective steel cross-section is reduced (Broomfield 2007). Cracking occurs when the stresses induced by the increasing rust layer exceed the tensile capacity of concrete especially in structures where the reinforcement is placed relatively close to the surface of the concrete. The cracking accelerates the penetration of agents which are harmful to concrete and may facilitate further damage as well as causes unsightly visual defects to the concrete structures, which can be especially unwanted on concrete facades and balconies. Cracking can be considered as a limit based on the appearance or serviceability of the structure where the needed intervention would be patch repairs and coatings. Visual damage which has advanced further leads to spalling, where a whole segment of the concrete cover will fall from the concrete surface. The rate of the corrosion process depends on many things, such as the cover depth, diameter of the reinforcing steel as well as temperature and the availability of moisture and oxygen (Ahmad 2003). Earlier research (Tuutti 1982, Andrade and Castillo 2003) indicates that corrosion rate during the propagation phase is highly affected by drying and wetting cycles of the structure. These cycles are in natural

conditions formed by weather parameters such as temperature, relative humidity, rainfall, solar radiation etc.

The popularization of open data policy in the European Union (Directive 2013/37/EU) as well as in Finland is making high frequency (time step < 3h) weather data more easily accessible also to professionals working outside the academia and available for practical service life design. This paper discusses a way of utilizing the available weather data in the field of corrosion modelling.

The ability to model or forecast corrosion rates on concrete facades will enhance the capability of realtors among other stakeholders to react on upcoming repair needs. This kind of model would be able to predict the residual service life of a certain structure, but it could also be used in creating renovation strategies for a larger building stock by revealing the order of importance or the urgency of single renovation projects. Such a tool could be used also in moving towards a predictive upkeep of realty (Lahdensivu 2012) and the confidence of making long term contracts between realty owners, renovation engineers and contractors.

1.2 The objective of this research

The objective of this study is to determine the individual and combined effect of weather parameters on the rate of reinforcement corrosion on already-carbonated concrete structures exposed to natural outdoor environment. This is accomplished by combining long-term corrosion rate measurement data to weather data from the location of the measurements from the same time period. A service life design model was generated to correlate the critical weather parameters directly to the corrosion rate of the reinforcement inside the concrete facade panel structures.

2. Background

2.1 The outdoor air climatic conditions

Outdoor air climatic conditions include variables such as air temperature and relative humidity, wind speed and direction, precipitation, short-wave solar radiation and long-wave thermal radiation. Depending on the application, also other variables such as outdoor air carbon dioxide concentration might be of interest. The outdoor air conditions are almost constantly changing, so to describe them with sufficient accuracy it is necessary to use measured data from meteorological stations.

As consecutive years are typically different from each other, different methods exist to take this variability into account in different studies: One approach is to use suitably chosen test/design

reference years (Sanders 1996) that have been pre-evaluated to represent the phenomena at hand (e.g. building energy consumption or the hygrothermal behaviour of building envelope structures). A second approach is to conduct simulations with large reference periods (normally 30 years) which represent current climate and minimize the effect of yearly variation. Monte Carlo methods can be used to reduce the amount of computational work. (Hagentoft et al. 2015). With shorter known measurement periods, such as the monitoring period discussed later in this article, the outdoor air conditions from that specific period can be used directly.

2.2 The Finnish climate

In the Köppen Climate Classification system Finland lies in the borderline between the humid continental and the subarctic climate (Köppen-Geiger Dfc), in which warm summers and freezing winters are typical. Similar climate to Finland (by the classification) is found in the rest of Scandinavia and in large parts of Russia and Canada. (Kottek et al. 2006).

Although the Finnish climate is relatively steady considering the latitudes, it still varies significantly from the mild and relatively rainy coastal area to the drier inland. Most of the rain and sleet in wintertime arrives with southerly to westerly winds. Rain events with wind from other directions have been rare. (Jylhä et al. 2009). Based on (Pakkala et al. 2014) in the present climate the amount of the precipitation in the form of rain and sleet is 20 % higher in the coastal area (Helsinki-Vantaa airport) than inland (city of Jyväskylä). As well, due to strong winds, 74 % of the rain and sleet load in the coastal area hits the vertical surfaces while the corresponding share inland is about 54 %. If the influence of prevailing wind directions and velocities is taken into account, the amount of rain and sleet affecting the vertical facade surfaces is up to 64 % higher in the coastal area than inland. Also the allocation of visible damage observed on existing concrete facades and balconies indicates a higher stress level in the coastal area than inland (Lahdensivu et al. 2013).

2.3 Wind-driven rain estimation

The standard SFS-EN ISO 15927-3 (2009) presents a factor I_{WA} (Wall annual index) which can be used to convert the amount of precipitation, unit [mm], collected by a free-standing driving-rain gauge in a flat open country to present the amounts of precipitation that impacts on a real wall.
The wall annual index is a simplified way of assessing the wind-driven rain against building facades. More sophisticated methods to model wind-driven rain include e.g. the semi-empirical SB model by Straube and Burnett (2000) and the CFD model by Blocken and Carmeliet (2002; 2007) based on the studies of Choi (1994). The both models take into account more precisely the distribution of the wind-driven rain in different areas of the facades. The CFD model is the most advanced but it also needs

significantly more demanding computing (Blocken et al. 2010). Although the wall annual index is a simplified method, it gives adequate results for e.g. comparing the different locational effects on the amount of wind-driven rain on facades. Compared to the CFD modelling it underestimates the amount of wind-driven rain near the top of the façade but overestimates the amount on the top 2.5 metres with high buildings and low rain intensity. The higher the rain intensity the more it underestimates the amount of wind-driven rain. The underestimation increases near the edges of the building. (Blocken et al. 2010).

2.4 Corrosion rate

2.4.1 Corrosion monitoring

Reinforcement corrosion can be monitored in terms of three measurement parameters: half-cell potential, concrete resistivity, and corrosion current density (Ahmad 2003). Andrade and Castillo (2003) subjected concrete specimens to both laboratory induced environments and natural environment in Madrid during a time period of five years. The authors monitored temperature, RH and precipitation as well as corrosion potential, current density and resistivity of the samples. The main influencing factors were temperature and rain events and their cyclical variation daily and seasonally. Cold climates were hypothesized to pose greater risk for corrosion due to lesser ability of the concrete to dry. It was also observed that the natural environment imposes fluctuations in the reinforcement corrosion behaviour that cannot be fully predicted by laboratory experiments. Al-Neshawy (2013) presented an automated system for monitoring temperature and relative humidity in concrete facades (RHT-MAPS -system) composed of a set of T and RH sensors, network components and analysis software. The system was utilized in predicting seasons/months with high corrosion risk. It was stated that more parameters such as wind-driven rain and solar radiation would increase the reliability of the predictions.

The ability to use linear polarization resistance (LPR) technique (Stern & Geary 1957) to monitor instantaneous corrosion rate was tested over gravimetric measurements by Law et al. (2004). The authors monitored carbonation and chloride induced corrosion in reinforced concrete samples under cycles of wetting and drying in the laboratory over a period of approximately three years. LPR method was found to overestimate weight loss regardless of the way of corrosion initiation (carbonation or chloride ingress). However, in carbonation induced uniform corrosion the method was found to give more reliable results of corrosion rate than for localized chloride induced corrosion. Karthick et al. (2014) evaluated the functionality of both embedded potential sensors and corrosion rate monitoring probe sensors (LPR) as well as surface mounted systems. The embedded systems were found to be the most reliable in the test period of 24 months. New solutions and materials for reference electrodes are

actively studied (Tang et al. 2015; Maruthapandian et al. 2016) to improve the stability of corrosion rate measurements.

2.4.2 Classification of corrosion rate

Many studies on the response of concrete reinforcement to either simulated atmospheric conditions or natural environment have been conducted over the years (e.g. Parrott 1987, Rasheeduzzafar 1992). Corrosion current densities on levels normally found on concrete reinforcement were classified and related to the diameter loss of steel by Andrade and Alonso (2001). According to the proposed classification, corrosion level is regarded high when corrosion current densities exceed 1.0 μA/cm^2. It equals to an approximate metal loss of 10 μm/year. Corrosion current densities of 0.5–1.0 μA/cm^2 are regarded as moderate corrosion level. On the other hand, the corrosion level at current densities below 0.1 μA/cm^2 is regarded as negligible. Recently, a neural network based model was proposed to describe the corrosion level based on long term measurements of the relative humidity of concrete facade panels (Taffese & Sistonen 2016).

3. Research methods and material

The research material is composed of a long-term corrosion current density measurement data on concrete facades and vertical balcony structures (frame panels) and long-term weather observation data corresponding to the measurement time span. The corrosion current density data was measured from the facades and balconies of two residential buildings in Finland: an inland location at Fysiikanpolku 5, Tampere, built in 1978 and a coastal area at Joupinrinne 4, Espoo, built in 1978 (Fig 1). The sites are further denoted as “Inland” and “Coastal area” respectively. The measurements were arranged on one facade and on one balcony tower adjacent to the facade. The instrumented structures were at both measurement sites facing southern directions: at Inland southeast (154 degrees from north, clockwise) and at Coastal area southwest (223 degrees from north, clockwise).

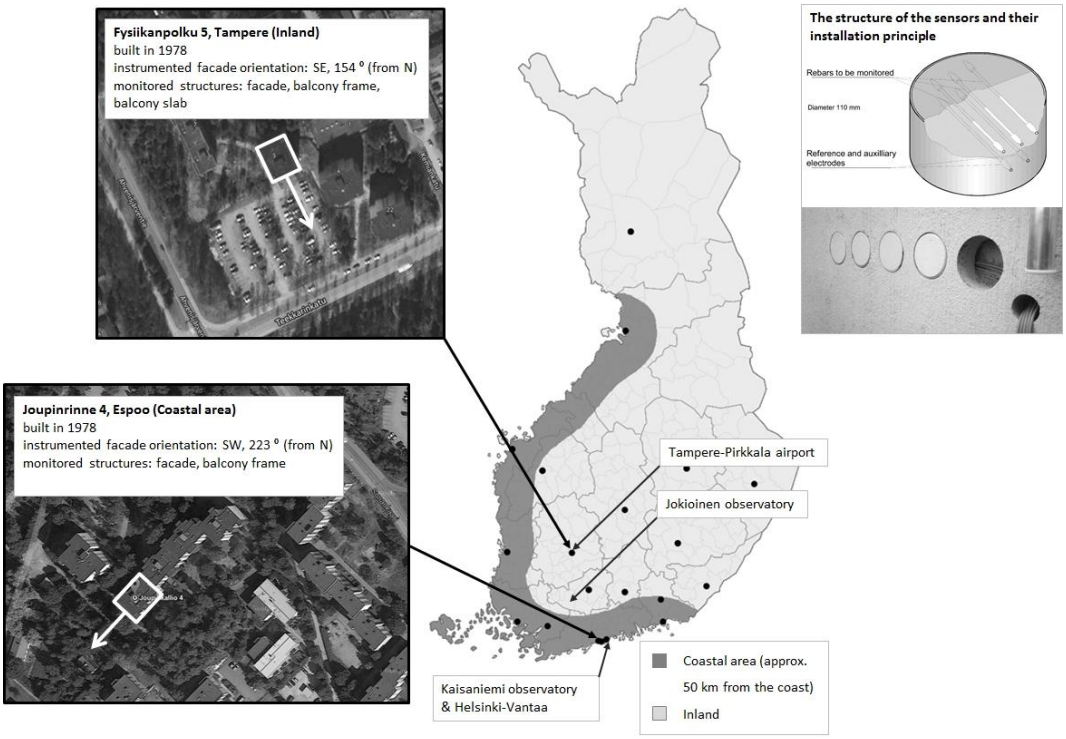

Figure 1 The structure of the measurement device and the geographical locations of the corrosion measurements in Tampere and Espoo, and the weather data in Tampere-Pirkkala airport (supplemented with solar radiation data from Jokioinen) and in Kaisaniemi observatory in Helsinki.

3.1 Field measurement data on corrosion current density

Corrosion rate data on concrete facades and balconies was available for the regression study from past monitoring period (Mattila & Pentti 2008) from the beginning of December 2000 until the end of year 2002 comprising a total of 25 months. The average measuring interval was roughly three hours through the whole monitoring period. The arrangement of the measurements and the measurement device are described also in (Mattila 2007, Mattila & Pentti 2008).

For the monitoring purposes, special cylindrical sensors (Fig. 1) composed of concrete, the monitored rebars and reference and auxiliary electrodes were manufactured, prepared and mounted into structures of existing buildings. The sensors utilized LPR-technique to measure the instantaneous corrosion rates. The basic idea of the sensors was to simulate reinforced concrete structures where reinforcing steel is corroding in carbonated concrete.

The diameter of sensors was 110 mm and the thickness 60 mm, which is the typical thickness of the outer panels of Finnish concrete façade stock. The sensors were prepared to contain

reinforcement bars and suitable electrodes for the monitoring of corrosion rate. The steel bars were made of ordinary cold drawn reinforcement with the diameter of 4 mm and nominal yield strength of 500 MPa. The cover depths of the rebars in the sensors were 5, 10 and 15 mm. The composition of the concrete used in the sensors was selected so that the concrete would represent the grade used in concrete facades in Finland during 1970's as well as possible. The specified concrete grade used in facade panels in Finland was C20/25 from 1965 until 1989. The cement type used in these precast panels is mostly CEM I ordinary Portland cement. The cubic strength of the concrete in the sensors was 25 MPa with a water-cement ratio of 0.8. The concrete sensors were exposed to accelerated carbonation in 4 % carbon dioxide according to (Dunster 2000) prior to installing on the monitored structures. The sensors on vertical surfaces were mounted into holes drilled through the outer leafs of concrete panels or balcony side walls. The sensors were coated with open silicate paint which would not affect the transportation of moisture compared to uncoated concrete.

Monitored data was available from three types of structures: 1) facade surfaces (outer leaf of sandwich panel representing an exterior wall of a heated building with thermal insulation of 90 mm mineral wool), 2) bearing side wall of a concrete panel balcony (representing a "cold" vertical structure) and 3) bottom surface of a balcony slab in an open balcony (representing a "cold" horizontal structure). 9 sensors were installed in each building: four sensors in facade panels, three in supporting side wall of balconies and two sensors on the bottom surface of balcony slabs. The sensors in the facades were mounted in a horizontal row in the middle of the uppermost wall panel row facing south. In the balconies, the sensors were mounted in the half height of the uppermost side wall facing south.

3.2 Weather observation data

The weather observation data was composed of the temperature and relative humidity of the surrounding air, the amount of rainfall (using daily observations together with 15 min weather radar data), the wind direction and velocity and direct and diffuse solar radiation on a horizontal surface. The obtained data is characterized in Table 1. The weather observation data was collected for this study by Finnish Meteorological Institute (FMI) and it was then further refined to form four weather parameters: Temperature (T, [ºC]), relative humidity (RH, [%]), amount of wind-driven rain on the measured wall surface (I_{WA}, [mm]), amount of direct and diffuse solar radiation on the measured wall surface (RAD, [kJ/m^2]) to perform the

regression analysis. The data was obtained from observation stations nearest to the case buildings with a time resolution of three hours.

Table 1 Description of the research data

Measured variable	Time resolution	Location of measurement in inland	Distance to the Inland site at Fysiikanpolu 5, Tampere (km)	Location of measurement in coastal area	Distance to the Coastal area site at Joupinrinne 4, Espoo (km)
Corrosion current density	3 h	Fysiikanpolku 5, Tampere	Directly on site	Joupinrinne 4, Espoo	Directly on site
Temperature of the surrounding air	3 h	Tampere-Pirkkala Airport	12.7	Kaisaniemi, Helsinki	15.4
Relative humidity of the surrounding air	3 h	Tampere-Pirkkala Airport	12.7	Kaisaniemi, Helsinki	15.4
Amount of rainfall	24 h	Tampere-Pirkkala Airport	12.7	Kaisaniemi, Helsinki	15.4
Wind direction and velocity	3 h	Tampere-Pirkkala Airport	12.7	Kaisaniemi, Helsinki	15.4
Solar radiation	3 h	Jokioinen observatory	79	Kaisaniemi, Helsinki	15.4
Weather radar data	15 min	Fysiikanpolku 5, Tampere	Directly on site (radar dislocation 54 km)	Joupinrinne 4, Espoo	Directly on site (radar dislocation 13 km)

3.3 Weather radar data

Weather radar data from FMI was used to improve the temporal resolution and location of rainfall estimation. The measured quantity in this study was reflectivity, measured in 500 m radial resolution every fifteen minutes over the research sites. The reflectivity (backscatter signal from raindrops) is related to the sum of raindrop diameters to sixth power inside the measuring volume. The inverse relation from reflectivity to rain rate is based on climatological raindrop size distribution. However, in the case of instantaneous radar

measurement, this can differ from the real rainfall rate typically by factor from 0.5 to 4, depending on precipitation type and distance from radar. So the short term radar rainfall measurements should always to be fitted with nearby in-situ surface rainfall observation if possible. In this study the weather radar data was calibrated by adjusting the monthly amount to the surface rainfall observation.

The weather radar data from both sites was missing the time period of approximately 1.5 months from Feb 19th to Apr 1st 2001. In addition five single days were missing from the Inland site data and two single days from the Coastal area site data. This missing data was replaced by the daily rainfall observations. Since the time resolution used in the final analysis is one month the representativeness of the data is still considered good. This may, however, be of influence on the analysis of the spring season.

3.4 Preparing of the weather parameters

3.4.1 Temperature and relative humidity (T, RH)

The temperature and relative humidity measurements were nearly continuous with the time resolution of three hours from both geographical locations. The temperature measurements contained only single isolated missing readings (< 10 readings in the 25 month period of 3h resolution), which were interpolated from the surrounding readings to obtain a continuous data set. The relative humidity data contained single isolated missing readings (a total of 89 readings in the 25 month period of 3h resolution) which were treated in a similar manner to the temperature data. Data from Inland, however, contained also a longer period of missing readings of 2.5 days (from 12:00 am 21st June 2002 to 6:00 am 24th June 2002, in all 20 readings). This period was ignored in the further analysis. The impact on the modelling of these missing readings was considered minor. After these corrections the temperature and RH data was used as such for the modelling purposes. The unit for the temperature was (°C) and for the RH (%).

3.4.2 Wind-driven rain (I_{WA})

The wall annual index given in the standard SFS-EN ISO 15927-3 (2009) was used to estimate the amount of wind-driven rain on a real wall (Eqs. 1 and 2). The weather radar data (15 min resolution) calibrated with the surface rainfall observations was used as the rainfall and wind direction and velocity was obtained from the weather observations (3h resolution).

The precipitation data was summed to match the 3-hour data. The data was available for the whole period when the corrosion current density were measured, i.e. collected from the beginning of December 2000 until the end of year 2002 comprising a total of 25 months.

The airfield annual index I_A is presented as:

$$I_A = \frac{2}{9} \frac{\sum v r^{\frac{8}{9}} \cos(D - q)}{N} \qquad (1)$$

Where

v = hourly mean wind speed [m/s]

r = hourly rainfall total [mm]

D = hourly mean wind direction from north [°]

θ = the angle between north and a line normal to the wall [°]

N = number of years for which data is available

The summation is taken over all hours for which $\cos(D - \theta)$ is positive. Finally, the effects of the building site (obstruction etc.) were taken into account by Eq.2.

$$I_{WA} = I_A C_R C_T O W \qquad (2)$$

Where

I_A = the airfield annual index calculated by Eq. (1)

C_R = a terrain roughness coefficient

C_T = a topography coefficient

O = an obstruction factor

W = a wall factor.

The constants used in calculating the Wall index I_{WA} were chosen based on the actual locations and surroundings of the studied buildings and the directions of the measured facades and balconies (Fig 1). In both cases the C_R was calculated with Terrain category III (Suburban or industrial areas and permanent forests) and the height above ground (z) was 21 metres. The topography coefficient C_T takes into account the increase of mean wind speed over isolated hills and escarpments near the building subjected to the study. The obstruction factor O depends on the horizontal distance to the nearest obstacle which is at least as high as the wall

subjected to the study. The wall factor W is, in the case of flat roof multi-storey building, 0.5 for the top 2.5 m of the wall and 0.2 for remainder. The values used in the calculation were C_R=0.93, C_T=1, O=1 and W=0.5.

3.4.3 Solar radiation (RAD)

The solar radiation to different wall surfaces was calculated from the meteorological data that included the global and diffuse solar radiation on a horizontal surface. First the diffuse radiation was subtracted from the global radiation to acquire the direct radiation on a horizontal surface. The amount of direct radiation was then converted on the vertical surfaces (Fig 1) by a factor C based on a solar position algorithm (Reda & Andreas 2008) taking into account transient solar angles at a given latitude and longitude. After calculating these angles the basic trigonometric functions were used to calculate the component of the beam solar radiation perpendicular to the studied wall. The final solar radiation parameter (RAD) on the facade surface was composed of the beam solar radiation perpendicular to the studied wall and the diffuse radiation components by adding them up in one parameter. The solar position angle algorithm was implemented in the R software (R Core Team 2014).

In reference (Reda & Andreas 2008) the uncertainty in the solar position angles is stated to be of approximately ±0.0003° in the time period from year 2000 BCE to 6000 CE. The results were in line with the reference cases in the appendices of the report. The results of the algorithm were also evaluated qualitatively by analyzing the plots of elevation and azimuth angles and of the relative proportions of solar radiation on the wall and on the ground surface. The beam solar radiation perpendicular to the studied wall was controlled by comparing and limiting it to the solar constant 4898.9 kJ/m^2 (Kopp & Lean 2011) representing the maximum available solar radiation on earth's surface.

3.5 Multi linear regression

Multi linear regression was used to determine the partial influence of single or a sequence of weather parameters to the observed corrosion current density. This study concerns corrosion rate inside concrete and weather properties of the surrounding air (and not the temperature and/or moisture inside concrete) as monthly values. Each of the studied structures, locations, weather parameters and isolated time periods were cross tabulated with corrosion rate forming

in all 525 regression calculations. The regression was calculated according to Eq. (3) by fitting the equation by the least squares method.

$$I_{corr} = b_0 + b_1 \times x_1 + (b_2 \times x_2 + b_3 \times x_3 + b_4 \times x_4) + n \qquad (3)$$

Where,

I_{corr} = average monthly corrosion current density (the dependent variable)

β_0 = interception term

β_1, x_1 = coefficient and monthly parameter of independent variable 1 (weather parameter)

β_2, x_2 = coefficient and monthly parameter of independent variable 2 (weather parameter, optional)

β_3, x_3 = coefficient and monthly parameter of independent variable 3 (weather parameter, optional)

β_4, x_4 = coefficient and monthly parameter of independent variable 4 (weather parameter, optional)

v = error term

In concrete the response to the changes in temperature and moisture of the concrete itself follow physical laws e.g. on diffusion which are fundamentally nonlinear. Transient fluctuation of e.g. the moisture content inside concrete is dependent on moisture difference, depth and material properties. Thereby, the moisture content of concrete reacts with a delay to changes in the surrounding environment. If transient correlation between the parameters was to be studied, a linear model could therefore not be used. However, a linear relationship can be assumed between monthly averages of corrosion rate and monthly averages of weather parameters when the sampling time step of the variables (averages or sums calculated over one month) is considerably longer than the actual fluctuation of the sampled parameter (less than one hour). A multi linear regression assumes linear relationship between the dependent and multiple independent variables. The residual plots of the regression generally showed a random pattern with an even number of positive and negative residuals around the neutral axis, which indicated a good fit with the linear model.

4. Results and discussion

4.1 The corrosion rates in facade and balcony structures

At the Inland site the monthly average corrosion current densities were 0.05–2.08 µA/cm^2 on facades (Fig. 2-5). The current densities on the balcony frame panels were found to have been higher with monthly averages of 0.37–3.40 µA/cm^2. Corrosion rates were highest in the autumn and winter seasons and lowest in the summer season. The yearly averages were 0.84 µA/cm^2 (year 2001) and 0.32 µA/cm^2 (year 2002) for the facades and 1.48 µA/cm^2 (year 2001) and 0.80 µA/cm^2 (year 2002) for the balcony frame panels. The year 2002 has thereby been remarkably milder regarding corrosion propagation than the year 2001. Peaks in the corrosion rate on both facade panels and balcony frame panels were observed during Dec 2000, Apr 2001, Sep 2001 and Feb 2002 with no distinguishable pattern visible. This implied that the consecutive years have been different regarding the corrosive environmental conditions. The current densities measured as a reference from the bottom surface of a balcony slab (sheltered from rain) were very low with monthly averages of 0.01–0.16 µA/cm^2. In the bottom surface of the slab the shelter from wetting is shown clearly as negligible corrosion rates.

At the Coastal area site the monthly average corrosion current densities on facades were 0.11–1.26 µA/cm^2 (Fig. 2-5). Similarly, the corrosion current densities on balcony frame panels were higher with monthly average values of 0.28–2.19 µA/cm^2. The yearly averages were lower than in inland with values of 0.61 µA/cm^2 (year 2001) and 0.37 µA/cm^2 (year 2002) for the facades and 1.26 µA/cm^2 (year 2001) and 0.79 µA/cm^2 (year 2002) for the balcony frame panels. Similarly to inland the year 2002 was milder regarding corrosion propagation than the year 2001. Distinguishable peaks in the corrosion rate were observed during Dec 2000, Oct 2001, Feb 2002 and Jul 2002. In addition, smaller variation between consecutive months was visible. Reference measurement from the bottom surface of a balcony slab was not available at this site.

The measured corrosion current densities were compared to the weather parameters T (Fig. 2), RH (Fig. 3), I_{WA} (Fig. 4) and RAD (Fig. 5) recorded from the same time period inland (left) and at coastal area (right). Similar trends can be observed between the isolated weather parameters and the corrosion current density. The outside air temperature and relative humidity tend to evolve as monthly averages rather steadily not fully grasping the whole

variability in corrosion rate (Figs. 2 and 3). These parameters mainly affect the conditions for the drying of concrete. On the other hand, solar radiation is highly concentrated on certain seasons (spring, summer) and the change between seasons is dramatic (Fig. 5). The change in solar radiation is not visible in corrosion rate with such a big effect. Thus, the influence of the solar radiation is presumed to be minor, like temperature and relative humidity, and mainly affect the conditions for the drying of concrete. An observation was, however, made that the level of corrosion rate tends to be generally lower during the seasons with high level of solar radiation.

The wind-driven rain is the only weather parameter that shows high variability also within seasonal changes, even though most of the rain is still concentrated in the autumn (Fig. 4). The representativeness of the wind-driven rain to the corrosion rate is observed to be fairly good. However, it alone will not explain all of the changes in the corrosion rate as observed e.g. in the Inland site data during 6-7/2002 (Fig. 4).

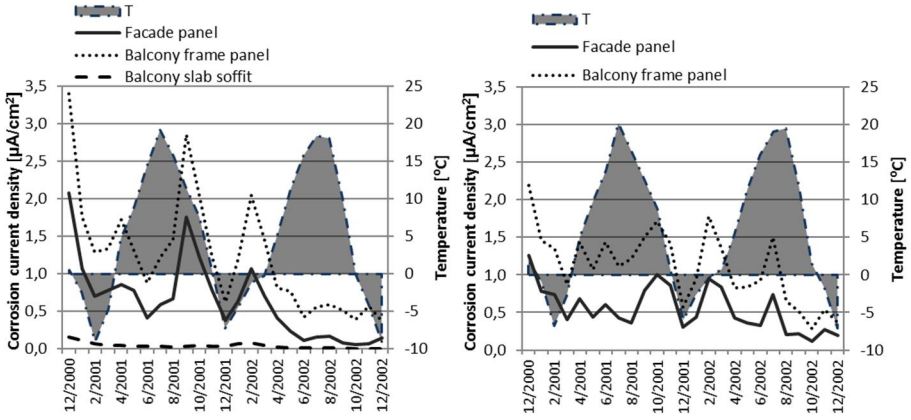

Figure 2 Corrosion rate contrasted to the monthly average outside air temperature T inland (left) and at coastal area (right)

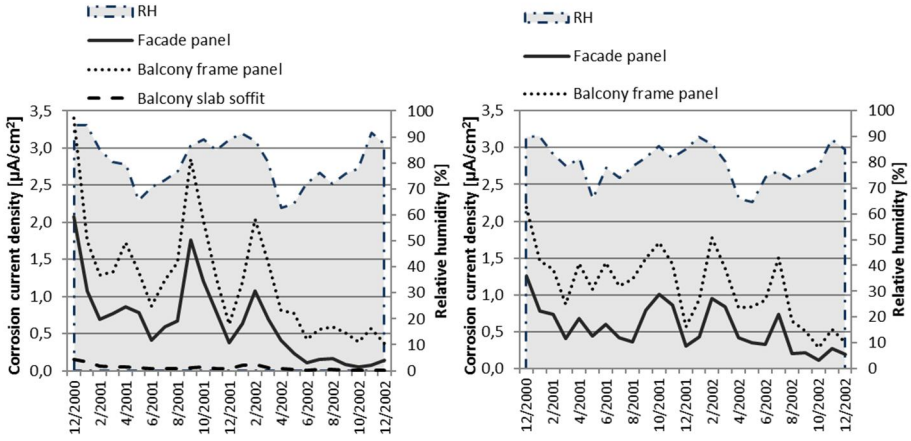

Figure 3 Corrosion rate contrasted to the monthly average RH of the outside air inland (left) and at coastal area (right)

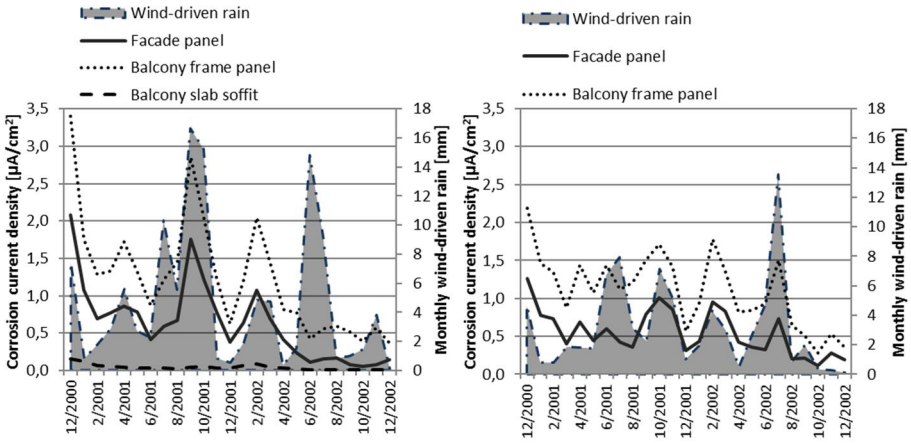

Figure 4 Corrosion rate contrasted to the monthly wind-driven rain amount I_{WA} inland (left) and at coastal area (right)

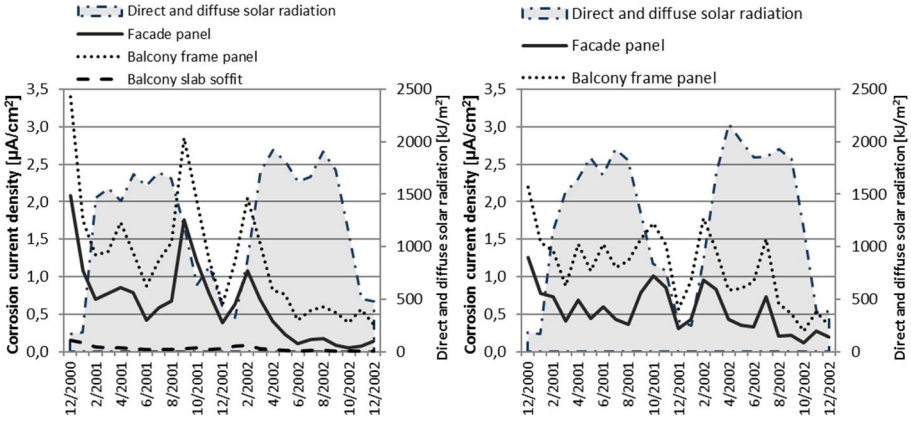

Figure 5 Corrosion rate contrasted to the monthly solar radiation amount RAD inland (left) and at coastal area (right)

Even though the highest peaks of the corrosion rate do not follow a certain pattern, the corrosion rate is as expected high during the autumn season. It is known to be a season when the ability of the structure to dry is greatly decreased keeping concrete wet for longer time periods once it is wetted by wind-driven rain. Rainfall is also in summer in Finland fairly large but, since the moisture caused by wind-driven rain generally can dry before it can have an effect on corrosion, the corrosion rates have been kept low in summer. During the summer season, when more variables play a role in determining the corrosion rate, the situation is more susceptible to changes and more unstable to predict. The highest monthly averages of corrosion rate were observed during winter mainly because of the lower ability of the structure to dry.

An initial presumption is often made that the corrosion rates will be higher on sites located in the coastal regions. However, this difference in corrosion rate between the coastal and inland

locations is not clearly visible in the research data. Actually, the overall monitored corrosion level was higher in the inland site (Figs. 2 – 5). This observation can be attributed to a higher amount of rainfall in the inland than in the coastal area during the monitoring period. Inherently, the corrosion rates have been 11–18 % higher inland than in the coastal region. This observation stresses the importance of the micro climate around the building and on the building site in regard of degradation rate. In this context, the micro climate means the actual weather conditions and exposure around a building which are influenced by the surrounding structures and vegetation as well as facade orientation and details.

The comparison of the measured corrosion rates from facades to balcony structures in both Inland and Coastal area sites (Fig. 6) shows that the both structures behave similarly, i.e. their intercorrelation is strong, under the same environmental conditions. The similar behaviour on its part verifies the measurements and reveals that the variations in the corrosion rates are caused by the variation in the environmental conditions and not e.g. by measurement setup related bias issues. Generally, the corrosion current densities on the balcony frame panels were approximately 1.5 times higher than on the facades.

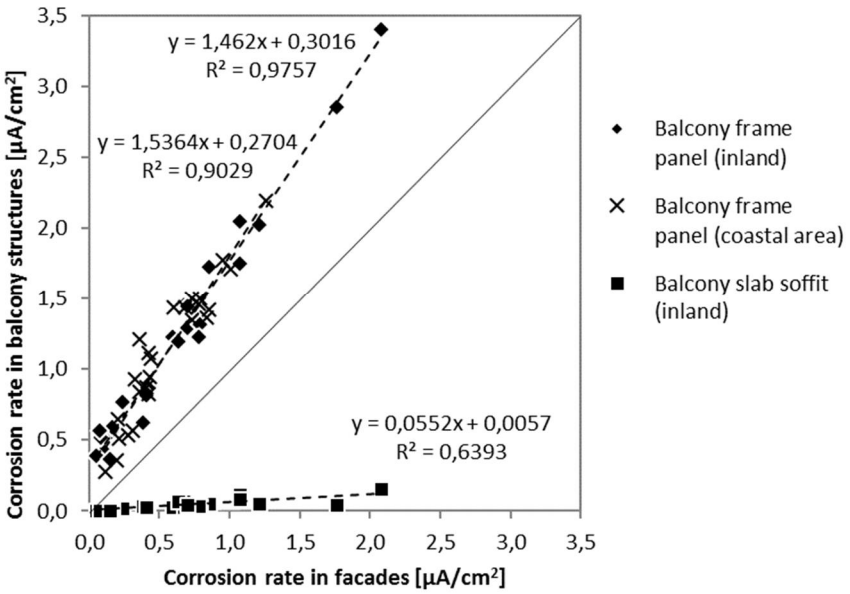

Figure 6 Comparison of the measured monthly corrosion rates in facades and in balconies at inland and coastal location

On the balcony frames this is presumed to be a result from both a more susceptible location for wetting (in the far edge of the facade) and worse conditions for drying (cold structures, no heat flux). The corrosion rate on the soffit surface of balcony slabs (not affected by wind-

driven rain) was only a fraction of the rates on the facades. This illustrates clearly that the wind-driven rain has a significant impact on the corrosion rates of the vertical weather exposed structures. On the other hand, sheltering structures from wetting (e.g. the balcony soffit) will result in greatly decreased corrosion risk and -rate. The different impact of the wind-driven rain on the different vertical walls is a result from weather, wall orientation, external shelter/obstruction and rainwater control of the wall itself.

4.2 Regression of the weather parameters to corrosion rate

The ability of the weather parameters to predict corrosion rates were tested with an extensive regression analysis. Judging by a preliminary analysis on the total time period of 25 months the overall representativeness of the single weather parameters is fairly low (series "The 25 mo period" in Figs. 7 and 8). However, division of the time period into seasons reveals the parameters that have the most effect over the year cycle.

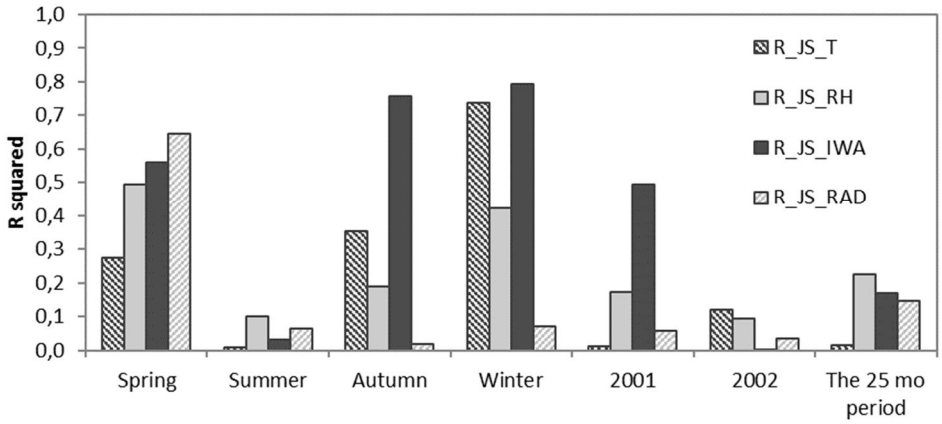

Figure 7 The correlation of single isolated weather variables to the corrosion rate on facades at the inland site

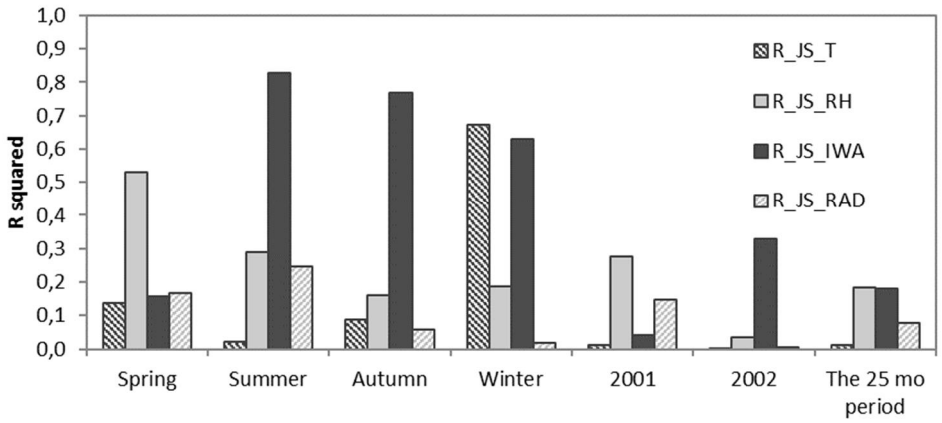

Figure 8 The correlation of single isolated weather variables to corrosion rate on facades in the coastal area site

In the results in Figs. 7 and 8 the seasonal evaluation shows generally high correlation between the wind-driven rain and the corrosion rate. However, it is low in summer season at the Inland site due to the rain event at 6-7/2002 and in spring at the Coastal area site due to a non-captured rise in corrosion rate at 4/2001, both visible in Fig. 4. The effect of the solar radiation is high during spring but its representativeness in the other seasons is low. The correlation between the RH and the corrosion rate is also high during spring. In the other seasons the effect is more random. The correlation between the temperature and the corrosion rate is remarkable in winter for two reasons: first, the temperature drop below 0 ºC greatly hinders the corrosion process and, secondly, the precipitation able to penetrate concrete (liquid form) requires a temperature of over 0 ºC. As a result, the effect of the temperature on the corrosion rate in winter is positive. This is contrary to the other seasons where the effect of the temperature is negative due to the increased drying of the structure.

4.3 Modelling of the corrosion rate with multiple parameters

The regression model was formed on the basis of linear regressions between the monthly averaged weather parameters of temperature (*T*, ºC), relative humidity (*RH*, %), wind-driven rain (I_{WA}, mm) and solar radiation (*RAD*, kJ/m^2) and the corrosion rate. The relationships of these parameters were illustrated in Figs. 2-5. From the large number of analyses (525 analyses with different combinations of weather parameters, seasons, etc.) the best performing combinations were judged by the coefficient of determination (R^2) of the model. At first separate models were produced for both inland and the coastal area as well as for facades and balconies. Their functionality was cross checked by attempting to use the coastal area model inland and vice versa. A fairly good fit (R^2 of 0.49–0.53) was achieved in the cross checking (Fig. 9). Finally, a combined model was composed where spring, autumn and winter seasons were from inland and the summer season from the coastal area data (Table 2). This allowed a slightly better fit for both geographical locations (R^2 for inland 0.71 and for the coastal area 0.55). Similar analysis was carried out also with the data from inland balcony slab soffits. However, no comparative data from the coastal area was available for it. Table 2 shows the parameters and coefficients that can be applied in the modelling of the reinforcement corrosion rate on concrete facades and balcony frames together with monthly weather data.

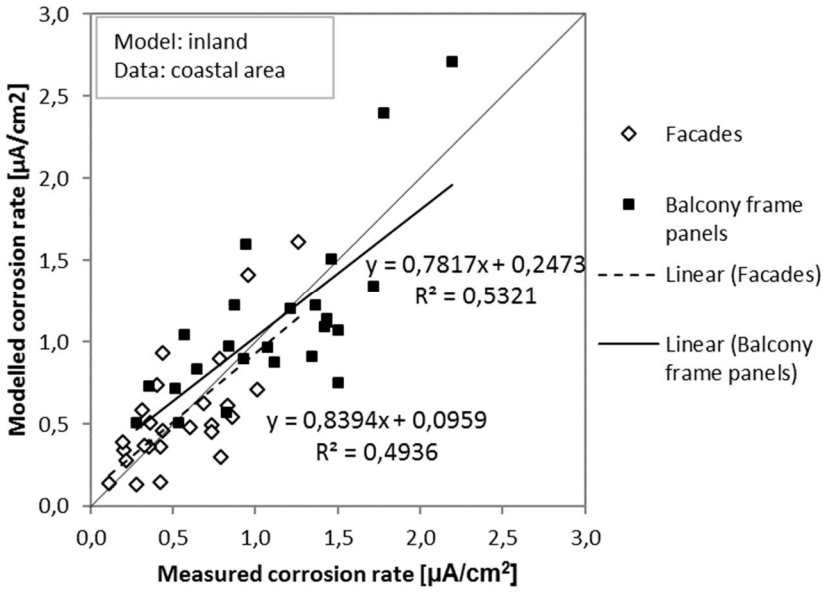

Figure 9 The correlation between the model generated from the inland data and the measured corrosion rate in the coastal area

Table 2 Regression models for reinforcement in facade panels (with heat flux) and balcony frame panels (cold structures). The R^2 values represent the goodness-of-fit of the specific season to the origin data.

Season	Origin	R^2 (facades)	R^2 (balconies)	Parameter	Coefficient (facades)	Coefficient (balconies)
Spring	inland data	0.45	0.85	β_{IWA}	0.035	0.126
				β_{RAD}	-0.0008	-0.0007
				β_0 (intercept)	1.913	2.091
Summer	coastal area data	0.95	0.96	β_{RH}	0.011	0.065
				β_{IWA}	0.037	0.047
				β_{RAD}	-0.0006	-0.0007
				β_0 (intercept)	0.562	-2.749
Autumn	inland data	0.69	0.78	β_{IWA}	0.084	0.122
				β_0 (intercept)	0.112	0.472
Winter	inland data	0.79	0.85	β_T	0.068	0.101
				β_{IWA}	0.134	0.235
				β_0 (intercept)	0.857	1.420

The model of every season is based on the influence of wind-driven rain which was shown by the measurements to have the dominating effect over the fluctuation of the corrosion rate in all seasons. In addition, the model utilizes the effect of solar radiation during spring and summer, the effect of relative humidity in summer and the effect of temperature in the winter season.

5. Application to service life design

The corrosion rates during the lifetime of the concrete structures at the inland and coastal area sites were estimated using the model with the coefficients presented in Table 2. A record of 30-year weather data from the time period 1979-2009 was used in preparing the weather parameters. The weather data was available for the coastal area site from Helsinki-Vantaa airport (distance to the site 15 km) and for the inland site from Jokioinen observatory (distance to the site 79 km), see Fig. 1. Fig. 10 shows the evolution of the corrosion rate over time as the function of the weather parameters at both locations and illustrates that the long-term effect of environmental actions alone on the corrosion rate was, according to the model, quite steady. High effect of the wind-driven rain is demonstrated by the comparison of the modelled corrosion rates on vertical concrete surfaces to the ones on the balcony slab soffit (Fig. 10) as well as the monthly measured values (Fig. 4). Phenomena which may slow down corrosion rates, such as the effect of the growing rust layer, are not in this model taken into account. The possible corrosion retarding phenomena should be considered in addition to the environmental actions especially in cases where the studied propagation phases are long.

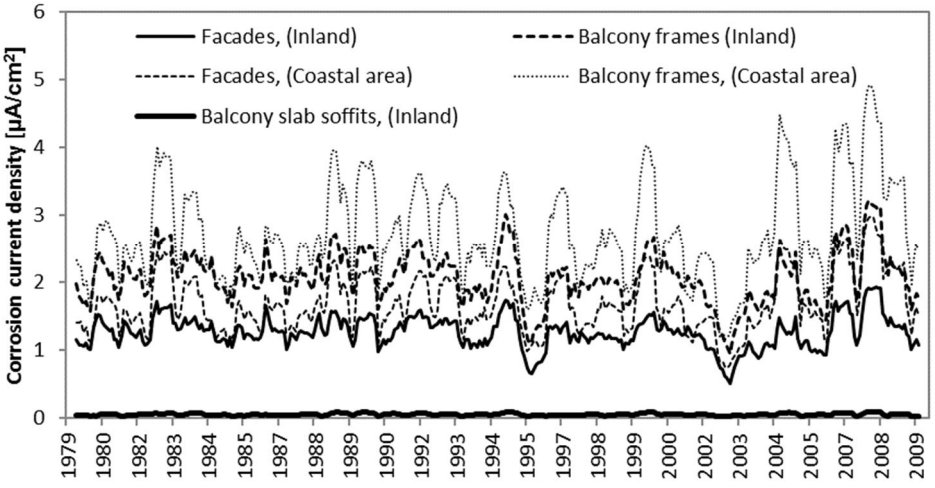

Figure 10 Corrosion rates extrapolated to the time period 1979-2009 in inland and in the coastal area (Moving average, n=9)

The modelled corrosion current densities on the Facades at the coastal area were by average 0.5 µA/cm^2 higher than inland. The overall average level was 1.2 µA/cm^2 inland and 1.7 µA/cm^2 at the coastal area. These corrosion rates correspond to a steel loss of 14.6 µm/year and 19.6 µm/year, respectively, derived from the Faraday's law. Based on the classification in (Andrade & Alonso, 2001) the corrosion levels can be considered high. In the studied 30-year period, corrosion propagated in the coastal area 34 % faster than inland. This modelled result at first seems to contradict the measurements presented in chapter 4.1. However, the lower corrosion rate in the measurements in the coastal area than inland has resulted in lower actual wind-driven rain amount during the finite measurement period. The total wind-driven rain amount over the 30-year period is opposite which results in higher long-term corrosion rate in the coastal area than inland. In other words, the model suggests a high relationship with the corrosion rate to the amount of wind-driven rain and a simple classification based solely on the geographical location is not in every situation enough to describe it. In this study, both of the facades were facing southern direction, but were not situated exactly the same which may cause some of the difference.

The modelled corrosion rates in the balcony frames are at both sites generally higher than in the facades. The average corrosion rate in the balcony frames was 2.1 µA/cm^2 inland and 2.7 µA/cm^2 at the coastal area corresponding to a steel loss of 24.2 µm/year and 31.7 µm/year, respectively. The corrosion rate was, thus, 62–66 % higher in the balcony frame panels than in the facades. There may be two reasons for this: (1) The balcony frame panels that are located at the far end upper corner of the facade are more susceptible to wind-driven rain than facade panels due to wind flow around the building, (2) The facade panels are affected by a heat flux through the outer wall. Although very small, it may improve the drying capability of the facade panels.

The corrosion rate information in Fig. 10 can be used to estimate the remaining service life of the concrete facade and balcony frame panels in regard of reinforcement corrosion. However, the estimate may be pessimistic since any corrosion retarding phenomena are not taken into account. Corrosion is in these structures commonly initiated by the carbonation of the concrete cover. The time of corrosion initiation of these structures is estimated to be 10–30 years in the facade panels (painted brush finished concrete) and 10–20 years in the balcony frames according to the square root relationship (Tuutti 1982) utilizing carbonation coefficients measured from 947 concrete buildings similar to the ones discussed in this paper

(Lahdensivu 2012). After initiation, corrosion will propagate at rates which are greatly dependent on the surrounding weather conditions as discussed in this paper. The metal loss due to active corrosion can be derived from Fig. 10 for the facades and balconies at the inland and costal area sites.

The selection of a suitable end of service life for these structures regarding visual cracking of the concrete cover is discussed in (Köliö et al. 2015). A critical corrosion penetration of 14.5–90.4 μm (depending on the reinforcement cover/diameter-ratio and the corrosion environment) was found experimentally for concrete facade panels. Thus, the extension to service life during the active corrosion phase can be approximately 1–6 years. If the corrosion rates on the balcony frames are considered in similar manner, the active corrosion phase in these structures is approximately 0.5–2.9 years. This extension to the service life is considered relatively minor. However, these structures which are facing southern directions are subjected to the most severe weather. In structures more sheltered from e.g. wind-driven rain the extension in service life can be remarkably higher.

6. Conclusions

A model to describe the evolution of the corrosion rates as a function of weather parameters was produced using a regression analysis between environmental conditions and field measurements of the corrosion rate. The regression analysis was performed on concrete facade panels and balcony frame panels at two geographical locations in Finland. The following conclusions can be drawn from the study:

i. After initiation, the corrosion rate in outdoor concrete structures, such as facades and balconies, is highly correlated with on-site weather parameters. The corrosion rates vary on concrete structures on seasonal and yearly basis. However, the highest correlation was found between the corrosion rate and wind-driven rain, the amount of which can differ greatly from year to year. The corrosion rates in the studied structures can be classified high.
ii. A versatile regression model based on field measurements was created between weather parameters and the corrosion rate of the reinforcement in outside air concrete structures. This model can be used to estimate corrosion rates in similar concrete structures in varying weather conditions. This analysis is a part of a future work to be conducted. The model was in this study validated by cross-checking with the data

from the two different locations. Final validation of the modelled result requires suitable reference data.

iii. Based on the developed regression model an analysis of 30-year weather data was undertaken. The results show that on a long time scale the effect of environmental actions on the corrosion rate on concrete facades and balconies was relatively steady. The average predicted corrosion rate after initiation on facades facing southern directions was estimated 1.2–1.7 μA/cm^2 corresponding to 14.6–19.6 μm/year metal loss. Similarly, on balcony frames the predicted corrosion rate was estimated 2.1–2.7 μA/cm^2 corresponding to 24.2–31.7 μm/year metal loss in the most severe cases. More information is needed on possible corrosion retarding effects of e.g. the diffusion resistance of corrosion products to describe the service life in detail.

iv. The geographical location of the structure (inland or at the coastal area) cannot be used alone to assess the environmental stress level of the building site. The stress level is significantly affected also by the micro climate around the building (e.g. shelter from surrounding terrain or vegetation) as well as the design of the details of the facade. Information on the micro climate is needed either as field measurement data or as classification. However, the generated model indicated that, over a long time period, corrosion is approximately 30 % faster in coastal area than in inland, mainly because of the higher amount of wind-driven rain.

7. Acknowledgements

This study was made possible by the Doctoral Programme of Built Environment (RYM-to) under the funding of the Academy of Finland (grant number T20500/913615/RYM-TO).

References

Ahmad S (2003) Reinforcement corrosion in concrete structures, its monitoring and service life prediction – a review. Cement & Concrete Composites 25:459-471.

Andrade C, Alonso C (2001) On-site measurements of corrosion rate of reinforcements. Construction and Building Materials 15:141–145.

Andrade C, Castillo A (2003) Evolution of reinforcement corrosion due to climatic variations. Materials and Structures 54:379–386.

Al-Neshawy F (2013) Computerised prediction of the deterioration of concrete building facades caused by moisture and changes in temperature. Aalto University, Doctoral dissertations 96/2013, Helsinki.

Blocken B, Carmeliet J (2007) On the errors associated with the use of hourly data in wind-driven rain calculations on building facades. Atmospheric Environment 41(11):2335–2343.

Blocken B, Carmeliet J (2002) Spatial and temporal distribution of driving rain on a low-rise building. Wind and Structures 5(5):441–462.

Blocken B, Dezsö G, van Beeck J, Carmeliet J (2010) Comparison of calculation models for wind-driven rain deposition on building facades. Atmospheric Environment 44:1714–1725.

Broomfield, J. 2007. Corrosion of steel in concrete. 2nd ed. Oxon: Taylor & Francis.

Choi E (1994) Determination of wind-driven rain intensity on building faces. Journal of Wind Engineering and Industrial Aerodynamics 51:55–69.

Directive 2013/37/EU. On the re-use of public sector information.

Dunster, A.M. 2000. Accelerated carbonation testing of concrete. Building Research Establishment. Information paper IP 20/00. Watford.

Fasullo E (1992) Infrastructure: The battlefield of corrosion. ASTM STP 1137.

Hagentoft C-E, Janssen H, Roels S, van Gelder L, Das P (2015) Reliability of Energy Efficient Building Retrofitting - Probability Assessment of Performance and Cost. ECBCS Annex 55, Chalmers.

ISO 15927-3 (2009) Hygrothermal performance of buildings. Calculation and presentation of climatic data. Part 3: Calculation of a driving rain index for vertical surfaces from hourly wind and rain data.

Jylhä K, Ruosteenoja K, Räisänen J, Venäläinen A, Tuomenvirta H, Ruokolainen L, Saku S, Seitola T (2009) The changing climate in Finland: estimates for adaption studies. ACCLIM project report. Finnish Meteorological Institute. Reports 2009:4. 78 p. + 36 app. (in Finnish, extended English abstract)

Karthick S, Muralidharan S, Saraswathy V, Thangavel K (2014) Long-term relative performance of embedded sensor and surface mounted electrode for corrosion monitoring of steel in concrete structures. Sensors and Actuators B 192:303–309.

Kopp G, Lean JL (2011) A new, lower value for total solar irradiance: Evidence and climate significance. Geophysical Research Letters 38:1–7.

Kottek M, Grieser J, Beck C, Rudolf B, Rubel F (2006) World Map of the Köppen-Geiger climate classification updated. Meteorologische Zeitschrift, 15(3):259–263.

Köliö A, Honkanen M, Lahdensivu J, Vippola M, Pentti M (2015) Corrosion products of carbonation induced corrosion in existing reinforced concrete facades. Cement and Concrete Research 78 Part B:200–207.

Lahdensivu J (2012) Durability Properties and Actual Degradation of Finnish Concrete Facades and Balconies. Tampere University of Technology, TUT Publ. 1028.

Lahdensivu J, Varjonen S, Pakkala T, Köliö A (2013) Systematic condition assessment of concrete facades and balconies exposed to outdoor climate. Int. J. of Sustainable Building Technology and Urban Development 4:199–209.

Law D, Claims J, Millard S, Bungey J (2004) Measurement of loss of steel from reinforcing bars in concrete using linear polarization resistance measurements. NDT&E International 37:381–388.

Maruthapandian V, Muralidharan S, Saraswathy V (2016) Spinel NiFe2O4 based solid state embeddable reference electrode for corrosion monitoring of reinforced concrete structures Construction and Building Materials 107:28-37.

Mattila J (2007) Effect of balcony glazing on the durability of concrete structures in nordic climate. Portugal SB 2007 - Sustainable Construction, IOS Press. Pp. 241-248.

Mattila J, Pentti M (2008) Residual service-life of concrete façade structures with reinforcement in carbonated concrete in Nordic climate. Tailor Made Concrete Structures, Taylor & Francis Group, London. Pp. 75-79.

Page CL (1988) Basic principles of corrosion. In: Schiessl P, editor. Corrosion of steel in concrete. London: Chapman and Hall. Pp. 3–21.

Pakkala T A, Köliö A, Lahdensivu J, Kiviste M (2014) Durability demands related to frost attack for Finnish concrete buildings in changing climate. Building and Environment 82:27–41.

Parrott LJ (1987) A review of carbonation in reinforced concrete. Cement and Concrete Association, Slough, UK.

R Core Team (2014) R: A Language and Environment for Statistical Computing. R Foundation for Statistical Computing, Vienna, Austria.

Rasheeduzzafar DFH, Al-Saadoun SS, Al-Gahtani AS (1992) Corrosion cracking in relation to bar diameter cover and concrete quality. J. Mater. Civ. Eng. 4:327-342.

Reda I, Andreas A (2008) Solar Position Algorithm for Solar Radiation Applications. NREL National Renewable Energy Laboratory, Colorado, USA.

Sanders C (1996) Environmental Conditions. ECBCS Annex 24, KU Leuven, Belgium.

Stern M, Geary A (1957) Electrochemical polarization, I. A theoretical analysis of the shape of polarization curves. Journal of the Electrochemical Society, pp. 56–63.

Straube J, Burnett E (2000) Simplified prediction of driving rain on buildings. Proc. of the International Building Physics Conference, Eindhoven, The Netherlands, 18–21 September 2000, pp. 375–382.

Taffese WZ, Sistonen E (2016) Neural network based hygrothermal prediction for deterioration risk analysis of surface-protected concrete façade element. Construction and Building Materials 113:34-48.

Tang Y-B, Wang S-N, Chen L, Fan Z-H (2015) Preparation and properties of embeddable Ag/AgCl gelling reference electrode for rebars corrosion monitoring in concrete. China Ocean Engineering 29(6):925-932.

Tilly G (2011) Durability of concrete repairs, in Concrete repair - a practical guide. New York, Taylor & Francis. pp. 231-247.

Tuutti K (1982) Corrosion of steel in concrete. Swedish Cement and Concrete Research Institute. CBI Research 4:82, 304 p.

Tampereen teknillinen yliopisto
PL 527
33101 Tampere

Tampere University of Technology
P.O.B. 527
FI-33101 Tampere, Finland

ISBN 978-952-15-3774-5
ISSN 1459-2045